HEVIN PROTEINA MATRIZELULARRAREN PARTE-HARTZEA ALKOHOLISMOAN: POSTMORTEM GIZA GARUNEAN ETA ANIMALIA-EREDUETAN BURUTUTAKO LANA

INVOLVEMENT OF THE MATRICELLULAR PROTEIN HEVIN IN ALCOHOL USE DISORDER: EVIDENCE FROM POSTMORTEM HUMAN BRAIN AND ANIMAL MODELS

Amaia Núñez del Moral

DOKTOREGO TESIA/DOCTORAL THESIS

2023

eman ta zabal zazu

Universidad del País Vasco

Euskal Herriko Unibertsitatea

Doktorego Tesi hau hurrengo erakunde eta proiektuen diru-laguntzei esker gauzatu da:

- Doktorego-aurreko Eusko Jaurlaritzaren diru-laguntza (2019-2022).
- The European Foundation for Alcohol Research (ERAB, EA 18 19)
- European Molecular Biology Organization (EMBO) short-term fellowship (2021)
- Eusko Jaurlaritza (IT1512-22)
- Centro de Investigación Biomédica en Red de Salud Mental (CIBERSAM)
- Fundación Vital (2018)
- FP7 Marie Curie Actions Career Integration Grant (FP7-PEOPLE- 2013-CIG #618807)
- Brain & Behavior Research Foundation (NARSAD, #17566)

Doktorego Tesi honetatik hurrengo artikulu zientifikoak lortu dira (Annexes 1 and 2):

- Nuñez-delMoral A., Brocos-Mosquera I., Vialou V., Callado L.F., Erdozain A.M. Characterization of Hevin (SPARCL1) Immunoreactivity in Postmortem Human Brain Homogenates. *Neurosciences*, (2021), 15; 467:91.
- Nuñez-delMoral A., Bianchi P.C., Brocos-Mosquera I., Anesio A., Palombo P., Camarini R., Cruz F.C., Callado L.F.,Vialou V., Erdozain A.M. A novel role for the matricellular protein hevin in alcohol use disorder. *Aurkeztua.*

LABURDURAK/ABBREVIATION LIST

2-AG:	2-arakidonilglizerol
3'UTR:	3'-untranslated region
5-HT:	5-hidroxitriptamina (serotonina)
ADAMTS4:	Tronbospondina 4 motibodun desintegrina eta metaloproteasa/A disintegrin and metalloproteinase with thrombospondin motifs 4
ADH:	Alkohol deshidrogenasa
AEB:	Amerikako Estatu Batuak
AED:	Autismoaren espektroaren gaitza
ALDH:	Aldehide deshidrogenasa
AMP:	Adenosina monofosfatoa
AMPA:	α-amino-3-hydroxy-5-metil-4-isoxazol-azido propionikoa/α-amino-3-hydroxy-5-methyl-4-isoxazole-propionic acid
AMY:	Amygdala
ANOVA:	Norabide nbakarreko bariantza-analisia/Analysis of variance
ATP:	Adenosina 5'-trifosfatoa
AUD:	Alcohol use disorder
BDNF:	Garunetik eratorritako faktore neurotrofikoa
CAU:	Caudate nucleus
CB:	Cerebellum
CB1:	1. motako hartzaile kannabinoidea
CB2:	2. motako hartzaile kannabinoidea
CCN:	cyr61-CTGF-NOV
cDNA:	DNA osagarria/Complementary DNA

CNS:	Central nervous system
COMP:	Kartilagoaren proteina oligomerikoa
CPu:	Dorsal striatum
CSF/LZR:	Likido zefalorraquideoa/Cerebrospinal fluid
CYT/ZIT:	Zitosola/Cytosol
DAPI:	4',6-diamidino-2-fenilindol
DMEM/F12:	Dulbecco's Modified Eagle Medium: Nutrient Mixture F-12
DTT:	Ditiotreitol
EAE:	Etanolaren aldizkako edatearen egitaraua
EC:	Zelulaz kanpoko kaltzioari lotzeko domeinua
EMA:	Europako Sendagaien Agentziak/ European Medicines Agency
FDA:	Amerikako Estatu Batuetako Elikagaien eta Drogen Administrazioak/ U.S. Food and Drug Administration
FS:	Folistatinaren antzeko domeinua
GABA:	Azido γ-aminobutrikoa/ γ-aminobutyric acid
GFAP:	Zuntzetako proteina astrozitiko glial azidoa /Glial Fibrillary Acidic Protein
GFP:	Proteina fluoreszente berdea/Green fluorescent protein
GHB:	Gamma-hidroxibutiratoa
GLAST/EAA1:	Na+-dependent glutamate/aspartate transporter/ excitatory amino acid transporter 1
GPCR:	G-proteinekin lotutako hartzaileak/G-protein-coupled receptors
GWAS:	Genoma osoko asoziazio- azterlana/Genome-wide association study
HIP:	Hippocampus
HT:	Homogeneizatu totala
IL:	Interleukina

KD:	Knockdown
KFA:	Kortikotropinaren faktore askatzailea
LC–MS/MS:	Kromatografia likidoa-tandem masa espektometria/ Liquid chromatography-tandem mass spectrometry
LTD:	Iraupen handiko depresioa
LTP:	Iraupen handiko indartzea
LZR:	Likido zefalorraquideoa
MAGL:	Monoazilglizerol lipasa
MALDI-TOF:	Matrix-Assisted Laser Desorption/Ionization - Time-Of-Flight
MAM:	Meprin, A5 protein, PTPm
MMP-3:	Matrizeko metaloproteasa-3/Matrix metalloproteinase-3
mQH2O:	Milli-Q® ura
MRI:	Errezonantzia magnetikoko bidezko irudigintza/ Magnetic resonance imaging
NAc:	Nucleus accumbens
NMDA:	Azido N-metil-D-aspartikoa/N-methyl-D-aspartic acid
NSZ:	Nerbio sistema zentrala
P2:	Mintzetan aberastutako frakzioa/Membrane-enriched fraction
PBS:	Fosfatato-indargetzaile soluzioa
PFA:	Paraformaldehidoa
PFC:	Prefrontal cortex
PMD:	Postmortem atzerapena/ Postmortem delay
RIPA:	Erradio-immunoprezipitazio entseguaren indargetzailea
RT-qPCR:	Polimerasaren erreakzio kateatuaren alderantzizko transkripzio kuantitatiboa/Quantitative reverse transcription polymerase chain reaction

SDS-PAGE:	Sodio dodezil sulfato-poliakrilamida gel elektroforesia
SEM:	Batez bestekoaren errore estandarra
SLF:	SPARC-antzeko fragmentua/SPARC-like fragment
SMECs:	Kontaktu kitzikagarri anizkoitzeko adarrak/Spines with multiple excitatory contacts
SPARC:	Jariatutako proteína azidoa zisteinan aberastua/ Secreted protein acidic and rich in cysteine
SSRI:	Serotonina berrabiarazteko inhibitzaile selektiboak
TH:	Total homogenate
TNF:	Tumoreen nekrosi-faktorea
TSP:	Tronbospondina
VTA:	Area tegmental bentrala/Ventral tegmental area
WT:	Basatia/ Wild-type
ZKM:	Zelulaz kanpoko matrizea

AURKIBIDEA/INDEX

1. SARRERA

1.1. ALKOHOLISMOA

1.1.1. ALKOHOLISMOAREN EPIDEMIOLOGIA

Nahiz eta etanolaren kontsumoa oso hedatuta eta onartua egon, alkoholismoa munduko ekonomian, gizartean eta osasunean eragin negatibo handien dutenen gaitz psikiatrikoetako bat da (Heilig et al., 2021; Rehm et al., 2009). Osasunaren Mundu Erakundearen 2018ko alkoholaren eta osasunaren txostenaren arabera ("Global status report on alcohol and health 2018" *World Health Organization* (WHO, 2018)) 2016an alkoholismoak munduko heriotzen % 5,3a eta gaixotasun-karga osoko % 5,1a (ezgaitasuna, doitutako bizi-urteari dagokionez edo *disability-adjusted life year (DALY)*) eragin zituen.

Espainian 2010. eta 2017. urteen artean batez beste 15.500 heriotza eta heriotza estandarizatuen % 4a alkohola edatearen ondorio izan ziren (Observatorio Español de las Drogas y las Adicciones, 2021a). Aipatzekoa da Espainian 2018. urtetik 2019. urtera alkoholismoagatik tratatutako pertsonen kopurua % 5,5 igo zela (25.753 kasu 2018an vs 27.209 kasu 2019an) (Observatorio Español de las Drogas y las Adicciones, 2021b). Gainera, Espainiako gobernuak 15 eta 64 urte bitarteko biztanleei egindako inkesta baten arabera, 2019an etanola izan zen gehien kontsumitu zen droga, egunero % 8,8k eguneroko kontsumoa egiten zutelarik (2017ko datuekin alderatuta 1,4 puntu gehiago) (Observatorio Español de las Drogas y las Adicciones, 2021a). Biztanleria beran % 5,2k alkohol-kontsumo arriskutsua egiten zela aurkeztu zuen, alkohol-kontsumo arriskutsuak hurrengo definizioa duelarik: kontsumitzailearentzat edo haren hurbileko senideentzat ondorio negatiboak izateko probabilitateak areagotzen dituen kontsumo-eredua.

Gainera, alkoholaren gehiegizko kontsumoa faktore kausala da 200 gaixotasun baino gehiagotan: gaitz mentaletan, minbizietan, zirrosi hepatikoan eta gaixotasun kardiobaskularretan, besteak beste (WHO, 2018). Halaber, azkenengo datu epidemiologikoek erakusten dute alkoholarekin erlazionatutako heriotza gehienek hurrengo arrazoiengatik gertatzen direla, bai munduan bai Espainian: zauriengatik, minbiziengatik eta gaixotasun digestibo, kardiobaskular eta infekziosoengatik (Observatorio Español de las Drogas y las Adicciones, 2021b; WHO, 2018).

Alkohola droga arriskutsuena eta kaltegarriena da kontsumitzaileen inguruko pertsonentzat (heroina baino gehiago). Izan ere, kontsumitzaileen osasunari kalte egiteaz

gain, haren gertuko senideei ere kalte egiten baitie modu askotan: etxeko indarkerian, trafiko-istripuetan, sexu-transmisiozko infekzioetan, delituetan, senideen antsietatean eta depresioan, ondasunen kalteetan eta lapurretetan parte hartzen du, besteak beste (Karriker-Jaffe et al., 2018; Nutt et al., 2010). Alkoholismoak eragindako galera ekonomikoa ere nabarmena da edari alkoholdunen kontsumo-tasa handia duten herrialdeetan. Europan adibidez kalkulatzen da herrialde bakoitzaren urteko guztizko kostua 1.000 milioi eurotik 7.800 milioi eurora bitartekoa izan zela 2012an (0,04-barne produktu gordinaren % 0,31a), gastu handiena ospitalizazioen ondorioz izan zelarik (Laramée et al., 2013).

1.1.2. ALKOHOLISMOAREN EZAUGARRI KLINIKOAK

Alkoholismoak bi sintoma nagusi ditu, gizabanakoari bere funtzioak normaltasunez garatzea eragozten diotenak: etanolaren kontsumoaren gaineko kontrolaren galera eta alkohola abstinentzian kontsumitzeko premia etengabea (desira edo *"craving"* ingelesez) (Spanagel et al., 2016; Weiss eta Porrino, 2002). Beste droga-menpekotasun askorekin batera, alkoholismoak sintoma fisiko negatiboak sortzen ditu abstinentzian, eta gero eta dosi handiagoak eskatzen ditu efektu positibo berberak lortzeko (tolerantzia) (Spanagel et al., 2016). Etanolaren menpekotasunaren zikloa elkarrekin lan egiten duten bi prozesu nagusik osatzen dute: errefortzu positiboak eta errefortzu negatiboak (Koob, 2021; Koob eta Volkow, 2016). Errefortzu positiboa etanolaren kontsumoaren emaitza da eta drogak dituen ezaugarri onuragarriei lotuta dago (Koob eta Volkow, 2016). Errefortzu negatiboa edatearen etenak eragiten du, eta hurrengo ezaugarriak ditu: abstinentziaren sintoma fisikoak eta egoera afektibo negatiboa (antsietatea, disforia, estresa eta suminkortasuna, besteak beste) (Koob, 2021; Koob eta Volkow, 2016). Horrela, abstinentzian, errefortzu positiboak drogaren ezaugarri onuragarriak bilatzea bultzatzen du, errefortzu negatiboak sintoma fisiko eta afektibo negatiboak etetera bultzatzen duen bitartean (Koob, 2021; Koob eta Volkow, 2016).

Nahiz eta jakina den etanolaren kontsumo akutuak eta kronikoak eragiten dituen garuneko neurobiologiaren aldaketek prozesu horietan (baita desiran eta tolerantzian ere) parte hartzen dutela (Abrahao et al., 2017; Koob eta Volkow, 2016), ikerketa biomedikoa oraindik argitzen saiatzen ari da zeintzuk diren etanolaren mekanismo zehatzak garunean sortzen dituen ondorioak eragiteko.

1.1.3. ALKOHOLISMOAREN EZAUGARRI GENETIKOAK

Beste gaixotasun neuropsikiatriko batzuk bezala, alkoholismoa faktore anitzeko gaixotasun konplexu bat da, non gene ezberdinek elkarreraginean jarduten duten, baita ingurumen-faktoreekin ere (Kendler et al., 2008). Horrek zaildu egiten du faktore genetiko edo ingurumen-faktore komun bat aurkitzea kasu guztietan. Zenbait ikerketek alkoholismoa garatzeko heredagarritasuna zenbatekoa den argitu nahi izan dute, 1960an lehen ikerketa lana argitaratu zelarik (Kaij eta Rosenthal, 1961). Bitxia bada ere, alkoholikodun gurasoa zuten bikien eta adopziozko haurren jarraipena egin zuten azterketen meta-analisi batean ikusi zen gaitz honen heredagarritasuna % 50etik hurbil zegoela (Verhulst et al., 2015).

Hainbat meta-analisik aztertu dute zer erlazio dagoen bariazio genetikoen eta alkoholismoa garatzeko sentikortasunaren eta edateko portaeren artean, eta horietako batzuetan etanolaren entzima metabolizatzaileen geneak parte har dezaketela aurkitu dute (Lopez-Leon et al., 2021). Alkohol deshidrogenasak (ADH) kontsumitutako etanolaren zatirik handiena gibelean metabolizatzen du eta oxidazio-erreakzio horretan azetaldehidoa sortzen da (Wilson eta Matschinsky, 2020). Horretaz gain, beste bi entzimak ere alkohola metabolizatzeko gai dira antzeko oxidazio-erreakzioan, neurri txikiagoan bada ere: P450 zitokromoa (CYP2E1) eta katalasa (Wilson eta Matschinsky, 2020). Ondoren, bigarren urrats oxidatzaile batean, aldehido deshidrogenasa (ALDH) entzimak azetaldehidoa azetato bihurtzen du (Wilson eta Matschinsky, 2020) **(1.1. irudia)**. ADH eta ALDH mota desberdinak daude, ehunetan zehar modu ezberdinean adierazten direnak eta aktibitate kataboliko ezberdina dutenak. Egiaztatu da ADH eta ALDH forma batzuek aldaera genetikoak dituztela talde etnikoen artean, entzimaren ahalmen katabolikoa aldatzen dutenak eta, beraz, organismoan etanolaren eta bere metabolitoen metaketa ere aldatzen da. Horrek, aldi berean, etanolaren efektuak eta edateko jarrera ezberdinak eragiten ditu aldaera genetikoen arabera (Wall et al., 2016). Horrela, *ADH1B*2, ADH1C*1* aleloak etanola azetaldehidoaren bihurketa handiagoarekin lotu dira, eta *ALDH2*2* aktibitate entzimatikoa gutxitzearekin (Edenberg eta McClintick, 2018; Zaso et al., 2019). Azkeneko emaitza beti odoleko azetaldehido maila handitzea da, zeinaren toxikotasunak ondorio kaltegarriak eragiten ditu eta, ondorioz, etanol gutxiago kontsumitzen da (Wall et al., 2016). Asiarren artean alelo horiek beste talde etniko batzuetan baino ohikoagoak dira (hau da, *ADH1B** asiarren ipar-ekialdeko % 80tan dago vs europako kaukasiarren % 10ean baino

gutxiagotan), eta, ondorioz, populazio hori babestuago dago alkoholismoa garatzeko (Wall et al., 2016; Zaso et al., 2019).

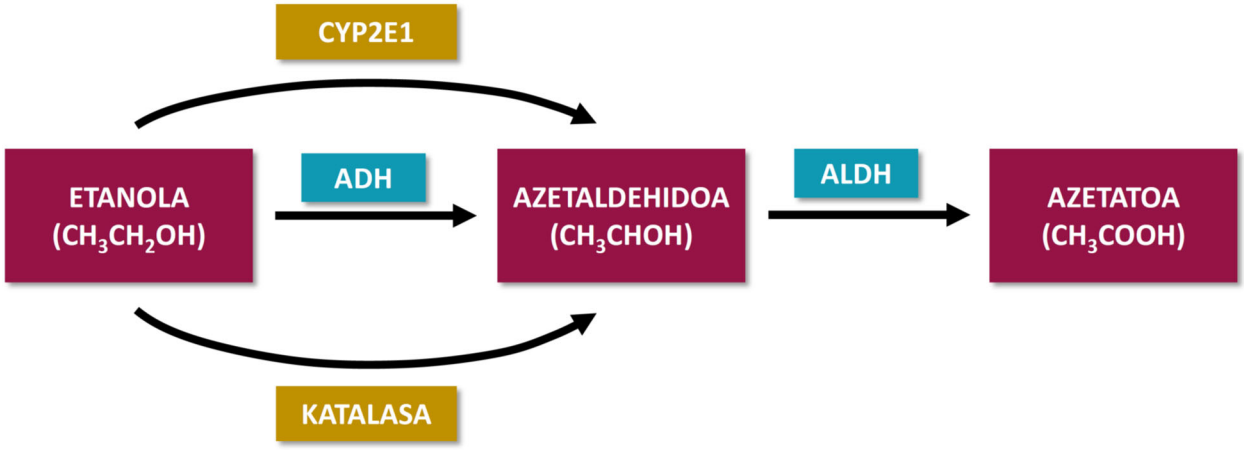

1.1. irudia. Etanolaren metabolismoaren hiru bidezidor garrantzitsuenak erakusten dituen irudi eskematikoa. ADH, alkohol deshidrogenasa; ALDH, aldehido deshidrogenasa; CYP2E1, P450 2E1 zitokromoa.

Gainera, neurotransmisore hartzaileen aldakuntza genetikoak alkoholismoa garatzeko sentikortasunarekin ere erlazionatu dira (Lopez-Leon et al., 2021). Badirudi hainbat bariazio genetiko D1, D2 eta D4 hartzaile dopaminergikoen geneetan (*DRD1*, *DRD2* eta *DRD4,* hurrenez hurren) alkoholismoa garatzeko arrisku handiagoarekin lotuta egon daitezkeela (Batel et al., 2008; Daurio et al., 2020; Jung et al., 2019). Nukleotido bakarreko polimorfismo bat 5-hidroxitryptamina (serotonina, 5-HT) 2A ($5\text{-}HT_{2A}$) hartzailearen genean alkoholismoa garatzeko arriskuarekin ere lotu egin da (Cao et al., 2014). Halaber, jatorri europarra zuten pertsonetan egindako meta-analisi batek agerian utzi zuen $GABA_A$ hartzailearen *GABRA2* geneak alkoholismoaren garapenean parte hartzen zuela (Li et al., 2014). Era berean, aleatorioko entsegu kontrolatu baten datuek iradokitzen dute *GABRA2* genearen polimorfismo bat lotuta dagoela etanolaren dosiaren menpeko erantzun euforikoarekin (Yang et al., 2017). Beste $GABA_A$ hartzaile gene asko alkoholismoaren sintomatologiaren ezaugarri ezberdinekin ere erlazionatu dira: *GABRA4, GABRA5* eta *GABRA6*, besteak beste (Koulentaki eta Kouroumalis, 2018). Beste sistema batzuetako elementuen geneetan gertatzen diren aldaketak alkoholismoaren arrisku-faktore gisa ere deskribatu dira, adibidez interleukina (IL) -10 genea (*IL10*), tumorearen nekrosi faktorearen (TNF) genea eta garunetik eratorritako faktore neurotrofikoaren (BDNF) genea (Egervari et al., 2021; Lopez-Leon et al., 2021; Zhou et al., 2020).

Hala eta guztiz ere, oraindik eztabaida handia dago bariazio genetiko horien eta alkoholismoaren arteko loturari buruz, emaitzak aldakorrak baitira ikerketen artean (Forero et al., 2015; Lopez-Leon et al., 2021). Gainera, genoma osoko asoziazio-azterlan (*genome-wide association studies* edo *GWAS*, ingelesez) asko egin dira alkoholismoaren nukleotido bakarreko polimorfismo komunak identifikatzeko helburuarekin, baina horietako bat ere ez lortu du oraindik (Deak et al., 2019; Lopez-Leon et al., 2021).

Azkenik, heredagarritasunarekin batera, geneen eta ingurumenaren arteko elkarrekintzaren garrantzia ere nabarmentzen da ikerketa genetikoetan (Agrawal eta Lynskey, 2008; Verhulst et al., 2015). Izan ere, ingurumen-estresoreek eta estresarekin lotutako gaitzek kromatinaren arkitektura eta, beraz, adierazpen genikoa aldatzen dutela deskribatu da, eta horrek, azkenean, alkoholarekiko menpekotasuna errazten duten alterazio neurobiologikoak eragiten ditu (Palmisano eta Pandey, 2017; Pucci et al., 2019). Etanolaren kontsumoa bera alkoholismoaren garapena bultzatzen duten aldaketa epigenetikoekin erlazionatu da, ziurrenik egoera afektibo negatiboa sustatuz (Egervari et al., 2021; Kyzar eta Pandey, 2015). Alegiakoa da, alkoholaren kontsumoarekin lotutako aldaketa epigenetikoen mekanismoa, neurri batean behintzat, etanolaren metabolismoak gibelean sortzen duen azetatoarekin lotuta dagoela ; zeren eta azetato horrek azetil-KoA sintetasa 2 entzimak katalizatutako garuneko histonen azetilazioan parte hartzen du (Mews et al., 2019).

1.1.4. ALKOHOLISMOAREN NEUROBIOLOGIA

1.1.4.1. Alkoholismoan parte hartzen duten neurotransmisio-sistemak

Etanola substantzia toxikoa da, eta bere erabilera akutuak antsiolisia, giharretako erlaxazioa, analgesia, sedazioa, amnesia, hipotermia eta anestesia eragiten ditu dosiaren mende. Denbora luzez kontsumitzeak aldaketak eragiten ditu organismo osoan, hala nola: sistema kardiobaskularrean, digestiboan, muskulueskeletikoan, metabolikoan eta immunitate- arnasketa-, gernu-, ugalketa- eta nerbio-sistemetan (Emanuele et al., 2002; La Vignera et al., 2013; Shield et al., 2014; Timary et al., 2012; Varga et al., 2017; Vonghia et al., 2008). Alkohola modu kronikoan kontsumitzen denean (hau da, alkoholismoan), organismoa etanolaren ondorioak orekatzen saiatzen da. Ondorioz, abstinentzian kontrako sintomak agertzen dira. Horrela, nerbio-sistema zentralean (NSZ) anedonia, antsietatea, goragalea, dardarak edo hipertermia ager daitezke; kasu larrienetan, konbultsio

epileptikoak, delirium tremens sindromea edo, esku-artze medikorik gabe, heriotza sortuz (Anton et al., 2020; Witkiewitz et al., 2019).

Biztanleriaren kontsumo-maila altuak kontuan hartuta, harrigarria dirudi zein informazio gutxi dagoen etanolaren itu molekularrei buruz, abusuzko beste substantzia batzuekin alderatuta (Abrahao et al., 2017; Most et al., 2014; Nestler eta Lüscher, 2019). Etanolaren mekanismo molekularrari buruzko lehen teorietako bat hurrengoa izan zen. Etanola tamaina txikia duenez, itu zehatzik ez daukanez eta bere banaketa organismoan uraren antzekoa denez, proposatu zen alkoholaren kontsumo akutuak mintz lipidiko neuronalak kaltetzen zituela, beraien jariakortasuna handiagotuz; eta etanolaren kontsumo kronikoak, ostera, mintz lipidikoen zurruntzea eragingo zuen, konpentsazio-mekanismo gisa (Chin eta Goldstein, 1981; Pang et al., 1980; Peoples et al., 1996). Hala ere, mintz neuronalak kaltetzeko beharrezkoak diren odoleko etanol kontzentrazioak, klinikoki esanguratsuak direnak baino askoz handiagoak dira (Goldstein, 1984), eta gaur egun badakigu alkoholak burmuineko itu zehatzekin elkarreragiten duela, zeinek aktibitate neuronala aldatzen dute (Abrahao et al., 2017).

Etanolak NSZren depresioa eragiten du $GABA_A$ hartzaileen bidezko transmisio GABAergikoaren potentziazioagatik eta NDMA (azido N-metil-D-Aspartikoa) hartzaileen bidezko transmisio glutamatergikoaren inhibizioagatik (Costardi et al., 2015). Horrez gain, etanolak beste neurotransmisio-sistema batzuk ere modulatzen ditu (adibidez sistema dopaminergikoa, opioidea eta serotoninergikoa), eta garuneko hainbat elementuri eragiten die, besteak beste, zelula glialei, zelula neuralen mezulari sekundarioei eta sistema neuroimmune eta neuroendokrinoei (Nutt et al., 2021).

1.1.4.1.1. Sistema GABAergikoa

Azido γ-aminobutrikoa edo GABA ugaztunen garuneko neurotransmisore inhibitzaile nagusia da, eta hiru hartzaile dituela uste da: $GABA_A$, $GABA_B$ eta $GABA_C$. $GABA_A$ hartzailea bost proteina azpi-unitatez osatutako ioi-erreten bat da, zeinaren bidez kloruro-ioiak (Cl^-) zelularen konpartimentu zitoplasmatikora pasatzen dira. Zelula barruko Cl^- kontzentrazioaren igoerak zelula hiperpolarizatzen du, beste neurotransmisoreen despolarizazio seinaleak blokeatuz (Whiting et al., 1995). $GABA_A$ hartzailearen isoformen kopurua ez dago argi, 19 azpi-unitate ezberdin baitaude elkarren artean bil daitezkeenak heteropentamero azpimota anitzak sortzeko. Hartzailearen isoforma desberdinak adieraz

daitezke zelula beraren barruan eta kokapen sinaptiko ezberdinekin. Gainera, bere aktibazioak inhibizio presinaptiko zein postsinaptikoan parte hartzen du (Khatri et al., 2019; Sigel eta Steinmann, 2012).

GABA eta substantzia GABA mimetikoek $GABA_A$ hartzaileetan eragiten dute, hiru leku nagusitan: 1) GABA gunea, droga agonista eta antagonistek jarduten duten ustezko lotura gunea, 2) pikrotoxina gunea, erreten ionikoa blokeatzen duena (modulatzaile alosteriko negatiboak gune honetan eragiten dute) eta 3) bentzodiazepina gunea, erretenaren irekiera sustatzen duena (modulatzaile alosteriko positiboak eragiten duten gunea). Etanola $GABA_A$ hartzailearen modulatzaile alosteriko positibo bat da, zeinak nagusiki zelulaz kanpoko domeinuan jarduten du, zehazki δ azpiunitatean, bentzodiazepina guneetako bat. Horrela, etanolak GABA neurotransmisorearen ekintza ahalbidetzen du, bentzodiazepinak eta barbiturikoak bezala (Olsen, 2018). Aurretik aipatu den moduan, $GABA_A$ hartzaileek azpi-unitate ezberdinez osatuta daude, garun-atalaren eta zelula motaren arabera. Beraz, etanolak tonu GABAergikoan duen eragina aldakorra da garun atal bakoitzak δ azpiunitateak dituzten hartzaileen kantitatearen arabera, adibidez accumbens nukleoan, hipokanpoan, talamoan, kortexean edo zerebeloan (Förstera et al., 2016). Etanolak $GABA_A$ren hartzaileen azpi-unitateen fosforilazioaren bidez, beraien funtzioa alda dezakeela frogatzen duten ebidentziak ere badaude (Kumar et al., 2012; Werner et al., 2016).

Bestalde, denboran zehar mantendutako alkohol-kontsumoak, abstinentzia-aldi errepikakorrekin batera, $GABA_A$ren hartzaileen barneratzea eta desentsitizazioa eragiten du, inhibizio-tonuaren beherakada orokorrarekin; eta horrek azkenean etanolak sistema GABAergikoan dituen efektuen tolerantzia eragiten du (Kumar et al., 2009; Olsen eta Liang, 2017). Aitzitik, alkoholaren kontsumoa bat-batean eteten edo murrizten denean, konpentsazio mekanismoak ez daude jada substantziaren bidez blokeatuta, eta abstinentzia-sindromea agertzen da, tonu inhibitzailearen eta kitzikagarriaren arteko desorekaren ondorioz. Horrela, homeostasiaren ondoriozko galera abstinentzia-sintoma gisa agertzen da (Heinz et al., 2020).

Azkenik, etanolak $GABA_B$ hartzaileen funtzioari ere eragiten dio. $GABA_B$ G-proteinekin (GPCR) lotutako hartzaile inhibitzaileak dira, eta $GABA_A$ hartzaileak baino erantzun motelagoa ematen dute. $GABA_B$ hartzaileen aktibazioak zelulen mintzaren hiperpolarizazioa eragiten du hiru mekanismoen bidez: potasio erretenen irekiera,

potentzial-diferentziarekiko mendekotasuna duten kaltzio-erretenen (*voltage-gated calcium channels*, ingelesez) inaktibazioa eta adenilatoaren zikloaren inhibizioa (Terunuma, 2018). Gainera, etanolak eragindako $GABA_B$ hartzaileen funtzioaren sustapena eta baklofeno sendagaiak ($GABA_B$ agonista) alkoholarekiko menpekotasuna tratatzeko erabilera iradokitzen du alkoholismoan hartzaile horien parte hartzea esanguratsua izan daitekeela (Ariwodola eta Weiner, 2004; Egervari et al., 2021; Federici et al., 2009; Logge et al., 2022).

1.1.4.1.2. Sistema glutamatergikoa

Glutamatoa garuneko neurotransmisore kitzikagarri nagusia da eta bi hartzaile mota ezberdinen bidez jarduten du, hauek ere etanolaren eraginpean daudelarik: ioi-erreten ligatuak (hartzaile ionotropikoak) eta GPCRak (hartzaile metabotropikoak) (Goodwani et al., 2017). Hartzaile ionotropikoak ioi-erretenak dira, eta, ligando baten bidez aktibatzen direnean, beraien erdiko poroa irekitzen da. Horri esker, ioi espezifikoen sarrera zelulara edo irteera zelulatik gertatzen da, zelula barneko tentsioa aldatuz. Hiru azpidibisiok osatzen dute talde hau: NMDA, AMPA (α- amino-3-hydroxy-5-metil-4-isoxazol-azido propionikoa) eta kainato hartzaileak (Reiner eta Levitz, 2018; Rodriguez-Chavez et al., 2021). Aldiz, errezeptore metabotropikoek G-proteinen bidez jarduten dute, zeinek zelulaz barneko mezulari sekundarioak modulatzen dituzte, eta hauek, ondoren, zelula-mintzean ioi-erretenak aktibatzen dituzte. Mekanismo horren bidez, hartzaile metabotropikoek ligando baten aurrean (adibidez, etanola edo glutamatoa) duten erantzuna, hartzaile ionotropikoena baino motelagoa da (Reiner eta Levitz, 2018). Etanolaren efektuak, batez ere, hartzaile ionotropikoen bidez ematen dira, eta, zehatzago, NMDA hartzailearen bidez, zeinak etanolarekiko sentikortasun handiena erakusten duen hartzailea da (Naassila eta Pierrefiche, 2019).

NMDA hartzailearen katioi-erretena lau azpiunitatez osatuta dago, egoera inaktiboan Mg^{2+} ioien igarotzea blokeatzen duelarik. Glutamatoaren askapenak eta AMPA hartzaileen bidezko despolarizazio postsinaptikoak Mg^{2+} NMDA hartzailearen ioi-erretenaren erditik desagertzea eragiten du, Na^+, Ca^{2+} and K^+ katioien fluxua erretenetik igarotzea ahalbidetuz. Horren ondorioz, mintz neuronala despolarizatu eta zelulaz barneko mezulari sekundarioak aktibatu egiten dira, funtzio zelularrean eraginez (Reiner eta Levitz, 2018).

Nahiz eta etanolak NMDA hartzaileetan eragiteko erabiltzen duen mekanismo zehatza ezezaguna den, oro har, bere kontsumo akutuak hartzaile hauen aktibitatea gutxitzen du.

NMDA hartzaileek etanolarekiko duten sentsibilitatea zelulaz kanpoko Mg^{2+} kontzentrazioaren, garun atalaren eta hartzailearen azpi-unitatearen konposizioaren eta fosforilazioaren mende dago (Boikov et al., 2020; Cuzon Carlson, 2018; Lovinger et al., 1989, 1990). Gainera, etanolak AMPA eta kainato hartzaileak inhibitzen ditu eta hartzaile glutamatergiko metabotropikoak modulatzen ditu (Costa et al., 2000; Gerace et al., 2021; Joffe et al., 2018; Johnson eta Lovinger, 2020; Wirkner et al., 2000). Horrela, etanolak droga depresore gisa jokatzen du, garuneko seinaleztapen sistema kitzikagarri nagusia inhibituz, hau da, sistema glutamatergikoa.

Egokitze-mekanismo gisa, berriz, etanola etengabe kontsumitzeak NMDA hartzaileen sentsibilizazioa eta gehiegizko adierazpena eragiten du, alkoholismoa duten subjektuen postmortem giza garunean deskribatu den bezala (Freund eta Anderson, 1996, 1999; Michaelis et al., 1993) **(1.2. irudia)**. Etanolaren edate kronikoak eragindako NMDA hartzailearen gainaktibitateak plastikotasun sinaptikoa aldatzen du, iraupen handiko indartzea (LTP) garuneko hainbat eremutan erraztuz, zeinek drogei lotutako errefortzuan, oroitzapenetan eta gehiegizko kontsumoan parte hartzen dute (adibidez, area tegmental bentrala *(ventral tegmental area* edo VTA, ingelesez), accumbens nukleoa eta hipokanpoa) (Burnett et al., 2016). Etanolaren presentzian, hau da alkohola kontsumitzen denean, seinale kitzikagarriaren gehiegizko erantzun hori tonu inhibitzaileak konpentsatzen du. Etanolaren gabezian ordez, lehen esan bezala (ikus 1.1.4.1.1 atala), seinaleztapen GABAergikoaren murrizpenak eta kitzikapen tonuaren handipenarekin batera egoera hiperglutamatergikoa eragiten du. Ondorioz, abstinentzia-sintomak (hau da, takikardia, goragalea, dardarak, buruko mina, anedonia eta antsietatea) eta drogarekiko desira (*craving*) agertzen dira (Krystal, n.d.; Roberto et al., 2021; Spanagel eta Kiefer, 2008) **(1.2. irudia)**.

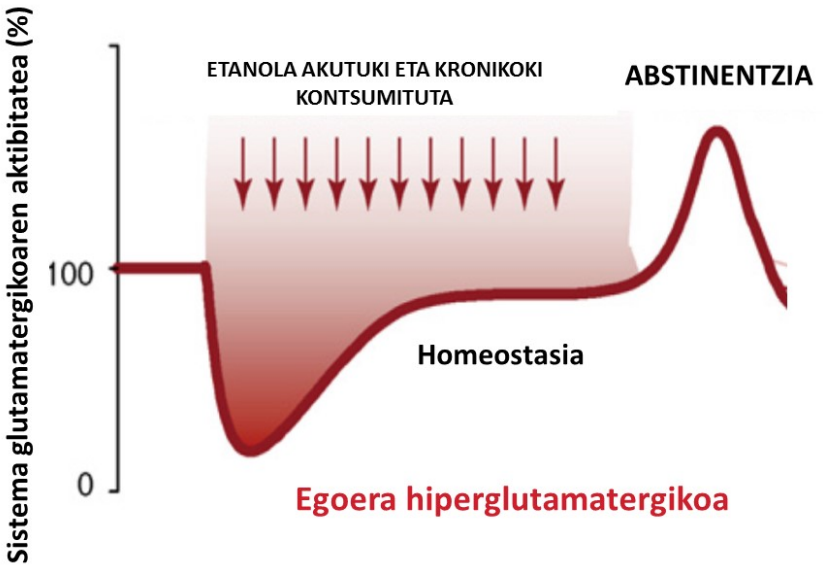

1.2. irudia. Sistema glutamatergikoaren aktibitatearen aurrera egitea alkoholismoan. Etanola hartzeak sistema glutamatergikoa inhibitzen du. Kontsumoa luzatzen denean, ordez, aktibitate glutamatergikoa handitzen da homeostasira iristeko. Farmakoaren gabezian (abstinentzia) etanolak eragindako inhibizioa desagertzen da, eta horrek egoera hiperglutamatergikoa eragiten du. *Spanagel eta Kiefer, 2008-tik moldatua*.

1.1.4.1.3. Sistema dopaminergikoa

Sari-sistemaren erdigunea VTAn dago, non neurona dopaminergikoak hurrengo nukleoetara proiektatzen diren: accumbens nukleoa, estriatu dortsala, amigdala, hipokanpoa, kortex aurrefrontala eta beste eskualde linbiko batzuk. Zirkuitu honen bidez dopaminak adikzioen motibazio jarrera modulatzen du (Klein et al., 2019).

Abusu edo indartze naturaleko beste edozein droga bezala (elikadura edo sexua, adibidez), etanolak sistema dopaminergiko mesokortikolinbikoa aktibatzen du, batez ere accumbens nukleoan dosiaren menpeko dopaminaren askapena handituz (Buck et al., 2021; Clarke et al., 2014; Di Chiara eta Imperato, 1988; Loftén et al., 2021; Yan, 1999; Yim eta Gonzales, 2000). Accumbens nukleoaren dopamina maila gora egitea hurrengo arrazoiengatik: dopamina VTAren neurona dopaminergikoen terminal sinaptikoen askapena gertatzen da eta etanolak neurona GABAergikoenkin eta hartzaile opioideekin elkarreragiten du (Cowen eta Lawrence, 1999; Gessa et al., 1985; Gilpin, 2008; Spanagel et al., 1992; Yim eta Gonzales, 2000). Izan ere, garezur barneko etanolaren autoadministrazioa areagotu egiten da etanola zuzenean VTAn ematen denean (Rodd, Bell, et al., 2004; Rodd, Melendez, et al., 2004). Gainera, abstinentziako animalia ereduetan, dopaminaren askapena estriatuan jaisten da eta VTAren neurona dopaminergikoen igorpena murriztu egiten dira. Horiek berreskuratu

daitezke alkoholaren autoadministrazioaren berreskurapenarekin (*reinstatement*, ingelesez), dopaminaren gabeziak alkoholaren abstinentzian dagoen errefortzu negatiboarekin zerikusia duela iradokiz (Rossetti et al., 1992; Weiss eta Porrino, 2002).

Gainera, alkoholismorik gabeko subjektuekin alderatuta, alkoholismoa duten pazienteek D_2 hartzaile dopaminergikoen maila baxuagoak dituzte estriatuan eta talamoan (Heinz et al., 2004; Volkow et al., 1996). D_2 estriatal horien urritasuna, alde batetik, etanolaren kontsumoa kontrolatzeko ezintasunarekin erlazionatu da; eta, bestetik, drogaren kontsumoarekin lotutako seinaleek (*cues-mediated*, inglesez) eragindako neurona-sareen gainaktibazioarekin, zeinek arretan, jokabidearen kontrolean eta desiran parte hartzen dute (Gleich et al., 2021; Heinz et al., 2004; Volkow et al., 1996, 2017; Zorick et al., 2019). Izan ere, estriatuan D_2 hartzaileen seinaleztapenaren handipenak alkoholismoa pairatzeko sentikortasuna duten subjektuentzako babes-faktorea izan daitekeela ematen du (Volkow et al., 2017). Dopamina garraiatzailearen murrizketa ere badago alkoholismoa duten subjektuetan, kasu honetan defizit kognitiboekin lotuta dagoela dirudiena (Grover et al., 2020; Tupala et al., 2000; Yen et al., 2015).

Hala eta guztiz ere, ikerketa lan batzuetan 6-hidroxidopamina neurotoxinak eragindako neurona dopaminergikoen desagertzea animalien accumbens nukleoan ez zuen etanolaren autoadministrazioaren jarrera aldatzen (Ikemoto et al., 1997; Koistinen et al., 2001). Era berean, beste ikerketa lan batean etanolaren autoadministrazioa ez zen eten dopamina mailak handitu zirenean, accumbens nukleoan dopaminaren birxurgapena inhibitzearen ondorioz (Engleman et al., 2000). Datu horiek adierazten dute sistema mesolinbiko dopaminergikoaren aktibazioa ez dela etanolaren indartze-efektu akutuen erantzule bakarra, eta, beraz, baieztatu egiten dute alkoholaren autoadministrazioan beste mekanismo batzuk parte hartzen dutela (Koob eta Volkow, 2010, 2016).

1.1.4.1.4. Opioide-sistema

Opioide endogenoen bidezko sistemaren aktibazioa sarien efektu atseginekin lotuta dago. Izan ere, gizakietan hartzitzaile μ-opioidearen eskuragarritasunaren eta sari-erantzunen arteko alderantzizko lotura dago (Nummenmaa et al., 2018).

Alkoholismoan, neurotransmisore sistema honek paper kritikoa du. Hainbat azterlanen arabera, peptido opioideen (adibidez, β-endorfina) eta μ- eta/edo δ- hartzaile opioideen dentsitate altuagoek parte har dezakete etanolaren kontsumo handiaren hastapenean eta

mantentzean;aldiz, κ- opioide hartzaileen edo dinorfina mailen handipena etanolaren gehiegizko kontsumoa inhibitzen dutela dirudi (Wang, 2019). Izan ere, arratoietan etanolaren administrazio akutuak endorfinen askapena areagotzen du accumbens nukleoan eta, saguetan, etanol kronikoaren edateak μ-hartzaileen funtzionalitatea handitzen du, morfinaren efektu onuragarriak indartuz (Olive et al., 2001; Shibasaki et al., 2013). Gainera, gizakietan egindako ikerketa batek erakusten du, kontrolekin alderatuta, ohiko gehiegizko alkoholaren kontsumoa (*heavy drinkers*, ingelesez) egiten dutenek opioide endogenoen askapen handiagoa dutela kortex aurrefrontalean eta accumbens nukleoan alkohol-kontsumoaren ondorioz (Mitchell et al., 2012). Datu horiek pentsarazten dute opioide-sistema sistema mesokortikolinbikoarekin lotuta egon daitekeela, etanolak eragindako dopamina askatzea blokeatu egin baitaiteke μ-hartzailearen antagonista bat administratuz (Job et al., 2007).

Hala eta guztiz ere, sistema dopaminergikoaz gain, beste mekanismo batzuek ere parte har dezakete opioide-sistemarekin lotutako alkohol-kontsumoan, hala nola naltrexona opioide antagonista alkohol-kontsumoa, desira eta berriz gaixotzea (bererorketa edo *relapse*, ingelesez) murrizteko gai da gizakietan (Burnette et al., 2022); baina seinaleztapen dopaminergikoaren galera accumbens nukleoan ez du etanolaren autoadministrazioa eteten (ikus 1.1.4.1.3. atala).

Gainera, ikerlan batean jakinarazi da korrelazio positiboa dagoela μ-hartzaileen erabilgarritasunaren eta alkoholarekiko desiraren larritasunaren artean paziente alokoholiko detoxifikatuen estriatu bentralean (Heinz et al., 2005). Azkenik, alkoholismo larria duten subjektuen estriatuko postmortem ehunetan μ-hartzaileen maila txikia detektatu da, etanolak eragindako opioide endogenoen askapenari aurre egiteko mekanismo neuromodulatzaile gisa (Hermann et al., 2017). Horrek azal lezake μ-hartzaile antagonisten (adibidez, naltrexona) eraginkortasun eza alkoholismoko paziente batzuengan (Hermann et al., 2017).

1.1.4.1.5. Sistema serotoninergikoa

Serotoninak (5-hydroxytryptamina, 5-HT) garuneko hainbat funtziotan hartzen du parte, hala nola janguraren kontrolean, lokomozioan, erabakiak hartzean, memorian, ikaskuntzan, ziklo zirkadianoen erregulazioan, aldartean, bulkadan eta adikzioan (Lv eta Liu, 2017).

Oro har, animaliei eta gizakiei buruzko hainbat azterlanen arabera, transmisio serotoninergikoaren hazkundea alkohol gutxiago kontsumitzearekin lotuta dago, eta alderantziz (Müller et al., 2020). Gizakiengan, postmortem garunean egindako ikerketa batek erakutsi zuen alkoholismoa zuten pazienteetan 5-HT_{1A} hartzailearen mRNA adierazpen handiagoa ematen zela (Thompson et al., 2012). Gainera, alkoholismoa duten subjektuek 5-HT_{1A} hartzailearen dentsitate murriztua dute aurreko zingulu-kortexean, eta 5-HT_{1B} hartzaileen handipena dute estriatu bentralean (Hu et al., 2010; Storvik et al., 2009).

Gainera, serotonina garraiatzailearen erabilgarritasuna handitzen duen aldaera genetiko batek nerabezaroan alkohola edatea sustatzen du (Hinckers et al., 2006). Era berean, serotonina garraiatzailearen erabilgarritasun txikiagoa deskribatu da alkoholismoa duten pazienteetan eta alkoholismoa pairatzen zuten subjektuen postmortem ehunetan, ziurrenik erantzun neuromodulatzaile gisa (Heinz et al., 1998, 2000; Ho et al., 2011; Kärkkäinen et al., 2015; Mantere et al., 2002; Storvik et al., 2006, 2008; Szabo et al., 2004). Aldiz, serotonina garraiatzailearen adierazpenaren handipena ere jakinarazi da alkoholismoko subjektuen postmortem kortex aurrefrontalean eta aurreko zingulu-kortexean, bere aldaketek garun ataleko espezifikotasuna izan dezaketela iradokiz (Underwood et al., 2018).

Bestalde, alkoholismoa zuten pazienteetan serotonina-sintesia ere aldatuta aurkitu da, garun atal espezifikotasuna erakutsiz (Nishikawa et al., 2009). Izan ere, serotoninaren metabolitoen mailen igoera detektatu egin da giza odolean eta gernuan etanol dosi bakar baten ondoren, serotoninaren askapena etanola edatearen ondorioz ematen dela iradokiz (LeMarquand et al., 1994). Serotonina-mailen gutxipena ikusi izan da alkoholismoa duten pazienteen likido zefalorraquideoan (LZR) eta plaketetan eta etanol-abstinentziaren aldi goiztiarrean zeuden pazienteen plaketetan. (Bailly et al., 1993; Nedic Erjavec et al., 2021; Virkkunen et al., 1995).

Karraskarietan, 5-HT_{1B} hartzailearentzako knock-out saguek etanol gehiago edaten dute eta lokomozio-koordinazio hobeagoa dute sagu basatiekin (*wild type*, ingelsez) alderatuta, hartzaile honek alkohol-intoxikazioan parte hartzen duela iradokiz (Crabbe et al., 1996). Izan ere, 5-$HT_{1A/1B}$ hartzailearen agonista partzialek etanolaren kontsumoa murrizten dute saguetan (Belmer et al., n.d.; Patkar et al., 2017, 2019). Horretaz gain, etanolaren gaitasun atsegingarriak murriztu egiten dira 5-HT_{2A} hartzailea blokeatzen denean eta etanolaren autoadministrazioak 5-HT_{2A} hartzailearen adierazpena handitzen du, hartzaile horrek

etanolaren propietate indargarrietan parte har dezakeela adieraziz (Alexander et al., 2012; Roberts et al., 1998). Halaber, etanolak seinale serotoninergikoak areagotzen ditu serotonina eta 5-HT_3 hartzailearen lotura erraztuz eta ioi-erretena irekita dagoen denbora luzatuz (Sung et al., 2000; Zhou et al., 1998). Etanolak, gainera, 5-HT_3 hartzailea zelula kultur ezberdinetan aktibatzen du ere (hau da, oozitoetan, kortexean eta gongoil neuronetan) (Harris et al., 1995; Lovinger eta White, 1991; Sung et al., 2000); eta 5-HT_3 hartzailearen blokeoak etanolaren autoadministrazioa eta kontsumoa murrizten ditu, baita estresak eragindako alkoholaren kontsumoaren berrezarpena eragin (Hodge et al., 1993; Lê et al., 2006; Sellers et al., 1994). Era berean, etanola emateak zelulaz kanpoko serotonina mailak handitzen ditu dosiaren mende hainbat garun ataletan, hala nola accumbens nukleoan, VTAn, kortex aurrefrontalean eta hipokanpoan (Bare et al., 1998; Deehan et al., 2016; Easton et al., 2013; Kalinichenko et al., 2019; Pavón et al., 2019; Szumlinski et al., 2007; Yan, 1999).

1.1.4.1.6. Sistema endokannabinoidea

Endokannabinoideak zenbait prozesu fisiologikoen seinaleztapenean parte hartzen duten neurotransmisore lipofiloak dira. Besteak beste, oroimena, mina, seinale immunologikoak, gosea, gogoa edo estresa erregulatzen dute (Lu eta Mackie, 2021). Gaur egun, bi hartzaile kannabinoide deskribatuta daude, biak Gi/o proteina inhibitzaileari akoplatuta daudenak: 1. motako hartzaile kannabinoidea (CB_1), garuneko terminal presinaptikoetan adierazten dena nagusiki (Herkenham et al., 1991; Schurman et al., 2020); eta 2. motako hartzaile kannabinoidea (CB_2), ehun periferikoen zelula immuneetan adierazia batez ere, eta neurri txikiagoan nerbio-sistema zentralean adierazten dena (Atwood eta Mackie, 2010; Munro et al., 1993; Schurman et al., 2020; Van Sickle et al., 2005). Azpimarratzekoa da, CB_1 hartzaileek espresio handia dutela sari-sistema mesokortikolinbikoa osatzen duten garun ataletan, drogekin lotutako sarietan eta motibazioan paper bat iradokiz (Manzanares et al., 2018).

Hartzaile horientzat hobekien ikertutako ligandoak N-arakidoniletanolamina (anandamida edo AEA) eta 2-arakidonilglizerol endokannabinoideak (2-AG) dira. Endokannabinoideek seinale kitzikagarri eta inhibitzaileak modulatzen dituzte zenbait neurotransmisoreen askapena inhibituz, hala nola glutamatoa eta GABA edo dopamina mesolinbikoa (Lu eta Mackie, 2021). Horrek, aldi berean, funtzio sinaptikoari eragiten dio, eta berehalako ondorioak edo ondorio iraunkorrak eragiten ditzake, hala nola iraupen handiko depresioa

(LTD) (Bilbao et al., 2020; Sidhpura eta Parsons, 2011). Alkoholaren gehiegizko kontsumoak sariarekin, motibazio portaerarekin, ikaskuntzarekin eta oroimenarekin zerikusia duten garuneko eremuetako plastikotasun sinaptikoaren modulazio endokannabinoidea eten dezake (Serrano eta Natividad, 2022; Zlebnik eta Cheer, 2016).

Ikertzaileek ebidentzia zientifiko argia aurkitu dute sistema endokannabinoidearen eta alkoholismoaren fisiopatologiaren loturaren artean (Erdozain eta Callado, 2011). Horrela, alkoholaren esposizio akutuak eta kronikoak murriztu egiten du endokannabinoide bidezko ELDa, eta horrek areagotu egin dezake seinaleekin lotutako (*cue-related,* ingelesez) ikaskuntza eta ezagutze-memoria (*recognition memory*, ingelesez) (Clarke eta Adermark, 2010; DePoy et al., 2013; Peñasco et al., 2020). Orokorrean, badirudi CB_1 hartzaileen antagonismoak etanolaren hartzea jaisten duela eta bere aktibazioak, ordez, kontsumoa sustatzen duela (Henderson-Redmond et al., 2016). Garrantzitsua da aipatzea, gure ikerketa taldeak alkoholismoa duten subjektuen postmortem giza garunean egindako ikerketa batek CB_1 hartzailearen hiperfuntzioa eta hipofuntzioa erakutsi zituela nukleo kaudatuan eta zerebeloan, hurrenez hurren (Erdozain et al., 2015). Gainera, kortex aurrefrontalean CB_1 hartzailearen adierazpenaren handipena detektatu zen suizidioaren ondorioz hil ziren subjektu alkoholikoetan. Azterketa horretan, gainera, monoazilglicerol lipasa (MAGL) entzima endokannabinoidearen aktibitate txikiagoa aurkitu zen alkoholismoa zuten subjektuetan, heriotzaren kausaz gain (Erdozain et al., 2015). Kontrara, CB_1 hartzailearen adierazpenaren antzeko murrizketa ikusi da kalamu-erretzaileen eta alkoholismoa duten pazienteetan; eta adierazpenaren murrizketa hori iraunkorragoa da bigarrenetan lehenengoetan baino, alkoholak CB_1 funtzioan eragin handia duela iradokiz (Ceccarini et al., 2014; Hirvonen et al., 2012, 2013).

Alkoholak karraskarien garunean ere endokannabinoideen mailak aldatzen ditu. Hala ere, honen gaineko dauden datuak aldakorrak dira ikerketa lanen artean, ziurrenik, ezberdintasun metodologikoak eta faktore esperimentalak direla eta, hala nola: erabilitako animalia-eredua, alkoholaren esposizioaren programa (iraupena, aldia) eta abstinentzia aldi baten presentzia edo absentzia (Serrano eta Natividad, 2022). Hala ere, arratoien amigdalan eta kortex aurrefrontalean ikusi da CB_1 hartzaileen murrizketa gertatzen dela etanol akutuaren eta etanol-abstinentziaren ondoren, baita endokannabinoide mailen murrizketa ere (Rubio et al., 2008, 2009). Ikerketa batzuen arabera, etanolak sistema

endokannabinoidean dituen ondorioetan sexu-desberdintasun handiak ere egon daitezkeela iradokitzen dute (Henricks et al., 2017).

1.1.4.1.7. Bestelako sistemak

Bere egitura molekular txikiaren eta bere propietate anfifilikoen ondorioz, etanolak beste sistema neurokimiko eta endokrino askori eragiten die. Horrela, etanolak hartzaile nikotinikoa modulatzen du, eta ondorio ezberdinak ditu hartzailearen azpi-unitatearen osaeraren arabera (Miller eta Kamens, 2020). Era berean, etanolak glizina hartzaileen aktibitatea sustatzen du bere azpi-unitateekiko espezifikotasunarekin. Horrela erantzun ezberdinak sortzen ditu hartzaile motaren arabera, adibidez etanolaren lehentasunean eta kontsumoan, antsietatean edo deskoordinazio motorrean (Blednov et al., 2015; Förstera et al., 2017).

Alkoholaren esposizioaren arabera (hau da akutua vs luzarokoa edo errepikakorra) aldaketa ezberdinak ikusi dira eroankortasun handiko kaltzioak aktibatutako potasio-erretenean (BK erretena, *large conductance calcium-activated potassium channel*, ingelesez) (Dopico et al., 2014); eta erreten horretako asaldurak alkoholak eragindako portaera depresiboarekin eta hipolokomozioarekin erlazionatu dira, besteak beste (Bettinger eta Davies, 2014; Oh et al., 2017). Etanolak erasandako beste ioi-erretena G-proteinari loturiko barrutik zuzendutako K^+ erretena (GIRK; *G-protein-coupled inwardly rectifying K^+ channel*, ingelesez) da, zeinek aktibitate handipena jasaten du etanolarekin zuzenezko elkarreraginaren ondorioz (Bodhinathan eta Slesinger, 2013). Bitxia bada ere, GIRK erreteneko esanahia aldatzen duen mutazio batek etanolak eragindako analgesia desagerrarazten du; eta alkoholaren edate kronikoa, aldiz, haren aktibazioa eteten du (Cannady et al., 2018; Kobayashi et al., 1999)

Sari eta errefortzu erantzunekin batera, bultzatzaile negatiboak ere badaude, drogarik ezean estresa eta beldurraren erantzunak indartzen dituztenak, drogaren bilatzea eta desira indartuz. Kortikotropinaren faktore askatzailea (KFA edo *corticotropin-releasing factor*, inglesez) errefortzu negatiboetako bitartekari bat da. KFAak seinaleztapen GABAergikoa areagotzen du amigdalan eta etanolaren esposizio akutuak indartu egiten du transmisio hori, KFA hartzailearen sentsibilitatea handitzen duelako. Hori, batez ere animalia emeetan ematen da eta etanolak transmisio inhibitzailea areagotzeko KFAren askapena sustatzen duela iradokitzen du (Bajo et al., 2008; Cruz et al., 2012; Rodriguez et al., 2022). Etanol kronikoa hartzeak KFA hartzailearen jarduera ere gutxitzen du hipokanpoan, KFA neuronen

jarduera oztopatuz stria terminalis-aren ohe-nukleoan (BNST; *bed nucleus of the stria terminalis*, ingelesez) (Marty et al., 2020; Snyder et al., 2019). Bere aldetik KFAak transmisio kitzikatzailea modulatzen du alkoholarekiko menpekotasuna erakusten duten arratoien amigdalan (Varodayan et al., 2017).

Etanolak sistema purinergikoan ere eragiten du, zeinak adenosina, adenosina monofosfatoaren (AMP) hidrolisi produktu bat eta adenosina 5'-trifosfato (ATP) bezalako purinez osatuta dagoen. Sistema hori etanolaren kontsumoaren ondorioekin erlazionatu zen lehenik, jakinarazi zenean nukleosido-garraiatzaile baten inhibitzaile batek (zelulaz kanpoko adenosinaren mailak erregulatzen dituenak) deskoordinazio motorra eta loa eragin zituela, etanolaren dosi altuen kontsumoaren antzekoa (Dar et al., 1983). Adenosina A_1 hartzaileen aktibazioa etanolak eragiten dituen ataxia, efektu antsiolitiko eta lasaigarriekin erlazionatu da; adenosina A_2 hartzaileen aktibazioa bere efektu hipnotikoekin, propietateak indartzearekin eta motibazio portaerarekin lotu den bitartean (Asatryan et al., 2011; Borea et al., 2018; Fang et al., 2017). Etanolaren kontsumo kronikoa eta abstinentzia adenosina A_1 hartzaileen murrizpena eta NMDA eta AMPA hartzaileen handipena eragiten ditu aldi berean (Bolewska et al., 2019); etanola kontsumitzeak, berriz, adenosinaren mailak handitzen ditu (Butler eta Prendergast, 2012; SanMiguel et al., 2019). Gainera, kafeinak, adenosinaren antagonista dena, alkoholaren abstinentziaren sintomak murrizten ditu (Pitchon et al., 2013; SanMiguel et al., 2019). Nahiz eta berriki egindako ikerketa batek kafeina eta adenosina A_{2A} hartzaileen aktibazioak etanolaren kontsumoa handitzen dutela erakutsi, aurreko ikerketek jakinarazi dute adenosina A_2 hartzaileen antagonismoak etanolaren autoadministrazioa gutxitzen duela saguetan, dopamina D_2 hartzaileen antzeko moduan (Arolfo et al., 2004; Mailliard eta Diamond, 2004; SanMiguel et al., 2019). Horrek erregulazio sinergikoa gertatzen dela iradokitzen du, bi hartzaileak estriatuko neuronetan kolokalizatzen direlako (Arolfo et al., 2004; Mailliard eta Diamond, 2004). Horrez gain, orain dela gutxi egindako ikerketa batek erakutsi du, etanolari erantzunez, astrozitoetatik ATParen eta adenosinaren askapena ematen dela eta hauek astrozitoen eta neuronen arteko zelulaz barneko komunikazioan parte hartzen dutela (Kim et al., 2021a).

Azkenik, neurona noradrenergikoek errefortzu, estres eta antsietate-erantzunekin lotuta dauden prosentzefaloaren eskualde linbikoak inerbatzen dituztelako, sistema noradrenergikoaren gehiegizko jarduera alkoholismoaren desirarekin, berrerortzearekin

eta errefortzu negatiboarekin lotu da (Downs eta McElligott, 2022; Haass-Koffler et al., 2018). Berriki egindako ikerketa batek erakusten du sistema noradrenergikoak ere paper garrantzitsua betetzen duela alkoholismoaren neurobiologian (Varodayan et al., 2022). Zehazki, ikerketa horretan aurkitu zuten arratoien amigdalan dauden α_1-hartzaileek seinaleztapen GABAergikoa sustatzen dutela, etanola neurrian hartzen dela kontrolatuz; β-hartzaileek, aldiz, gehiegizko edaria gidatzen duten bitartean. Gainera, postmortem laginak erabiliz ikusi zuten α_{1B} -hartzailearen mRNA-aren handipena alkoholismoa zuten gaixoen amigdalan.

1.1.4.2. Garunaren egitura-aldaketak alkoholismoan

Etanolaren esposizioak eragindako garuneko atrofia oso aztertua izan da. Izan ere, giza ehun postmortem-ean egindako lehen lanetako batek entzefaloaren, bizkarrezur-muinaren eta nerbio periferikoen asaldura makro- eta mikroskopikoen ilustrazioak erakusten ditu, etanolaren intoxikazio akutuak eta alkoholismoak eragindakoak (Courville, 1955). Neuroirudi teknika modernoek, hau da, erresonantzia magnetiko bidezko irudiak (EMI) alkoholaren kontsumoak eragindako egitura aldaketak egiaztatu dituzte, hainbat lanetan jakinarazi denez. Horrela, gai grisaren galera nabarmena aurkitzen da eskualde kortikal eta azpikortikaletan; eta zehazki, kortex aurrefrontalean, zingulu-kortexean, insulan, estriatuan, talamoan eta hipokanpoan (Daviet et al., 2022; Li et al., 2021). Alkoholaren gehiegizko hartzeak materia grisean dituen ondorioak bat datoz alkoholismoaren kontsumoaren progresioarekin eta iraupenarekin, meta-analisi baten jakinarazi duenaren arabera (Yang et al., 2016). Gai zurian detekta daitezkeen alterazio gehienak mikroestrukturalak dira (adibidez, tiamina eskasia demielinizazioarekin lotuta dago) eta pazienteen adinarekin eta alkoholaren dosiarekin mendekotasun handia dute (Hampton et al., 2019). Etanolak eragindako kalteak garuneko egitura zehatzetan aldaketak eragin ditzake haien funtzioetan, eta horrek, aldi berean, jokabide adiktiboa bultzatzen du (Nutt et al., 2021; Zou et al., 2018).

Kortex aurrefrontala garuneko funtzio exekutiboez arduratzen denez (hau da, judizioa, arazoen ebazpena, erabakiak hartzea, planifikazioa, jokabide soziala eta bulkaden kontrola, besteak beste) (Friedman eta Robbins, 2022; Jones eta Graff-Radford, 2021), alterazioak kortex aurrefrontalean alkoholismoan gertatzen den gaitasun horien galerarekin lotuta egon litezke (Koob eta Volkow, 2016; Le Berre et al., 2017). Garrantzitsua da, alkoholismoa duten pazienteen kasuan, kortex aurrefrontaleko zitoeskeletoaren murrizpena ikusi dela,

hipokanpoan, nukleo kaudatuan eta zerebeloan α- eta β- tubulina zitosolikoen murrizpenarekin batera (Erdozain et al., 2014; Labisso et al., 2018).

Era berean, amigdalan, hipokanpoan eta estriatu bentralean bolumen txikiagoa zegoela adierazten zuen ikerketa batek frogatu zuen, halaber, korrelazioa zegoela amigdala-bolumenaren galera garrantzitsuaren eta alkoholarekiko desiraren larritasunaren eta berrerortzearen artean (Wrase et al., 2008), segur aski bulkaden kontrol faltagatik. Horrez gain, alkoholismoa duten eta talamo-bolumen txikiagoa duten pazienteek alkoholaren gehiegizko kontsumoa berrabiarazteko joera handiagoa erakusten dute (Segobin et al., 2014).

Alkoholismoaren ondoriozko Papez-en zirkuituko egitura aldaketak ere deskribatu dira; zehazki, mamila gorputzen, talamoaren, hipokanpoaren eta zingulu-kortexaren bolumenaren murrizpen orokorra deskribatu da (Cardenas et al., 2007; Pitel et al., 2012; Sullivan et al., 1995; Sullivan eta Pfefferbaum, 2009; Topiwala et al., 2017; Wilson et al., 2017). Hala ere, oraindik ez da frogatu korrelazio zuzenik alkoholismoa duten subjektuetan gertatzen den oroimen-episdokioaren galeraren eta garuneko Papez-en zirkuituaren narriadura makroskopikoaren artean (Chanraud et al., 2009).

Zerebeloak koordinazio motorrean ez ezik, adikzioaren garapenean eta mantentzean ere parte hartzen du, drogek eragindako oroitzapenak sendotuz (Miquel, 2016). Eta, garun atal gehienetan bezala, bere bolumenean murrizpena ere jasaten du alkoholaren gehiegizko kontsumoaren ondorioz (Cardenas et al., 2007; Sullivan eta Pfefferbaum, 2009). Zerebeloaren egituraren asaldura ezagutza emozionaleko eta sozialeko, prozedura memoria eta ataxiako alterazioekin lotu da (Shanmugarajah et al., 2016; Sullivan eta Pfefferbaum, 2019). Alabaina, alkoholaren Wernicke-Korsakoff sindromea (alkohol gehiegi edatearen ondoriozko tiamina urritasunak eragindakoa) diagnostikatzeko ezaugarrietako bat honako hau da: zerebeloaren atrofia, bolumen-galera eta erresonantzia magnetikoaren bidez aurkitutako Wernicke lesioak (Praharaj et al., 2021).

Azkenik, azpimarratu behar da burmuinaren bolumena murriztea ez dela beti atzeraezina. Hots, abstinentziarekin batera gai grisak bere bolumena handituz doa, erregioaren menpe eta modu ez-linealean, eta horrek, garrantzitsua izan daiteke abstinentzia mantentzeko (Durazzo et al., 2015; Gazdzinski et al., 2005; Nutt et al., 2021; Zou et al., 2018). Nahiz eta gai zuria alkohola edatearen etetearekin ere berreskura daitekeen, badirudi berreskuratze

honek gai grisak baino erraztasun txikiagoa duela (Alhassoon et al., 2012; Cardenas et al., 2007; Pfefferbaum et al., 2014; Segobin et al., 2014).

1.1.5. ALKOHOLISMOAN ERABILTZEKO TRATAMENDU FARMAKOLOGIKOAK

Alkoholismoaren kontrako tratamenduaren helburua da pazienteei edateari uzten laguntzea (abstinentzia) edo kontsumo kaltegarria murriztea, haien osasuna hobetzeko eta abstinentzia sintomak murrizteko. Beste edozein gaixotasun psikiatrikotan bezala, ingurumen-faktoreek zeregin garrantzitsua dute alkoholismoa garatzeko eta mantentzeko. Horregatik, farmakoterapiarekin batera, jokabide-terapia kognitiboak eta motibazio-terapiak bezalako esku-hartze psikosozialak funtsezkoak dira (Ray et al., 2020). Gainera, eragin desiragaitzek eta eskura dauden farmakoen eraginkortasun aldakorrak beharrezkoa egiten dute sendagai seguruagoak eta eraginkorragoak garatzea.

Alkoholismoaren kontrako tratamendu farmakologikoa Europako Sendagaien Agentziak (EMA; *European Medicines Agency*, ingelesez) edo Amerikako Estatu Batuetako (AEB) Elikagaien eta Drogen Administrazioak (FDA; *U.S. Food and Drug Administration*, ingelesez) onartutako lau medikamentuk baino ez dute osatzen gaur egun: disulfirama, akanprosatoa, naltrexona eta nalmefenoa (azken hori EMAk bakarrik onartu du alkoholismoa tratatzeko). Hala ere, beste medikamentu batzuek edatea murriztu eta abstinentzia luzatzen dutela ere frogatu dute (Burnette et al., 2022). Hurrengo paragrafoetan, konposatu aipagarrienak laburki berrikusiko dira.

Disulfirama tratamendu farmakologiko abertsiboa da. Horrek esan nahi du bere ekintza-mekanismoa berrerortzea saihestean oinarritzen dela, etanola kontsumitzean ondorio kaltegarriak eta desatseginak eraginez. Zehazki, disulfiramak ALDH alkoholaren entzima metabolizatzailearen aktibitatea inhibitzen du eta horrek azetaldehido- azetato bihurketa eragozten du. Ondorioz, etanola kontsumitzeak azetaldehidoa organismoan metatzea eragiten du, eta erreakzio desatsegina eragiten du: goragalea, gorakoak, hipotentsioa, takikardia, izerdia eta buruko min larria, besteak beste. Bere erabilerak dituen mugak direla eta (hau da, tratamenduarekiko atxikimendu handia behar da eraginkorra izateko), disulfirama gomendatzen da soilik abstinentzia mantentzeko eta inoiz ez alkoholaren kontsumoa murrizteko (Kranzler eta Soyka, 2018).

Akanprosatoa edo kaltzio N-azetilhomotaurinatuak gizakietan alkoholaren abstinentziak eragindako antsietatea eta desira murrizten ditu, baina tratatutako pazienteen azpimultzo

batek baino ez du lortzen erantzun onena (Ho et al., 2022). Plazeboarekin kontrolatutako hainbat probatan frogatu da akanprosatoa eraginkorra dela alkoholaren berrerortzearen kopurua murrizteko eta abstinentzia-aldia handitzeko (Jonas et al., 2014; Witkiewitz et al., 2012). Bere ekintza-mekanismoa erabat ulertzen ez den arren, badirudi akanprosatoak sistema glutamatergikoaren tonua murrizteko duen gaitasuna inplikatuta dagoela alkoholismoa tratatzeko duen eraginkortasunean (Kalk eta Lingford-Hughes, 2014).

Naltrexona antagonista opioide ez-selektiboa da, eta hartzitzaile μ-opioideentzako afinitate handia aurkezten du; eta, beraz, endorfinak eragindako askapen dopaminergikoa murrizten du sari bidezidor mesolinbikoan (ikus 1.1.4.1.4. atala). Nahiz eta animalia-ereduetan alkoholaren kontsumoa gutxitu eta meta-analisi batean naltrexonarekin tratatutako pazienteek abstinentzia luzeagoa eta berrerortzeko arrisku murriztua ezagutarazi, naltrexonak alkoholaren kontsumoa gutxitzeko neurrizko eragina baino ez duela ematen du (Burnette et al., 2022; Jonas et al., 2014; Swift eta Aston, 2015). Gainera, naltrexonak opioideen abstinentzia sindromea sortarazi dezakeenez, substantzia honekin tratatutako pazienteek opiodeen kontsumoaren monitorizazioa behar dute (Kranzler eta Soyka, 2018).

Nalmefeno beste antagonista opioide bat da, naltrexona baino erdibizitza luzeagoa duena. Hartzaile μ-opioideen antagonista izateaz gain, κ-hartzaileen agonista partziala ere bada. (Soyka et al., 2016; Swift, 2013). Zentro anitzeko hiru saiakuntza klinikok eragin zuten EMAk nalmefeoa onartzea. Ikerketa horiek jakinarazten zuten nalmefenoa eraginkorra zela alkoholaren kontsumoa murrizten, beharrezkoa zenean bakarrik hartzen bazen eta ez modu jarrai batean. Baina haien metodologiak oso kritikatuak izan ziren, nalmefenoaren eragina plazeboarekin konparatzen baitzuten, eta ez naltrexona bezalako zuzeneko konparatzaileekin (Naudet et al., 2016). Naltrexonarekin gertatzen den bezala, opioideak hartzen dituzten pazienteek monitorizazioa behar dute nalmefeno tratamenduarekin (Kranzler eta Soyka, 2018).

Gamma-hidroxibutiratoa (GHB) inhibizio GABAergikoa sustatzen duen sendagai lasaigarria da. Badirudi GHBk alkoholaren eragina imitatzen duela, bere abstinentziaren sintomak eta desira murriztuz. Nahiz eta Europako herrialde batzuetan GBHaren erabilera alkoholismoa tratatzeko onartuta dagoen, abusuzko droga gisa kontsumitzeko duen potentziala bere erabilera paziente zehatzetara mugatzen du (Shen, 2018).

Baklofenoa $GABA_B$ hartzaileen agonista da, espastikotasuna tratatzeko erabilia (Minozzi S et al., 2018). Alkoholismoa baklofenoarekin tratatzeko egindako saiakuntza klinikoek emaitza mistoak erakusten dituzte. Horrela, kontrolatutako eta aleatorizatutako saiakuntza batzuek abstinentzia-tasak handitu zirela adierazi bazuten ere, ikerketa handienak ez zuen ezberdinatsunik aurkitu baklofenoaren eta plazeboaren artean, ziurrenik ikerketa hauetan sartutako subjektuen banakoen arteko aldagarritasun handiagatik (Minozzi S et al., 2018; Witkiewitz et al., 2019) .

Bareniklina hartzaile nikotinikoen agonista partziala da eta bere erabilera nagusia nikotinarekiko menpekotasuna da (King et al., 2022). Erretzaileak diren eta ohiko gehiegizko alkoholaren kontsumoa egiten duten subjektuekin egindako giza ikerketetan, bareniklinaren tratamenduak etanolaren kontsumoa eta desira jaitsi zituen plazeboarekin alderatuta (Hurt et al., 2018; Nocente et al., 2013). Hala ere, beste proba kliniko batean bareniklinkak ez zuen lortu drogen seinaleekin lotutako desira murriztea, plazeboarekin alderatuta (Miranda et al., 2020). Hala eta guztiz ere, badirudi aukera oparoa dela erretzaile astunak diren paziente alkoholikoentzat, albo-ondorio txikiak dituelako (Burnette et al., 2022).

Ondansetron farmako antiemetikoa eta $5\text{-}HT_3$ hartzaileraren antagonista bat da, zeinak alkoholismoaren garapen goiztiarra duten pazienteetan (25 urte baino lehen) eraginkortasuna erakutsi du, batez ere ohiko gehiegizko alkoholaren kontsumoa eta depresioa eta antsietatea (Johnson et al., 2002; Kranzler et al., 2003). Hala ere, orain dela gutxiko saiakuntza kliniko batek ez zuen ondansetronen dosi baxuekin ondorio onuragarririk aurkitu alkoholismoa tratatzeko (Seneviratne et al., 2022). Beraz, beste tratamendu farmakologikoen antzera, froga gehiago behar dira ondansetronek alkoholismoan duen erabilgarritasuna baieztatzeko.

Alkoholismoa tratatzeko antikonbultsibanteak erabiltzea (topiramatoa, gabapentina, karbamazepina, azido balproikoa) tonu glutamatergikoa murrizteko eta transmisio GABAergikoa handitzeko duten gaitasunean oinarritzen da. Era honetan, abstinentzia sintomak blokeatzea du helburu abstinentzia luzatzeko. Hala ere, meta-analisien eta saiakuntza klinikoen ikerketek ez dute ebidentziarik aurkitu konposatu horien eraginkortasunari buruz alkoholismoaren tratamenduan (Palpacuer et al., 2018; Rojo-Mira et al., 2022).

Azkenik, serotonina berrabiarazteko inhibitzaile selektiboak (SSRI) bereziki gomendagarriak dira alkoholismoa duten pazienteek antsietatea edo depresioa bezalako gaitz bat ere dutenean (Gimeno et al., 2017). Nahiz eta SSRI tratamenduarekin etanol gutxiago hartzen dela frogatzen duten ikerketa batzuk egon, kalitate gutxikoak dira (hau da, abstinentzia-egunen indizearen ebidentzia baxua dago, depresioaren larritasunaren, eragin desiragaitzen eta tratamendu etetearen datuak falta dira), eta gehien bat alkoholismoaren depresio-sintomak tratatzera bideratuta daude (Agabio et al., 2018). Era berean, alkoholismoa tratatzeko antipsikotikoen erabileraren eraginkortasuna eskizofrenia duten komorbilitatean bakarrik frogatu da (Ceraso et al., 2020; Kishi et al., 2013). Eta, neurri txikiagoan, oldarkortasun tasa altuak dituzten pazienteetan eraginkorrak dira, abstinentzia mantentzen laguntzeko edo edateko latentzia luzatzeko helburuarekin erabili direlarik (Anton et al., 2017).

1.2. PROTEINA MATRIZELULARRAK

Zelulaz kanpoko matrizea (ZKM) burmuinaren bolumenaren % 20 inguru hartzen du, eta zelula neuronal eta endotelialak inguratzen ditu, euskarri biokimiko eta estrukturala emanez (Nicholson eta Hrabětová, 2017). Neuronek eta zelula glialek sintetizatuta, ZKMa osatzen duten molekulak proteoglikanoak (agrekana, brebikana, adibidez), azido hialuronikoa, proteina fibrosoak (kolagenoak, fibronektina), atxikipen zelularreko molekulak (integrinak, kadherinak) eta glikoproteinak (adibidez, tronbospondinak (TSPak), tenaszinak, SPARC (jariatutako proteina azidoa zisteinan aberastua, baita osteonektina edo BM-40 moduan ezaguna), hevina) **(1.3. irudia)**. ZKMan beste molekula mota batzuk ere aurki daitezke, hala nola hazkuntza-faktoreak, zitokinak edo proteasak, zeinek ZKMko beste molekulekin elkar eragin dezaketen (Song eta Dityatev, 2018). Oso onartua dago ZKMko molekulek garunaren funtzioan zuzenean parte hartzen dutela (Barros et al., 2011), eta badago ZKMko glikoproteinen azpitalde bat, bere ezaugarri bereziengatik garrantzia hartzen ari dena: proteina matrizelularrak alegia.

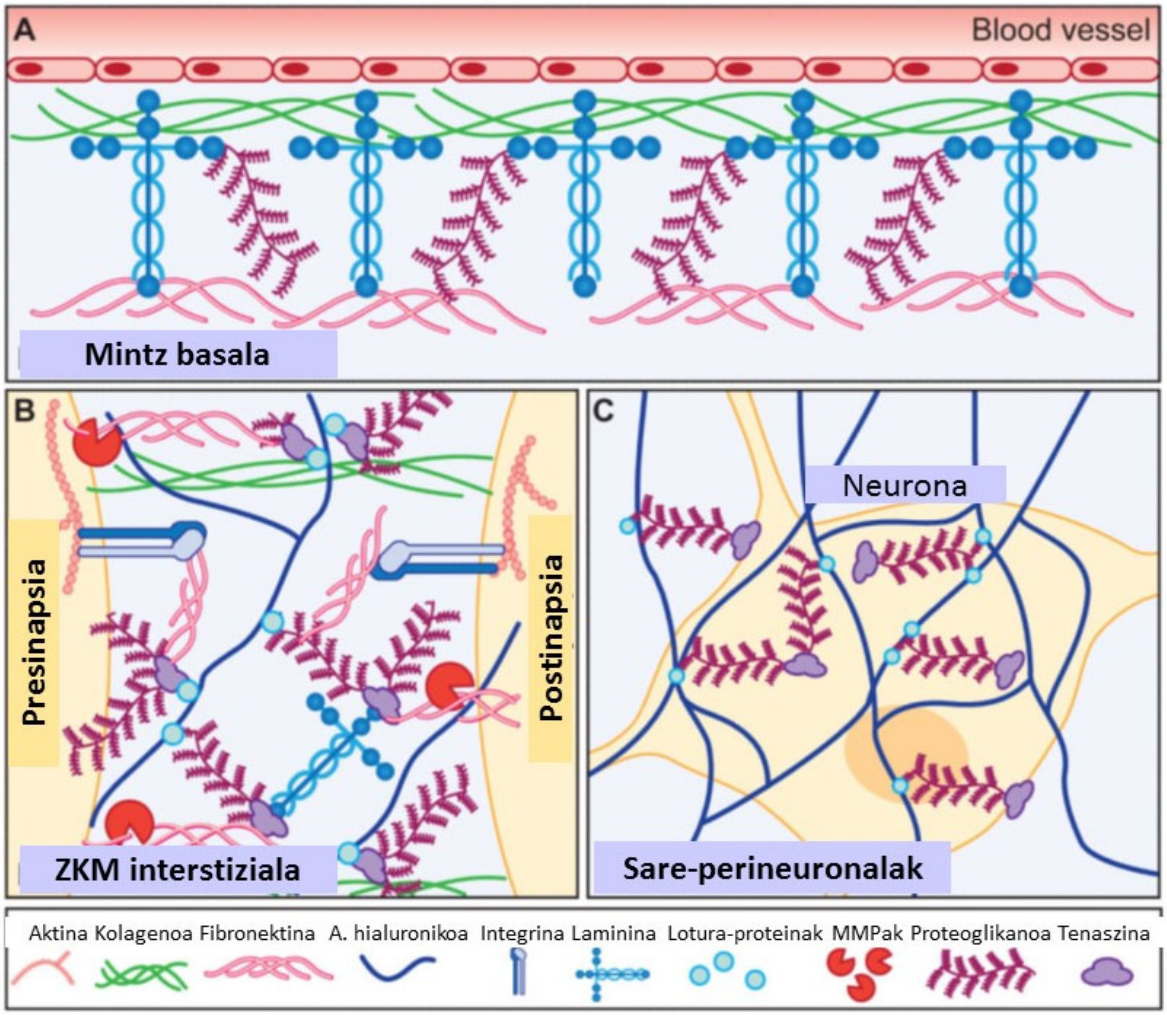

1.3. irudia. Garuneko zelulaz kanpoko matrizearen (ZKM) konpartimentuen eta horien konposizio molekularraren irudikapen eskematikoa. **(A)** Mintz basala, odol-garun mugaren zati bat odol hodien alde basolateralean kokatuta dagoena eta lamininek, fibronektinek, kolagenoek eta proteoglikanoek osatzen dituztena. **(B)** ZKM interstiziala neuronak eta zelula glialak inguratzen ditu garuneko parenkiman eta, aurrekoez gain, matrizearen metaloproteasak (MMP), azido hialuronikoak, tenaszina-R eta lotura-proteinak (agrekana eta brebikana, besteak beste) ere osatzen dute. **(C)** Sare perineuronalak neuronak inguratzen dituzten dentsitate altuko eta sareta itxurako egiturak dira eta proteoglikanoak, azido hialuronikoa, tenaszina-R eta lotura proteinak osatzen dute. ZKMko molekulek elkarren artean eta zelulen gainazaleko molekulekin (adibidez, integrinekin) elkarreragiten dute. *Lasek, 2016-tik moldatua.*

"Matrizelular" kontzeptua Paul Bornstein-ek definitu zuen 1995ean. Bornstein-ek ZKMko glikoproteinen talde berezi hori kontzeptualizatu eta definitzeko beharra ikusi zuen, zeren eta berak egiaztatu zuen glikoproteina haietako batzuek funtzio biologiko konplexuen bidez zelulen jardueran zuzenean eragiten ziotela eta gainerako ZKMko proteinen ezaugarriekin bat ez zetozen (Bornstein, 1995). Proteina matrizelularrak biltzen eta bereizten dituzten ezaugarriak berrikusi egiten dira hurrengo artikuluetan: Bornstein (2009a), Bornstein eta Sage, (2002), Murphy-Ullrich eta Sage (2014); eta honela laburbil daitezke: 1) ZKMko molekulek ez< bezala, ez dute egitura-funtziorik, baizik eta zelula-zelula eta zelula-ZKM

interakzioak modulatzen dituzte, 2) propietate desitsaskorrak dituzte, 3) ZKMko hazkuntza-faktoreekin, zelulen gainazaleko hartzaileekin, zitokinekin eta proteasekin elkarreragiten dute zelulen jarduera modulatzeko **(1.5 irudia)**, 4) beraien espresioa zelulen ingurunearen arabera aldatzen da, eta oso altua da garapenean zehar eta lesio edo gaixotasun baten ondorioz.

Hasiera batean matrizelulartzat hartzen ziren proteina bakarrak TSP-1, SPARC eta tenaszin-C ziren. Hala ere, pixkanaka-pixkanaka, izendapen matrizelularreko baldintzak betetzen dituzten molekula gehiago aurkitu dira, hala nola TSP-2, SPARC familiako beste kide batzuk (hau da, hevin (SPARCL1 edo SC1), glipikanak, CCN (cyr61-CTGF-NOV), galektinak eta autotaxina) (Jayakumar et al., 2017; Sage eta Bornstein, 1991). Doktorego Tesi honek hevina proteina du ardatz, beste proteina matrizelularretatik bereizten dituen zenbait propietate dituena (ikus 1.2.2.4 atala).

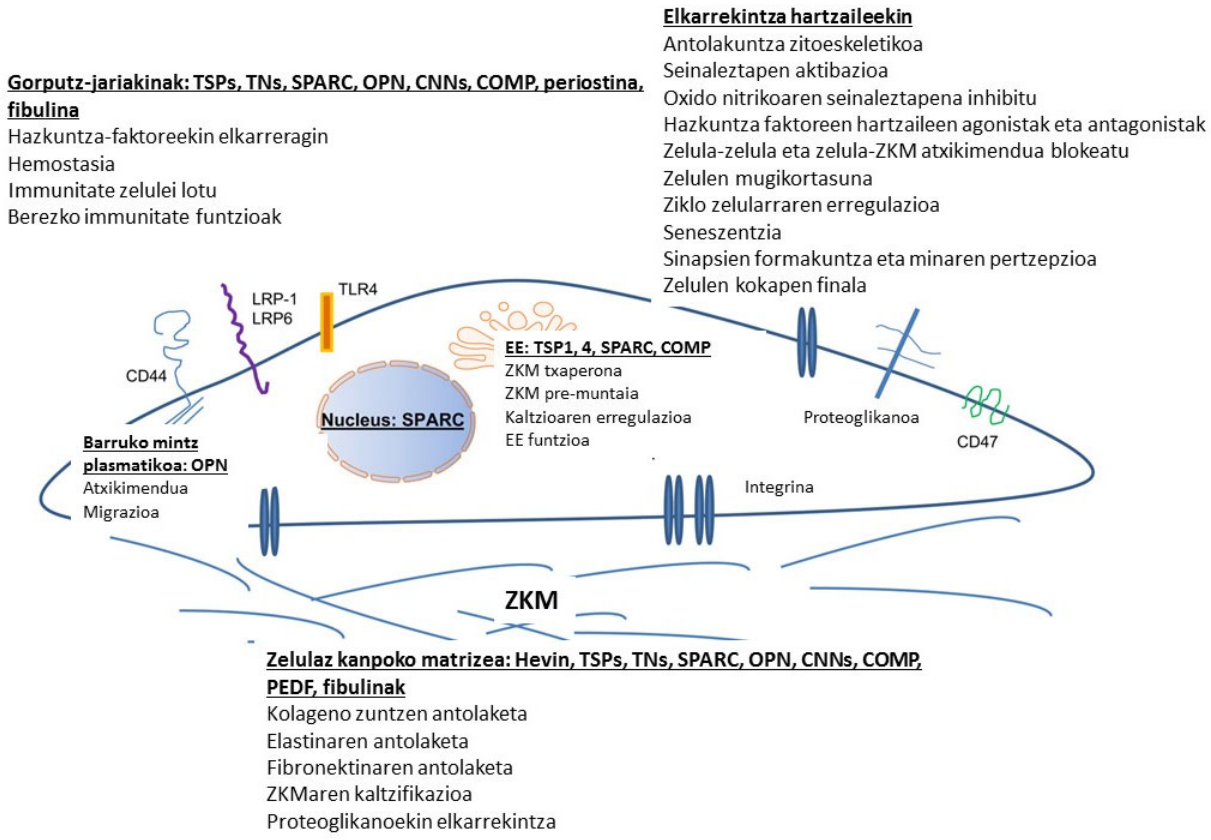

1.4. irudia. Proteina matrizelularren zenbait funtzio erakusten duen irudikapen eskematikoa. Funtzio horiek zelula barneko edo kanpoko kokapenaren eta beste molekulekin (zelulaz kanpoko matrizeko (ZKM) molekulak, gorputz jariakinetako molekulak, zelula hartzaileak, barruko mintz plasmatikoan edo erretikulu endoplasmatikoan (ER) dauden molekulak) duten elkarreraginaren arabera erakusten dira. CCN, cyr61-CTGF-NOV; COMP, kartilagoaren proteina oligomerikoa (edo baita TSP-5); OPN, osteopontina; SPARC, jariatutako proteina azidoa zisteinan aberastua; TN, tenaszina; TSP, tronbospondina. *Murphy-Ullrich eta Sage, 2014-tik moldatua*.

1.2.1. PROTEINA MATRIZELULARRAK PLASTIKOTASUN SINAPTIKOAREN BITARTEKARI GISA

Lehen esan bezala, proteina matrizelularrek zelulak modulatzen dituzte itu molekularrekin duten elkarrekintzaren bidez. Horrela, garunean, plastikotasun sinaptikoa modulatzen dute neuronekin eta zelula glialekin elkareraginez. Atal honetan proteina matrizelular indibidualen deskribapen labur bat egiten da, hevinarena izan ezik, Doktorego Tesi honen intereseko proteina delako, 1.2.2 atalean luze deskribatuko da eta.

SPARC proteina kaltzioari eta kolagenoari lotzen zaio, garapenean adierazten da gehienbat eta funtzioa anti-sinaptogenikoa du (Kucukdereli et al., 2011). β3-integrina konplexuen bidezko elkarreginaren bidez, SPARCek AMPA hartzaileen egonkortzea sinapsietan inhibitzen du, eta horrela transmisio kitzikagarria kontrolatzen du sinapsi helduetan (Jones et al., 2011). Garapen garaian, SPARC sinapsien ezabatzea sustatzen du neurona kolinergikoetan, zirkuitu neuronalen funtzioa fintzeko (López-Murcia et al., 2015). Gainera, SPARCek zelula-ZKM elkarrekintza, hazkuntza-faktoreen seinaleztapena eta zelulen migrazioa, atxikipena eta ugalketa ere erregulatzen ditu (Brekken eta Sage, 2001; Murphy-Ullrich, 2001).

Zelula endotelialen ugalketa eta migrazioa inhibitzeko duten gaitasunaren ondorioz, TSPak antiangiogeniko gisa definitu izan dira normalean, baina horrez gain ZKMko molekulekin eta zelulen gainazaleko hartzaileekin ere elkarreragiten dute garatzen ari den garunean sinapsiak sortzen laguntzeko (Bornstein, 2009b; Christopherson et al., 2005; Eroglu et al., 2009; Xu et al., 2010). Hala ere, sinapsi hauek presinaptikoki aktiboak dira, baina postsinaptikoki isilak, mintz postsinaptikoan duten glutamatoaren AMPA hartzaileen faltagatik; eta beraz, horrek adierazten du heltze sinaptikoa erregulatzen duten beste faktore batzuk egon behar direla (Christopherson et al., 2005; Eroglu et al., 2009). Gainera, hipokanpoko neurona gazteen kulturetan TSP-1 sinapsi kitzikagarriak sortzeko gai da, baina TSPek seinale kitzikagarriak gutxitzen dituztela ere jakinarazi da, sinapsian AMPA hartzaileen metaketaren inhibizioagatik eta glizina-hartzaile inhibitzaileen handipenagatik (Hennekinne et al., 2013; Xu et al., 2010). TSPek zelula barneko muskelina proteinarekin interakzionatzen dute aktina zitoeskeletoaren organizazioan eraginez (Adams et al., 1998). Hori dela eta, morfologia sinaptikoa erregulatu dezaketela ere iradoki da (Adams et al., 1998; Risher eta Eroglu, 2012).

Tenaszina-C garunaren garapena ematen den bitartean adierazten da nagusiki (Bartsch et al., 1992; Ferhat et al., 1996; Irintchev et al., 2005). Šekeljić eta Andjus 2012-ko lanean berrikusten den moduan, tenaszina-C-ren knock-out saguek aktibitate neuronal hondatua erakutsi zuten proteinaren gabezia zegoen garun ataletan. Horrek, aldi berean, iradokitzen du tenaszina-C plastikotasun sinaptikoan parte hartzen duela, L-motako Ca^{2+} tentsioaren menpeko erretenekiko (*L-type* Ca^{2+} *voltage-dependent channels* (L-VDCC), ingelesez) elkarrekintzaren eta ondorengo zelula barneko Ca^{2+} postsinaptikoaren kontzentrazioaren igoeraren bidez (Šekeljić eta Andjus, 2012). Gainera, tenaszina-C-k neurona-glia interakzioetan parte hartzen du hazkunde axonalean eta beraien orientazioa eta garapenean zehar ematen den migrazio neuronala erregulatzeko (Jones eta Bouvier, 2014-an berrikusia)

Glipikanak sinapsiak antolatzen dituzten proteinak dira, zehazki, itsaskortasun sinaptikoa, heldutasuna eta plastikotasuna eta bisorkuntza axonala erregulatzen dituztenak (Kamimura eta Maeda, 2021; Miyata eta Kitagawa, 2017). Glipikanek sinapsi kitzikagarri postsinaptiko aktiboen formakuntza sustatzen dute, AMPA hartzailearen GluA1 azpiunitatea handituz eta, beraz, baita gertaera sinaptiko glutamatergikoen maiztasuna eta anplitudea ere (Allen et al., 2012).

CCN familiako osagai batzuk zenbait nahasmendu neurologikoetan aldatuta daudela dirudien arren (adibidez Alzheimerren gaixotasunean, albo-esklerosi amiotrofikoan edo garuneko traumatismoan), oraindik ez dago argi zein den haien funtzio zehatza (Malik et al., 2015). Adibidez, CCN1-aren mRNA-ren adierazpena handitu egiten da hartzaile azetilkoliniko muskarinikoak estimulatzen direnean eta ikasketa eta oroimen prozesuetako plastikotasun sinaptiko kolinergikoarekin lotu da (Albrecht et al., 2000). Bestetik, CCN3-ak oligodendrozitoen diferentziazioa eta mielinazioa bultzatzen dituela ematen du (de la Vega Gallardo et al., 2019).

1.2.2. HEVIN, PROTEINA MATRIZELULARRA

1.2.2.1. Egitura molekularra

Hevin (SPARC-like 1, SC1 edo MAST9 bezala ere ezaguna) 664 aminoazidoko glikoproteina bat da, gutxi gorabeherako 71 kDa-eko pisu molekularra duena. Egiturari dagokionez, seinale-peptidoak, N-terminal domeinu azidoak, folistatina-antzeko (FS) domeinuak eta

zelulaz kanpoko kaltzioari lotzeko (EC) domeinuak C-terminalean osatzen dute (Bendik et al., 1998; Girard eta Springer, 1995; Hambrock et al., 2003) **(1.5. irudia)**.

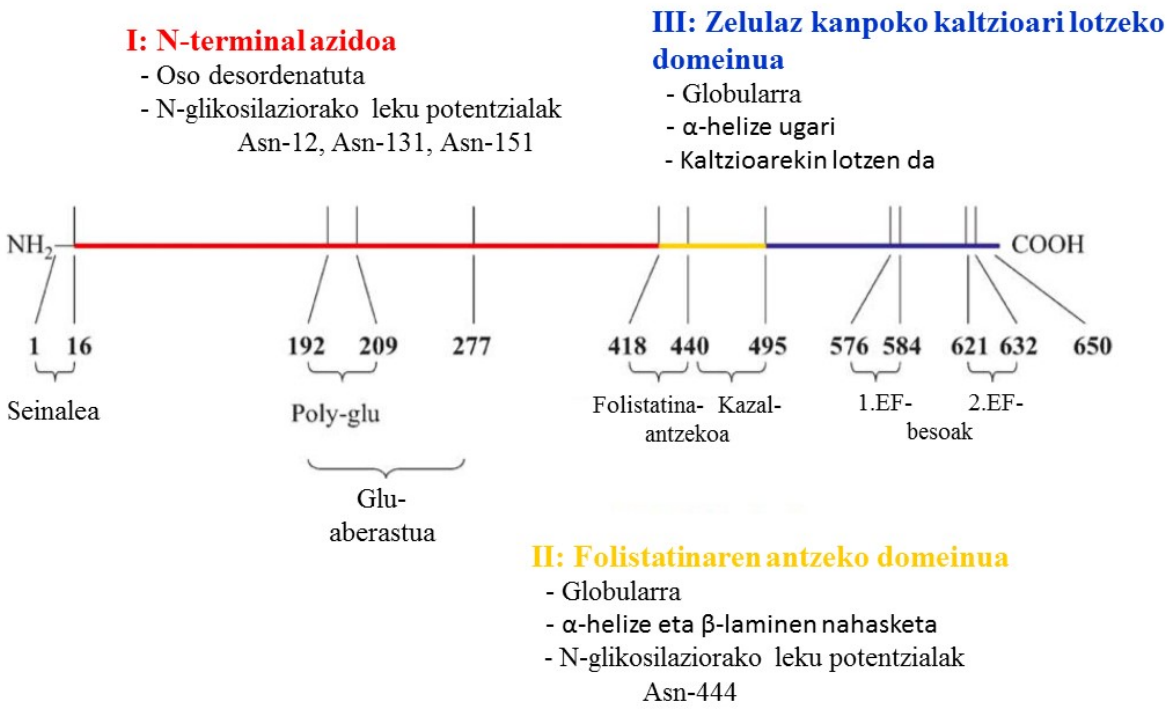

1.5. irudia. Hevinen egitura proteikoa erakusten duen irudi eskematikoa, non N-terminal domeinu azidoa, folistatinaren antzeko (FS) domeinua eta zelulaz kanpoko kaltzioari lotzeko (EC) domeinua erakusten diren, N-glikosilaziorako toki potentzialekin. *Sullivan eta Sage, 2004-tik moldatua*.

SPARC proteinaren antzeko egitura duenez, hevin proteinak SPARC -like 1 moduan ere izendatzen da. Izan ere, biek oso kontserbatuta dagoen EC domeinuaren % 62ko sekuentzia eta FS domeinuaren sekuentziaren % 56koa partekatzen dute (Fan et al., 2021; Girard eta Springer, 1995). Bi proteinetan FS domeinuak egituraz antzekoak diren bitartean, EC domeinuek alde handiak dituzte. Ezberdintasun horien ondorioz, FS-EC tandem-aren interfazea txikiagoa da hevinean, FS domeinua EC domeinutik urrunduta dagoelarik (Fan et al., 2021). FS domeinuak epidermiseko hazkuntza faktorearen (EGF edo *epidermal growth factor,* ingelesez) antzeko errepikapen bat eta Kazal domeinuak osatzen dute, hevin proteinaren zisteina hondar gehienak ditu, bi Cu^{2+}-loturarako tokiak ditu eta N-lotutako karbohidrato konplexu bat (Fan et al., 2021; Yan eta Sage, 1999). Horrez gain, eskualde horretan N-glikosilazioareko hainbat toki proposatu dira (Asn-444) (Girard eta Springer, 1995; Hambrock et al., 2003). FS domeinuak neurexina eta neuroligina atxikipen zelularreko proteinei lotzen zaie, azkenengo honi kaltzioaren menpeko erreakizoaren bidez, eta beraz, domeinu hau funtsezkoa da neurexina-neuroligina zubi transsinaptikoak sortzeko

(Fan et al., 2021; Singh et al., 2016). EC domeinua α-helikoidala da eta bi EF-beso ditu (1. EF-besoa: His^{586}-Ala^{618} eta 2. EF-besoa: His^{625}-Phe^{651} amino azidoak gizakietan; 1. EF-besoa: His^{572}-Ala^{604} eta 2. EF-besoa: His^{611}-Phe^{637} amino azidoak saguetan) eta kaltzioaren menpeko eta kontzentrazio txikiko afinitatetarekin I eta V kolagenoei lotzen dela ikusi izan da orain dela gutxi, SPARC proteinak kolagenoekin duen elkarrekintza antzeko batekin (Fan et al., 2021; Hambrock et al., 2003; Maurer et al., 1995). EF-besoak beharrezkoak dira hevin proteina zuzen tolesteko eta bere garraiorako erretikulu endoplasmatikotik zelulaz kanpoko matrizeraino (Taketomi et al., 2022). Azkenik, duela gutxi aurkitu da hevinaren C-terminalak (FS-EC tandem domeinuak barne) interakzioan diharduela kaltzion izeneko (*calcyon*, ingelesez) neuronentzako espezifikoa den proteina besikular baten N-terminalarekin, burmuineko lesioen ondoren ematen den sinapsien berreskurapenean parte hartuz (ikus 1.2.2.3. atala) (Kim et al., 2021b).

Hevinean N-terminala gutxien kontserbatutako eremua da eta kaltzioarekin elkarreragiten du α-helizeak dauden eskualdeak egonkortzeko (Brekken eta Sage, 2001). N-glikosilazio potentzialeko gune batzuk proposatu dira domeinu honetan (Asn- 12, Asn-131, Asn-151), baita O-glikosilazio posibleak ere (Girard eta Springer, 1995; Halim et al., 2013; Hambrock et al., 2003). Gainera, eremu hau hevinen funtzio sinaptogenikoan parte har dezakeela postulatu da, hevinek eragindako sinaptogenesia antagonizatzen duten bi proteinek eremu hau ez daukatelako; zehazki, SPARC proteina eta SPARC-antzeko fragmentua (SLF edo *SPARC-Like fragment*, ingelesez) (hevinen proteolisi produktua dena) dira proteina horiek (Fan et al., 2021; Kucukdereli et al., 2011).

1.2.2.2. Kokalekua

Hevin proteina matrizelularra hainbat ehunetan eta zelula-motatan adierazten da. Garapen garaian hevin gizakietan eta karraskarietan detektatzen da. Gizakietan garunean, heste mehe eta handietan, biriketan, gibelean, pankrean eta hestegorrian adierazten da (Klingler et al., 2020; Mongrédien et al., 2019; Strunz et al., 2019). Eta karraskarietan garunean, hestean, pankrean, erretinan, bihotzean, guruin adrenaletan, epididimoan eta biriketan adierazten da, eta maila baxuetan giltzurrunean (Girard et al., 1999; Johnston et al., 1990; Klingler et al., 2020; Kucukdereli et al., 2011; Lloyd-Burton eta Roskams, 2012; Mendis, 1996a, 1996b; Mothe eta Brown, 2000; Soderling et al., 1997).

Proteina matrizelular gehienak garunaren garapenean adierazten diren bitartean, hevin oso adierazia dago karraskarien garun helduetan (Eroglu, 2009; Johnston et al., 1990; Kucukdereli et al., 2011; Lively et al., 2007b; Lloyd-Burton eta Roskams, 2012; Weaver et al., 2011; Weaver et al., 2010). Hevin saguen garun atal guztietan aurkitzen da, bere adierazpen astrozitiko altuagatik eta neurona mota ezberdinetan duen espresioagatik, bereziki neurona parbalbumina-positibo GABAergikoetan eta baita beste azpimota neuronal batzuetan ere adierazten da: zenbait neurona glutamatergiko eta zerebeloaren Bergmann glian (Mendis, 1996a; Mongrédien et al., 2019). Gainera, mikroskopia elektronikoak eta irudi konfokalak hevin aurkitu dute sinapsien inguruko prozesu astrozitikoetan, mintz postsinaptikoetan eta garun karraskari helduen zirrikitu sinaptiko kitzikagarrietan (Johnston et al., 1990; Jones et al., 2011; Kucukdereli et al., 2011; Lively et al., 2007b; eta Brown, 2008a; Risher et al., 2014; Singh et al., 2016; Weaver et al., 2010).

Hevin gizaki helduen LZRan eta garunean ere detektatzen da, zehazki kortex aurrefrontalean, nukleo kaudatuan, garun-enborrean eta gongoil sentsorialen neuronetan (Halim et al., 2013; Hashimoto et al., 2016; Mongrédien et al., 2019; Nilsson et al., 2009; Yin et al., 2009). Garrantzitsua da saguaren eta giza garun helduaren arteko konparazioak agerian utzi duela hevinarentzako antzeko zelula-adierazpena bietan (Mongrédien et al., 2019; Weaver et al., 2011). Eta beraz, horrek hevin proteina aztertzeko animalia-ereduak erabil daitezkeela iradokitzen du.

Azkenik, hevin hainbat tumoretan ere adierazten da (hau da, meningiometan, biriketako minbizi ez-zelularrean, kartzinoma gastrikoan eta prostatako eta koloneko kartzinometan), ehun konektiboan eta muskulu eskeletikoan, non lotune neuromuskularrean aurkitzen den (Bendik et al., 1998; Brayman et al., 2021; Brekken et al., 2004; Dalan et al., 2017; Gagliardi et al., 2017; Nelson et al., 1998; Ringuette et al., 1998).

1.2.2.3. Funtzioak

Hevinek sinapsi kortikal eta talamokortikal kitzikatzaileen eraketa eta mantentzea sustatzen du (Espírito-Santo et al., 2021; Gan eta Südhof, 2019, 2020; Kim et al., 2021b; Kucukdereli et al., 2011; Risher et al., 2014; Singh et al., 2016). Hevinen gaitasuna sinapsi kitzikatzaileak induzitzeko bi mekanismo ezberdinetan oinarritzen da gutxienez.

Lehena Singh et. al. -ek deskribatu zuen 2016an. Lehen esan bezala, hevinek konexio talamokortikal kitzikagarriak sustatzen eta egonkortzen ditu zubi transsinaptiko bat eratuz,

zeinak neurexin-1α presinaptikoaren eta neuroligin-1B postsinaptikoaren loturaz osatuta dago (Singh et al., 2016). Zubi transsinpatiko horrek NMDA hartzaileen erreklutamendua eta horien funtzioa areagotzen ditu, ziurrenik neuroliginekin duten elkarreraginaren bidez (Singh et al., 2016).

Bigarren mekanismoak, Gan eta Südhof-ek 2020an deskribatu berri duenak, iradokitzen du hevinek sinaptogenesi kitzikagarria sustatzen duela neurexina/neuroligina loturak aparteko eran (Gan eta Südhof, 2020). Handik gutxira, 2021ean Fan et.al., hevinaren C-terminalak neurexinekin zein neuroliginekin elkarreragiten duela frogatu zuen, hevinak aipatutako bi mekanismoen bidez sinaptogenesi kitzikagarria bultza dezakeela baieztatuz, neurexinen eta neuroliginen mekanismo independentea erabat ulertzen ez den arren. Era berean, hevin hurrengo proteinekin lehiatzen dela ere frogatu zuten: 1) neuroliginei lotzeagatik glikosilfosfatidilillinositol proteina duen MAM (meprin, A5 proteina, PTPm) domeinua (edo MDGA) izeneko proteina sinaptiko antolatzaile batekin lehiatzen da, MDGAk neurexina-neuroligina zubi transsinaptikoak ezegonkortzen ditu; eta 2) hevinek SPARCarekin (eragin sinaptogenikorik ez duena) lehiatzen da neurexinaren eta neuroliginaren loturagatik (Fan et al., 2021). Hori dela eta, proposatu da hevin jariatzen dela neurexinen eta neuroliginen lotura sustatzeko ez ezik, SPARC eta MDGA proteina inhibitzaileak blokeatzeko ere (Fan et al., 2021; Kucukdereli et al., 2011). Gainera, 1.2.2.1 atalean esan bezala, hevin V kolagenoarekin lotzen da neurexinaren eta neuroliginaren bestelako lekuetan. Ematen du hevin eta V kolagenoaren arteko elkarrekintza neurexina-neuroligina zubi transsinaptikoak ZKMko toki egokira ainguratzea duela helburu, zubien lokalizazioa eta antolaketa erregulatuz (Ramirez et al., 2021) **(1.6. irudia)**.

Garrantzitsua da hevinek selektiboki sustatzen dituela konexio kitzikagarri funtzionalak, baina ez duela inhibitzaileetan eragiten; eta transmisio kitzikagarriak baina ez inhibitzaileak potentziatzeko gai ere bada, batez ere NMDA hartzailearen adierazpena eta erantzunak areagotuz (Gan eta Südhof, 2020). Gainera, hevinek sinapsiaren eraketa eta AMPA hartzaileen dentsitatea handitzen ditu neurona kortikaletan, neuronentzako espezifikoa den kaltzion proteina besikularren bidezko AMPA hartzaileen barneratzaea ostopatuz (Kim et al., 2021b) **(1.6. irudia)**. Lehen esan bezala, hevinen produktu proteolitikoak, SLF zatiak, luzera osoko hevinen funtzio sinaptogenikoa antagonizatzen duela dirudi, ziurrenik sinaptogeniesia erregulatzeko helburuarekin (Kucukdereli et al., 2011). Horrez gain, hevinek kontaktu kitzikagarri anizkoitzeko adarren (*spines with multiple excitatory contacts (SMECs)*,

ingelesez) eliminazioa kontrolatzen du garapenean zehar (Risher et al., 2014). Prozesu hori beharrezkoa da adar dendritikoen garapen egokia eta egonkortze sinaptikoa behar bezala emateko (Risher et al., 2014).

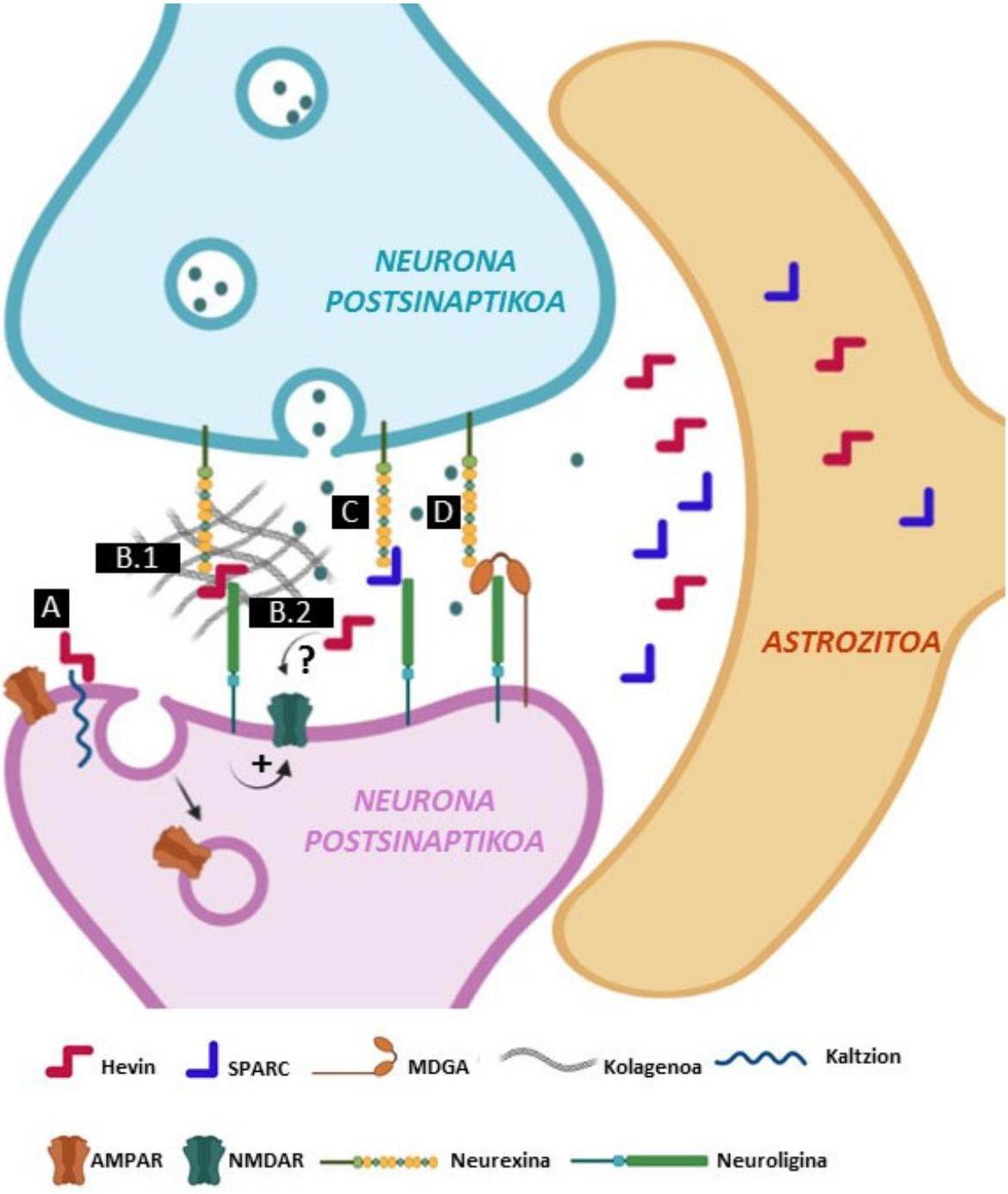

1.6. irudia. Hevinek sinapsi kitzikatzaileetan dituen funtzioak erakusten dituen irudikapen eskematikoa. (A) Hevin kaltzion proteinari lotzen da AMPA hartzailearen (AMPAR) barneraketa blokeatuz, beraien espresioa mintz postsinaptikoetan handiagotuz. **(B)** Hevinek sinaptogenesia eta NMDA hartzaileen (NMDAR) errekrutatzea induzitzen du bi mekanismoen bidez: 1) neurexina-neuroligina zubi transsinaptikoen menpekoa (B.1), 2) neurexina-neuroligina zubien aparteko mekanismoa (B.2). Hevinen eta kolageno V-aren arteko elkarrekintzak neurexina-neuroligina zubiak egonkortu eta ZKMra ainguratzen ditu (B.1). **(C)** SPARC eta MDGA hevinekin lehiatzen dira neurexinaren eta neuroliginaren loturarengatik, hevinen efektu sinaptogenikoa ostopatuz.

Hevin proteina anti-itsasgarria da, zelulen migrazioa modulatzen duena. Horrela, garatzen ari den garun-kortexean zelula glial erradialen migrazio neuronala gelditzeko seinale gisa funtzionatzen du, neuronak garuneko geruza zuzenera bideratuz (Gongidi et al., 2004). Era berean, garatzen ari den zerebeloan hevinen mRNAn Bergmann zelula glialetan adierazten da eta proteina zuntz erradialei atxikitzen zaie zelula granularren migrazioan bitaterkotzeko (Mendis et al., 1994). Hevinek zelula endotelialen atxikimendu fokala mintz basaletan inhibitzen du ere (Girard eta Springer, 1996).

Lehen esan bezala, hevin tumore askotan adierazten da, eta horietako batzuetan bere espresioa murriztuta dago. Ematen du hevinen adierazpen murriztuak prostatako metastasian tumore-zelula endoteliorekiko atxikimendua sustatzeko eta, beraz, zelulen migrazioa amaitzeko beharraren ondorioa dela (Hurley et al., 2012; Nelson et al., 1998). Ehun batzuetan hevinek zelulen ugaritzea oztopatzen eta zelulen zikloa inhibitzen badu ere, beste batzuetan (hau da, zelula linfoideak) zelulen ugalketa sustatzen du (Claeskens et al., 2000; Framson eta Sage, 2004; Oritani et al., 1997). Horrela, hevinek tumore supresorea edo faktore onkogeniko gisa joka lezake tumore motaren arabera (Gagliardi et al., 2017). Adibidez, adenokartzinoma gastrikoan hevinen adierazpenaren murrizketa bere tumoreak suprimitzeko funtzioen inaktibazioarekin erlazionatu da (Jakharia et al., 2016). Funtzio kontraesankor hori hevinak ehun motaren arabera hartzaile ezberdinekin elkarreragiteko duen gaitasunagatik azal daiteke (Sullivan eta Sage, 2004). Gainera, egiaztatu da hevina antiangiogenikoa dela, odol-hodien morfologia eta osotasuna sustatzen dituela, eta kanpoko matrize dermikoaren egitura modulatzen duela kolageno zuntz-muntaketaren erregulazioaren bidez (Regensburger et al., 2021; Sullivan et al., 2006).

1.2.2.4. Hevinen papera gaitz neuropsikiatrikoetan

Gero eta ikerketa gehiagok nabarmentzen dute astrozitoen papera alkoholismoaren garapenean, funtzionalki promiskuoak diren zelula glial horiek sinapsietan duten funtsezko funtzioa dela eta (Allen eta Eroglu, 2017). Izan ere, duela gutxi frogatu da astrozitoek, ATP eta adenosina askatuz, etanolak eragiten duen neuronen zelulaz barneko kaltzio kontzentrazioaren areagotzea sustatzen dutela (Kim et al., 2021a). Gainera, astrozitoen aktibazioak etanolaren kontsumoa areagotzen du eta dosi baxuetan hiperlokomozioa eta dosi altuetan efektu lasaigarriak bultzatzen ditu (Erickson et al., 2021).

Horrela, frogatuta geratu da jariatutako faktore astrozitikoek, hala nola proteina matrizelularrek, helduen plastikotasun neuronalean parte hartzen dutela gaixotasun psikiatrikoetan, adikzioen gaitzak barne (Lacagnina et al., 2017; Nagai et al., 2019; Walker et al., 2020; Wang et al., 2021). Proteina-familia hau alkoholismoaren jaio aurreko eta jaio osteko animalia-ereduetan alteratuta dago (Miguel-Hidalgo, 2018; Trindade et al., 2016). Zehazki, frogatu egin da etanolarekiko esposizioak jaio aurretik (in utero) astrozitoen fenotipoa biziki aldatzen duela eta hevin proteinaren adierazpena eragiten duela. Horrek iradokitzen du alkoholak hevinen espresioa aldatu dezakeela eta, beraz, hevinek alkoholismoaren plastikotasun neuronalean inplikatuta egon daitekeela (Trindade et al., 2016).

Hevin beste gaitz psikiatriko eta neurogarapenekoekin ere lotu izan da. Adibidez, saguen estresarekiko portaeraren egokitzapenari buruzko ikerketa batean, hevinen espresioa eragin zen sagu erresilienteen accumbens nukleoan eta birus-transgenesiaren bidezko hevinen gainespresioa alderantzikatu egin zuen mehatxu-sozialaren (*social defeat,* ingelesez) efektuak saguetan, antidepresore-moduan jokatuz (Vialou et al., 2010).

Postmortem garuneko laginetan egindako ikerketa batek, “cDNA microarray” teknologia erabiliz, hevin genearen gainadierazpenaren berri eman zuen autismoaren espektroaren gaitza (AEG) zuten subjektuetan (Purcell et al., 2001). Mutazioak, polimorfismoak eta kopien kopuruaren aldaketak (CNV edo *copy number variation*s, ingelesez) hevin genean AEG-ren eta eskizofreniaren gaineko ikerketetan ere aurkitu dira (De Rubeis et al., 2014; Jacquemont et al., 2006; Kähler et al., 2008). Gainera, neurexinen eta neuroliginen mutazioak ere aurkitu dira AEGn, zeinek hevinen mutazioekin batera, iradokitzen dute hevinez osatutako zubi transsinaptikoek zeregin garrantzitsua izan ditzaketela patologia honetan (De Rubeis et al., 2014). Konexio talamokortikalek ere alterazioak erakusten dituzte AEGn, hipotesi hau bermatuz (Nair et al., 2013). Era berean, orain dela gutxiko lan batek erakusten du *SPARCL1* genearen mutazioetako batek, EF-besoaren motiboa falta duen hevinentzat kodifikatzen duenak, hevina erretikulu endoplasmatikoan metatzea eragiten duela (Taketomi et al., 2022). Eta horrek, hevinen jariaketa kaltzen du eta txarto tolestutako proteinen erantzunak aktibatzea eragiten du (Taketomi et al., 2022). Hevinen alterazioak erakusten dituen beste neurogarapenako gaitz bat Fragile X sindromea da, non hevin proteinaren adierazpenaren erregulazio okerra deskribatu da, garun atal espezifikotasunarekin (Wallingford et al., 2017).

Hevin, halaber, neuroendekapenezko gaitzen biomarkatzaile potentzial gisa ere hartu da, kontrolekin konparatuta haren adierazpena aldatu egiten delako hurrengo gaixotasunak dituzten banakoen LZRan: narriadura kognitibo arina, albo-esklerosi amiotrofikoa eta Parkinsonen eta Alzheimerren gaixotasunak (Collins et al., 2015; Strunz et al., 2019; Vafadar-Isfahani et al., 2012; Yin et al., 2009). Izan ere, Alzheimerren gaixotasuna duten pazienteetan, hevin genearen bi nukleotido bakarreko polimorfismo gaixotasunaren progresioaren azelerazioarekin erlazionatu dira (Seddighi et al., 2018).

Horretaz gain, garun helduan duen funtzio fisiologikoa aztertu da batez ere garuneko gaixotasunen animalia ereduetan, hala nola, garuneko lesioa, infartu iskemikoa eta epilepsia. Zehazki, hevinen adierazpena astrozito erreaktiboetan indartzen da infartu iskemikoaren edo karraskari helduen garuneko lesio lokalizatuaren ondoren, ziurrenik heriotza neuronala konpentsatzeko (Lively et al., 2011; Lively eta Brown, 2007a; McKinnon eta Margolskee, 1996; Mendis, 1996a; Mendis et al., 2000). Era berean, hevin-kaltzion elkarrekintzak, garun helduaren lesio baten ondoren, antolaketa eta berreskurapen sinaptikoan parte hartzen du, zeinetan matrizeko metaloproteasa-3k (MMP-3) ere inplikatuta dago (Kim et al., 2021b).

2. HIPOTESIA ETA HELBURUAK

HIPOTESIA

Hevinek plastikotasun estrukturalean eta sinaptikoan duen funtzioa kontutan izanda, bere espresioaren alterazioa alkoholismoarekin lotutako plastikotasun neuronalaren aldaketetan parte har zezakeen. Hori dela eta, hevin proteinak alkoholismoaren fisiopatologiarekin nahastuta egon liteke eta, beraz, patologia honen prebentzio, diagnostiko eta tratamendurako itu berria izan liteke.

Hipotesi hori frogatzeko hurrengo helburuak ezarri egin ziren:

HELBURUAK

1) Hevin proteinaren adierazpena karakterizatzea kontrol-subjektuetatik abiatutako giza ehunean.
2) Hevinen mRNA-ren eta proteinaren adierazpena alkoholismoa zuten subjektuen eta subjektu-kontrolen artean konparatzea postmortem giza garunean.
3) Etanolaren administrazioak hevin proteinaren adierazpenean dituen ondorioak aztertzea saguen garunean eta plasman.
4) Saguen accumbens nukleoaren astrozitoetan hevinaren adierazpena jaisteak alkoholaren kontsumoaren gain dauzkan ondorioak aztertzea.

3. SUBJEKTUAK, MATERIALAK ETA METODOAK

3.1. GIZA LAGINAK

3.1.1. GARUNEKO ETA LIKIDO ZEFALORRAKIDEOKO POSTMORTEM LAGINAK

Giza laginak Auzitegi Medikuntzako Euskal Institutuan (Bilbo, Espainia) egindako autopsietatik lortu ziren, 1999. eta 2019. urteen artean. Lan hau postmortem giza laginekin ikertzeko Espainiak duen lege-politika eta berrikuspen etikoko kontseiluei jarraituz egin zen.

Heriotza baieztatu eta berehala, gorpua 4 °C-tan gorde zen. Garuneko disekzioak autopsiarekin batera egin ziren kortex aurrefrontala, hipokanpoa, nukleo kaudatua eta zerebeloko laginak biltzeko, eta berehala -70 °C-tan gorde ziren, esperimentua egin arte. Likido zefalorrakideoko (LZR) laginak ere autopsian lortu ziren, eta -70 °C-tan gorde ziren, esperimentua egin arte. Subjektu guztien odol-laginak ere hartu ziren, beraien azterketa toxikologikoa egiteko Auzitegi Medikuntzako Euskal Institutuan eta Toxikologiako Institutu Nazionalean (Madril). Horrela, estandarizatutako hainbat metodo erabiliz (adibidez, erradioimmunoentsegua, immunoentsegu entzimatikoa, errendimendu handiko kromatografia likidoa eta gas kromatografia-masa-espektrometroa) heriotzaren unean etanola, antidepresiboak, antipsikotikoak eta beste psikofarmako batzuren odol-kontzentrazioa zehaztu zen. Bildu bezain laster, lagin guztiak kodetu egin ziren, subjektu konfidentzialtasuna gordetzeko.

Doktorego Tesi honetan erabilitako kasu guztiei atzera begirako bilaketa bat egin zitzaien heriotza aurreko diagnostiko psikiatriko bat lortzeko, DMS-IV, DMS-IV-TR eta DMS-Vn oinarritua (American Psychiatry Association, 1994; 2000; 2013). Bilaketa horri esker, subjektuak hiru taldetan sailkatu ahal izan ziren: heriotza aurretik gaixotasun neuropsikiatriko gabeko subjektuak (kontrol-taldea), heriotza aurretik alkoholismoko diagnostikoa zuten subjektuak (alkoholismo-taldea) eta heriotza aurretik depresio nagusiko diagnostikoa zuten subjektuak (depresio-taldea). Bestelako diagnostiko psikiatrikoren bat zuten subjektuak azterketatik kanpo geratu ziren.

Giza ehunean hevinen adierazpena karakterizatzeko (ikus 4.1. atala) honako lagin hauek erabili ziren (subjektu horien ezaugarri demografikoak **3.1 taulan** laburbiltzen dira):

- Antigorputzak balioztatzeko, 4 subjektu kontrolen kortex aurrefrontalen “Pool” prestakina (hau da, subjektu guztien laginen nahasketa).

- Hevinen adierazpena konparatzeko garun atalen eta frakzio azpizelularren artean, 6 subjektu kontrolen kortex aurrefrontala, hipokanpoa, nukleo kaudatua eta zerebeloa erabili ziren.
- Aldagai ezberdinak hevinen adierazpenean izan dezaketen efektua neurtzeko alkoholismoaren ikerketako 25 subjektu kontrol eta beste 4 emakume kontrol erabili ziren.
- 4 subjektu kontrolen LZRko laginak erabili ziren.

Hevinen adierazpena alkoholismoaren azterketak (ikus 4.2. atala) 25 subjektu kontrol, 25 subjektu alkoholismoko diagnostikoarekin eta 25 subjektu depresio diagnostikoarekin hartu zituen. Talde bakoitzeko subjektu guztiak bat zetozen adinarekin, sexuarekin, postmortem atzerapenarekin (PMD, heriotzaren eta autopsiaren arteko denbora-tartea) eta biltegiratze-denborarekin. Lau parametro horiek ez ziren estatistikoki desberdinak izan taldeen artean ($p>0,05$, norabide bakarreko bariantza-analisia (*one way* ANOVA), ikus 3.2. taula). Esperimentu guztietan, talde bakoitzarekin bat zetozen subjektuen laginak paraleloan prozesatu ziren. Subjektu guztien ezaugarri demografikoen deskribapen osoa **3.2. taulan**.

Entsegu mota	Laginen kopurua (n)	Adina (BB±SEM)	Sexua
Antigorputzen espezifikotasuna, degradazioa eta entsegu entzimatikoak	4 subjektu kontrolen pool prestakina	45±2	4G
Adierazpen erregionalalaren eta azpizelularraren entseguak	6 KAF 6 HIP 6 KAU 6 ZB	44±1	6G
Korrelazioa aldagai ezberdinekin	29 KAF	50±2	11E/18G
Likido zefalorrakideoa	4	65±7	4G

3.1. taula. Subjektuen ezaugarri demografikoak eta hevinen adierazpenaren giza karakterizazioan sartutako subjektuen kopurua. BB, batez bestekoa; E, emakumea; G, gizona; KAF, kortex aurrefrontala; HIP, hipokanpoa; KAU, nukleo kaudatua; ZB, zerebeloa; SEM, batez bestekoaren errore estandarra.

Kasua	Sexua	Adina (urteak)	PMD (orduak)	Biltegiratze-denbora (hilabeteak)	Heriotza-mota eta kausa	Diagnostiko psikiatrikoa	Drogak odolean
A1	G	59	22	11	Naturala/ Zirrosia	Alkoholismoa	(-)
K1	G	57	3	18	Istripua/ Trafikoa	Kontrol	(-)
D1	G	55	20	95	Suizidioa/ Trena	Depresioa	Antidepresibo
A2	G	59	19	159	Naturala/ HKP	Alkoholismoa	(-)
K2	G	58	16	201	Istripua/ Trafikoa	Kontrola	(-)
D2	G	60	18	170	Suizidioa/ Urkatzea	Depresioa	Antidepresibo
A3	G	61	34	20	Naturala/ HKP	Alkoholismoa	Etanola
K3	G	62	9	45	Naturala/ HKP	Kontrola	(-)
D3	G	62	15	96	Suizidioa/ Labana	Depresioa	Antidepresibo
A4	G	51	23	23	Naturala/ HKP	Alkoholismoa	(-)
K4	G	51	14	108	Istripua/ Trafikoa	Kontrola	Etanola
D4	G	51	24	200	Suizidioa/ Urkatzea	Depresioa	Antidepresibo
A5	G	55	11	36	Naturala/ HKP	Alkoholismoa	(-)
K5	G	56	13	96	Naturala/ HKP	Kontrola	(-)
D5	G	56	3	128	Naturala/ Tronboenbolismoa	Depresioa	Antidepresibo
A6	G	61	27	162	Naturala/ HKP	Alkoholismoa	(-)
K6	G	61	23	202	Istripua/ Trafikoa	Kontrola	(-)
D6	G	60	24	111	Suizidioa/ Salto	Depresioa	Antidepresibo
A7	G	52	17	85	Naturala/ HKP	Alkoholismoa	(-)
K7	G	54	16	112	Istripua/ Zapalketa	Kontrola	(-)
D7	G	50	23	143	Suizidioa/ Gun	Depresioa	Antidepresibo
A8	G	47	28	88	Naturala/ HGI	Alkoholismoa	Etanola
K8	G	46	24	129	Naturala/HKP	Kontrola	(-)
D8	G	49	27	18	Naturala/HKP	Depresioa	Antidepresibo
A9	E	50	14	95	Naturala/ HGI	Alkoholismoa	Etanola
K9	E	50	10	129	Naturala/HKP	Kontrola	(-)
D9	E	49	19	164	Suizidioa/ Salto	Depresioa	Antidepresibo
A10	E	38	22	165	Naturala/ HKP	Alkoholismoa	(-)
K10	E	36	20	123	Istripua/ Train	Kontrola	(-)
D10	E	36	32	152	Suizidioa/ Droga intoxikazioa	Depresioa	Antsiolitikoak/ Antidepresibo
A11	E	71	16	125	Naturala/ HKP	Alkoholismoa	(-)
K11	E	71	22	155	Istripua/ Trafikoa	Kontrola	(-)
D11	E	70	7	92	Suizidioa/ Salto	Depresioa	Antidepresibo
A12	G	64	9	104	Naturala/ HKP	Alkoholismoa	Etanola
K12	G	64	22	46	Naturala/ HKP	Kontrola	(-)
D12	G	65	12	145	Suizidioa/ Urkatzea	Depresioa	Antidepresibo
A13	G	73	2	168	Naturala/ HKP	Alkoholismoa	Etanola
K13	G	73	10	202	Istripua/ Salto	Kontrola	(-)
D13	G	73	11	39	Suizidioa/ Urkatzea	Depresioa	Antidepresibo
A14	G	52	27	114	Naturala/ HKP	Alkoholismoa	(-)
K14	G	51	19	101	Istripua/ Trafikoa	Kontrola	(-)
D14	G	53	22	87	Suizidioa/ Urkatzea	Depresioa	Antidepresibo
A15	G	49	10	115	Naturala/ HKP	Alkoholismoa	Etanola
K15	G	48	10	123	Naturala/HKP	Kontrola	(-)
D15	G	50	24	118	Suizidioa/ Gun	Depresioa	Antidepresibo

A16	G	56	24	129	Naturala/ HKP	Alkoholismoa	Etanola
K16	G	55	22	130	Naturala/HKP	Kontrola	(-)
D16	G	56	22	119	Suizidioa/ Gun	Depresioa	Antidepresibo
A17	E	54	7	142	Naturala/ HKP	Alkoholismoa	Etanola
K17	E	51	10	84	Naturala/HKP	Kontrola	(-)
D17	E	54	18	169	Suizidioa/ Urkatzea	Depresioa	Antidepresibo
A18	G	60	6	143	Naturala/ HKP	Alkoholismoa	(-)
K18	G	60	19	87	Naturala/ HKP	Kontrola	(-)
D18	G	61	5	198	Naturala/ Aneurisma	Depresioa	Antidepresibo
A19	G	46	11	149	Naturala/ Hemorragia	Alkoholismoa	(-)
K19	G	47	17	205	Naturala/ HKP	Kontrola	(-)
D19	G	47	18	167	Suizidioa/ Urkatzea	Depresioa	Antidepresibo
A20	E	44	11	163	Naturala/ HKP	Alkoholismoa	(-)
K20	E	45	12	130	Naturala/ HKP	Kontrola	(-)
D20	E	43	24	143	Naturala/HKP	Depresioa	Antidepresibo
A21	G	53	25	158	Naturala/ HKP	Alkoholismoa	(-)
K21	G	54	23	159	Istripua/ Salto	Kontrola	(-)
D21	G	53	39	191	Suizidioa/ Pistola	Depresioa	Antidepresibo
A22	G	65	5	159	Naturala/ HKP	Alkoholismoa	Etanola
K22	G	67	22	166	Naturala/ HKP	Kontrola	(-)
D22	G	65	11	94	Suizidioa/ Droga intoxikazioa	Depresioa	Antsiolitikoak/ Antidepresibo
A23	E	50	23	159	Naturala/ HKP	Alkoholismoa	Etanola
K23	E	45	8	21	Naturala/ Hemorragia	Kontrola	(-)
D23	E	49	18	142	Suizidioa/ Ito	Depresioa	Antidepresibo
A24	G	57	17	147	Naturala/ HKP	Alkoholismoa	(-)
K24	G	55	20	37	Istripua/ Trafikoa	Kontrola	(-)
D24	G	57	21	92	Suizidioa/ Salto	Depresioa	Antidepresibo
A25	E	46	19	156	Naturala/ HKP	Alkoholismoa	Etanola
K25	E	43	3	40	Istripua/ Trafikoa	Kontrola	(-)
D25	E	45	21	89	Suizidioa/ Urkatzea	Depresioa	Antidepresibo
BB ± SEM							
$A_{1\text{-}25}$	7E/18G	54.9±2	17.2±2	119±10			
$K_{1\text{-}25}$	7E/18G	54.4±2	15.5±1	114±12			
$D_{1\text{-}25}$	7E/18G	54.8±2	19.2±2	126±9			

3.2. **taula. Hevinen papera alkoholismoan aztertzeko giza garunean egindako ikerlanean sartu diren subjektuen ezaugarri demografikoak, postmortem atzerapena (PMD), biltegiratze denbora, heriotza mota eta kausa, diagnostiko psikiatrikoa eta datu toxikologikoak.** Beheko partean kuantifikatu daitezkeen aldagaien batez bestekoa eta batez bestekoaren errore estandarrak erakusten dira. A, alkoholismoa; K, kontrola; D, depresioa; E, emakume; G, gizona; HKP, hutsegite kardio-pulmonarra; HGI, hemorragia gastrointestinala; BB, batez bestekoa.

3.1.2. GARUNEKO TUMOREEN LAGINAK

Gurutzetako Ospitaleko Neurokirurgia Zerbitzuan (Bizkaia, Espainia) egindako kraniotomietan tumore zati txikiak bildu ziren eta zuzenean -70 ºC-tan gorde ziren, esperimentuak egin arte. Neuropatologoek laginak hartu zituzten NSZko tumoreen, Osasunaren Mundu Erakundearen babespean dagoen Nazioarteko Sailkapenaren arabera diagnostikatzeko. Azterketa horretan 3 astrozitoma anaplasiko (III. gradukoak) eta 3 meningioma diagnostikatu ziren. Pazienteen ezaugarri demografikoak **3.3 taulan** laburbiltzen dira. Esperimentu guztietan laginak paraleloan prozesatu ziren.

Entsegu mota	Lagin kopurua (n)	Adina (BB ± SEM)	Sexua (E/G)
Astrozitoma	3	49±8	3G
Meningioma	3	61±7	2E/1G

3.3. taula. Pazienteen ezaugarri demografikoak. BB, batez bestekoa; E, emakume; G, gizona; SEM, batez bestekoaren errore estandarra.

3.1.3. ODOL-LAGINAK

Odol laginak lau kontrol subjektu bizidunetatik atera ziren zain-barnetik, odola biltzeko Vacutainer® zitratodun hodietara (Becton Dickinson & Company), eta berehala prozesatu ziren. Odol-bilketa Euskal Herriko Unibertsitateko (EHU) Medikuntza eta Erizaintza Fakultatean egin zen (Leioa, Espainia). Parte-hartzaile guztiek idatziz, txostenaren bidezko baimena eman zuten ikerketan parte hartzeko, eta ez zuten gaixotasun psikiatrikorik aurkezten DSM-IV, DMS-IV-TR edo ICD-10 irizpideen arabera. Lau subjektuak emakumeak ziren eta batez besteko adina 28 ± 3 urtekoa izan zen (urteak ± batez bestekoaren errore estandarra, SEM). Esperimentu guztietan laginak paraleloan prozesatu ziren.

3.2. ANIMALIAK ETA TRATAMENDUAK

Animalien zaintza eta esperimentu guztiak Europar Batasuneko legeekin eta neurozientzietako ikerketetan animaliak erabiltzeko politikekin bat etorriz burutu ziren (Europako Batzordearen 2010/63/EB Zuzentaraua). Hevinentzako 129/FBV knockout saguak Cagla Eroglu doktorearengandik (Duke Unibertsitatea, Ipar Carolina, AEB, ikus 3.2.1 atala) lortu ziren. Peritoneo barneko (i.p. edo *intraperitioneal*, ingelesez) etanola emateko eta hevinen adierazpenaren gutxipena (edo knocdown, KD) egiteko erabili ziren C57BL/6J saguak Janvier Labs-etik (Le Genest-Saint-Isle, Frantzia) lortu ziren. Doktorego Tesi honetako sagu guztiak Paris-Seine Biologia Institutuko (Paris, Frantzia) animalia-instalazioetan mantendu ziren. Zehazki, saguak kaioletan bostnaka egon ziren egon ziren, baldintza estandarretan: 23 °C eta 12 orduko argi eta iluntasun zikloan, *ad libitum* janari eta urarekin. Kasu guztietan, esperimentuak 2 eta 4 hilabete bitarteko adineko C57BL/6J sagu arretan egin ziren.

3.2.1. HEVINERAKO KNOCKOUT SAGUEN GARUNEKO LAGINAK

Cagla Eroglu doktoreak (Duke Unibertsitatea, Ipar Carolina, AEB) hevinerako 129/FBV kockout saguak (hevin adirazten ez duten saguak) sortu zituen, transkripzioaren hasiera kodoian bigarren exoiaren birkonbinazio homologoa erabiliz (McKinnon et al., 2000). C57BL/6J homozigotoak lortu ziren 129/FBV saguak C57BL/6J-ekin 10 belaunaldiz gurutzatuz. Esperimentuak 2-4 hilabeteko adina zuten 2 hevin-gabeko eta 2 sagu basatien (*wild-type*, WT) garunak erabiliz egin ziren. Hevin knockout eta WT saguei burua moztu zitzaien eta azkar garunak atera ziren. Garunak disekzionatu ziren eta berehala biltegiratu ziren -70 °C-tan, Western blot-erako prestatu arte (ikus 3.5.2.1.1. atala).

3.2.2. PERITONEO BARNEKO ETANOLAREN ADMINISTRAZIOA

Lau etanol tratamendu egin ziren 2-4 hilabeteko C57BL/6J saguetan. Kasu guztietan, saguak modu kronikoan tratatu ziren 13 egunez, bai gatz soluzioarekin, bai etanolarekin eta ez ziren injektatu hurrengo 3 egunetan (abstinentzia); azkenik, berrezartze dosi bat eman zitzaien, gatz soluzioarekin edo etanolarekin **(3.1 irudia)**. Hona hemen lau tratamendu-taldeak:

- 1. taldea: gatz soluzioarekin tratamendu kronikoa + abstinentzia + gatz soluzioarekin berrezartze-dosia (gazia-gazia edo S-S), eta kontrol-taldea da.

- 2. taldea: gatz soluzioarekin tratamendu kronikoa + abstinentzia + etanolarekin berrezartze-dosia (gazia-etanola edo S-S), eta etanolaren efektu akutua imitatzen du.
- 3. taldea: etanolarekin tratamendu kronikoa + abstinentzia + gatz soluzioarekin berrezartze-dosia (etanola-gazia edo E-S), eta etanolaren tratamendu kronikoa imitatzen du.
- 4. taldea: etanolarekin tratamendu kronikoa + abstinentzia + etanolarekin berrezartze-dosia (etanola-etanola edo E-S), eta abstinentzia ondoko berrerortzea imitatzen du.

Tokiko lehentasuna eragiten duen etanol dosia (1,75 g etanol/kg) edo % 0,9ko NaCl gatzezko soluzioa peritoneo barnean injektatu ziren (Nocjar et al., 1999). Saguak azken injekzioa jaso eta 24 ordu ondoren deslokalizazio zerbikalez akabatu ziren eta garuneko disekzioak berehala egin ziren. Hurrengo bost garun ataletan atal bakoitzeko bi zulaketa egin ziren: kortex aurrefrontala, amigdala, hipokanpoa, estriatu dortsala eta accumbens nukleoa. Odola EDTA duten hodietan bildu zen (1 µl 0,5M EDTA pH 8,0), 10 min, 17000 x g-tan eta 4 °C-tan (Eppendorf Centrifuge 5427 R, FA-45-48-11 errotorea) zentrifugatu ziren, eta plasma laginak hodi freskoetara aldatu ziren. Laginak 70 °C-tan gorde ziren Western blot-erako prestatu arte (ikus 3.5.2.1.2. atala garuneko laginen prestakinetarako eta 3.5.2.1.3. atala saguen plasma prestakinetarako).

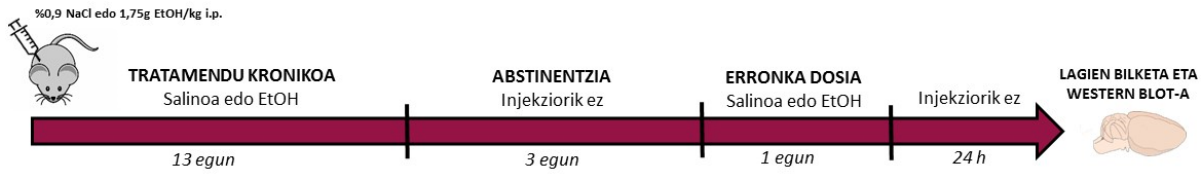

3.1. irudia. C57BL/6J saguetan egindako tratamenduen irudikapen eskematikoa.

3.2.3. KIRURGIA ESTEREOTAXIKOA ETA BIRUSEN BIDEZKO INFEKZIOA

Accubens nukleoaren astrozitoetan hevinen adierazpena murrizteko asmoz (KD edo *knockdown*, ingelesez) C57Bl6/J sagu helduak anestesiatu ziren 100 mg/kg-ko ketamina eta 10 mg/kg-ko xilazina zuen % 0,9 NaCl-ko nahasketa batekin. Hevin KD lortzeko 7 sagu injektatu ziren AAV2.5-GFAP-EmGFP-miR-Hevin birusarekin (9,4. 1012 vg/ml) eta 7 sagu AAV5.GFAP.eGFP.WPRE.hGH (9,1. 1012 vg/ml, Ipar Carolinako Unibertsitatea, Amerikako

Estatu Batuak (AEB)) birus kontrolarekin injektatu ziren. Injekzioak accumbens nukleoaren bi aldeetan egin ziren (bregmari dagokionez) honako koordenatu hauek erabiliz: +1,6, erdialbokoa: +1,45, dortsobentrala: -4,3, erdiko lerrotik 10°-ko angeluarekin. Birusaren 500 nl injektatu zitzaizkion sagu bakoitzari 100 nl/min-tan. Portaera-probak kirurgia egin eta 3 astera egin ziren, eta saguak aldian-aldian monitorizatu ziren. Injekzioaren kokapen egokia eta transgenearen adierazpena immunohistokimikaren bidez berretsi ziren (ikus 3.5.4. atala)

3.3. HEVIN ADIERAZTEN DUTEN ZELULAK

BON giza zelula kartzinoideak Bruno Gasnier doktorearengandik lortu ziren (Saints-Pères Paris Institute for the Neurosciences - CNRS UMR, Frantzia) eta geroago Vincent Vialou doktoreak prozesatu zituen (Neurosciences Paris Seine - Institut de Biologie Paris Seine, Sorbonne Université, Frantzia). Zelulak 1:1 DMEM/F12n mantendu ziren % 10 behi fetuaren serumarekin eta 100 U-100 µg/ml penizilin-streptomizinarekin, 37 °C -tan % 5 CO2 inkubagailu hezean. BON zelulak modu iragankorrean transferitu ziren saguen hevin cDNArekin (Source Biosciences, Erresuma Batua) edo simulatutako transfekzioa egin zen, Lipofektamina 2000 transfekzio-protokolo estandarra erabiliz (Thermo Fisher Scientific Conference). Zelulak pH 7,4ko 5 mM Tris-HCl-an lixatu ziren sonikazioaren bidez (Vibra-Cell Klinics Bioblock Scientific), eta -70 °C-tan kontserbatu ziren elektroforesiko-karga indargetzailean (100 mM DTT, % 2 SDS, % 8 glizerola, % 0,01 bromofenol urdina), poliakrilamidazko elektroforesi-gelean kargatu ziren arte (ikus 3.5.2.3. atala).

3.4. MATERIALAK

3.4.1. ANTIGORPUTZAK

Doktorego Tesi honetan erabilitako antigorputz primarioak eta sekundarioak **3.4 taulan** azaltzen dira:

Lagina eta esperimentu mota	Antigorputz primarioa	Antigorputz primarioaren diluzioa	Antigorput sekundarioa	Antigorputz sekundarioaren diluzioa
Giza garuna (hevinen antigorputzaren balioztaketa; karakterizazioa eta alkoholismoaren ikerketa)	Ahuntzean sortutako anti-giza hevin Ag.(R&D systems, AF2728)	1:3000*	Alexa Fluor® 680 konjugatuta astoan sortutako anti-ahuntza Ag. (Life Technologies, A21084)	1:5000
	Saguan sortutako anti-giza hevin Ag. (Santa Cruz Biotechnology, sc-514275)	1:500	Alexa Fluor® 680 konjugatuta astoan sortutako anti-sagua Ag. (Life Technologies, A21084)	1:3000
	Ahuntzean sortutako anti-sagua hevin Ag. (R&D systems, AF2836)	1:2000	Alexa Fluor® 680 konjugatuta astoan sortutako anti-ahuntza Ag. (Life Technologies, A21084)	1:5000
	Saguan sortutako anti- β-actin Ag. (Sigma-Aldrich, A1978)	1:100000	DyLight™ 800 konjugatuta astoan sortutako anti-sagua Ag. (Rockland, 610-745-002)	1:5000
	Ahuntzean sortutako anti-sagua biotina Ag. (ThermoFisher™, B-2763)	1:200	Alexa Fluor® 680 konjugatuta astoan sortutako anti-ahuntza Ag. (Life Technologies, A21084)	1:5000
Giza garuna (frakzio azpizelularren balioztaketa)	Saguan sortutako anti-giza Syntaxin1A Ag. (Merck Millipore, MAB336)	1:2000	DyLight™ 800 konjugatuta astoan sortutako anti-sagua Ag. (Rockland, 610-745-002)	1:3000
	Untxian sortutako anti-giza VGLUT1 Ag. (Salah El	1:1000	DyLight™ 800 konjugatuta astoan sortutako anti-untxia	1:3000

	Mestikawy-k emandakoa)		Ag. (Rockland, 611-745-127)	
	Ahuntzean sortutako anti-giza NR2A Ag. (Santa Cruz Biotechnology, sc-1468)	1:1000	IRDye® 800 konjugatuta untxian sortutako anti-ahuntza Ag. (Rockland, 605-432-013)	1:3000
	Saguan sortutako anti-giza PSD95 Ag. (Merck Millipore, MAB1596)	1:1000	DyLight™ 800 konjugatuta astoan sortutako anti-sagua Ag. (Rockland, 610-745-002)	1:3000
	Untxian sortutako anti-giza Stathmin Ag. (Cell Signaling Technology, #3352)	1:200	DyLight™ 800 konjugatuta astoan sortutako anti-untxia Ag. (Rockland, 611-745-127)	1:3000
	Untxian sortutako anti-giza Iκβ-α Ag. (Santa Cruz Biotechnology, Sc-371)	1:500	DyLight™ 800 konjugatuta astoan sortutako anti-untxia Ag. (Rockland, 611-745-127)	1:3000
Saguen garuna eta plasma (alkoholismoaren ikerketa)	Ahuntzean anti-sagua hevin (R&D systems, AF2836)	1:2000	Alexa Fluor® 680 konjugatuta astoan sortutako anti-ahuntza Ag. (Life Technologies, A21084)	1:5000
	Untxian sortutako anti- β-actin Ag.(Abcam, Ab8227)	1:5000	DyLight™ 800 konjugatuta astoan sortutako anti-untxia Ag. (Rockland, 611-745-127)	1:5000
Immunohistokimika (birusen bidezko infekzioaren balioztaketa)	Ahuntzean sortutako anti-sagua hevin Ag. (R&D systems, AF2836)	1:2000	Cy™3 AffiniPure saguan sortutako anti-ahuntza IgG Ag. (Jackson Immunoresearch, 205-165-108)	1:2000
	Oiloan sortutako anti-GFP Ag. (A010-pGFP-5, Badrilla)	1:2000	Cy™3 AffiniPure astoan sortutako anti-oiloa IgY Ag. (Jackson Immunoresearch, 703-165-155)	1:2000

3.4. taula. Lagin mota eta esperimentuaren arabera erabilitako antigorputzen xehetasun komertzialak eta diluzioak. *1:3000 diluzioa hevinen seinale immunoerreaktiboa detektatzeko erabili zen eta 1:100 diluzioa hevinen immunoprezipitaziorako. Ag., antigorputza.

3.4.2. ZUNDAK

RT-qPCRrako zundak Thermo Fisher Scientific™-etik lortu ziren, eta guztiak TaqMan® adierazpen genikoaren egiaztapen gisa inbentariatuta zeuden. Ikerketa honetan erabilitako zundak hauek izan ziren: Hs00949886_m1 hevinen genearentzat, Hs99999905_m1 glizeraldehido 3-fosfato deshidrogenasaren (GAPDH) genearentzat eta Hs01945436_u1 S13 erribosoma-proteinaren (RPS13) generentzat.

3.4.3. BEKTORE BIRALAK

- AAV2.5-GFAP-EmGFP-miR-hevin: AAV1 eta AAV2 birus adeno-elkartuen arteko hibridoa, zuntzetako proteina astrozitiko glial azidoa (GFAP) bideratutako, proteina fluoreszente berdea esmeralda (EmGFP) eta hevin micro-RNA (miR-hevin) adierazten dituena (Dr. Vincent Vialou doktorea, Neurosciences Paris Seine - Institut de Biologie Paris Seine, Sorbonne Université, France).

- AAV5.GFAP.eGFP.WPRE.hGH: birus adeno-elkartuaren 5. serotipoa, zeinak GFAP promotore astrozitikoak bideratuta, honako hauek adierazten ditu: proteina fluoreszente berde indartua (eGFP), marmotaren hepatitisaren birusaren transkripzio osteko erregulazio-elementua (WPRE), adierazpen transgenikoa areagotzeko, eta giza hazkuntzako hormona (hGH), poliadenilizazioko seinale gisa (poliA), RNA egonkortzen duena (Ipar Karolinako Unibertsitatea, Estatu Batuak).

3.4.4. BESTELAKO ERREAKTIBOAK

Agilent technologies (Santa Clara, CA, AEB): Agilent RNA 6000 Nano Kit-a.

Bio-Rad Laboratories (Hercules, CA, AEB): Bio-Rad proteina entsegua (Bradford protein assay), DC proteina entsegua, amonio persulfatea (APS); N,N,N’,N’-tetrametiletilendiamina (TEMED), Precision Plus Dual™ Color Protein Standards.

Bio-techne®, R&D Systems (Minneapolis, MN, AEB): giza hevin proteina errekonbinantea (2728-SL), giza ADAMTS4 (a disintegrin and metalloproteinase with thrombospondin motifs 4) proteina errekonbinantea (4307-AD).

BioWorld (Dublin, OH, AEB)**:** Acrilamida /Bis-Acrilamida 5:1 (30%)

Carlo Erba Reagents (Bartzelona, Espainia): metanola.

GE Healthcare (Buckinghamshire, Erresuma Batua): nitrozelulosa mintzak (pore size: 0,45 µm), Whatman TM 3MM zelulosa paperak.

Honeywell Fluka™ Chemicals (Charlotte, NC, AEB): glizerola, sukrosa.

Invitrogen™ (Bartzelona, Espainia)**:** ditiotreitol (DTT), TRIzol™ Reagent, PureLink™ RNA Mini kit-a RNA totalaren arazketarako, DEPC-treated water (nukleasarik gabeko ura), NuPage™ LDS 25% lagin indargetzailea, Fluoromount-G.

Merck (Darmstadt,Alemania): kloruro sodikoa (NaCl), kloruro potasikoa (KCl), disodio fosfatoa (Na_2HPO_4), monopotasio fosfatoa (KH_2PO_4), sodio bikarbonatoa ($NaHCO_3$), azido etilenediaminetetraazetikoa (EDTA), kaltzio kloruro dihidratoa ($CaCl_2{\cdot}2H_2O$), etanola 96%.

New England BioLabs® (Ipswich, MA, AEB): EndoF3 (Endoglicosidasa F3, P0771S), EndoH (Endoglicosidasa H, P0702S) and PNGaseF (N-Glicosidasa F, P0708S) entzima errekonbinanteak.

Panreac química S.A.U. (Bartzelona, Espainia): azido azetiko glaziala, azido klorhidrikoa (HCl).

Santa Cruz Biotechnology (Dallas, TE, AEB): A/G Plus-Agarosa (sc-2003) proteina.

Sigma-Aldrich® (Saint Louis, MO, AEB): tronbina entzima (605195), RNaseZAP™, 1-Bromo-3-kloropropanoa (BCP), glizina, Tris (hidroximetil)aminometano-hidrokloruroa (Tris-HCl), Erradio-immunoprezipitazio entseguaren indargetzailea (RIPA buffer), sodio dodezil sulfatoa (SDS), polioxietileno (20) sorbitan monolauratoa (Tween 20), Ponceau S, bromofenol urdina, proteasen inhibitzaileen nahasketa (Sigma Protease Inhibitor Cocktail, P8340), sodio ortobanadatoa (Na_3VO_4), sodio floruroa (NaF), OptiPrep™, N-(2-Hidroxietil)piperazina-N'-(azido 2-etanosulfonikoa), 4-(2- Hidroxietil)piperazina-azido 1-etanosulfonikoa (HEPES-free acid), Triton X-100, fenilmetilsulfonil floruroa (PMSF), azido etilendiaminotetraazetikoa (EDTA), 4',6-diamidino-2-fenilindola (DAPI, D9542), behiaren serumeko albumina (BSA).

Sino Biological (Eschborn, Alemania): MMP-3 (matrizearen metaloproteasa -3, 10467-HNAE) giza proteina errekonbinantea.

Source Bioscience (Nottingham, Erresuma Batua): sagu hevinen cDNA (IRAVp968E073D).

Thermo Fisher Scientific™ (Waltham, MA, AEB): TaqMan™ Fast Universal Master Mix (4367846), High-Capacity cDNA Reverse Transcription Kit-a (4368814), Lipofektamina 2000 Transfekziorako erreaktiboa eta Dulbecco's Modified Eagle Medium: Nutrient Mixture F-12 (DMEM/F12).

3.5. METODOAK

3.5.1. POLIMERASAREN ERREAKZIO KATEATUAREN ALDERANTZIKO TRANSKRIPZIO KUANTITATIBOA (RT-qPCR)

3.5.1.1. RNAren erauzketa

Alkoholismoko eta depresioko subjektuen eta beraien kontrolen kortex aurrefrontalean, hipokanpoan, nukleo kaudatuan, eta zerebeloan (ikus **3. 2. taula**) RNAren erauzketa eta arazketa egin zen. Lehenik eta behin, zelulen apurketa egin zen garuneko laginei (50-100 mg garun ehuna) 1 mL TRIzol® erreaktiboa (fenola eta guanidina tiozianatoko disoluzio monofasiko batean) gehituz eta mini errotagailu batekin homogeneizatuz. Homogeinatuak giro-tenperaturan inkubatu ziren 5 minutuz, eta gero zentrifugatu egin ziren 12000 x g 15 minutuz 4 ° C-tan (Eppendorfeko zentrifugagailua 5810 R, F45-30-11 errotorea). Lortutako gain-jalkiak (1 mL) hodi berrietara aldatu ziren eta 100 µL 1-bromo-3-kloropropanoko (BCP) gehitu ziren. Hodien edukiak vortex-arekin ondo nahastu ziren, 5 minutuz inkubatu ziren giro-tenperaturan eta 15 minutuz 12000 x g zentrifugatu ziren 4 ° C-tan. Zentrifugazio horrek nahasketa bat sortzen du, hiru fasetan banatua: beheko fase organiko bat (gorria), interfaze bat (zuria) eta RNA duen goiko fase urtsu bat (kolorerik gabekoa). Fase urtsuko 400 µL bildu ziren eta % 70eko etanol esterilaren bolumen bera (400 µL) gehitu ziren, vortex-arekin nahastu eta bolumen hori bilketarako flitrodun kartutxo bat daukan mikrohodi batera eraman zen. Mikrohodia kartutxoarekin 12000 x g zentrifugatu zen 30 segundo giro-tenperaturan. Porsezu horren ostean, RNA iragazki-kartutxoan bilduta zegoen, eta, guztira, hiru aldiz garbitu zen, bi garbiketa-soluzio komertzialekin eta ondorengo zentrifugazioekin (12000 x g 30 segundo). Azkenik, RNA iragazi paperetik askatzeko iragazpen-kartutxoa 100 µL askapen indargetzailearekin (RNAasarik gabeko ura) inkubatu zen minutu batez giro-tenperaturan eta gero 2 minutuz zentrifugatu 12000 x g-tan. RNA kontzentrazioa NanoDrop 1000 espektrometroan (Thermo Fisher Scientific™) neurtu zen. RNAaren integritate zenbakia (RIN) 2100 Bioanalizagailuan (Agilent Technologies) zehaztu zen Agilent RNA 6000 Nano Kit-a erabiliz. RIN balioak **3.5 taulan** agertzen dira. Araztutako RNA -20 °C-tan biltegiratu zen alderantzizko transkripzioa egin arte.

Kasua	KAF	HIP	KAU	ZB	Kasua	KAF	HIP	KAU	ZB
A1	6.6	5.5	6.6	6.5	*A14*	8.5	8.1	5.5	8.3
K1	8	8.1	9	9	*K14*	8.6	7.7	8.3	7.9
D1	8	8	6.8	8.8	*D14*	8.8	6.7	6.9	8.2
A2	7.3	7	8	8.9	*A15*	6.6	6.4	6.5	8.6
K2	7.5	7.5	8.5	9	*K15*	6.5	8.1	7.6	8.7
D2	7.4	8.4	8.1	9	*D15*	7.4	8.1	8.2	8.6
A3	6.7	6.7	6.9	7.9	*A16*	7.8	6.1	7.2	6.8
K3	8.4	7.8	7.4	7.8	*K16*	8.3	7.1	7.6	8.5
D3	8.1	6	6.1	7.4	*D16*	7.8	8	7.2	8.3
A4	6.9	7.3	7.7	8.3	*A17*	8.4	7.8	7.2	7.2
K4	8.1	8.1	8.4	8.6	*K17*	8.2	8.3	8.7	7.6
D4	7.8	8.4	7.3	8.7	*D17*	8	8.2	8.6	7.5
A5	8.4	6	6.4	7.6	*A18*	6.9	7.8	7.2	8.6
K5	7.1	7.9	7.2	8.1	*K18*	7.9	7.8	8.3	9
D5	8.6	7.8	8.3	7.8	*D18*	7.2	6.8	6.4	7.9
A6	7.2	6.6	7.9	8.4	*A19*	7.7	6.2	6.9	7.2
K6	8	6.5	6.2	8.5	*K19*	7.9	5.9	6.2	8
D6	6.8	7.6	6.1	7	*D19*	8	7	7.5	9
A7	7.3	6.1	5.8	9.9	*A20*	7.5	6	8.5	8.7
K7	8.2	7.9	8.1	8.6	*K20*	7.4	7.1	8	8.4
D7	7.7	6.1	8.5	7.9	*D20*	6.5	5.9	7.4	7.1
A8	6.8	5.1	5.6	5	*A21*	8.7	7.3	7	8.5
K8	8.5	7.7	5.2	8.9	*K21*	7.7	7.4	8.7	8.3
D8	6.8	7.5	5.9	8.6	*D21*	8	7.9	7.7	8.6
A9	8.3	6.7	8.7	6.2	*A22*	8	7.1	7.8	8.6
K9	8.2	7.8	8.9	8.4	*K22*	7.2	7.4	7.3	8.6
D9	7.9	6.1	8.2	7.3	*D22*	6.7	7.7	6.4	9.1
A10	7.2	6.4	6.6	7.3	*A23*	7.4	5.5	7.9	6.3
K10	8.2	6.1	8.7	9.6	*K23*	9.2	8.5	8.1	8.4
D10	7.2	5	6	6.8	*D23*	7.9	7.7	7	9.1
A11	6.8	7.1	8.3	8.7	*A24*	7	7.1	7.4	7.9
K11	6.5	6.8	6.9	5.8	*K24*	6.4	6.5	7.3	6.4
D11	7	8.9	8.9	9.1	*D24*	8.5	7.5	7.6	7.5
A12	8.2	8.5	7.8	8.8	*A25*	7.7	6.1	5.6	7
K12	8.6	7.5	8.7	7.4	*K25*	9	8.3	8	7.8
D12	6.9	7.4	8.6	8.7	*D25*	8.5	7.4	8	8
A13	7.6	6.9	7.4	8.1					
K13	6.9	7.6	7.4	8.5					
D13	8.1	7.4	8.6	8.8					

3.5. taula. Aztertutako lau garun atalen RIN baloreak subjektu bakoitzarentzat. KAF, kortex aurrefrontala; HIP, hipokanpoa; KAU, nukleo kaudatua; ZB, zerebeloa; A, alkoholismoa; K, Kontrola; D, depresioa.

3.5.1.2. Alderantzizko transkripzioa

Araztutako RNA laginen DNA osagarria (cDNA) lortzeko, alderantzizko transkripzioa egin zen High Capacity cDNA Reverse Transcription kit-a (Applied Biosystems™) erabiliz eta fabrikatzailearen zehaztapenei jarraituz. Lagin bakoitzaren RNA totalaren kontzentrazioaren arabera, horien bolumen egokia hartu zen eta Milli-Q® urarekin diluitu zen, guztietan DNAren azken kontzentrazio bera lortzeko (50 ng/L). Alderantzizko transkripzioaren baldintzak **3.6 taulan** agertzen dira.

	1. urratsa	2.urratsa	3.urratsa	4.urratsa
Tenperatura (°C)	25	37	85	4
Denbora	10 min	120 min	5 seg	∞

3.6. taula. Alderantzizko transkripzioaren baldintzak.

3.5.1.3. Polimerasaren erreakzio kateatua denbora errealean (qPCR)

Hevinen genearen adierazpena denbora errealeko polimerasaren erreakzio kateatuaren (qPCR) bidez aztertu zen, StepOne™ sistema (Applied Biosystems™) erabiliz. Analisia 5 µL-ko erreakzio-nahasketan egin zen, zeinetan 20 ng cDNA, TaqMan® Fast universal PCR Master Mix eta aldez aurretik diseinatutako gene-zunda (TaqMan® adierazpen genikoaren entsegua, ikus 3.4.2. atala) zeuden. Adierazpen geniko bakoitzak abiarazle aurreratuak eta alderantzizkoak zituen, eta FAM™ tindagaiari lotutako zunda. Hevinen mRNA-ren adierazpenaren zenbatekoak GAPDH eta RPS13 *housekeeping* geneen (modu osagarrian adierazten diren eta zeluletan mantentze-lanak betetzen dituzten molekulen geneak) adierazpenarekin normalizatu ziren. PCR plaka guztietan barne kontrol negatibo bat (cDNArik gabekoa) eta erreferentziazko kontrol lagin bat (garuneko eskualde bakoitzeko aztertutako lagin guztien cDNA nahasketa bat) sartu ziren geneen adierazpen-proba bakoitzeko. PCRaren baldintzak **3.7. taulan** agertzen dira.

	Hasierako desnaturalizazioa	40 ziklo	
		Desnaturalizazioa	Anplifikazioa
Tenperatura (°C)	95	95	65
Denbora	20 seg	1 seg	20 seg

3.7. taula. qPCR baldintzak.

3.5.1.4. Emaitzen analisi matematikoa

qPCRaren anplifikazio-urratsean, xede-geneak esponentzialki anplifikatzen dira (gertaera hau deskribatzen duen ekuazioa 3.1 ekuazioan agertzen da). Ondoriozko anplikonek seinale fluoreszentearen hazkunde lineala dute. Fluoreszentzia handitzen duen seinalearen fase esponentziala oso zehatza da. Seinalea atalasera iristen den ziklo-kopuruari (hondoko

zarataren gaineko balioa) atalase-zikloa (Ct) deitzen zaio, eta hasierako xede-cDNAren kopuruarekiko zuzenki proportzionala da. Horrela, Ct balioak lagin batean cDNA zehatz bat kuantifikatzea ahalbidetzen du, eta bereaz, bere mRNA adierazpen erlatiboa. Lagin bakoitzaren hevinen mRNA-ren adierazpen erlatiboa (ΔΔCt) Ct metodo konparatiboaren bidez kalkulatu zen, GAPDH eta RPS13 *housekeeping* geneen mRNA kopuruan oinarrituta, eta erreferentziazko lagin bateko (lagin guztien cDNA nahasketa bat duena) adierazpen erlatiboari dagokionez, non (ΔΔCt = (Ct (hevin)$_{lagina}$ - Ct (housekeeping)$_{lagina}$)- (Ct (hevin)$_{erreferentziazko\ lagina}$ - Ct (housekeeping)$_{errferentziazko\ lagina}$).

Datuen analisia StepOne Software v2.1 (Applied Biosystems™) erabiliz egin zen. mRNAren kantitate erlatiboa $2^{-\Delta\Delta Ct} \pm$ SEM moduan adierazi zen, non kontrol-taldearen batez bestekoa 100 balio erlatibotzat hartu zen.

$$Xn = X_0(1 + E_x)^n$$

3.1. ekuazioa. Anplifikazio esponentziala PCRan. Xn = n zikloko xede-molekulen kopurua; X_0 = xede-molekulen hasierako kopurua; E_X = xede-anplifikazioaren efizientzia (1 TaqMan ® Gene Expression Assays guztietarako), n = zikloen kopurua.

3.5.2. WESTERN BLOT

3.5.2.1. Laginen prestaketa

3.5.2.1.1. Hevin knockout eta sagu basatien garunen prestaketa

Zerebeloko laginak izotzaren gainean homogeneizatu ziren sonikazioaren bidez (Vibra-Cell™ Bioblock Scientific sonicator, Sonics®) 1/1000 diluzioan Sigma proteasen inhibitzaileen nahasketa duen RIPA indargetzailearen 200 µL -tan. Homogeneizazioaren ondoren, lagin bakoitzaren proteinen guztizko kontzentrazioak Bradford entseguaren bidez zehaztu ziren (ikus 3.5.2.2.1. atala). Kontzentrazio bereko diluzioak lortzeko eta laginak ingurune desnaturalizatzaile eta erreduzitzailean mantentzeko, 50 µg proteina totala zuten laginak NuPage™ LDS %25 indargetzailearekin (Invitrogen™) eta DTT 1M-ekin nahastu ziren. Nahasketa horiek -70ºC-tan biltegiratu ziren, poliakrilamidazko elektroforesi-gelean kargatu ziren arte (ikus 3.5.2.3. atala).

3.5.2.1.2. Etanolarekin tratatutako saguen garunen prestaketa

Etanolarekin tratatutako saguen zulaketak (ikus 3.2.2. atala) izotzaren gainean desizoztu ziren, eta proteasen eta fosfatasen inhibitzaileak gehituta zuen 100 µL homogeneizaziorako indagetzaile batekin (5 mM Tris-HCl pH 7,4, 50 l/g Sigma proteasen inhibitzaileen nahasketa, 5mM Na_3VO_4 eta 10 mM NaF) sonikatu ziren 15 segundo 3 aldiz (Q55 Sonicator, QSONICA Sonicators). Proteina totalaren kuantifikazioa Bradford metodoaren bidez egin zen (ikus 3.5.2.2.1. atala) eta kontzentrazioak berdindu egin ziren. Azkenik, elektroforesiko-karga indargetzailea (100 mM DTT, % 2 SDS, % 8 glizerola, % 0,01 bromofenol urdina) lagin guztiei gehitu zitzaien, erredukzio eta desnaturalizatzeko baldintzak lortzeko. Laginak -70 °C-tan gorde ziren poliakrilamidazko elektroforesi-gelean kargatu arte (ikus 3.5.2.3. atala). 6 saguen garun homogeneizatuak zituen kanpoko erreferentziazko lagin bat erabili zen, zeinak prestaketa prozesu bera jarraitu zuen.

3.5.2.1.3. Etanolarekin tratatutako saguen plasmen prestaketa

Saguen plasma laginak izotzetan desizoztu ziren. Proteasen eta fosfatasen inhibitzaileak gehituta zuen homogeneizaziorako indargetzaile baten 10 µL (5 mM Tris-HCl pH 7,4, 50 l/g Sigma proteasen inhibitzaileen nahasketa, 5mM Na_3VO_4 eta 10 mM NaF) gehitu zitzaien 50 µL-ko lagin bakoitzari. Ondoren, horiek sonikatu egin ziren 15 segundoz (Q55 Sonicator, QSONICA Sonicators) eta berehala elektroforesi-karga indargetzailea gehitu zitzaien (100 mM DTT, 2% SDS, 8% glizerol, 0,01% bromofenol urdina). Azkenik, -70 °C-tan biltegiratu ziren poliakrilamidazko elektroforesi-gelean kargatu ziren arte (ikus 3.5.2.3. atala).

3.5.2.1.4. Giza garunen eta garuneko tumoreen prestaketa

Izoztutako postmortem giza garun laginak moztu ziren meningeetatik, odoletik eta gai zuritik ahalik eta gehien garbitzeko. Ehun lagin bakoitza (0,4 g) Ultra-Turrax batekin homogeneizatu zen (IKA LabortechnIK), 3 bider 10 segundo 4 ºC-tan, proteasen eta fosfatasen inhibitzaileak gehituta zuen homogeneizaziorako indargetzaile baten 4 ml-rekin, homogeneizazio totaleko prestakina emanez. Esperimentu batzuetarako homogeneizazio totaleko prestaketa erabili zen, eta beste batzuetan frakzio post-nuklearra (S1), zitosolikoa eta/edo mintz neuronaletan aberastutako frakzioa (P2) erabili ziren, era honetan prestatu zirenak. Homogeneizatu totala 10 minutuz zentrifugatu zen (4 °C) 1100 x g-tan (Sorvall® RC-5C zentrifugatzailea, SM-24 errotorea), eta frakzio nuklearra zuen pellet-a kendu zen, S1 prestakina sortuz. S1 prestakinak berehala gorde ziren 4 ºC-tan, proteina kopurua neurtu

arte. Zatiketa azpizelularrerako, S1 berriz zentrifugatu zen 10 minutuz (4 °C) 40000 × g-tan. Zatiki zitosolikoari zegokion gain-jalki berria berehala gorde zen 4 ° C-tan, proteina kopurua neurtu arte. Pellet-a P2 zatiari zegokion. Hori 2 mL 5 mM Tris-HCl pH 7,4 indargetzailearekin garbitu zen (lehen aipatutako proteasa eta fosfatasaren inhibitzaileekin osatua) eta hirugarren aldiz zentrifugatu zen 10 minutuz (4 °C) 40000 × g-tan. Azkenik, pellet-a 1,2 ml-tan birsuspenditu zen, proteasa eta fosfatasaren inhibitzaileekin, eta 4 ° C-tan biltegiratu zen, proteina kantitatea zehaztu arte **(3.2 irudia)**.

Kasu guztietan, proteina-kantitatea Bradford metodoaren bidez neurtu zen (ikus 3.5.2.2.1. atala) lagina prestatu zen egun berean. Azterketa-talde bakoitzerako proteina totaleko kontzentrazio berdina zuten diluzioak prestatu eta berehala, elektroforesiko- karga indargetzailea (100 mDTT, % 2 SDS, % 8 glizerola, % 0,01 bromofenol urdina) gehitu zitzaien lagin guztiei, baldintza erreduzitzailean eta desnaturalizatzailean jartzeko. Azkenik, laginak -70 °C-tan gorde ziren, poliakrilamidazko elektroforesi-gelean kargatu arte (ikus 3.5.2.3. atala).

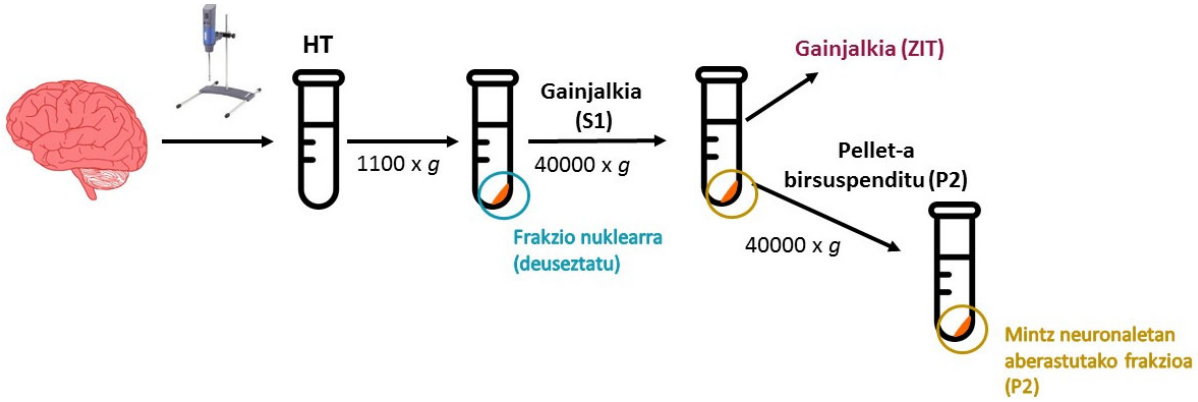

3.2. irudia. Giza ikerketako garun-ehunen prestakinak lortzeko urrats nagusiak erakusten dituen irudikapen eskematikoa. HT, homogeneizatu totala; S1, prestakin post-nuklearra; ZIT, frakzio zitosolikoa (disolbagarria); P2, mintz neuronaletan aberastutako frakzioa.

3.5.2.1.5. Giza likido zefalorrakideoaren prestaketa

Lau LZR laginak 10 minutuz zentrifugatu ziren (4 °C) 1100 x g-tan (Sorvall® RC-5C zentrifugatzailea, SM-24 errotorea) zelulak eta hondakinak kentzeko. Lortutako gain-jalkiak hodi freskoetan bildu ziren, gero proteinen edukia DC proteinen entseguaren bidez neurtu zen (ikus 3.5.2.2.2. atala) eta haien kontzentrazioak berdindu egin ziren. Lagin guztiei elektroforesiko- karga indargetzailea (100 mDTT, % 2 SDS, % 8 glizerola, % 0.01 bromofenol

urdina) gehitu zitzaien. Ondoren, laginak -70 °C-tan gorde ziren poliakrilamidazko elektroforesi-gelean kargatu arte (ikus 3.5.2.3. atala).

3.5.2.1.6. Giza odolen frakzioen prestaketa

Giza odol freskoaren zatiketarako, odol-lagin bakoitzeko 5 mL gehitu ziren poliki 5 mL dentsitate-zutabe batera (0,9 mL OptiPrep™, 0,85% (w/v) NaCl, 20 nM HEPES-NaOH pH 7.4, 1 mM EDTA) bi faseen nahasketa saihestuz, eta 15 minutuko (20 °C) 350 g-ko zentrifugazioa eginez kulunkako errotorean (Eppendorf™ zentrifugatzailea 5810 R, A-4-62 errotorea). Odol osoa lau fasetan banatu zen eta bakoitza bere aldetik berreskuratu zen, plasmari (goiko fasea), plaketei (tarteko geruza mehea), leukozitoei (tarteko geruza, plaketen azpian) eta eritrozitoei (beheko fasea) zegozkiela **(3.3. irudia)**. Plaketan eta leukozitoetan aberastutako frakzioen zatietan egon zitekeen seruma kentzeko, 5 minutuz zentrifugatu ziren, 20 °C -tan 600 × g-tan, eta gain-jalkiak deuseztatu ziren. Pellet-a 500 µL-ko soluzio batekin (0,85% (w/v) NaCl, 20 nM HEPES-NaOH pH 7,4, 1 mM EDTA) birsuspenditu zen eta berriro zentrifugatu egin zen. Homogeneizaziorako indargetzailea, proteasarekin eta fosfatasaren inhibitzaileekin osatua, odolaren frakzio bakoitzari gehitu zitzaion eta 15 segundoz (Q55 Sonicator, QSONICA Sonicators) sonikatu ziren. Proteina-edukia DC proteina entseguaren bidez neurtu zen (ikus 3.5.2.2.2. atala), eta odoleko frakzio bakoitzerako proteina totaleko kontzentrazio berdina zuten diluzioak prestatu ziren. Elektroforesiko- karga indargetzailea (100 mM DTT, 2% SDS, 8% glizerol, 0.01% bromofenol urdina) lagin guztiei gehitu zitzaien, eta berehala -70 ° C-tan biltegiratu ziren, poliakrilamidazko elektroforesi-gelean kargatu arte (ikus 3.5.2.3. atala).

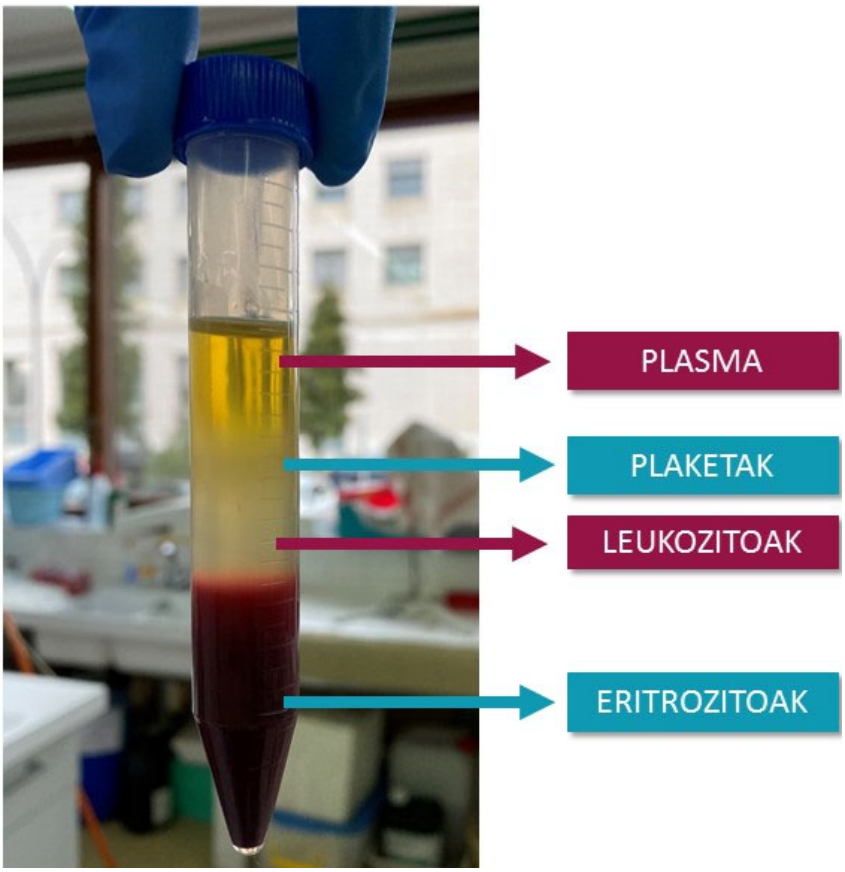

3.3. irudia. Odolaren zatiketaren ondorengo plasman (goiko fasea), plaketetan (tarteko geruza mehea), leukozitoetan (tarteko geruza, plaketen azpian) eta eritrozitoetan (beheko fasea) aberastutako faseak erakusten dituen irudia.

3.5.2.1.7. **Karakterizazio-entseguak**

3.5.2.1.7.1. Immunoprezipitazio-entsegua

4 subjektu kontrolen laginen nahasketa egiteko, kortex aurrefrontaleko postmortem-aren homogeneizatu totala prestatu zen. Horretarako garun ehuna lisi-indargetzaile batekin (10 mM Tris-HCl, 1% triton X-100, proteasa eta fosfatasa inhibitzaileekin (50 µL/g of Sigma Protease Inhibitor Cocktail, 5mM Na_3VO_4 and 10 mM NaF)) nahastu zen. Homogeneizatu totala osoa 10 minutuz zentrifugatu zen (4 °C) 1100 x g-tan (Sorvall® RC-5C zentrifugatzailea, SM-24 errotorea). S1 frakzioari zegokion gain-jalkia hodi fresko batera transferitu zen eta 1 h 4 °C-ra laborategiko gurpil kulunkari batean garbitu zen A/G Plus-Agarose proteina suspentzioaren (sc-2003, Santa Cruz Biotechnology) 30 µL-rekin, A/G bolatxoen loturak proteina ez-espezifikoekin kentzeko. Ondoren, nahasketa minutu batez zentrifugatu zen (4 °C) 2000 × g-n, eta A/G agarose bolatxoak zuen pellet-a bota zen. Garbitutako S1 frakziotik 1 mL-ko 3 alikuota jaso ziren. Bat erabili zen giza hevinen (anti-hSPARCL1 antigorputza; AF2728, R&D Systems) aurkako ahuntz antigorputz poliklonalarekin (1:100eko diluzioan)

immunoprezipitazioa egiteko. Horretarako, ordubetez 4 °C-tan inkubatu zen laborategiko errotazio-gurpilean. Beste alikuota bat lotura ez-espezifikoaren isotipoa kontrolatzeko erabili zen, eta horretarako, ahuntzaren IgG anti-sagu-biotinarekin (B-2763, Thermo Fisher Scientific™) immunprezipitatu zen 1: 200eko diluzioan, ordubetez 4 °C -tan inkubatuz laborategiko errotazio-gurpilean. Hirugarren alikuota -70 °C -tan gorde zen zuzenean kontrol gisa erabiltzeko. Alikuotak antigorputzekin inkubatu ondoren, A/G agarosa proteinaren suspentsioaren 75 µL gehitu zitzaien eta gau osoan zehar 4 °C -tan inkubatu ziren laborategiko errotazio-gurpilean. Hurrengo egunean, 1 minutuko hiru garbiketa egin ziren (4 °C-koa 2000 × g-n) proteasa eta fosfatasaren inhibitzaileekin osatutako lisis indargetzailearekin. Azkenik, antigorputz proteina konplexuaren askapenerako nahasteak 95 ºC-tan 7 minutuz berotu ziren elektroforesi-karga indargetzailean (100 mM DTT, 2% SDS, 8% glizerol, 0,01% bromofenol urdina). Ondoren, zentrifugatu egin ziren 1 minutuz (4 °C) 2000 × g-tan agarosa bolatxoak pellet-ean metatzeko Gain-jalkiak -70 °C-tan gorde ziren, poliakrilamidazko elektroforesi-gelean eta kromatografia likidoa-tandem masa espektometrian (LC-MS/MS) kargatu ziren arte (ikus 3.5.2.3. eta 3.5.3. atalak, hurrenez hurren).

3.5.2.1.7.2. Degligozidazio-entseguak

Fabrikatzaileen gomendioei jarraituz, giza kortex aurrefrontaleko nahasketatik (karakterizazioko nahasketa, 3.5.2.1.4. atalean prestatua) lortutako homogeneizatu totalaren 8 µg proteina totala edo giza hevin errekonbinatzaileko 50 ng (R & D Systems, 2728-SL) (kontrol positibo gisa), hurrengo hiru deglicosidasekin banan-banan tratatu ziren: EndoF3 (P0771S, New England Biolabs), EndoH (P0702S, New England Biolabs) eta PNGase F (P0708S, New England Biolabs). EndoF3 bidezko erreakzio entzimatikorako 50 U (U, substratuaren 1 µmol minutuero katalizatzen duen entzima kopurua, entseguaren baldintza espezifikoetan) erabili ziren; EndoH entzimaren bidezko erreakziorako 5000 U eta PNGase F entzimaren bidezko erreakziorako 1000 U erabili ziren. Laginak erreakzio-indargetzaile egokian inkubatu ziren (20 µl-ko azken bolumena lortuz) 5 orduz 37 °C -tan, entzimaren presentzian edo absentzian. Erreakzioa gelditu egin zen PMSF 2 mM-ko, DTT 100 mM-ko, Laemmli indargetzailea (% 2 SDS, % 8 glizerol, % 0,01 bromofenol urdina) gehituz eta 5 minutuz 98 °C–tan berotuz, poliakrilamidazko elektroforesi-gelean kargatu aurretik (ikus 3.5.2.3. atala).

3.5.2.1.7.3. Denboraren eta tenperaturaren menpeko degradazio-entseguak

Kortex aurrefrontaleko homogeneizatu totaleko nahasketak (karakterizazioko nahasketa, 3.5.2.1.4 atalean prestatua) erabili ziren hevinen proteolisia aztertzeko. Denboraren menpeko entsegurako, homogeneizatu totalak proteasen eta fosfatasaren inhibitzaileen aurrean edo ezean prestatu ziren, hevinen degradazioa eta inhibitzaileen efektua hobeto bistaratzeko. Lagin guztiak 37 °C-tan inkubatu ziren, 0 minututik 180 minutura. Zehazki, proteasen eta fosfatasaren inhibitzailerik gabeko laginak inkubatu ziren 0 eta 180 minutuz; inhibitzaileekin prestatutako laginak, berriz, 0, 30, 60, 90, 120, 150 eta 180 minutuz inkubatu ziren. Ondoren, laginei elektroforesiko-karga indargetzailea (100 mM DTT, 2% SDS, 8% glizerol, 0,01% bromofenol urdina) gehitu zitzaien eta 5 minutu 95 °C-tan berotu ziren, poliakrilamidazko elektroforesi-gelean kargatu aurretik (ikus 3.5.2.3. atala).

Tenperaturaren menpeko proteolisiaren entseguaren kasuan, laginak zuzenean inkubatu ziren elektroforesi indargetzailean (ikus 3.5.3.3. atala) 15 minutuz, 4 ° C eta 95 ° C arteko tenperatura ezberdinetan (5 ° C, 20 ° C, 37 ° C, 50 ° C, 65 ° C, 80 ° C eta 95 ° C). Laginak ez ziren gehiago berotu eta berehala kargatu ziren poliakrilamidazko elektroforesi-gelean (ikus 3.5.2.3. atala).

3.5.2.1.7.4. Digestio entzimatikoa hevin degradatzen duten entzimekin: ADAMTS4, MMP-3 eta tronbina-rekin

Kortex aurrefrontaLeko nahasketatik lortutako homogeneizatu totalaren (karakterizazioko nahasketa, 3.5.2.1.4 atalean prestatua) 140 µg proteina totala ADAMTS4ko 2 µg-rekin (tronbospondina 4 motibodun desintegrina eta metaloproteasa) edo MMP-3ko 0,4 µg-rekin (matrizeko metaloproteasa-3) nahastu ziren B1 inkubazio-indargetzailearen (50mM Tris-HCl, 125 mM NaCl, 5 mM $CaCl_2 \cdot 2H_2O$, pH 7,5) 100 µl-rekin eta 37 ºC-tan inkubatu ziren ordu batez edo 5 orduz. Tronbinaren kasuan, giza kortex aurrefrontaleko nahasketatik lortutako homogeneizatu totalaren 70 µg proteina eta entzimaren 1 U konbinatu ziren B2 indargetzailearen (20 mM Tris-HCl, 0,15 m NaCl, 2,5 mm CaCl2). 2H2O, pH 8,4) 50 µl-rekin eta 37 ºC-tan inkubatu ziren 15 orduz. Gainera, giza hevin errekonbinatzailearen 400 ng eta 20 ng (R&D Systems, 2728-SL) kontrol positibo gisa erabili ziren ADAMTS4/MMP-3 eta tronbinaren bidezko digestioetarako, hurrenez hurren. Kontrol negatiboetarako, laginak berdin tratatu ziren, baina entzimarik gabe. Kasu guztietan, erreakzioa gelditu egin zen

PMSF 2 mM, DTT 100 mM, Laemmli buffer (2% SDS, 8% glizerol, 0,01% bromofenol urdina) gehituz eta 10 minutuz 75 ° C-tan berotuz. Laginak -70 ° C-tan gorde ziren, poliakrilamidazko elektroforesi-gelean kargatu arte (ikus 3.5.2.3 atala).

3.5.2.2. Proteina totalaren edukiaren zehaztapena

3.5.2.2.1. **Bradford metodoa**

Giza LZR laginekin eta giza odolaren prestakinekin izan ezik, esperimentu guztietan Bradford metodoa erabili zen proteinen edukia neurtzeko (Bradford, 1976). Proteina totalaren edukia estrapolazio-kurbaren irismen linealaren gainetik egon ohi denez, 1:10 edo 1:15eko diluzioak prestatu ziren lagin bakoitzerako 5 mM Tris-HCl pH 7,4 indargetzailea erabiliz. Ondoren, diluzioaren 10 µL 96 putzuko plaketan jarri ziren, hiru aldiz lagin bakoitzerako, eta 200 µL Bradforden proteina entseguaren erreaktiboa 1:5 diluitua gehitu zen. Plakak 10 minutuz inkubatu ziren giro-tenperaturan. Absorbantzia 630 nm-ko uhin-luzeran zehaztu zen ElX808 Absorbance mikroplaken irakurgailuan (BioTek Instruments). Paraleloan, proteinen balioak erregresio linealaren bidez estrapolatzeko, BSArekin lerro estandar bat egin zen, 0 µg/mL eta 0,7 µg/mL arteko kontzentrazio-tartean. Ondoren, guztizko proteina kantitateak birkalkulatu ziren laginaren diluzioaren arabera. Erregresioaren analisi lineala eta datuen estrapolazioa GraphPad Prism 9 ® softwarearekin egin zen.

3.5.2.2.2. **DC proteina-entsegua**

Giza LZRaren eta giza odol-laginen prestakinen proteina-eduki totala DC proteina-entseguaren (Bio-Rad) bidez zehztu ziren. Aztertutako ehunen frakzioek proteina-edukia aldakorra zenez, diluzio desberdinak prestatu ziren bakoitzarentzat 5 mM Tris-HCl pH 7,4 indargetzailea erabiliz, proteasen eta fosfatasaren inhibitzaileekin osatua (50 µL/g of Sigma Protease Inhibitor Cocktail, 5 mM Na_3VO_4 and 10 mM NaF). Zehazki, LZRrako 1:2 diluzioa prestatu zen eta 1:20 diluzioa plaketa eta leukozitoen frakzioentzat, 1:30 diluzioa plasmarentzat eta 1:100 diluzioa eritrozitoak dituen frakzioarentzat prestatu ziren. Ondoren, diluzioaren 5 µL 96 putzuko plaketan jarri ziren, hirukoiztuta, A erreaktiboko 25 µL (DC proteina-entsegua) eta B erreaktiboko 200 µL (DC proteina-entsegua) gehituz. Plaka kontu handiz astindu zen, edukia nahastu eta 5 minutuz inkubatu zen. Absorbantzia 630 nm-ko uhin-luzeran zehaztu zen ElX808 Absorbance mikroplaken irakurgailuan (BioTek Instruments). BSArekin 0 µg/L eta 0,5 µg/L arteko kurba estandar bat egin zen paraleloan, absorbantzia estrapolatzeko. Laginetan proteinen azken kontzentrazioa zehazteko,

estrapolatutako proteinen kontzentrazioak kasu bakoitzean erabilitako diluzioaren arabera birkalkulatu ziren.

3.5.2.3. Elektroforesia poliakrilamidazko geletan

Tenperaturaren menpeko degradazioa aztertzeko laginen kasuan izan ezik, esperimentu guztietan laginak 95 °C-tan berotu ziren 5 minutuz, proteinak erabat desnaturalizatzeko elektroforesi gelean kargatu baino lehen. Proteina solubilizatuak SDS-PAGE (sodio dodezil sulfato-poliakrilamida gel elektroforesia) geletan ebatzi ziren. Esperimentu guztietan, erabilitako SDS-PAGE geletako goiko zatia % 5a poliakrilamida (gel pilatzailea) zen eta beheko zatia % 10a poliakrilamida (gel disolbatzailea) zen. Gelak elektroforesi indargetzaile batean murgilduta egon ziren denbora guztian (% 0,1 SDS, 192 mM glizina, 25 mM Tris-HCl, pH 8,3) korronte elektrikoaren transmisio eta proteinen banaketa zuzenerako. Desnaturalizatutako laginak gelean kargatu ondoren, gelei 60 V-ko korronte elektrikoa eman zitzaien 30 minutuz, eta horri esker, laginen proteina guztiak gelean pilatzeko. Ondoren, korronte elektrikoa 120 V-ra igo zen 2 ordu eta 30 minutuz, proteinak euren pisu molekularraren arabera bereizteko. Pisu molekularren identifikazio bisualerako, pisu molekularreko markatzaile bat (Precision Plus Protein™ Dual Color) gehitu zen gel guztietan. Gainera, seinale immunoerreaktiboaren kuantifikazio-kasuetan kanpoko erreferentzia-lagin bat sartu zen.

3.5.2.4. Transferentzia nitrozelulosa mintzean

Proteinak SDS-PAGE geletik nitrozelulosazko mintz batera transferitu ziren. Horretarako, transferentzia-sandwhich-a prestatu zen, zeinetan gela nitrozelulosazko mintza zuzenean ukitzen du eta kanpoko aurpegiak hiru Whatman paperez (3MM) eta esponja batez **(3.4A irudia)** inguraturik daude. Proteinak mintzera transferitzeko 110 V-ko korronte elektrikoa erabili zen. Prozesu guztia transferentzia-indargetzailean egin zen (25 mM Tris-HCl, 192 mM glizina, % 20 metanola, pH 8,3). Proteinen transferentzia zuzena baieztatzeko, nitrozelulosazko mintzak Ponceau S soluzioan inkubatu ziren (% 0,5 Ponceau S gorria, % 1 azido azetiko glaziala) 3 minutuz eta ondoren Milli-Q® urarekin garbitu ziren. Giza eta saguen odolen azterketako mintzak Ponceau-ren tindaketarekin eskaneatu ziren, proteina-eduki totalaren intentsitatea analizatzeko lagin bakoitzeko **(3.4B irudia)**. Azkenik, mintzak fosfatato-indargetzaile soluzioan (PBS) garbitu ziren (137 mM NaCl, 2,7 mM KCl, 12 mM Na2HPO4, 1,38 mKH2PO4, pH 7,4) Ponceaus S tindaketa erabat kentzeko.

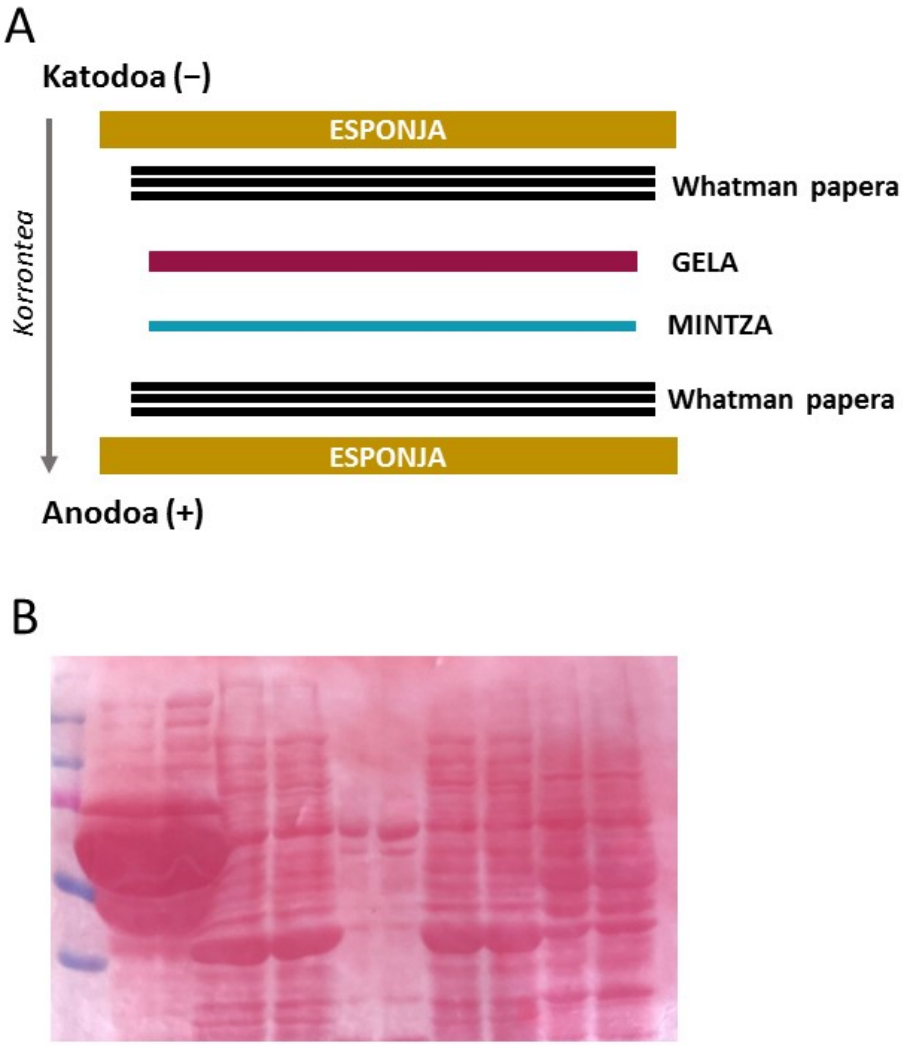

3.4. irudia. A) Transferentzia sandwhich-aren irudikapen eskematikoa. **B)** Ponceau S-rekin tindatutako nitrozelulosa mintz baten adibidea (kasu honetan gizakiaren odol-ikerketakoa).

3.5.2.5. Blokeoa eta immunodetekzioa

Seinale immunoerreaktibo ez-espezifikoa murrizteko, mintzak blokeo-soluzio batean inkubatu ziren 1 orduz giro-tenperaturan (% 5 esne lehor ez-koipetsua PBSn). Ondoren, mintzak antigorputz primarioekin inkubatu ziren **(4. taula)** inkubazio-soluzioan (% 5 esne lehor ez-koipetsua PBSn eta % 0,1 Tween 20), 4 °C-tan gau osoan zehar, etengabeko agitazioarekin. Giza hevinaren aurkako antigorputza balioztatzeko (R&D sistemak, AF2728), antigorputza peptido blokeatzailearekin inkubatu zen (R&D Systems 2728-SL, 1:150) 1 orduz giroko tenperaturan inkubazio soluzio berean nitrozelulosazko mintzaren inkubazioaren aurretik. Hurrengo egunean, mintzak PBST soluzioan garbitu ziren (PBS gehi % 0,1 Tween 20) 30 minutuz (10 minutu 3 aldiz) eta giro-tenperaturan 90 minutuz inkubatu ziren Ig-G-rekin konjugatutako antigorputz sekundario fluoreszentearekin **(4. taula)**

inkubazio-soluzioan diluituta. Mintzak PBST soluzioan garbitu ziren (PBS gehi % 0,1 Tween 20) 30 minutuz (10 minutu 3 aldiz), eta azken aldia PBS soluzioarekin. Azkenik, seinale immunoerreaktiboa (integratutako intentsitate balioak) Odyssey infragorrien irudi sistema (LI-COR Biosciences) erabiliz detektatu zen.

3.5.2.6. Seinale immunoerreaktiboaren kuantifikazioa

Kuantifikazioa Image Studio Lite 5.2 (LI-COR Biosciences) erabiliz egin zen. Inmunoerreaktibitate-balioak aktina-seinalearen arabera normalizatu egin ziren. Homogeneizatu totalaren nahasketa estandar bat gel horretan prozesatu zen kanpoko erreferentziazko lagin gisa erabilitzeko. Saguaren plasma laginetan, zelularik ez egoteak aktina seinalearen bidezko normalizazioa oztopatu zuen. Kasu horretan, Ponceau S-rekin tindatutako irudiakaztertu ziren eta lagin guztietan proteina kopuru bera zegoela zehaztu zen.

3.5.3. PROTEINEN IDENTIFIKAZIOA, KROMATOGRAFIA LIKIDOA-TANDEM MASA ESPEKTROMETRIA ERABILIZ (LC–MS/MS)

Hevin proteina, giza-hevinen kontrako antigorputzarekin immunoprezitatu zen (R&D systems, AF2728) (ikus 3.5.2.1.7.1. atala). Euskal Herriko Unibertsitateko (UPV/EHU, Leioa, Espainia) Proteomikako Unitatea-SGIker erakundeak laginak prozesatu zituen SDS-PAGE erabiliz, zeinetan ~130 and ~100 kDa-eko bandak eskuz moztu eta analizatu ziren LC-MS/MS-aren bidez. Gel zatiak DTTrekin (10 mM in 50 mM NH_4HCO_3, 56°C, 45 minutu) eta iodoazetamidarekin (25 mM in 50 mM NH_4HCO_3, 30 minutu giro -tenperaturan eta iluntasunean) inkubatu ziren, eta proteomikarako tripsinarekin (12.5 ng/µl in 50mM NH_4HCO_3, 37°C, gau osoan zehar) digeritu ziren. Berreskuratutako peptidoak SpeedVac-ean lehortu ziren (Thermo Fisher Scientific™) eta etxeko C18 (3M Empore C18) puntekin gatzgabetu ziren. Masa-espektrometriako analisiak EASY-nLC 1200 kromatografia likidoko sisteman egin ziren, Q Exactive HF-X masa-espektrometroarekin (Thermo Scientific) tartekatua, nanospray ioi-iturri baten bidez. Peptido gatzgabetuak Acclaim PepMap100 zutabe batean kargatu ziren (75 µm x 2 cm, Thermo Scientific) Acclaim PepMap RSLC (75 µm x 25 cm, Thermo Scientific) zutabe analitiko bati konektatuta. Peptidoen askapena azido formikoa % 0,1ean zeukan % 2,4 eta % 24 arteko azetonitrilo gradiente lineala erabiliz egin zen, 18 minututik gorako 300 nL/min-ko emarian. MS eskaner osoa 375etik 1800erako m/z-rekin hartu ziren 120.000-ko erresoluzioarekin 200 m/z-tan. 10 ioi gogorrenak zatikatu

egin ziren C-trap disoziazio energia handiagoa eta 28-ko kolisio energiaren bidez eta MS/MS espektroak 15.000 m/z-ko erresoluzioarekin grabatu ziren. Ioi-injekzioen gehienezko denbora 100 ms-koa izan zen azterketa egiteko eta 120 ms-koa MS/MS eskanerretarako, non 3 x 10^6 eta 5 x 10^5 AGC itu balioak erabili ziren azterketarako eta MS/MS eskanerretarako, hurrenez hurren (Elu et al., 2019). Fitxategi gordinak Proteome Discoverer 2.2-rekin(Thermo Scientific) prozesatu ziren eta UniProtKB-SwissProt Human (2020_02) datu-basearekin konparaketa-bilaketak egin ziren. Aitzindari eta zatikien masa-tolerantziak 10 ppm eta 0,02 Da-koak izan ziren, hurrenez hurren, eta zatiketa huts bat ere baimendu zen. Zisteinen karbamidometilazioa Meteoninen eraldaketa finkotzat eta oxidaziotzat jo zen. Peptidoa eta FDR proteina % 1ean zeuden.

3.5.4. IMMUNOHISTOKIMIKAKO ENTSEGUA SAGU-GARUNEAN

Saguei 150 mg/kg-ko pentobarbital (Euthasol ® 400 mg/mL) dosi hilgarria eman zitzaien eta % 4 paraformaldehido (PFA) fosfato soluzioan (PBS; 137 mM NaCl, 2,7 mKCl, 12 mM Na_2HPO_4, 1,38 mM KH_2PO_4, pH 7,4) bihotz barnetik perfunditu zen. Garunak % 4ko PFAn eta 4 °C-tan gorde ziren erabili arte. Garunak bibratomean moztu ziren (Leica VT1000 S, Leica biosystems) 40 µm-ko sekzio koronaletan. Garun-mozketak % 0,2 gelatina eta % 0,25 Triton X-100 zuen PBS soluzio batekin blokeatu ziren ordubetez giro-tenperaturan. Ondoren, sagu-hevinen aurkako antigoputzarekin (anti-mhevin; AF2836, R&D systems 1:2000 diluzioa) eta proteina fluoreszente berdearen aurkako antigorputzarekin (anti-GFP; A010-pGFP-5, Badrilla, 1:2000 diluzioa) inkubatu ziren blokeo-indargetzailean, 4 °C-tan gau osoan zehar. Garbitu ondoren, mozketak zegozkien zianina Cy™3-ri konjugatutako antigorputz sekundarioarekin inkubatu ziren **(4. taula)** 1:2000-ko diluzioan 2 orduz giro-tenperaturan. Mozketak DAPIrekin (4',6-diamidino-2-fenilindol, Sigma-Aldrich, D9542) inkubatu ziren 1: 15000-ko diluzioan 20 minutuz giro tenperaturan eta mikroskopiokorako porta batean jarri ziren eta kristalezko estalkia jarri zen Fluoromount-G erabiliz. Mozketa guztiak NanoZoomer 2.0-HT (Hama-matsu Photonics) batean eskaneatu ziren 20x bereizmenarekin. Laserraren intentsitatea eta eskuratzeko denbora bereiztuta ezarri ziren seinale inmuoerreaktibo bakoitzerako. Irudiak NDP.view2 (Hamamatsu Photonics) softwarea erabiliz aztertu ziren. Eskualde interesgarriak Paxinos saguaren burmuinaren atlasaren arabera identifikatu ziren (Paxinos & Franklin, 2001). Zelula positiboek gorputz zelularraren tindaketa indartsua adierazten dute eta DAPI-z tindatutako nukleo baten inguruan daude. Kolokalizazioa bi antigorputzen seinaleak zelula bereko soman egoteak

zehazten zuen. Accumbens nukleoko eskualde osoa ebaluatu zen. Ilustraziorako, NanoZoomer irudiak TIFF formatuan esportatu ziren NDP viewer programa erabiliz. Irudien kontrastea zuzendu zen, Photoshop CS6an moztu ziren eta Illustrator CS6an bildu ziren.

3.5.5. ETANOLAREN ALDIZKAKO EDATEAREN (EAE) EGITARAUA SAGUETAN

Saguen aldi aktiboko alkohol-kontsumoa neurtzeko, esperimentua hasi baino astebete lehenago, argi eta iluntasun zikloa aldatu zen argiak goizeko 9etan itzaliz eta gaueko 9etan piztuz. Horretarako ura eta janaria *ad libitum* jarri ziren. Esperimentua goizeko 9etan hasi zen, hevin murriztuta zeukaten saguak (KD, n = 7) eta kontrol-saguak (n = 7) egunero banaka jarriz. Saguak bi ur botiletara ohitu ziren 3 egunez. EAE egitaraua 18 egunetan egin zen guztira; ur eta etanol botilak egunero goizeko 9etan jartzen ziren eta arratsaldeko bostetan kentzen ziren eta berriro ura jartzen zitzaien. Kontsumitutako bolumena esperimentua hasi eta 4 ordu eta 8 ordu igaro ondoren neurtzen zen, eta botilen posizioa egunero aldatu zen botilen kokapeneko lehentasuna saihesteko. Etanolaren kontzentrazioa (w/v) 3 egunetik behin handitzen zen alkohola edatera bultzatzeko. Horrela, etanolaren hasierako kontzentrazioa% 5ekoa izan zen eta hurrengoak jarraitu zioten: % 10, % 15, % 20, 3 egun etanola ez zuen botilarekin (erretiratzea) eta bererorketa % 10 etanolarekin **(3.5 irudia)**. Etanol soluzioak prestatu ziren % 96 (v/v) etanola urarekin nahastuz. Ur botilek ur-lasterra zeukaten. Saguen pisua hiru egunetik behin neurtzen zen. Etanolaren lehentasuna (neurketa bakoitzerako bolumen totalarekiko kontsumitutako etanolaren ehunekoa non, % 50a bainoa handiagoa etanolaren lehentasuntzat hartzen zen) eta kontsumoa (neurketa bakoitzerako edandako g etanola/kg sagua) kalkulatu ziren sagu bakoitzarentzat, etanol kontzentrazio bakoitzeko hirugarren eguneko neurriak erabiliz.

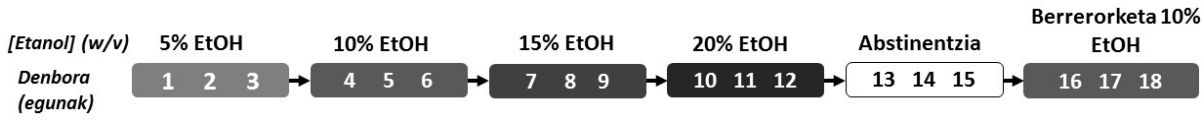

3.5. irudia. EAE egitarauaren eta esperimentuaren urrats bakoitzean erabilitako etanol kontzentrazioen irudikapen eskematikoa.

3.5.6. ANALISI ESTATISTIKOA

Kasu guztietan, analisi estatistikoa GraphPad Prism 9® softwarearen bidez egin zen eta emaitzak estatistikoki adierazgarritzat hartu ziren p balioa ≤ 0.05 zenean. RT-qPCR eta Western blot tekniketan lortutako datuen emaitzak zutabe-eta-bibote-ko grafiketan

erakusten dira non, “zutabeak” batez bestekoa 25 eta 75 kuartilak erakusten dituzte eta “biboteak” 5 eta 95 pertzentilak eraskusten dituzte. Datuen banaketari buruzko informazio zehatzagoa emateko, banakako datua gainjarri dira grafiketan.

Analisia egin aurretik, datu multzo guztiak bi irizpideren arabera egiaztatu ziren: (i) banaketa normala eta (ii) bariantzen berdintasuna. Banaketa normala D 'Agostino & Pearson normaltasun proba eginez egiaztatu zen. Bariazioen berdintasuna F-testarekin egiaztatu zen. Banaketa normalaren eta bariantza berdinen kasuan, konparazio estatistikoak egin ziren Student-en bakundutako t testarekin edo norabide bakarreko bariantza-analisiarekin (ANOVA), eta ondoren Dunnett-en konparazio anitzeko testarekin. Bestela, proba ez-parametrikoak erabili ziren.

Giza kontroleko garunean hevinen luzera osoko (~130 eta ~100 kDa) bi formetarako adierazpen azpizelularra eta erregionala. Hevinen mailen konparazioa homogeneizatu totaletan, frakzio zitosolikoan eta mintz neuronaletan aberastutako (P2) frakzioan eta kortex aurrefrontalean, hipokanpoan, kaudatu nukleoan eta zerebeloan 6 banako garuneko laginetan (n = 6) egin zen. Datuak Kruskal-Wallis-en test batekin aztertu ziren, eta ondoren Dunn-en konparazio anitzeko testa egin zen.

Sexu-desberdintasunak giza garuneko hevin banden adierazpenean. Datu multzoa aurrez-aurreko kortexaren 29 laginek osatzen zuten, 11 emakume eta 18 gizonenak. Student-en bakundutako t testa egin zen.

Hevin isoformen mailak giza garunean eta beraien korrelazioa Korrelazioa adinarekin, PMDarekin, biltegiratze-denborarekin. Pearson-en bi lerroko korrelazio-proba egin zen hevinen isoformeen mailak eta adinaren, PMDaren, biltegiratze-denboraren eta isoformen arteko korrelazioa zehazteko.

Giza astrozitoma eta meningioma garun-tumoreak. Hevinen luzera osoko *(~130 eta ~100 kDa)* formen adierazpena astrozitoman (n = 3), meningioman (n = 3) eta b kortex aurrefrontalean (n = 6) Mann-Whitney-ren testarekin aztertu ziren.

Postmortem giza garunean hevinen mRNAren eta proteinen adierazpen-mailen konparazioa alkoholismoa edo depresioa zuten subjektuen eta subjektu kontrolen artean. Datuak ANOVAren bidez aztertu ziren eta Dunnett-en konparazio anitzeko testa egin zen.

E*tanola ematearen eragina hevinen adierazpenean garunean eta plasman.* Saguaren burmuineko ~130 kDa-eko banda eta plasman detektatutako ~ 130 kDa eta ~ 47 kDa isoformeen adierazpena Kruskal-Wallis testarekin aztertu zen, ondorengo Dunn-en konparazio anitzeko testarekin.

Saguetan hevinen adierazpenaren murrizketak etanolaren lehentasunean eta kontsumoan duen eragina aztertzea. Hevin KD saguen eta sagu-kontrolen arteko aldeak Mann-Whitney testaren bidez kalkulatu ziren eta Friedman testa etanol kontzentrazioen arteko ezberdintasunak kalkulatzeko erabili zen.

4. RESULTS

4.1. CHARACTERIZATION OF HEVIN EXPRESSION IN HUMAN SAMPLES BY WESTERN BLOT

4.1.1. DETERMINATION OF HEVIN IMMUNOREACTIVITY SPECIFICITY

4.1.1.1. Validation of hevin antibodies

Three antibodies against hevin were tested for specificity by Western blotting on human prefrontal cortex total homogenate: anti-human hevin (R&D systems, AF2728), anti-mouse hevin (R&D Systems, AF2836) and anti-human hevin (Santa Cruz, sc-514275) antibodies.

Anti-mouse hevin (R&D Systems, AF2836) and anti-human hevin (Santa Cruz, sc-514275) antibodies were rapidly discarded, as neither showed specific immunoreactivity at the expected molecular weight **(Figure 4.1B, C)**. Conversely, anti-human hevin antibody (R&D systems, AF2728) showed two marked bands at the expected molecular weight **(Figure. 4.1A, left)**. More specifically, hevin immunoreactive upper band migrated at 130 kDa and the lower band at around 100 kDa, similar to what has been described by other authors (Brekken et al., 2004; Johnston et al., 1990; Kucukdereli et al., 2011; Lively & Brown, 2008a; Lively & Brown, 2008c; Mendis, 1996b; Weaver et al., 2010; Weaver et al., 2011). The signal intensity of both bands increased in a dose-dependent manner with the increase in protein concentration **(Figure 4.1A, right)**, suggesting specificity.

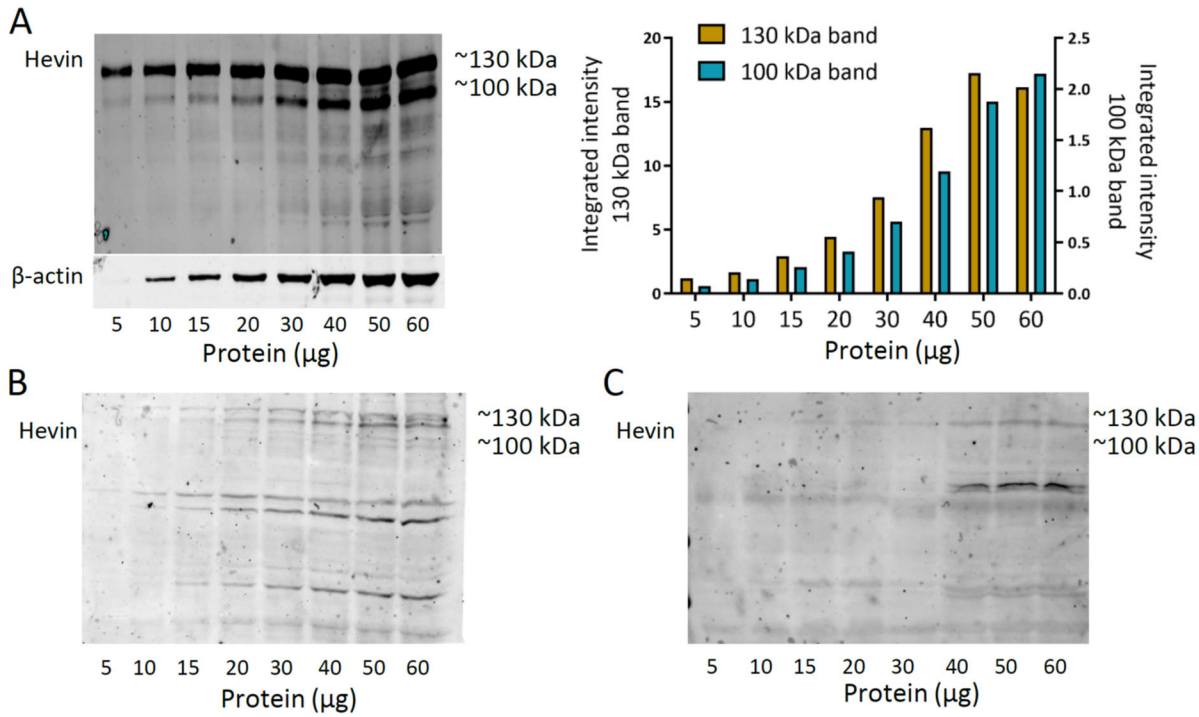

Figure 4.1. Validation of human hevin antibody specificity. (A) Protein dependent-curve of hevin immunoreactivity in prefrontal cortex total homogenate pool (5–60 mg) with goat anti-human hevin antibody (R&D AF2728, *right*) and the corresponding quantification of ~130 kDa and ~100 kDa hevin bands (*left*), **(B)** with goat anti-mouse hevin antibody and (C) with mouse anti-human hevin antibody. Blots A, B and C were run in parallel with the same sample and blot A was incubated with anti- β-actin antibody.

These two bands also appeared with the recombinant hevin protein (R&D systems, 2728-SL, **Figure 4.2A**) and their immunoreactivity was blocked by preincubating the antibody with the blocking peptide (recombinant human hevin, R&D systems, 2728-SL, **Figure 4.2A**), supporting the specificity of both bands corresponding to hevin. In addition, cell extracts and extracellular medium of BON cells transfected with mouse hevin were analyzed by Western blot. Hevin immunoreactivity was detected in hevin-transfected cells and their extracellular medium, but not in mock-transfected cells **(Figure 4.2B)**.

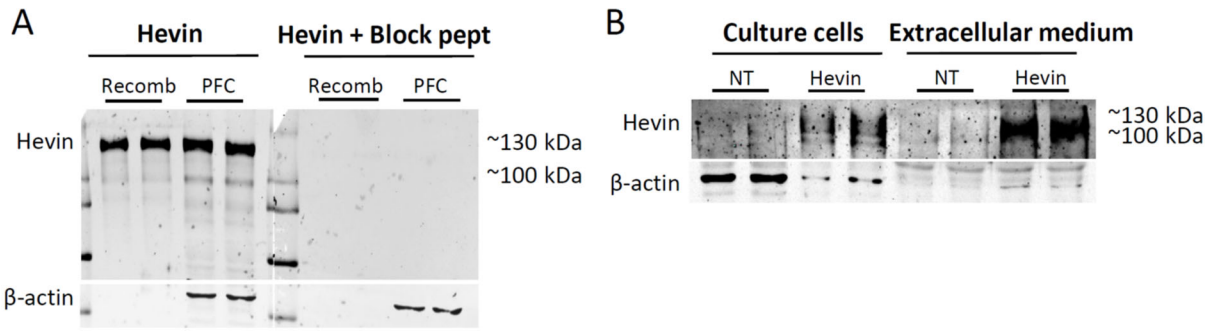

Figure 4.2. Validation of human hevin antibody specificity. (A) Hevin immunoreactivity with goat anti-human hevin antibody (R&D AF2728) in prefrontal cortex total homogenate and in human recombinant hevin (Recomb), in the presence or absence of its blocking peptide. **(B)** Hevin immunoreactivity with goat anti-human hevin antibody (R&D AF2728) in cell culture lysate and in the extracellular medium of mock-transfected (NT) and hevin-tranfected BON cells. Samples were run in duplicate. Blots were incubated with anti- β-actin antibody.

To further assess the specificity of the selected antibody (R&D AF2728), immunoprecipitation of hevin from total homogenate fraction of prefrontal cortex samples was performed. When the immunoprecipated fraction was run in SDS-PAGE and incubated with R&D AF2728 antibody, the same bands were revealed (~130 and ~100 kDa). Instead, they were absent when the sample was immunoprecipitated with control IgG (anti-mouse biotin, ThermoFisher™, B-2763, **Figure 4.3A**). Finally, in mouse brain TH samples, hevin immunoreactivity at ~120 kDa was observed with both anti-mouse hevin (R&D Systems, AF2836) and anti-human hevin (R&D Systems, AF2728) antibodies **(Figure 4.3B)**. Conversely, it was absent in hevin knockout mice. Altogether, these results demonstrate the specificity of the R&D anti-human hevin antibody. Therefore, this antibody was selected to further characterize hevin protein expression in human brain tissue.

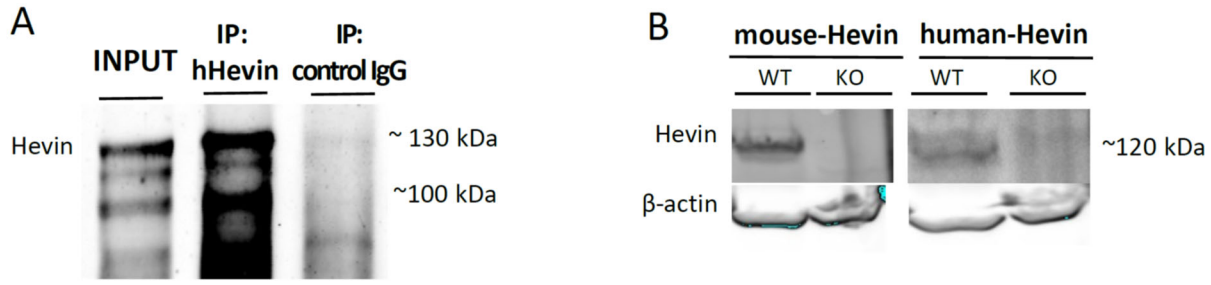

Figure 4.3. Validation of human hevin antibody specificity. (A) Immunoblotting with goat anti-human hevin antibody (R&D AF2728) after immunoprecipitating hevin protein with the same antibody or control IgG in prefrontal cortex total homogenate pool. The input loaded in the gel corresponds to 1:20 fraction of the tissue used in the assays. **(B)** Hevin immunoreactivity in wild-type (WT) and hevin knockout (KO) mouse cerebellum homogenates, with goat anti-mouse antibody (R&D AF2836) or goat anti-human hevin antibody (R&D AF2728). Blot B was incubated with anti- β-actin antibody.

4.1.1.2. Liquid chromatography-tandem mass spectrometry (LC-MS/MS) analysis of immunoreactive bands

Protein bands at ~130 and ~100 kDa were removed and analyzed by LC-MS/MS. This analysis unambiguously identified hevin protein (UniProtKB Q14515) in both bands, with a sequence coverage of 36% and 18%, respectively. Although more unique peptides were found in the ~130 kDa band (19 vs 8, possibly due to a higher amount of the ~130 kDa isoform), all but one of the peptides found in the 100 kDa isoform are common to the ~130 kDa and encompassed almost the entire protein sequence from amino acids A47 to R629 **(Figure 4.4)**. This proteomic analysis suggests that the 30 kDa difference observed between both bands does not correspond to splicing variants but it may be the result of differential post-translational modifications.

A **~130 kDa band**

MKTGLFFLCL LGTAAAIPTN ARLLSDHSKP TAETVAPDNT AIPSLRAEAE ENEKETAVST EDDSHHKAEK
SSVLKSKEES HEQSAEQGKS SSQELGLKDQ EDSDGHLSVN LEYAPTEGTL DIKEDMSEPQ EKKLSENTDF
LAPGVSSFTD SNQQESITKR EENQEQPRNY SHHQLNRSSK HSQGLRDQGN QEQDPNISNG EEEEEKEPGE
VGTHNDNQER KTELPREHAN SKQEEDNTQS DDILEESDQP TQVSKMQEDE FDQGNQEQED NSNAEMEEEN
ASNVNKHIQE TEWQSQEGKT GLEAISNHKE TEEKTVSEAL LMEPTDDGNT TPRNHGVDDD GDDDGDDGGT
DGPRHSASDD YFIPSQAFLE AERAQSIAYH LKIEEQREKV HENENIGTTE PGEHQEAKKA ENSSNEEETS
SEGNMRVHAV DSCMSFQCKR GHICKADQQG KPHCVCQDPV TCPPTKPLDQ VCGTDNQTYA SSCHLFATKC
RLEGTKKGHQ LQLDYFGACK SIPTCTDFEV IQFPLRMRDW LKNILMQLYE ANSEHAGYLN EKQRNKVKKI
YLDEKRLLAG DHPIDLLLRD FKKNYHMYVY PVHWQFSELD QHPMDRVLTH SELAPLRASL VPMEHCITRF
FEECDPNKDK HITLKEWGHC FGIKEEDIDE NLLF

B **~100 kDa band**

MKTGLFFLCL LGTAAAIPTN ARLLSDHSKP TAETVAPDNT AIPSLRAEAE ENEKETAVST EDDSHHKAEK
SSVLKSKEES HEQSAEQGKS SSQELGLKDQ EDSDGHLSVN LEYAPTEGTL DIKEDMSEPQ EKKLSENTDF
LAPGVSSFTD SNQQESITKR EENQEQPRNY SHHQLNRSSK HSQGLRDQGN QEQDPNISNG EEEEEKEPGE
VGTHNDNQER KTELPREHAN SKQEEDNTQS DDILEESDQP TQVSKMQEDE FDQGNQEQED NSNAEMEEEN
ASNVNKHIQE TEWQSQEGKT GLEAISNHKE TEEKTVSEAL LMEPTDDGNT TPRNHGVDDD GDDDGDDGGT
DGPRHSASDD YFIPSQAFLE AERAQSIAYH LKIEEQREKV HENENIGTTE PGEHQEAKKA ENSSNEEETS
SEGNMRVHAV DSCMSFQCKR GHICKADQQG KPHCVCQDPV TCPPTKPLDQ VCGTDNQTYA SSCHLFATKC
RLEGTKKGHQ LQLDYFGACK SIPTCTDFEV IQFPLRMRDW LKNILMQLYE ANSEHAGYLN EKQRNKVKKI
YLDEKRLLAG DHPIDLLLRD FKKNYHMYVY PVHWQFSELD QHPMDRVLTH SELAPLRASL VPMEHCITRF
FEECDPNKDK HITLKEWGHC FGIKEEDIDE NLLF

Figure 4.4. Validation of human hevin specificity by LC-MS/MS. The complete hevin amino acidic sequence with the unique peptides found in ~130 kDa **(A)** and ~100 kDa **(B)** bands marked in blue.

4.1.2. STUDY OF THE HEVIN GLYCOSYLATION PATTERN

In order to gain more insight into the structure of the carbohydrate moieties of each of the hevin bands observed in human brain, several deglycosylation assays were carried out. Human prefrontal cortex total homogenate pool and human recombinant hevin (R&D Systems, 2728-SL) were incubated in the presence of PNGase F, EndoF3 or EndoH deglycosylases, enzymes that remove different types of N-glycosylations.

PNGase F (almost all N-glycan, asparagine-linked chains hydrolyzing enzyme (Maley et al., 1989): high mannose, hybrid, bi-, tri- and tetra-antennary) produced a marked shift in both hevin bands in prefrontal cortex samples and recombinant protein, leading to lower molecular weight bands of ~125 and ~90 kDa **(Figure 4.5A,B)**. These results indicate that both hevin bands are glycosylated proteins.

EndoF3 (asparagine-linked fucosylated-bi-antennary and tri-antennary complex oligosaccharides cleaving enzyme) (Maley et al., 1989) produced a slight shift of both bands in prefrontal cortex and recombinant protein samples to lower molecular weight bands, although not as pronounced as with PNGaseF **(Figure 4.5A,B)**.

And finally, in the presence of EndoH enzyme (high mannose cleaving enzyme (Maley et al., 1989)), only a fraction of the ~130 kDa band suffered a migration shift in both prefrontal cortex and recombinant protein, which might suggest that this apparent unique band corresponds to a mix of slightly different isoforms or is even a doublet **(Figure 4.5A,B)**. Altogether these results confirm that both hevin bands are glycosylated in human brain but in a different way as it is rodent brain (Johnston et al., 1990).

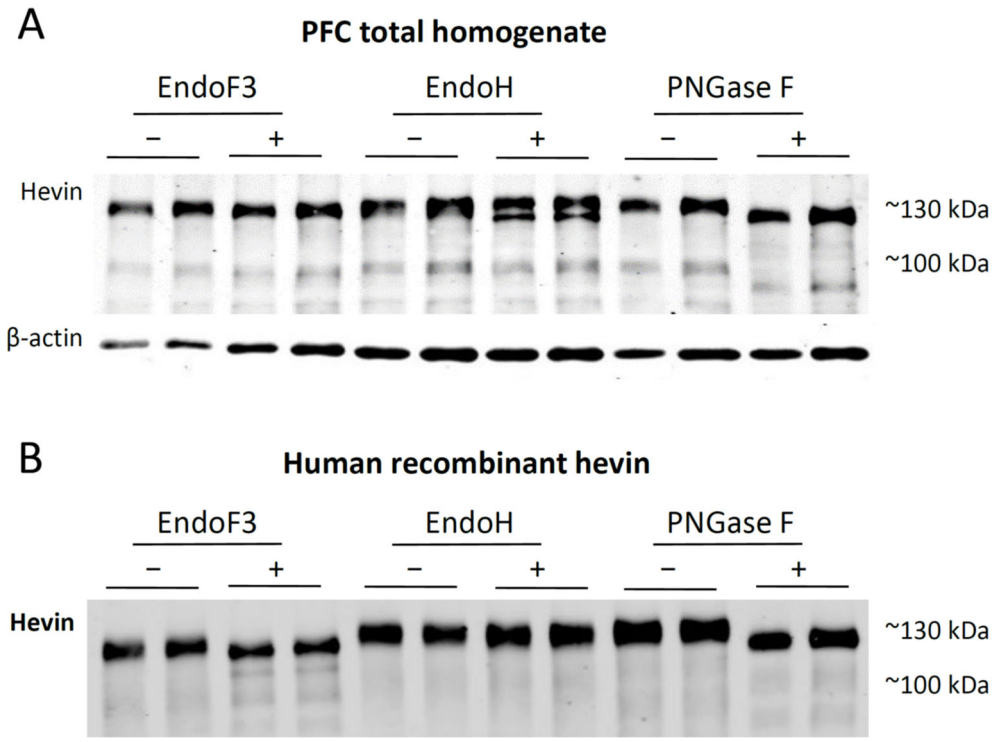

Figure 4.5. Glycosylation patterns of hevin in human brain. (A, B) Hevin immunoreactivity in a prefrontal cortex total homogenate pool **(A)** and in human recombinant hevin **(B)** after treatment with EndoF3, EndoH or PNGaseF enzymes for 5 h at 37°C. Samples were run in duplicate and experiments were performed in triplicates. A representative Western blot image for each experiment is shown. Blot A was incubated with anti- β-actin antibody.

4.1.3. STUDY OF THE ENDOGENOUS PROTEOLYSIS OF HEVIN

To determine if the ~100 kDa band derived from the ~130 kDa band via proteolytic degradation, prefrontal cortex total homogenate pool samples were incubated at 37°C in the absence of protease inhibitors for a range of times, then denatured at 95°C for 5 min, and immediately processed by Western blot. Immunoreactive intensity of both bands remained unchanged throughout the entire 3 h experiment **(Figure 4.6A)**, suggesting the absence of endogenous proteolysis.

The effect the temperature factor on hevin proteolysis was also tested. For this purpose, prefrontal cortex total homogenate pool samples were incubated for 15 min in temperatures ranging from 4 to 95°C and immediately processed by Western blot. Temperature-dependent proteolysis did not alter the intensity of neither of both bands **(Figure 4.6B)**. These results suggest that the lower ~100 kDa band is not a degradation product of the ~130 kDa band.

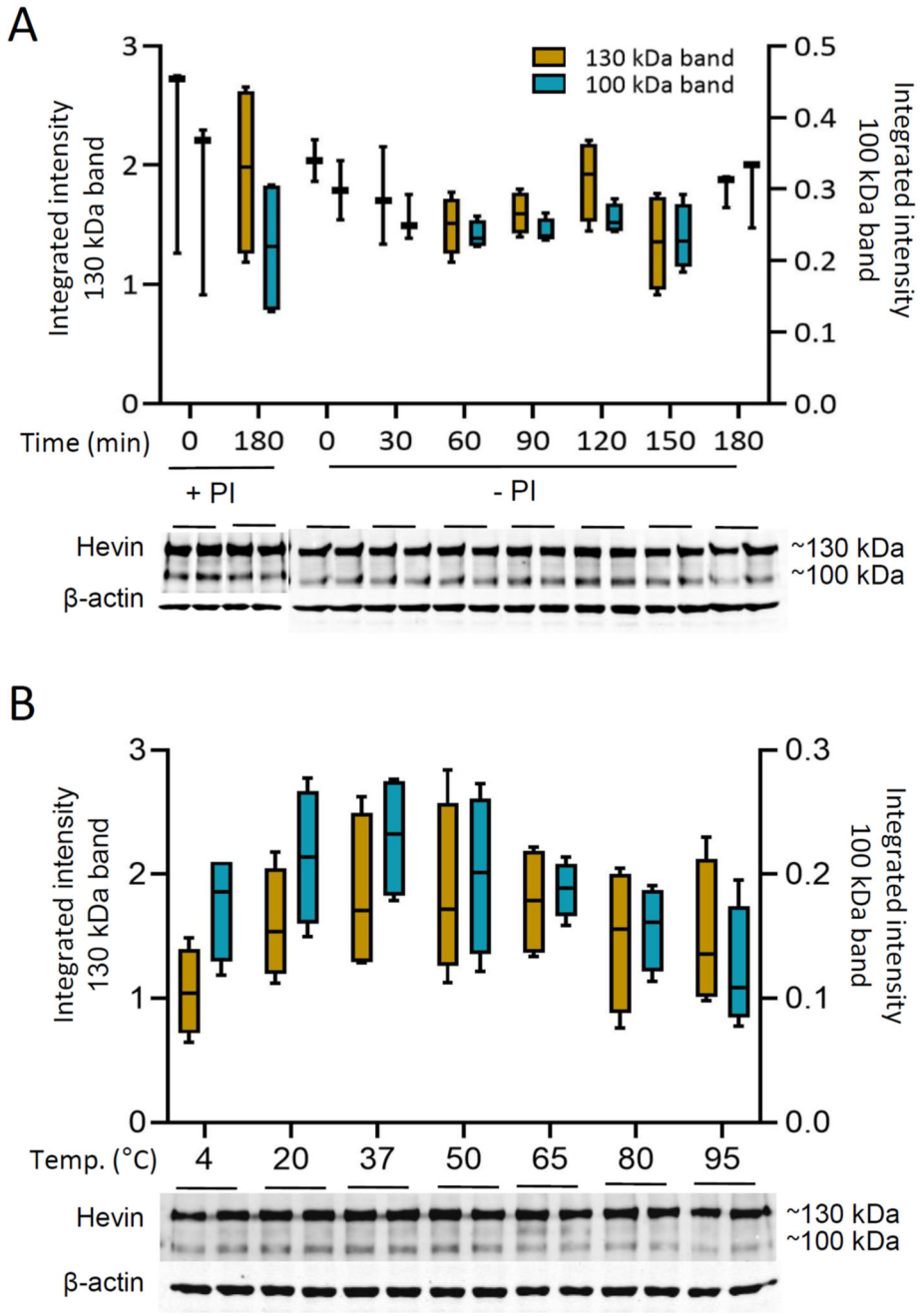

Figure 4.6. Proteolytic degradation of hevin in human brain. (A) Hevin immunoreactivity and corresponding β-actin-normalized quantification in a prefrontal cortex total homogenate pool (20 µg) after incubation with (+PI) or without (-PI) protease inhibitors for a duration of 0 to 180 min at 37°C. **(B)** Hevin immunoreactivity and corresponding β-actin-normalized quantification in a prefrontal cortex total homogenate pool (20 µg) after incubation at different temperatures (4°C–95°C) for 15 min. Samples were run in duplicate and experiments were performed in triplicate. A representative Western blot image for each experiment is shown. The quantification is represented in box-and-whiskers plots, where "box" shows the median and the 25th and 75th percentile and the "whiskers" depict the 5th and 95th percentile.

4.1.4. STUDY OF THE ENZYMATIC DIGESTION WITH THE HEVIN DEGRADING ENZYMES ADAMTS4, MMP-3 AND THROMBIN PROTEASES

The matrix metalloproteases ADAMTS4 (a disintegrin and metalloproteinase with thrombospondin motifs 4), MMP-3 (matrix metalloproteinase-3) and thrombin have been described to cleave hevin in rodent brains, giving as a product the C-terminal SPARC-like fragment (SLF), which shares a high homology with SPARC, a close homologue of hevin, and which antagonizes hevin's synaptogenic function (Weaver et al., 2011; Weaver et al., 2010). To confirm the sensitivity of human hevin towards ADAMTS4, MMP-3 and thrombin, proteolysis assays were performed by incubating prefrontal cortex total homogenate samples and human recombinant hevin with the three proteases.

As expected, incubation with ADAMTS4 or MMP-3 enzymes led in human prefrontal cortex to a marked decreased in the intensity of the ~130 kDa and ~100 kDa bands with a concomitant appearance of an intense ~40 kDa double band **(Figure 4.7A, arrow)**, which seems to correspond to SLF (Weaver et al., 2011; Weaver et al., 2010). Likewise, proteolysis of human recombinant hevin with the same enzymes decreased the intensity of full-length hevin protein bands. Surprisingly, the band corresponding to the hypothesized SLF had slightly greater molecular weight around 47 kDa **(Figure 4.7A, filled arrowhead)**. Importantly, the SLF fragment was identified in non-digested prefrontal cortex samples, although it showed lower intensity level compared to the ~130 kDa and ~100 kDa bands **(Figure 4.7A, open arrowhead)**. On the other hand, hevin proteolytic cleavage by thrombin in both prefrontal cortex and recombinant proteins, decreased levels of the ~130 kDa and ~100 kDa bands and produced many fragments higher than 50 kDa **(Figure 4.7B)**.

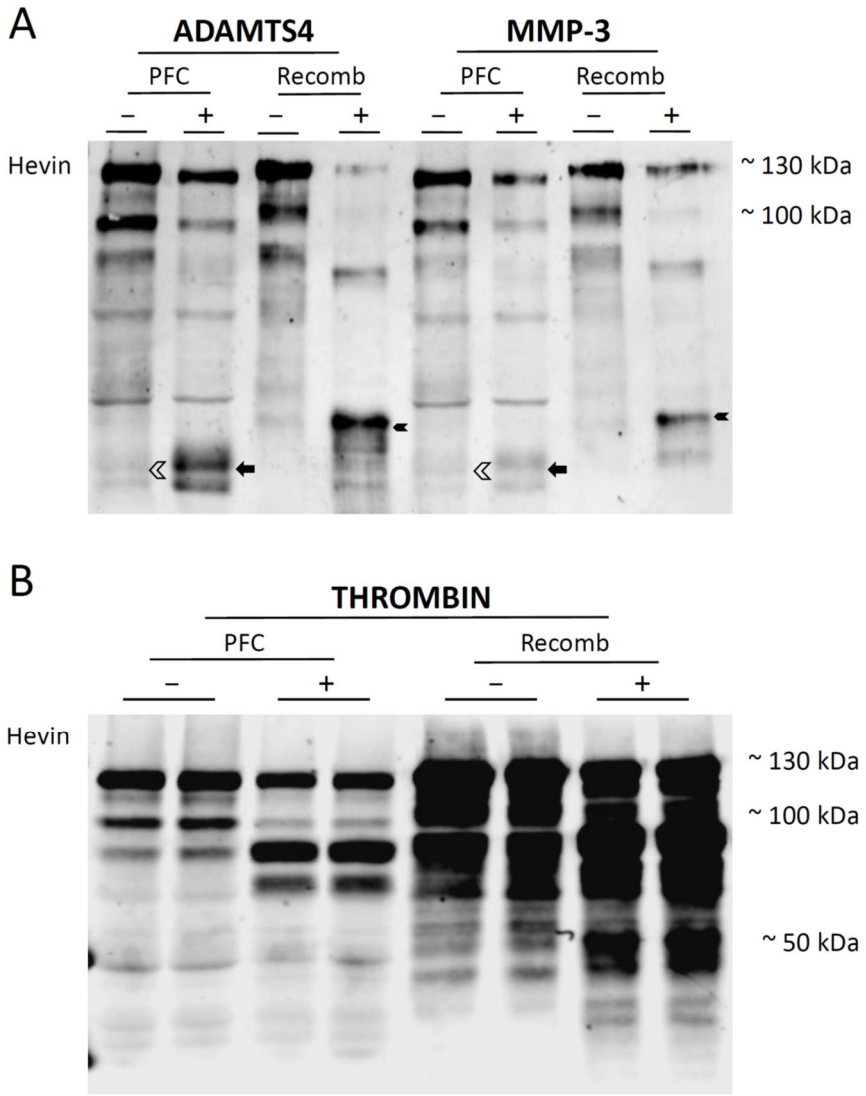

Figure 4.7. Sensitivity of human hevin to matrix metalloproteases and serine protease. (A) Hevin immunoreactivity in a prefrontal cortex total homogenate pool (50 µg) and in human recombinant hevin (140 µg) after treatment with ADAMTS4 or MMP-3 enzymes for 5 h at 37°C (*arrow*: ~40 kDa double band detected in digested- prefrontal cortex; *filled arrowhead*: ~47 kDa double band detected in digested-recombinant protein; *empty arrowhead*: hypothetical ~40 kDa SLF fragment in non-digested prefrontal cortex). **(B)** Hevin immunoreactivity of prefrontal cortex total homogenate pool (70 µg) or human recombinant hevin (20 ng) after incubation for 15 h at 37°C in the presence or absence of thrombin (1 U). Experiments were performed in triplicates and samples from thrombin assay were run in duplicate. A representative Western blot image for each experiment is shown. *PFC, prefrontal cortex.*

Finally, in both ADAMTS4 and MMP-3 dependent-proteolysis assays, more pronounced effects were detected when increasing the incubation time from 1 h to 5 h. A greater increase in the ~40 kDa double band from prefrontal cortex and in the ~47 kDa fragment from the human recombinant protein could be observed **(Figure 4.8 and Figure 4.9, respectively)**.

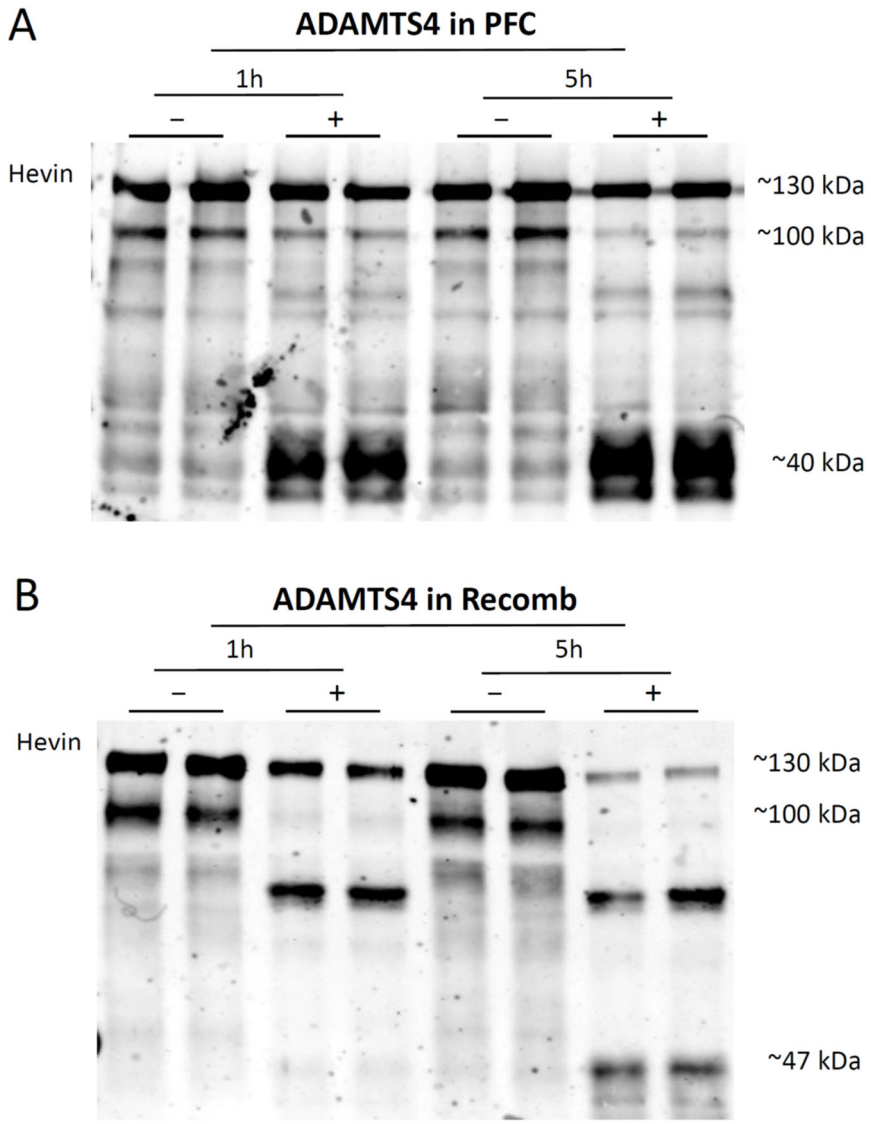

Figure 4.8. ADAMTS4-dependent proteolysis of human hevin. (A) Hevin immunoreactivity of prefrontal cortex total homogenate (50 µg) and **(B)** human recombinant hevin (140 µg) after 1 h or 5 h (37°C) incubation in the presence or absence of ADAMTS4 (2 µg) protease. Samples were run in duplicate and experiments were performed in triplicates. A representative Western blot image for each experiment is shown. *PFC, prefrontal cortex.*

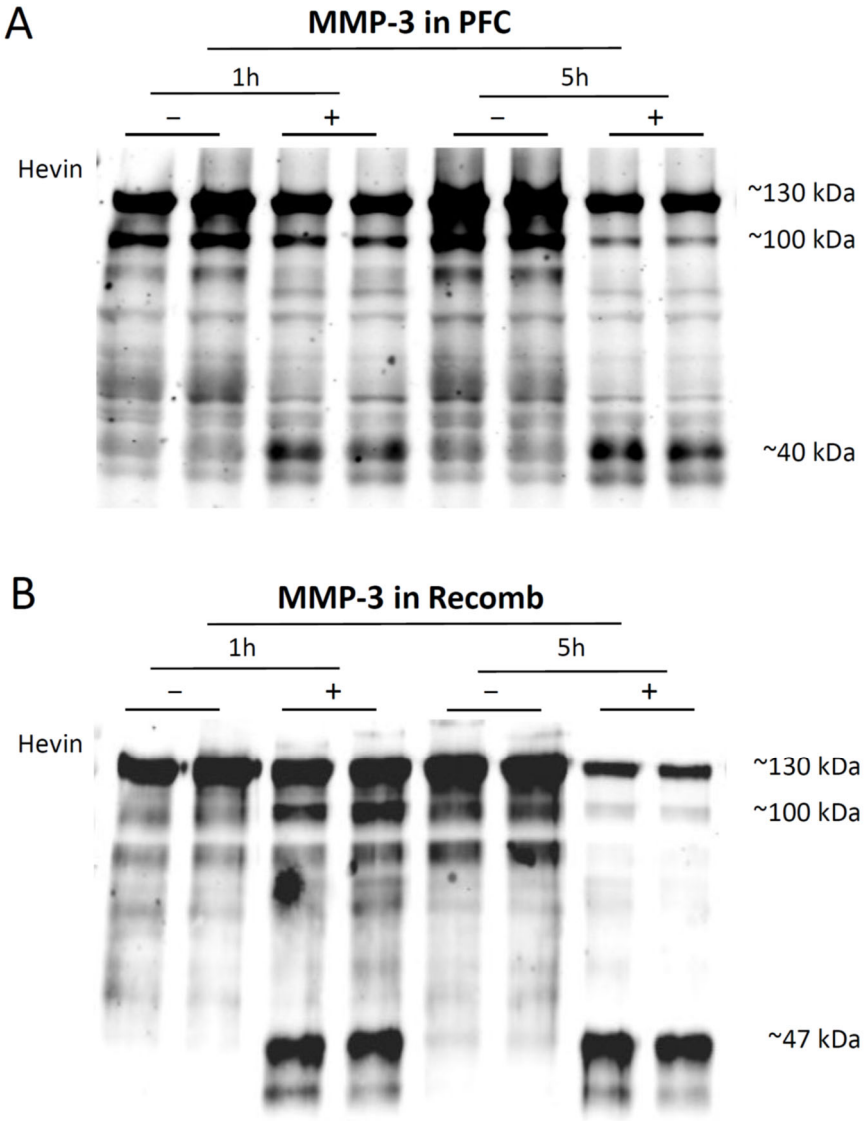

Figure 4.9. MMP-3-dependent proteolysis of human hevin. (A) Hevin immunoreactivity of prefrontal cortex total homogenate pool (50 µg) and **(B)** human recombinant hevin (140 µg) after 1 h or 5 h (37°C) incubation in the presence or absence of MMP-3 (0.4 µg) protease. Samples were run in duplicate and experiments were performed in triplicates. A representative Western blot image for each experiment is shown. *PFC, prefrontal cortex.*

4.1.5. EFFECTS OF SEX, AGE, POSTMORTEM DELAY AND STORAGE TIME ON HEVIN IMMUNOREACTIVITY

A large control group of 29 prefrontal cortex total homogenate samples (11 females and 18 males ranging from 18 to 71 years old) was analyzed in order to test the putative effects of the following variables in the expression of hevin: sex, age, PMD and samples' storage time.

Neither sex (11 females vs 18 males), nor age (18–71 years) showed significant differences or correlation with the immunoreactivity of any of the two detected bands (sex: ~130 kDa band p= 0.3544; ~100 kDa band p= 0.9787; age: ~130 kDa p= 0.9248 and ~100 kDa p= 0.0514; **Figure 4.10A-D**).

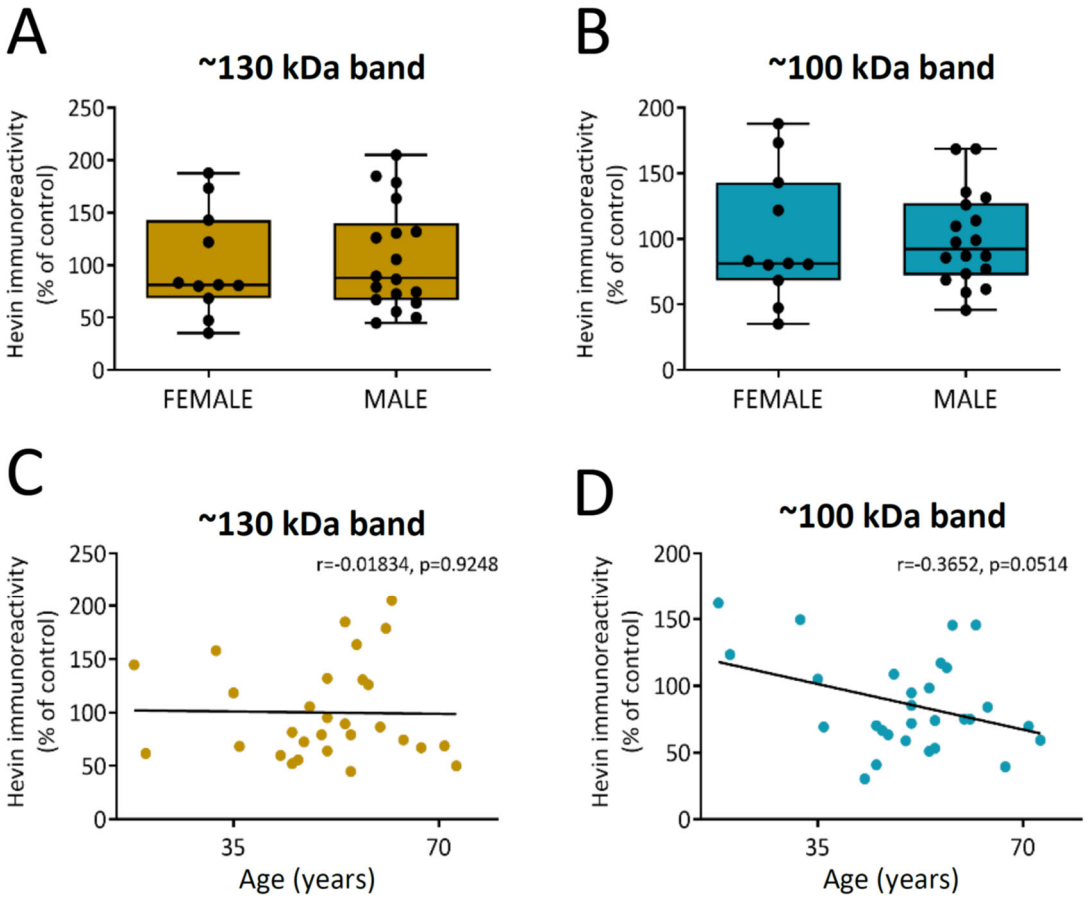

Figure 4.10. Influence of sex and age on hevin expression. (A, B) Sex comparison between 11 females and 18 males of ~130 kDa **(A)** and ~100 kDa **(B)** β-actin normalized hevin bands immunoreactivity in prefrontal cortex total homogenates. **(C,D)** Correlation of age with β-actin normalized ~130 kDa **(C)** and ~100 kDa **(D)** hevin bands immunoreactivity in total homogenate preparations from human prefrontal cortex of 29 control subjects. Statistical comparison between sexes was performed by two-tailed Student's t-test and correlation analyses by two-tailed Pearson´s correlation test (Pearson' r value, *p* value and the regression line are shown in each correlation graph). In the sexes comparison the quantification is represented in box-and-whiskers plots, where "box" shows the median and the 25th and 75th percentile and the "whiskers" depict the 5th and 95th percentile. Dots represent the average value of each individual in the performed experiments.

In the same way, no significant correlation was observed between hevin expression levels and neither postmortem delay (3-39 h) nor storage time (18-244 months; PMD ~130 kDa p= 0.5809 and ~100 kDa p= 0.3022; storage time ~130 kDa p= 0.5252 and ~100 kDa p= 0.9477; **Figure 4.11A-D**).

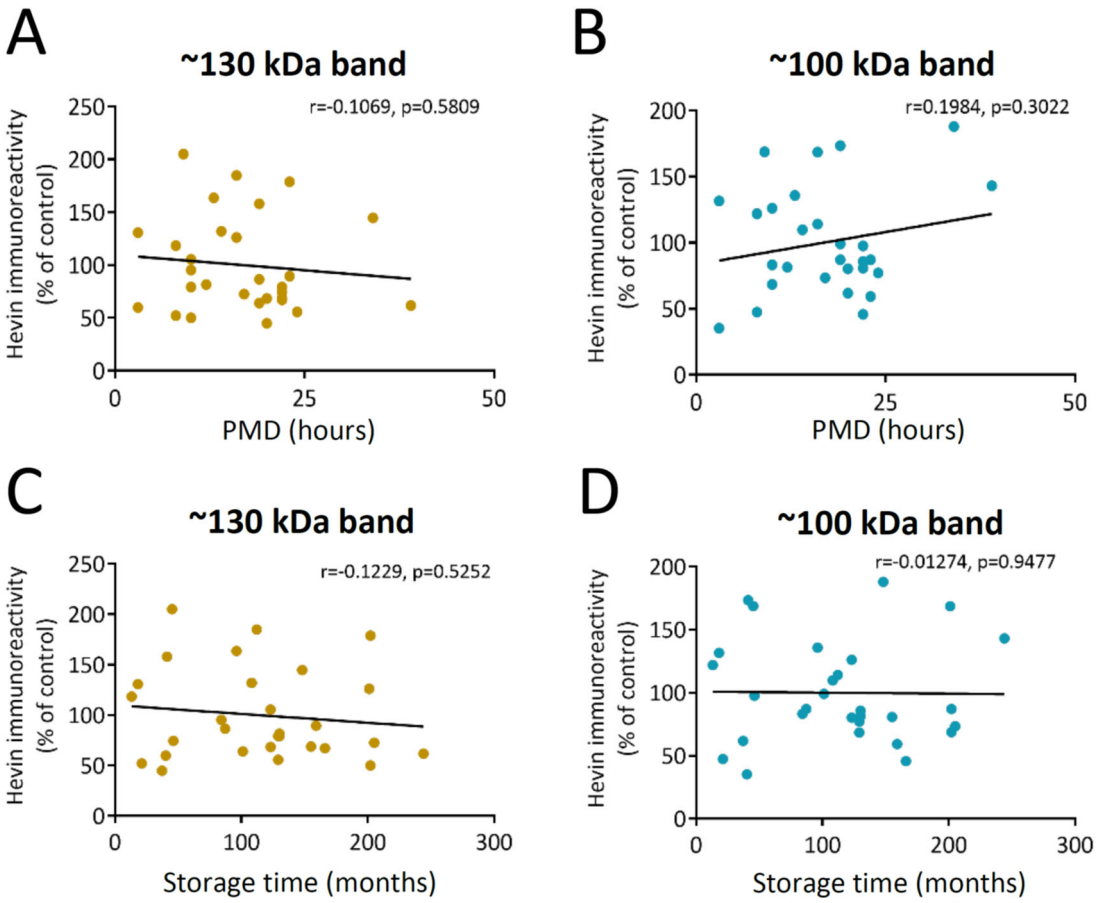

Figure 4.11. Influence of PMD and sample's storage time on hevin expression. Postmortem delay **(A,B)** and storage time **(C,D)** correlation with β-actin normalized ~130 kDa **(A,C)** and ~100 kDa **(B,D)** hevin bands immunoreactivity in total homogenate preparations from human prefrontal cortex of 29 control subjects. Correlation analyses were performed by two-tailed Pearson´s correlation test (Pearson' r value, *p* value and the regression line are shown in each correlation graph). Dots represent the average value of each individual in the performed experiments.

Interestingly, analyzing this large control group, a positive correlation between ~130 kDa and ~100 kDa bands (p< 0.0001) was found, indicating that subjects that showed high levels for one form also showed high levels for the other, and conversely **(Figure 4.12)**.

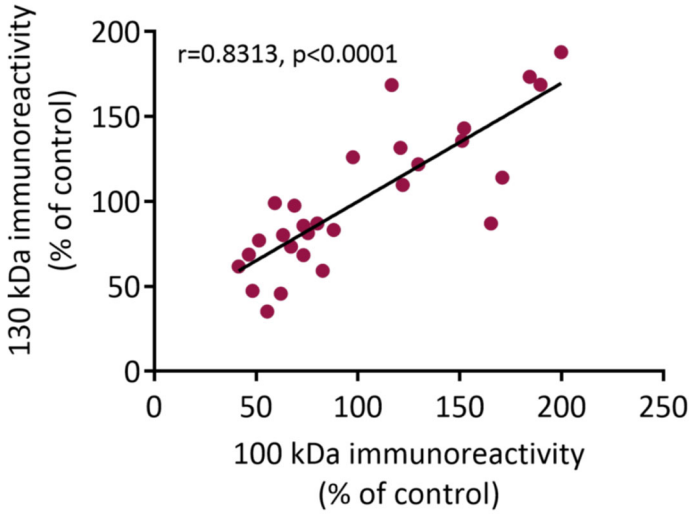

Figure 4.12. Correlation between both hevin isoforms. Statistical linear correlation between β-actin normalized ~130 kDa and ~100 kDa hevin bands immunoreactivity in total homogenate preparations from human prefrontal cortex of 29 control subjects. Correlation analysis was performed by two-tailed Pearson´s correlation test (Pearson' r value, *p* value and the regression line are shown). Dots represent the average value of each individual in the performed experiments.

4.1.6. CHARACTERIZATION OF HEVIN PROTEIN EXPRESSION IN POSTMORTEM HUMAN BRAIN

4.1.6.1. Validation of the human brain subcellular fractionation

In order to study the presence or absence of hevin in the cytosol and/or in the neuronal membranes, subcellular fractionation of human brain tissue was performed and the obtained fractions were analyzed by Western blot. By this way, both hevin immunoreactive bands (~130 and ~100 kDa) were also detected in cytosolic and neuronal membrane-enriched (P2) fractions from human prefrontal cortex samples **(Figure 4.13)**. To validate the complete subcellular fractionation, the three prepared fractions from human prefrontal cortex (total homogenate, cytosolic and P2) were incubated with antibodies against proteins anchored to the neuronal or vesicular membranes or cytosolic proteins **(Table 4)**. The immunodetected synaptic proteins were syntaxin1A, VGLUT1 (Vesicular glutamate transporter 1), NR2A (N-methyl D-aspartate receptor subtype 2A) and PSD95 (postsynaptic

density protein 95), while the immunodetected cytosolic proteins were stathmin and IκBα (NFκB inhibitor alpha).

The correct fractionation of human brain tissue was confirmed by the enrichment of the synaptic proteins (syntaxin1A, VGLUT1, NR2A and PSD95) in the P2 fraction, while they were almost absent in the cytosolic fraction and, vice versa, the enrichment of the cytosolic proteins (stathmin and IκBα) in the cytosolic fraction, with very low presence in the P2 fraction **(Figure 4.13)**.

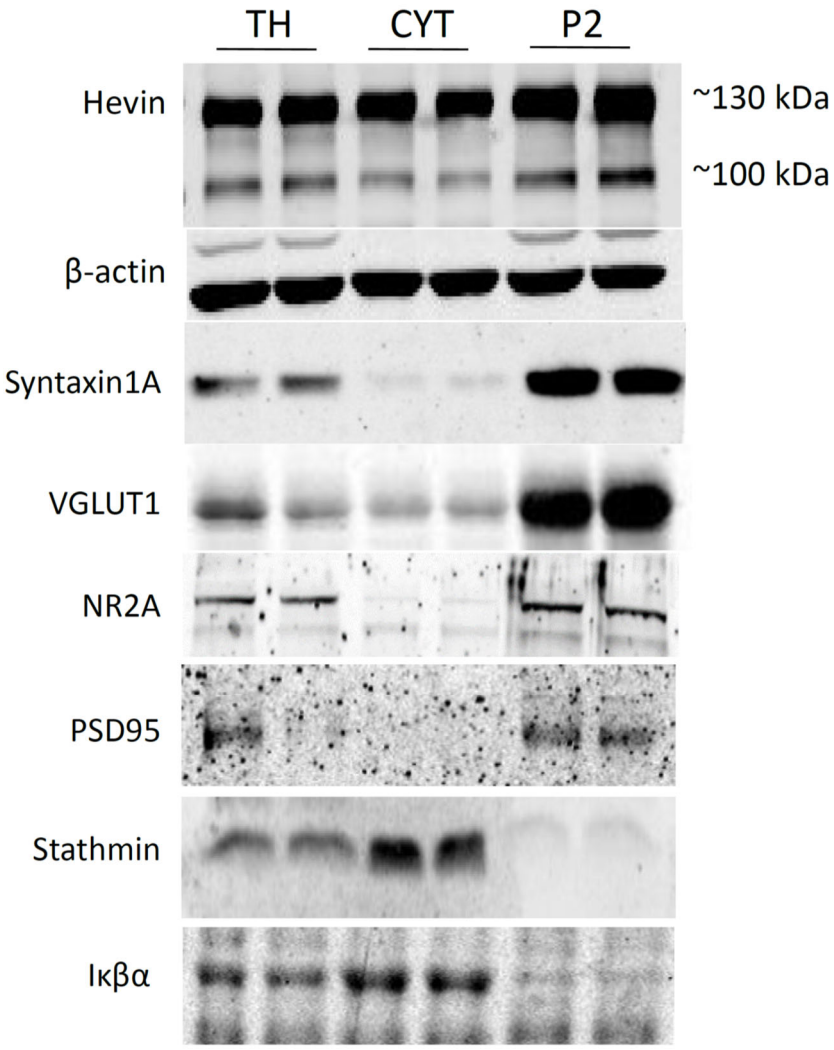

Figure 4.13. Validation of the subcellular fractionation of human prefrontal cortex pool samples. Enrichment of synaptic proteins (Syntaxin1A, VGLUT1, NR2A, PSD95) in P2 membrane fraction and enrichment of cytosolic proteins (Stathmin, IKβα) in the cytosolic fraction. Samples were run in duplicate and a representative Western blot images are shown. *TH: total homogenate, CYT: cytosol, P2: membrane-enriched fraction.*

4.1.6.2. Subcellular distribution of hevin in postmortem human brain

Using cellular fractionation of human brain samples, the subcellular distribution of both full-length forms of hevin (~130 and ~100 kDa) was studied by Western blot. The immunodetection and quantification of hevin was performed individually in four human brain areas (prefrontal cortex, hippocampus, caudate nucleus and cerebellum) from 6 control subjects' samples.

Both hevin ~130 and ~100 kDa bands were expressed in cytosolic and membrane-enriched (P2) fractions, with a strongly enhanced expression in the P2 fraction compared to the cytosolic one **(Figures 4.14-4.17)**. This subcellular expression pattern was observed in all assessed brain areas, almost all of them showing statistical significant differences between cytosolic and P2 fractions, with the exception of the 100 kDa hevin band of the prefrontal cortex **(Table 4.1)**.

	PFC	**HIP**	**CAU**	**CB**
~130 kD band	CYT: 92% ± 21 P2: 183% ± 15 (*p*= 0.0042)	CYT: 82% ± 23 P2: 186% ± 27 (*p*= 0.0110)	CYT: 63% ± 9 P2: 186% ± 17 (*p*= 0.0002)	CYT: 62% ± 6 P2: 325% ± 57 (*p*= 0.0001)
~100 kD band	CYT: 119% ± 24 P2: 189% ± 33 (*p*= 0.1168)	CYT: 85% ± 21 P2: 166% ± 32 (*p*= 0.0399)	CYT: 87% ± 12 P2: 175% ± 14 (*p*= 0.0014)	CYT: 70% ± 11 P2: 148% ± 28 (*p*= 0.0266)

Table 4.1. Data of the quantification and statistical analysis of the immunoreactivity of the two hevin bands (~130 kDa and ~100 kDa) in cytosol (CYT) and membrane-enriched fraction (P2) of different brain areas *(PFC: prefrontal cortex, HIP: hippocampus, CAU: caudate nucleus, CB: cerebellum)***.** Data were calculated as the percentage of the mean of the total homogenate fraction and shown as the mean of each fraction ± SEM (standard error of the mean). Kruskal-Wallis followed by Dunn's multiple comparisons test was used for each comparison.

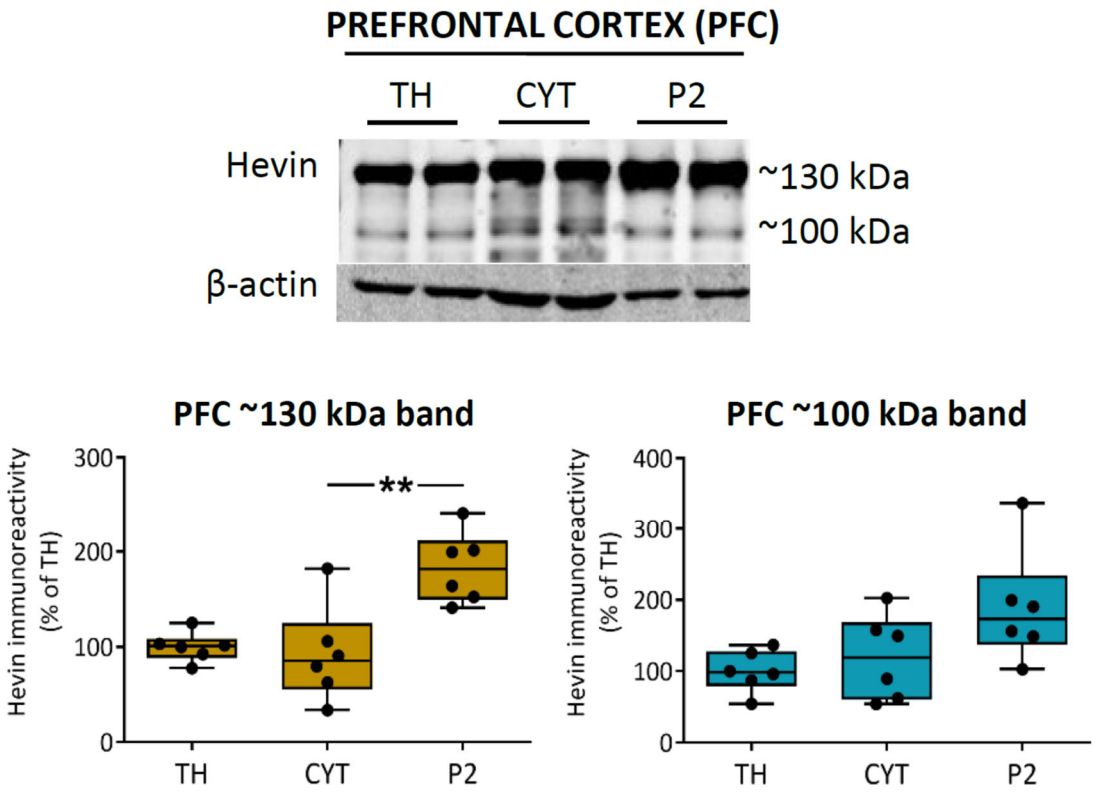

Figure 4.14. Expression of hevin in total homogenate, cytosolic and membrane-enriched (P2) fractions in human prefrontal cortex (PFC). β-actin-normalized hevin immunoreactivity and its ~130 kDa and ~100 kDa bands quantification in different cellular preparations (*TH: total homogenate, CYT: cytosol, P2: membrane-enriched fraction*) obtained from the prefrontal cortex (15 µg). Kruskal-Wallis followed by Dunn's multiple comparisons test was used for each comparison (**$p < 0.01$). Samples were run in duplicate and experiments were performed in triplicate. A representative Western blot image is shown in the figure. The quantification is represented in box-and-whiskers plots, where "box" shows the median and the 25th and 75th percentile and the "whiskers" depict the 5th and 95th percentile. Dots represent the average value of each individual in the performed experiments.

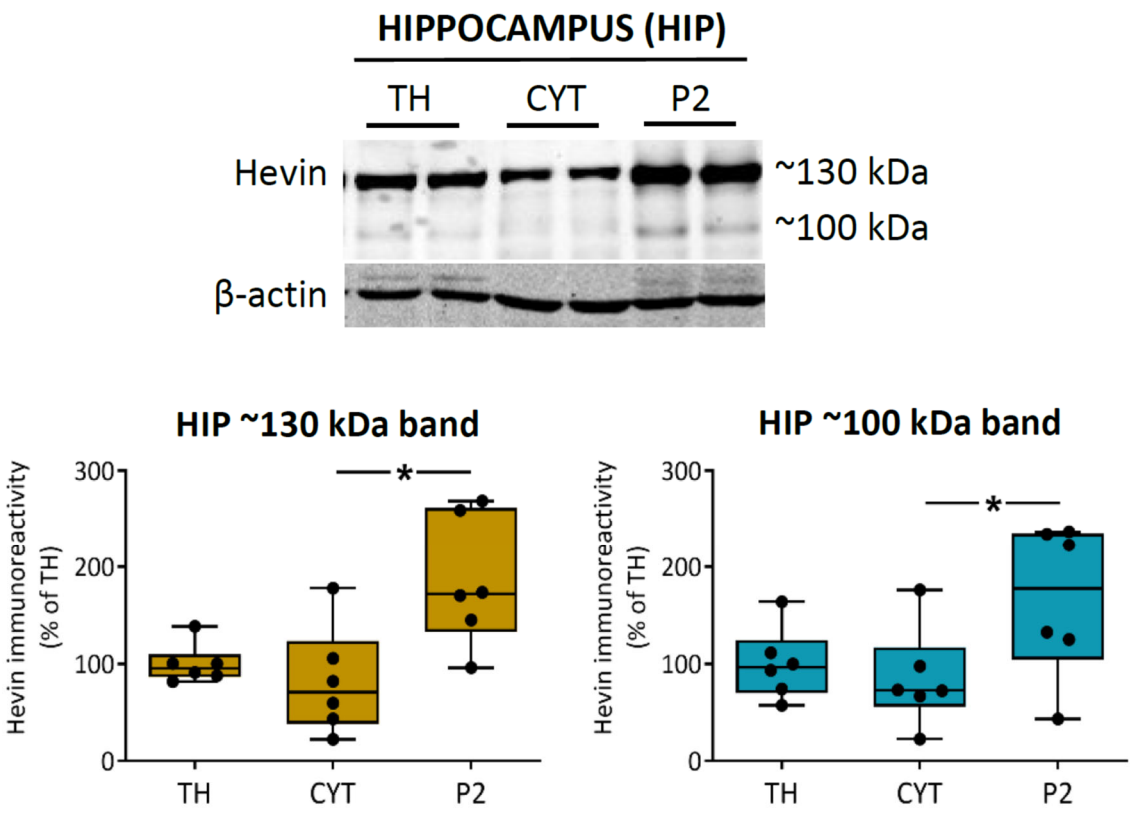

Figure 4.15. Expression of hevin in total homogenate, cytosolic and membrane-enriched (P2) fractions in human hippocampus (HIP). β-actin-normalized hevin immunoreactivity and its ~130 kDa and ~100 kDa bands quantification in different cellular preparations (*TH: total homogenate, CYT: cytosol, P2: membrane-enriched fraction*) obtained from the HIP (15 µg). Kruskal-Wallis followed by Dunn's multiple comparisons test was used for each comparison (*$p < 0.05$). Samples were run in duplicate and experiments were performed in triplicate. A representative Western blot image is shown in the figure. The quantification is represented in box-and-whiskers plots, where "box" shows the median and the 25th and 75th percentile and the "whiskers" depict the 5th and 95th percentile. Dots represent the average value of each individual in the performed experiments.

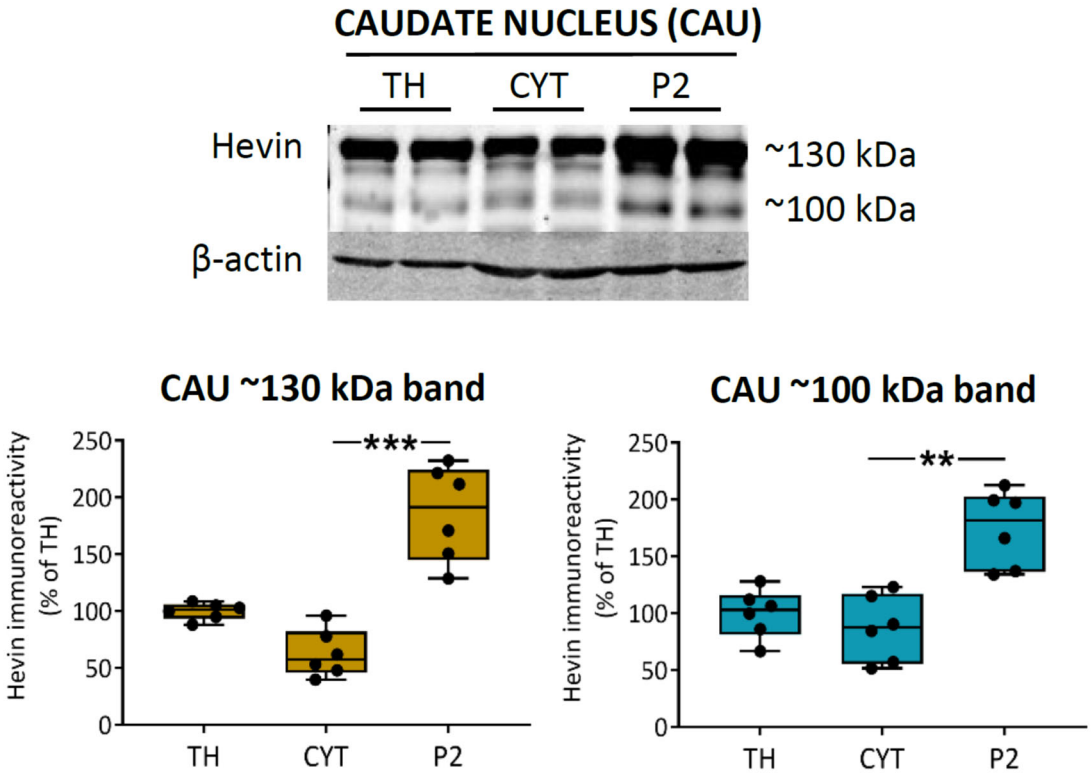

Figure 4.16. Expression of hevin in total homogenate, cytosolic and membrane-enriched (P2) fractions in human caudate nucleus (CAU). β-actin-normalized hevin immunoreactivity and its ~130 kDa and ~100 kDa bands quantification in different cellular preparations (*TH: total homogenate, CYT: cytosol, P2: membrane-enriched fraction*) obtained from the CAU (15 µg). Kruskal-Wallis followed by Dunn's multiple comparisons test was used for each comparison (**$p < 0.01$, ***$p < 0.001$). Samples were run in duplicate and experiments were performed in triplicate. A representative Western blot image is shown in the figure. The quantification is represented in box-and-whiskers plots, where "box" shows the median and the 25th and 75th percentile and the "whiskers" depict the 5th and 95th percentile. Dots represent the average value of each individual in the performed experiments.

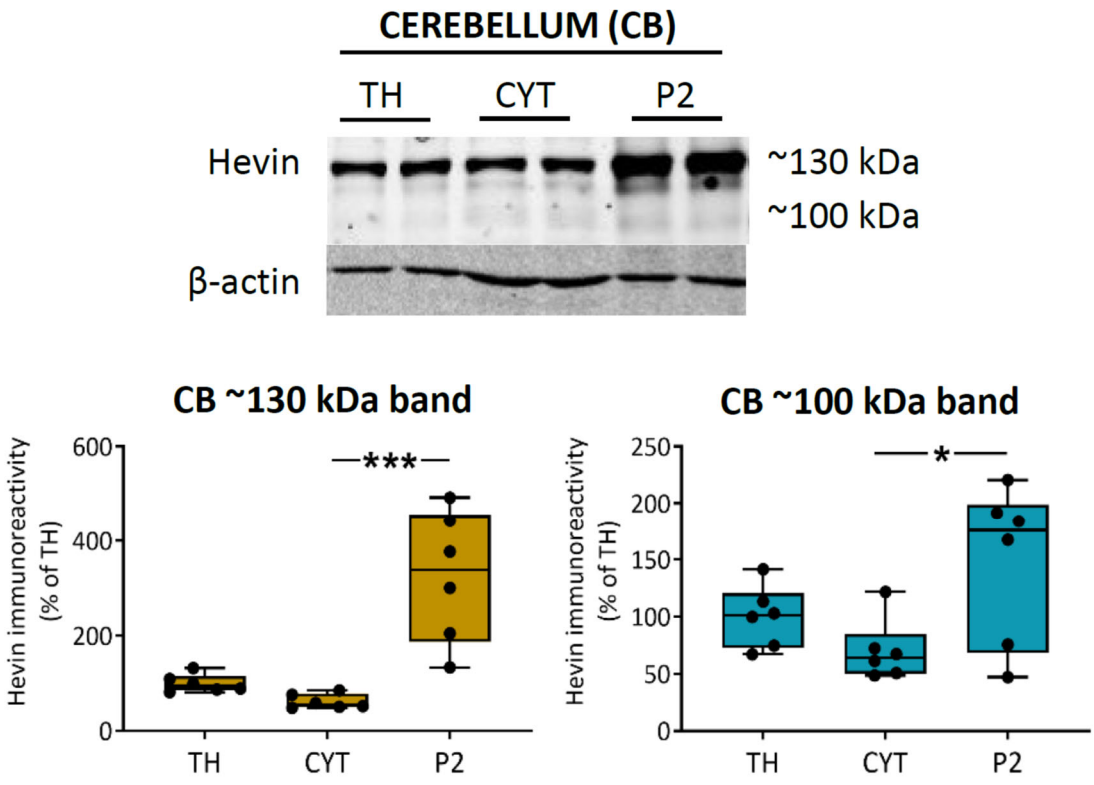

Figure 4.17. Expression of hevin in total homogenate, cytosolic and membrane-enriched (P2) fractions in human cerebellum (CB). β-actin-normalized hevin immunoreactivity and its ~130 kDa and ~100 kDa bands quantification in different cellular preparations (*TH: total homogenate, CYT: cytosol, P2: membrane-enriched fraction*) obtained from the cerebellum (15 µg). Kruskal-Wallis followed by Dunn's multiple comparisons test was used for each comparison (*$p < 0.05$, ***$p < 0.001$). Samples were run in duplicate and experiments were performed in triplicate. Samples were run in duplicate and experiments were performed in triplicate. A representative Western blot image is shown in the figure. The quantification is represented in box-and-whiskers plots, where "box" shows the median and the 25th and 75th percentile and the "whiskers" depict the 5th and 95th percentile. Dots represent the average value of each individual in the performed experiments.

4.1.6.3. Regional distribution of hevin in postmortem human brain

The expression pattern of the two full-length hevin forms (~130 and ~100 kDa) was also compared between different brain regions: prefrontal cortex, hippocampus, caudate nucleus and cerebellum by Western blot. Hevin immunodetection and quantification was performed in total homogenate, cytosol and membrane-enriched (P2) fractions. Samples containing 20 µg of total protein each from 6 control subjects were individually analyzed.

For each subcellular fraction (total homogenate, cytosol and P2), similar regional distribution was observed for the ~130 and ~100 kDa hevin forms, with the prefrontal cortex showing the highest expression of hevin bands in all cases. No differences were detected between the other brain regions **(Table 4.2 and Figures 4.18-4.20)**.

	TH	**CYT**	**P2**
~130 kD band	PFC: 100% ± 7	PFC: 100% ± 15	PFC: 100% ± 19
	HIP: 66% ± 6 ($p_{PFC\ vs\ HIP}$ = 0.0429)	HIP: 39% ± 8 ($p_{PFC\ vs\ HIP}$ = 0.0341)	HIP: 29% ± 8 ($p_{PFC\ vs\ HIP}$ = 0.0066)
	CAU: 78% ± 5 ($p_{PFC\ vs\ CAU}$ = 0.5337)	CAU: 47% ± 7 ($p_{PFC\ vs\ CAU}$ = 0.1812)	CAU: 54% ± 15 ($p_{PFC\ vs\ CAU}$ = 0.2592)
	CB: 50% ± 6 ($p_{PFC\ vs\ CB}$ = 0.0006)	CB: 38% ± 10 ($p_{PFC\ vs\ CB}$ = 0.0269)	CB: 48% ± 11 ($p_{PFC\ vs\ CB}$ = 0.1650)
~100 kD band	PFC: 100% ± 8	PFC: 100% ± 6	PFC: 100% ± 13
	HIP: 45% ± 7 ($p_{PFC\ vs\ HIP}$ = 0.0537)	HIP: 26% ± 6 ($p_{PFC\ vs\ HIP}$ = 0.0058)	HIP: 27% ± 9 ($p_{PFC\ vs\ HIP}$ = 0.0128)
	CAU: 54% ± 5 ($p_{PFC\ vs\ CAU}$ = 0.2592)	CAU: 37% ± 3 ($p_{PFC\ vs\ CAU}$ = 0.1986)	CAU: 61% ± 19 ($p_{PFC\ vs\ CAU}$ = 0.2825)
	CB: 21% ± 2 ($p_{PFC\ vs\ CB}$ < 0.0001)	CB: 17% ± 3 ($p_{PFC\ vs\ CB}$ = 0.0003)	CB: 23% ± 5 ($p_{PFC\ vs\ CB}$ = 0.0086)

Table 4.2. Data of the quantification and statistical analysis of the immunoreactivity of the two hevin bands (~130 kDa and ~100 kDa) in PFC (prefrontal cortex), HIP (hippocampus), CAU (caudate nucleus) and CB (cerebellum) of different cellular preparations *(TH: total homogenate, CYT: cytosol, P2: membrane-enriched fraction*). Data were calculated as the percentage of the mean of the prefrontal cortex and shown as the mean of each fraction ± SEM (standard error of the mean). Kruskal-Wallis followed by Dunn's multiple comparisons test was used for each comparison.

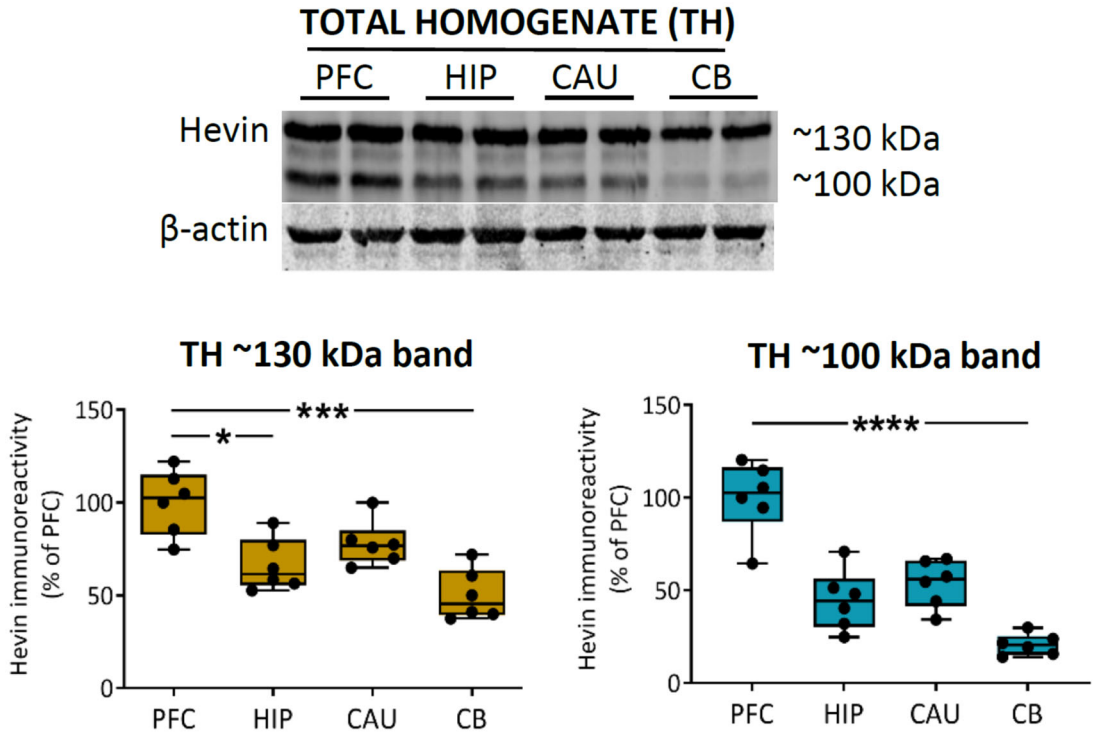

Fig. 4.18. Regional distribution of hevin in human brain total homogenate (TH) preparation. β-actin-normalized hevin immunoreactivity and its ~130 kDa and ~100 kDa bands quantification in different brain areas *(PFC: prefrontal cortex, HIP: hippocampus, CAU: caudate nucleus, CB: cerebellum)* from total homogenate preparation (20 µg). Kruskal-Wallis followed by Dunn's multiple comparisons test was used for each comparison (*$p < 0.05$, ***$p < 0.001$, ****$p < 0.0001$). Samples were run in duplicate and experiments were performed in triplicate. A representative Western blot image is shown in the figure. The quantification is represented in box-and-whiskers plots, where "box" shows the median and the 25th and 75th percentile and the "whiskers" depict the 5th and 95th percentile. Dots represent the average value of each individual in the performed experiments.

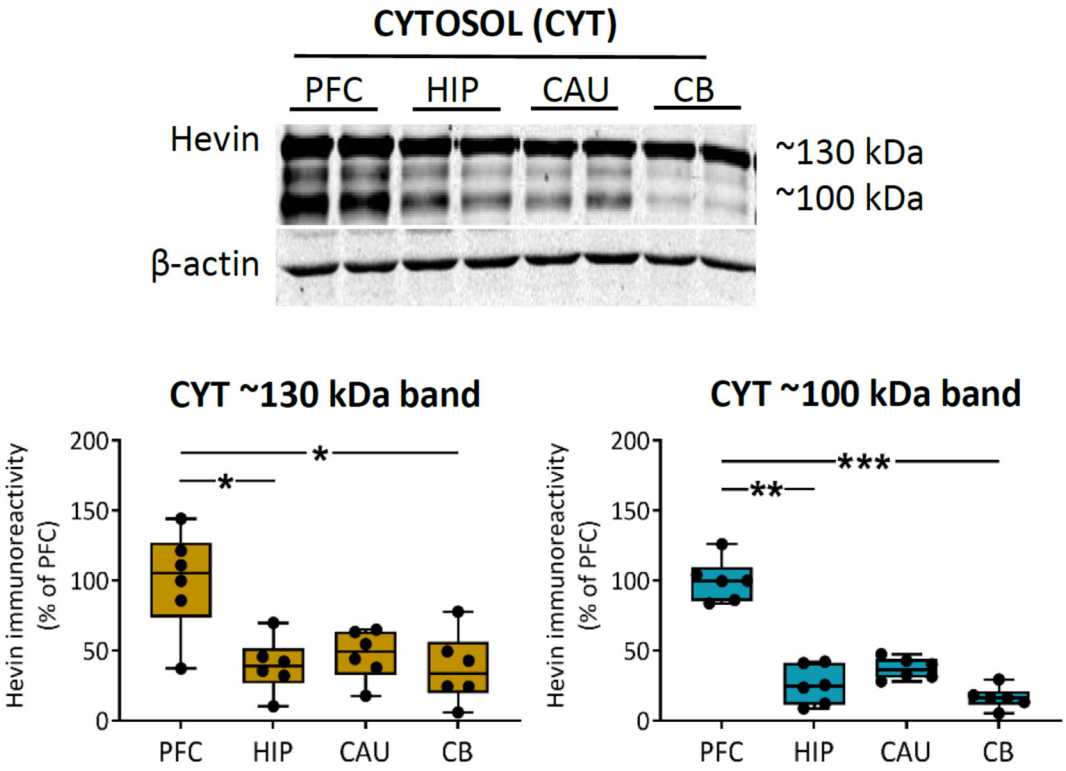

Figure 4.19. Regional distribution of hevin in human brain cytosol (CYT) preparation. β-actin-normalized hevin immunoreactivity and its ~130 kDa and ~100 kDa bands quantification in different brain areas *(PFC: prefrontal cortex, HIP: hippocampus, CAU: caudate nucleus, CB: cerebellum)* from cytosol preparation (20 µg). Kruskal-Wallis followed by Dunn's multiple comparisons test was used for each comparison (*$p < 0.05$, **$p < 0.01$, ***$p < 0.001$). Samples were run in duplicate and experiments were performed in triplicate. A representative Western blot image is shown in the figure. The quantification is represented in box-and-whiskers plots, where "box" shows the median and the 25th and 75th percentile and the "whiskers" depict the 5th and 95th percentile. Dots represent the average value of each individual in the performed experiments.

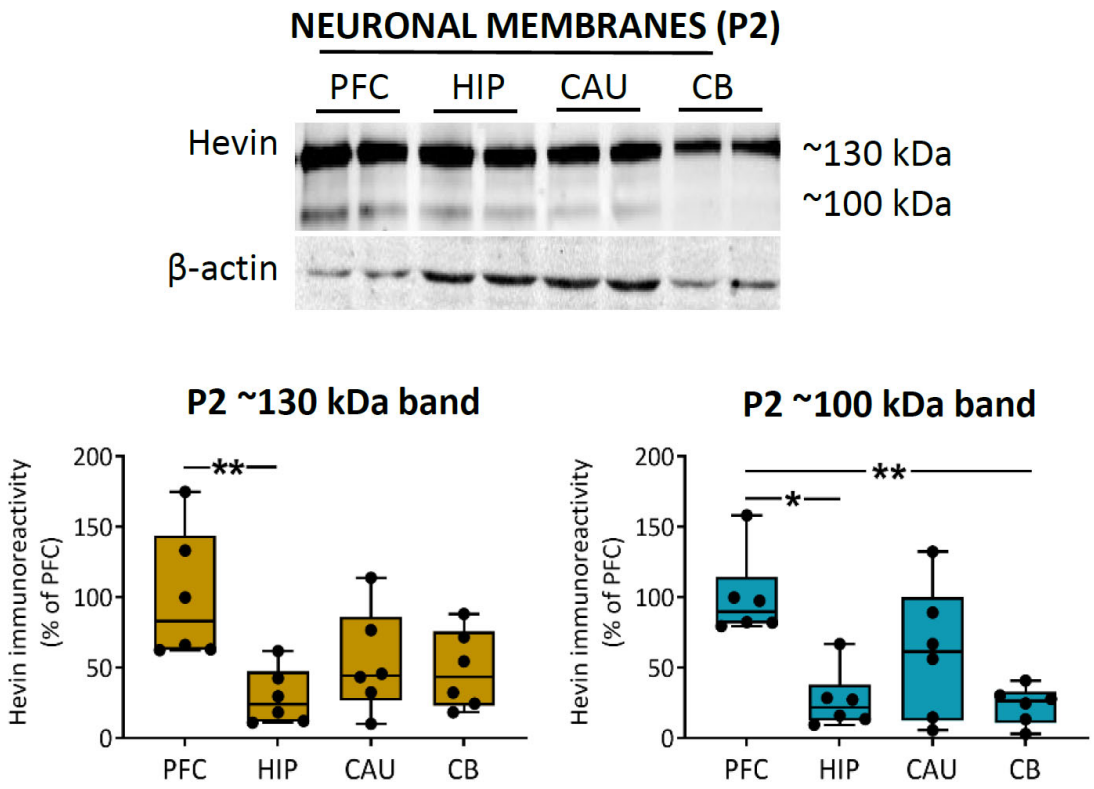

Figure 4.20. Regional distribution of hevin in human brain P2 preparation. β-actin-normalized hevin immunoreactivity and its ~130 kDa and ~100 kDa bands quantification in different brain areas *(PFC: prefrontal cortex, HIP: hippocampus, CAU: caudate nucleus, CB: cerebellum)* from P2 preparation (20 µg). Kruskal-Wallis followed by Dunn's multiple comparisons test was used for each comparison (*p< 0.05, **p< 0.01). Samples were run in duplicate and experiments were performed in triplicate. A representative Western blot image is shown in the figure. The quantification is represented in box-and-whiskers plots, where "box" shows the median and the 25th and 75th percentile and the "whiskers" depict the 5th and 95th percentile. Dots represent the average value of each individual in the performed experiments.

4.1.7. EVALUATION OF THE EXPRESSION LEVELS OF THE PROTEIN HEVIN IN ASTROCYTOMA AND MENINGIOMA HUMAN SAMPLES

The relative expression of both hevin forms (~130 kDa and ~100 kDa) was evaluated in astrocytoma (n=3) and meningioma brain tumors (n=3) by Western blot. Hevin protein expression was clearly detectable in both type of tumors **(Figure 4.21)**.

Interestingly, the hevin ~130 kDa immunoreactive band signal was significantly increased in astrocytoma tumors compared with prefrontal cortex total homogenates, and significantly decreased in meningioma tumors compared with prefrontal cortex (PFC) total homogenates (~130 kDa band: PFC 100% ± 7, astrocytoma 200% ± 37 and meningioma 15% ± 7, $p_{(\text{PFC vs astrocytoma})} = 0.024$, $p_{(\text{PFC vs meningioma})} = 0.024$). A lower immunoreactive signal intensity was detected in meningioma tumors in comparison to prefrontal cortex total homogenates for the ~100 kDa form, while no differences were detected between

prefrontal cortex total homogenates and astrocytoma samples (~100 kDa band: PFC 100% ± 8, astrocytoma 121% ± 44 and meningioma 4% ± 2, $p_{(PFC\ vs\ meningioma)} = 0.024$) **(Figure 4.21)**.

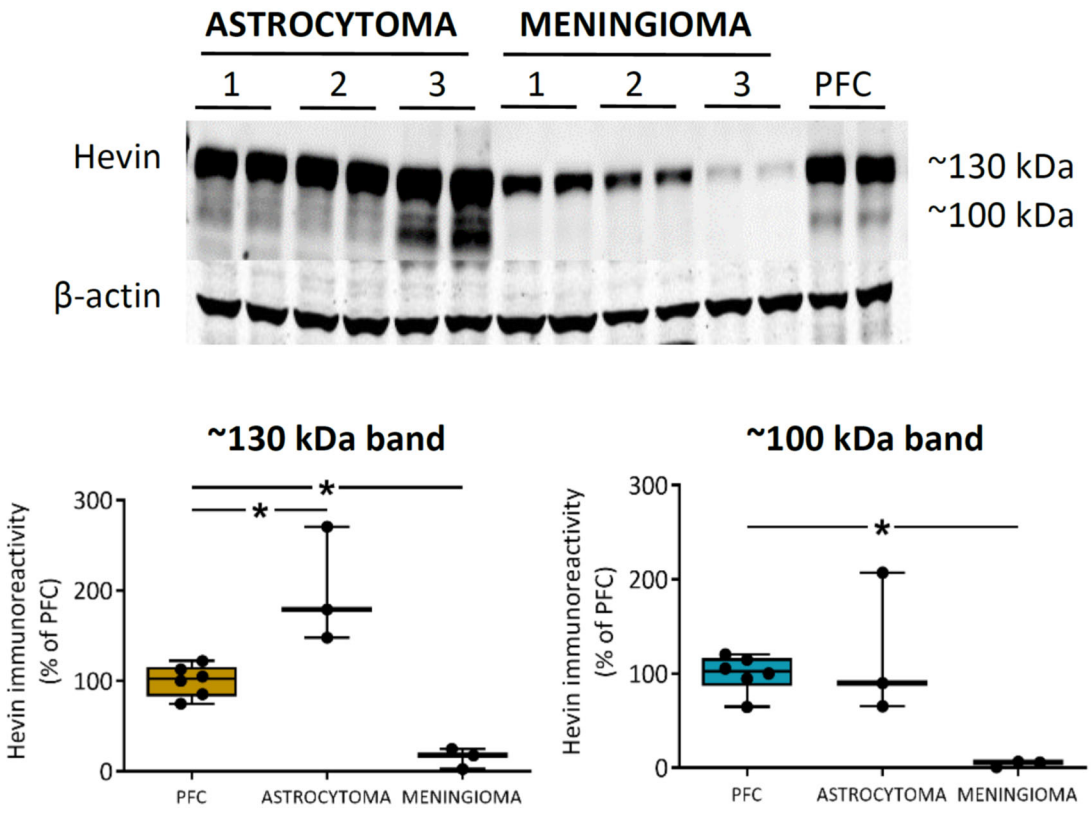

Figure 4.21. Hevin expression in astrocytoma and meningioma human samples. β-actin-normalized hevin immunoreactivity and its ~130 kDa and ~100 kDa bands quantification in total homogenate preparations of 3 astrocytoma , 3 meningioma and 6 prefrontal cortex samples . The statistical comparison was done by Mann-Whitney test (*$p < 0.05$). Samples were run in duplicate and experiments were performed in triplicate. A representative Western blot image is shown. The quantification is represented in box-and-whiskers plots, where "box" shows the median and the 25th and 75th percentile and the "whiskers" depict the 5th and 95th percentile. Dots represent the average value of each individual in the performed experiments. *PFC, prefrontal cortex.*

In order to assess if a differential alteration occurred for the both bands, the ~130 kDa/ ~100 kDa bands ratio was also calculated. This ratio was similar in both brain tumors (astrocytoma 34 ± 9 and meningioma 47 ± 13). However, it seems to be higher in both tumor types compared to control prefrontal cortex total homogenates (PFC ratio: 6 ± 1, astrocytoma ratio: 34 ± 9 and meningioma ratio: 47 ± 13, p= 0.024 in both cases) **(Figure 4.22)**.

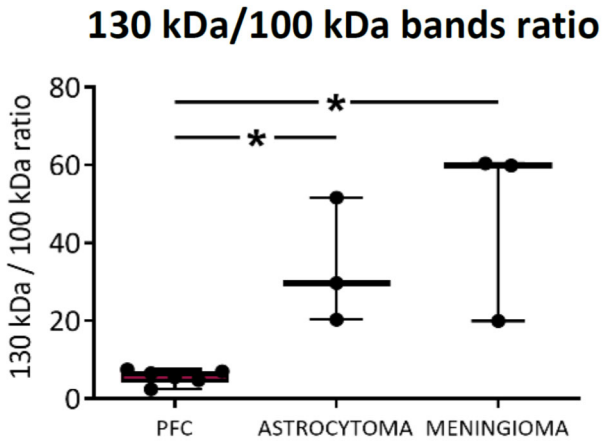

Figure 4.22. Relative expression of the hevin ~130 kDa and ~100 kDa bands in astrocytoma, meningioma and prefrontal cortex (PFC) samples. Relative expression levels of hevin bands calculated as ~130 kDa/ ~100 kDa ratio from total homogenate preparations of 3 astrocytoma, 3 meningioma and 6 prefrontal cortex samples. The statistical comparison was done by Mann-Whitney test (*p < 0.05). The quantification is represented in box-and-whiskers plots, where "box" shows the median and the 25th and 75th percentile and the "whiskers" depict the 5th and 95th percentile. Dots represent the average value of each individual in the performed experiments.

4.1.8. EVALUATION OF THE EXPRESSION LEVELS OF THE PROTEIN HEVIN IN HUMAN CEREBROSPINAL FLUID AND BLOOD FRACTIONS

Hevin protein expression was analyzed in 4 postmortem CSF samples from control subjects, and 4 plasma samples from living subjects. Hevin immunoreactive signal was detected in both CSF and plasma samples, with apparent higher levels in the CSF **(Figure 4.22)**. Significantly, a new pattern of hevin immunoreactivity was observed in both fluids. A shorter novel band of ~90 kDa band and the ~130 kDa band were detected, without the presence of ~100 kDa band **(Figure 4.23)**.

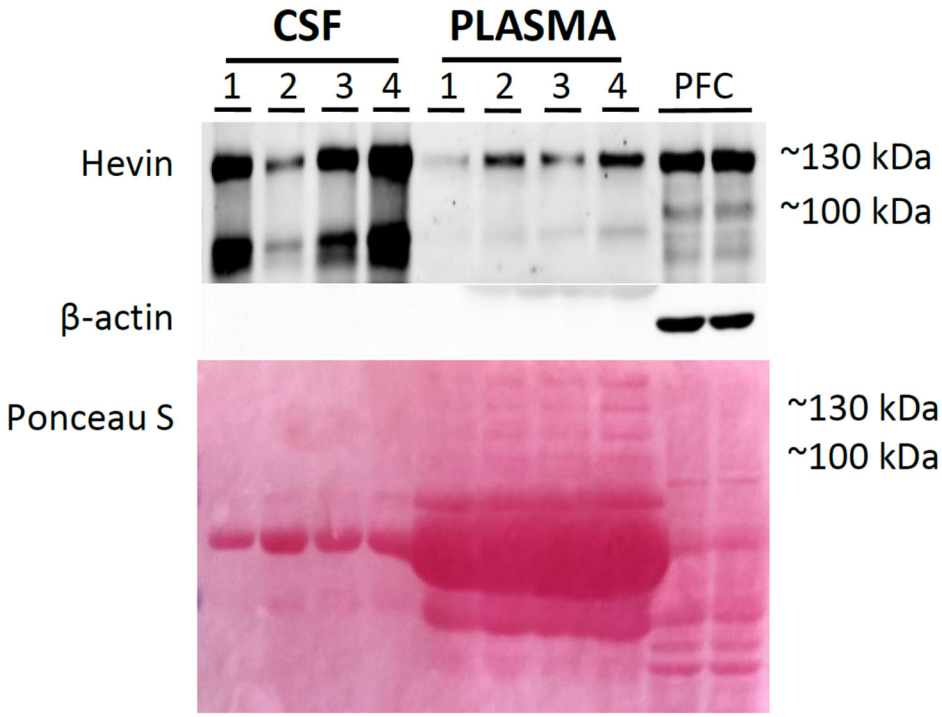

Figure 4.23. Hevin immunoreactivity in human CSF and plasma. Hevin immunoreactivity in CSF (n=4, 3.6 µg), plasma (n=4, 3.6 µg) and total homogenate prefrontal cortex control pool samples (15 µg). β-actin and Ponceau S staining are also shown. Prefrontal cortex pool sample was run in duplicate and experiments were performed in triplicate. A representative Western blot image is shown.

The presence of hevin in the plasma raised the question of what would be its source (i.e. where it would be released from). Therefore, the expression of hevin in different blood fractions (plasma, platelets, erythrocytes and leucocytes) was tested in order to assess if hevin is produced by blood cells or derives from other organs that would secrete it. Western blot analysis revealed that hevin, which was highly expressed in plasma, was absent in any other blood cell fraction **(Figure 4.24)**, suggesting that hevin is transported into the bloodstream and not synthesized by any blood cell type.

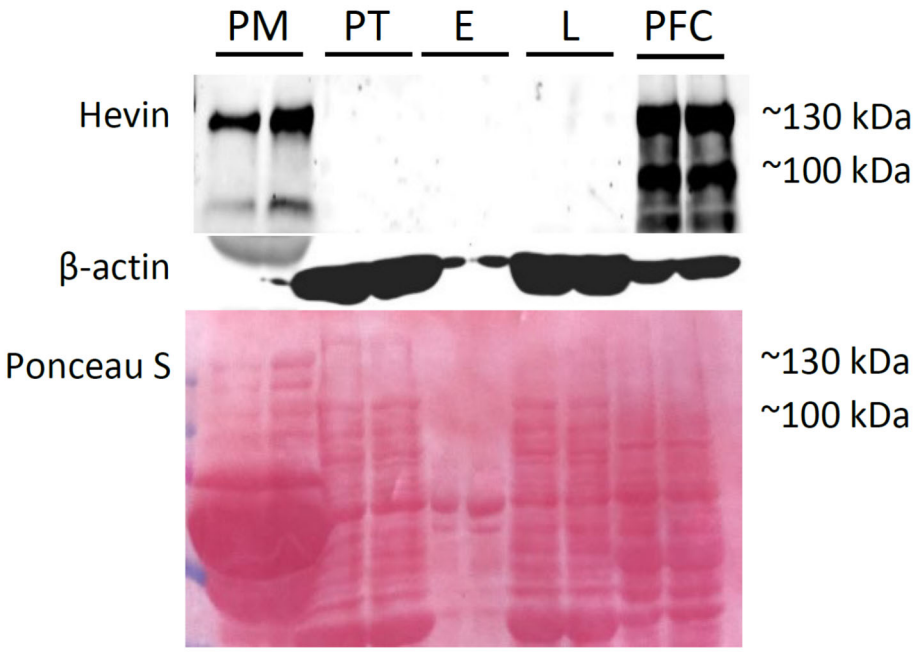

Figure 4.24. Hevin immunoreactivity in different blood fractions. Hevin is present in human plasma, but absence in any blood cell type *(PM: plasma, PT: platelets, E: erythrocytes, L: leucocytes)*. The same amount of protein was loaded for each sample (37 µg) with the exception of leucocytes (37 µg). β-actin and Ponceau S staining are also shown. Samples were run in duplicate and experiments were performed in triplicate. A representative Western blot image is shown.

4.2. THE HUMAN BRAIN STUDY FOR THE EVALUATION OF HEVIN'S ROLE IN ALCOHOL USE DISORDER

4.2.1. HEVIN mRNA EXPRESSION IN POSTMORTEM HUMAN BRAIN FROM SUBJECTS WITH ALCOHOL USE DISORDER

Hevin mRNA expression levels were measured by RT-qPCR in four human brain areas (prefrontal cortex, PFC; hippocampus, HIP; caudate nucleus, CAU; and cerebellum, CB) from 75 subjects. Individuals were divided into three experimental groups according to their antemortem psychiatric diagnosis: control (n=25), AUD (n=25) and a depression groups (n=25) (see section 3.1.1.). In all the studied brain areas a significant increase in hevin's mRNA was detected in the AUD group compared to the controls (PFC: AUD 159% ± 19, control 100% ± 5, p= 0.0028; HIP: AUD 172% ± 22, control 100% ± 7, p= 0.0058; CAU: AUD 192% ± 25, control 100% ± 7, p= 0.0028; CB: AUD 170% ± 25, control 100% ± 11, p= 0.0344). Conversely, no significant differences were detected between the depression and control groups **(Figure 4.25A-D)**.

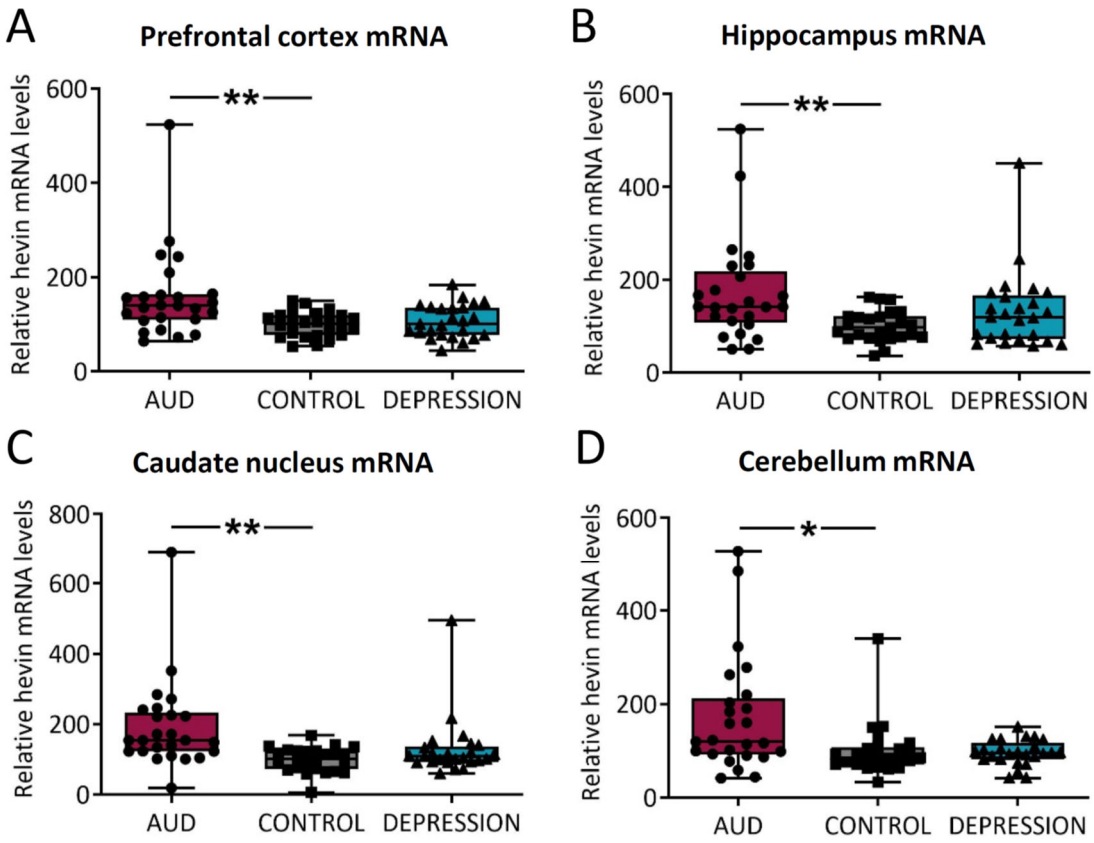

Figure 4.25. Hevin mRNA expression in the prefrontal cortex, hippocampus, caudate nucleus and cerebellum from human control, AUD and depression groups. (A-D) Relative hevin mRNA levels quantified by RT-qPCR in human postmortem samples from subjects with AUD (n=25), depression (n=25) and controls (n=25). One-way ANOVA followed by Dunnett's post hoc test was used for the comparison (*$p < 0.05$, **$p < 0.01$). Samples were run in triplicate. The quantification is represented in box-and-whiskers plots, where "box" shows the median and the 25th and 75th percentile and the "whiskers" depict the 5th and 95th percentile. Dots represent the average value of each individual in the performed experiments.

4.2.2. HEVIN PROTEIN EXPRESSION IN POSTMORTEM HUMAN BRAIN FROM SUBJECTS WITH ALCOHOL USE DISORDER

Hevin protein expression levels were measured in the same four human brain areas of the same control (n=25), AUD (n=25) and a depression (n=25) subjects (see section 4.2.1.) Specifically, both ~130 kDa and ~100 kDa hevin bands, previously described in human control subjects (see section 4.1 and/or Nuñez-delMoral et al., 2021) were measured in the post nuclear fractions of prefrontal cortex (PFC), hippocampus (HIP), caudate nucleus (CAU) and cerebellum (CB) by Western blot.

In accordance to the alterations observed in hevin's mRNA, a significant increase in ~130 kDa and ~100 kDa forms was detected in prefrontal cortex and cerebellum of the AUD group in comparison to the control group (PFC ~130 kDa band: AUD 126% ± 11, control 100% ± 9, $p = 0.0015$; PFC ~100 kDa band AUD: 146% ± 14, control 100% ± 8, $p < 0.0001$; CB ~130 kDa

band: AUD 132% ± 15, control 100% ± 11, p= 0.0344; CB ˜100 kDa band: AUD 138% ± 14, control 100% ± 6, p= 0.013) **(Figures 4.26, 4.27)**.

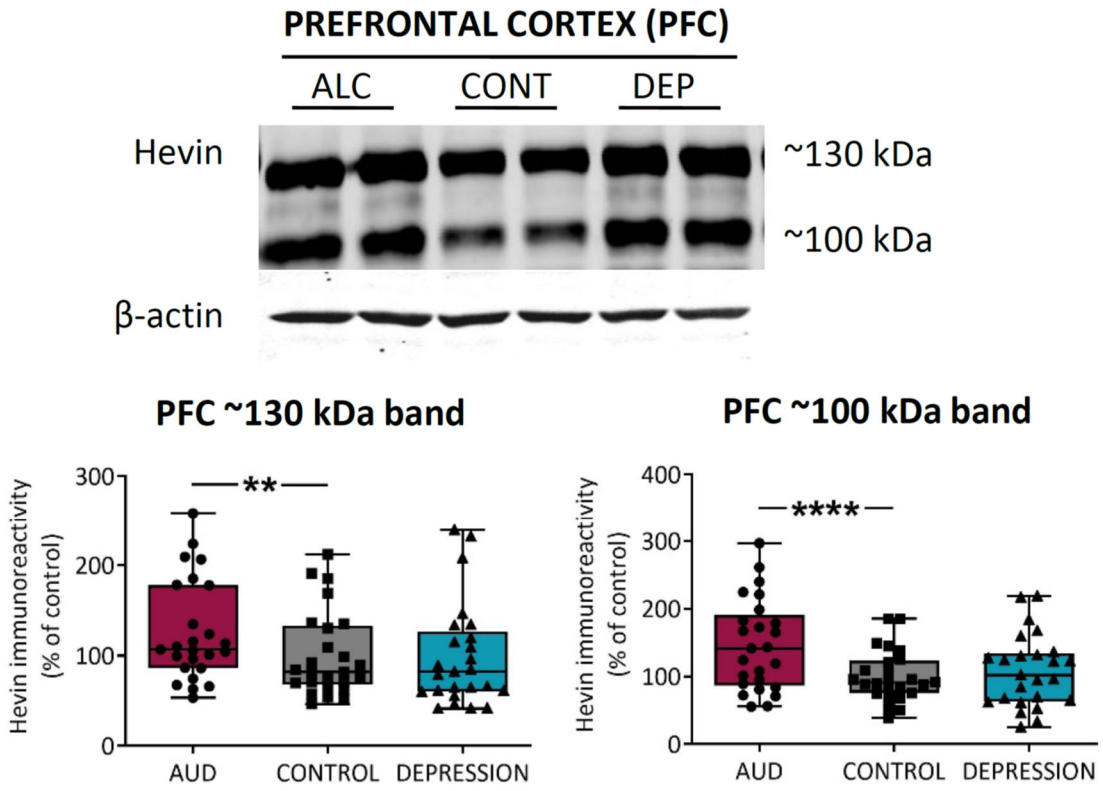

Figure 4.26. Expression of the two hevin forms in the prefrontal cortex (PFC) from human control, AUD and depression groups. β-actin-normalized hevin immunoreactivity and its ~130 kDa and ~100 kDa bands quantification in prefrontal cortex post nuclear fractions (~15 µg) from human control subjects and subjects with antermortem diagnosis of AUD or depression (n= 25). One-way ANOVA followed by Dunnett's post hoc test was used for the comparison (**p< 0.01, ****p< 0.0001). Samples were run in duplicate and experiments were performed in triplicate. A representative Western blot image is shown in the figure. The quantification is represented in box-and-whiskers plots, where "box" shows the median and the 25th and 75th percentile and the "whiskers" depict the 5th and 95th percentile. Dots represent the average value of each individual in the performed experiments.

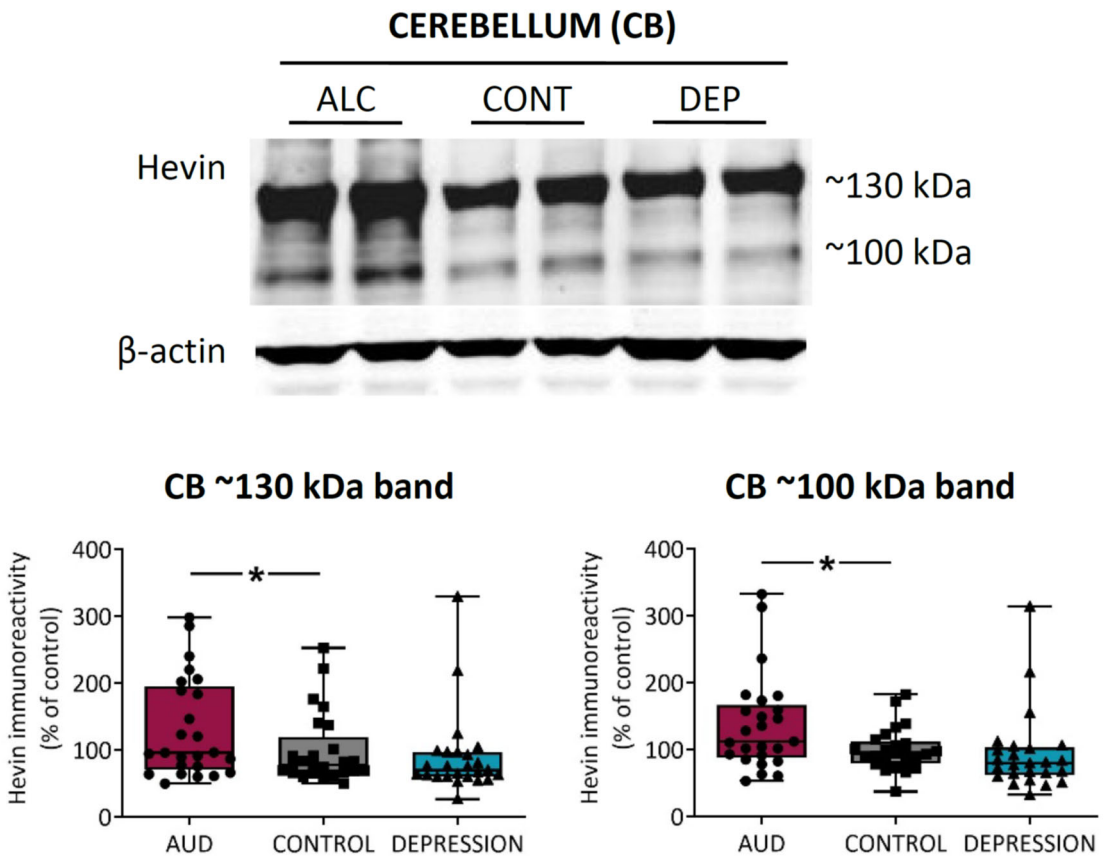

Figure 4.27. Expression of the two hevin forms in the cerebellum (CB) from human control, AUD and depression groups. β-actin-normalized hevin immunoreactivity and its ~130 kDa and ~100 kDa bands quantification in cerebellum post nuclear fractions (~25 µg) from human control subjects and subjects with antermortem diagnosis of AUD or depression (n= 25). One-way ANOVA followed by Dunnett's post hoc test was used for the comparison (*p< 0.05). Samples were run in duplicate and experiments were performed in triplicate. A representative Western blot image is shown in the figure. The quantification is represented in box-and-whiskers plots, where "box" shows the median and the 25th and 75th percentile and the "whiskers" depict the 5th and 95th percentile. Dots represent the average value of each individual in the performed experiments.

In the hippocampus, only the ˜100 kDa band was significantly increased in the AUD group in comparison to the control group (˜100 kDa band: AUD: 156% ± 30, control: 100% ± 14, p= 0.0384). Although the ˜130 kDa band showed a similar trend, the increase did not reach statistical significance (p= 0.0836, **Figure 4.28**). In contrast, no differences were observed in the expression of neither of the bands in the caudate nucleus, albeit the trend towards an increase in the upper band **(Figure 4.29)**. To note, Grubbs outlier test was performed in all analysis and it identified a significant outlier sample ($p \leq 0.05$) in the AUD group of the caudate nucleus. Therefore, that sample and their matched samples from the control and depression groups were excluded from the study in the caudate nucleus.

Finally, the depression group did not show statistical significant differences in the levels of protein expression in comparison to the control group in any brain area **(Figures 4.26-4.29)**.

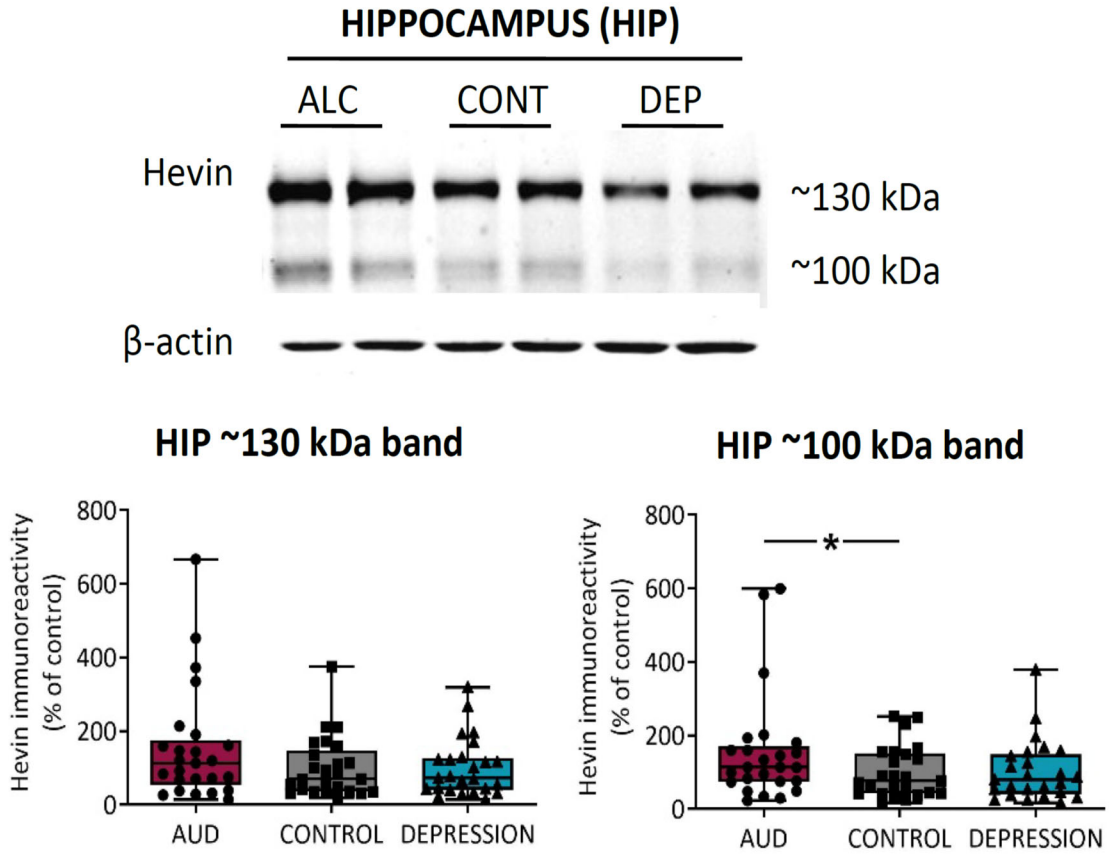

Figure 4.28. Expression of the two hevin forms in the hippocampus (HIP) from human control, AUD and depression groups. β-actin-normalized hevin immunoreactivity and its ~130 kDa and ~100 kDa bands quantification in hippocampus post nuclear fractions (~15 µg) from human control subjects and subjects with antermortem diagnosis of AUD or depression (n= 25). One-way ANOVA followed by Dunnett's post hoc test was used for the comparison (*p< 0.05). Samples were run in duplicate and experiments were performed in triplicate. A representative Western blot image is shown in the figure. The quantification is represented in box-and-whiskers plots, where "box" shows the median and the 25th and 75th percentile and the "whiskers" depict the 5th and 95th percentile. Dots represent the average value of each individual in the performed experiments.

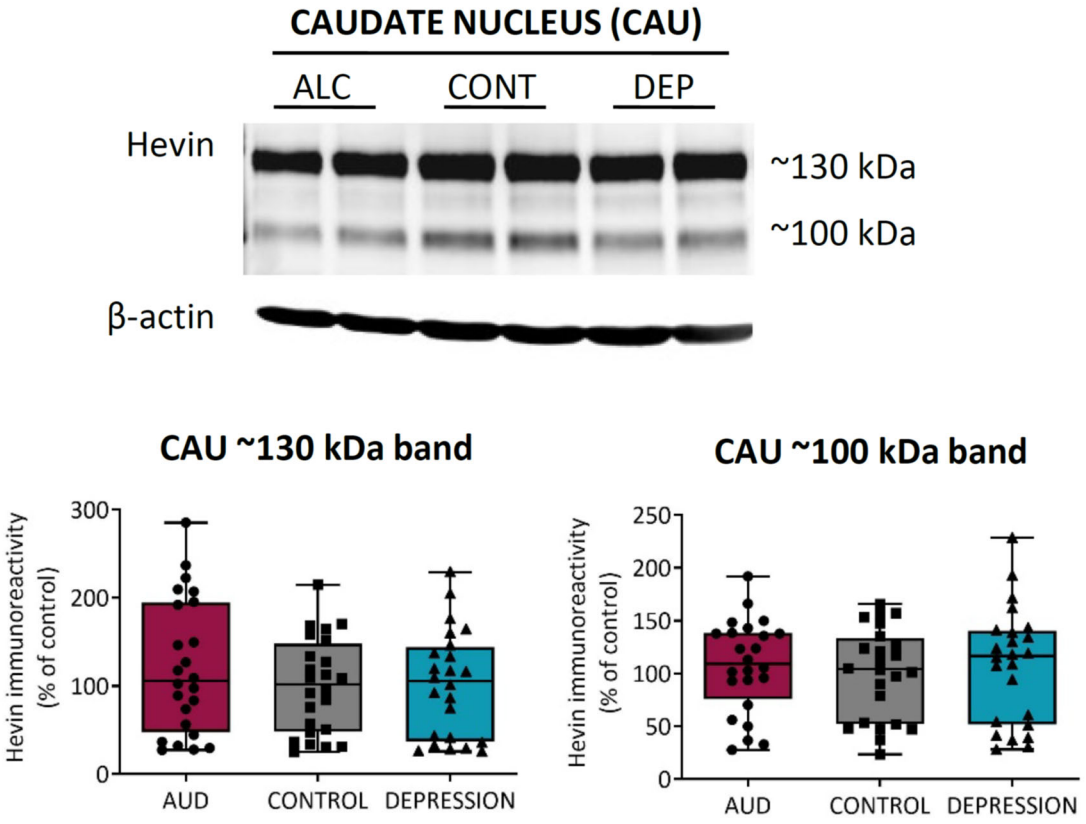

Figure 4.29. Expression of the two hevin forms in the caudate nucleus (CAU) from human control, AUD and depression groups. β-actin-normalized hevin immunoreactivity and its ~130 kDa and ~100 kDa bands quantification in caudate nucleus post nuclear fractions (~15 µg) from human control subjects and subjects with antermortem diagnosis of AUD or depression (n= 24). One-way ANOVA followed by Dunnett's post hoc test was used for the comparison. Samples were run in duplicate and experiments were performed in triplicate. A representative Western blot image is shown in the figure. The quantification is represented in box-and-whiskers plots, where "box" shows the median and the 25th and 75th percentile and the "whiskers" depict the 5th and 95th percentile. Dots represent the average value of each individual in the performed experiments.

4.3. THE ANIMAL STUDY FOR THE EVALUATION OF HEVIN'S ROLE IN ALCOHOL USE DISRODER

4.3.1. EVALUATION OF THE EFFECT OF DIFFERENT ETHANOL TREATMENTS ON HEVIN EXPRESSION IN MICE

4.3.1.1. Effect of ethanol treatments on hevin protein expression in mouse brain

In order to determine whether ethanol exposure alters hevin expression in mice's brain, hevin protein expression was analyzed after a challenge dose of ethanol or saline, with or without a history of prior ethanol exposure (see section 3.2.2.). Experiments were performed in total homogenates of the following five brain regions: nucleus accumbens, amygdala, frontal cortex, hippocampus and dorsal striatum. Samples containing around 10 µg of total protein were individually analyzed.

In contrast to human brain, mice did not express the ~100 kDa band, or its immunoreactive signal was too low to be analyzed, as it has been previously described (M. S. Weaver et al., 2010). Therefore, the present data correspond only to the ~130 kDa band.

The nucleus accumbens showed increased hevin levels after chronic ethanol administration followed by reinstatement (E-E) compared to saline treatment (S-S: 100% ± 5; E-E: 174% ± 16, p=0.0041), to acute ethanol treatment (S-E: 106% ± 10; E-E: 174% ± 16, p=0.0232) and, more markedly, to ethanol withdrawal schedule (E-S: 78% ± 11; E-E: 174% ± 16, p=0.0007) **(Figure 4.30.)**.

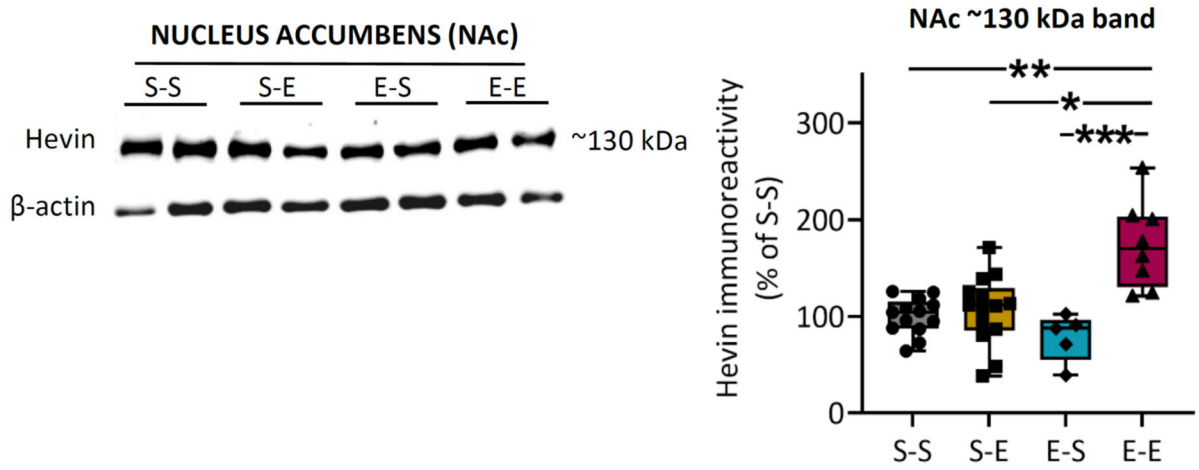

Figure 4.30. Effect of ethanol i.p. treatment on hevin protein expression in mouse nucelus accumbens (NAc). A representative Western Blot image for the mice nucleus accumbens and the graphics representing the β-actin-normalized quantification of the hevin ˜130 kDa band in the four administered ethanol treatments (S-S: saline – saline (n=13), S-E: saline – ethanol (n=14), E-S: ethanol-saline (n=5) and E-E: ethanol-ethanol (n=8)). Kruskal-Wallis followed by Dunn's post hoc test was used for the comparison (*p< 0.05, **p< 0.01, ***p< 0.001). Two different mouse samples were run for each treatment group and experiments were performed in triplicates. The quantification is represented in box-and-whiskers plots, where "box" shows the median and the 25th and 75th percentile and the "whiskers" depict the 5th and 95th percentile. Dots represent the average value of each individual in the performed experiments.

In addition, acute ethanol injection (S-E) reduced hevin protein levels in amygdala in comparison to the saline treatment (S-S) (S-S 100% ± 15, S-E 44% ± 4, $p_{(S\text{-}S \text{ vs } S\text{-}E)}$= 0.0471 **(Figure 4.31)**. No changes were observed in the other brain regions assessed **(Figure 4.32)**.

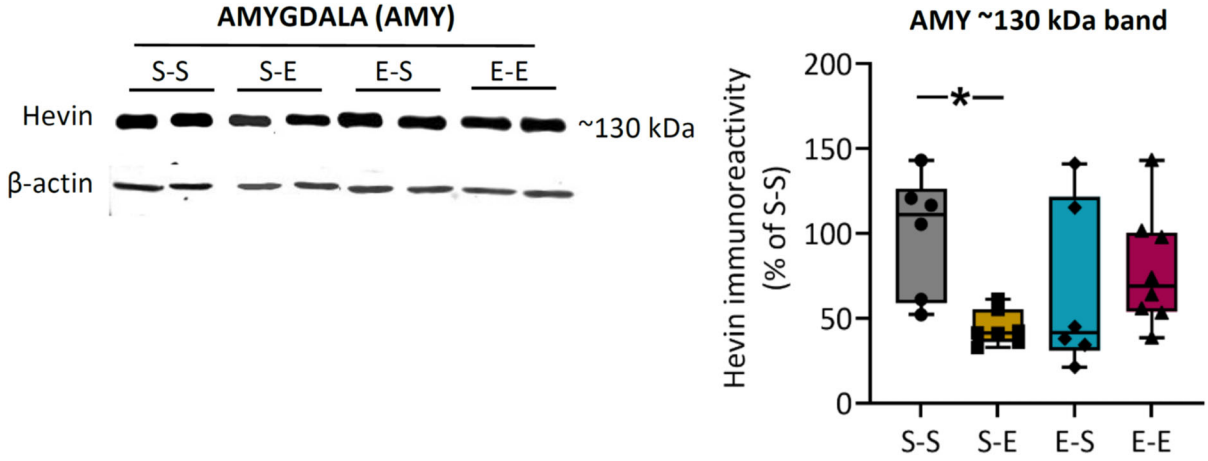

Figure 4.31. Effect of ethanol i.p. treatment on hevin protein in mouse amygdala (AMY). A representative Western Blot image for the mice amygdala and the graphics representing the β-actin-normalized quantification of the hevin ˜130 kDa band in the four administered ethanol treatments (S-S: saline – saline (n=6), S-E: saline – ethanol (n=7), E-S: ethanol-saline (n=6) and E-E: ethanol-ethanol (n=8)). Kruskal-Wallis followed by Dunn's post hoc test was used for the comparison (*p< 0.05). Two different mouse samples were run for each treatment group and experiments were performed in triplicates. The quantification is represented in box-and-whiskers plots, where "box" shows the median and the 25th and 75th percentile and the "whiskers" depict the 5th and 95th percentile. Dots represent the average value of each individual in the performed experiments.

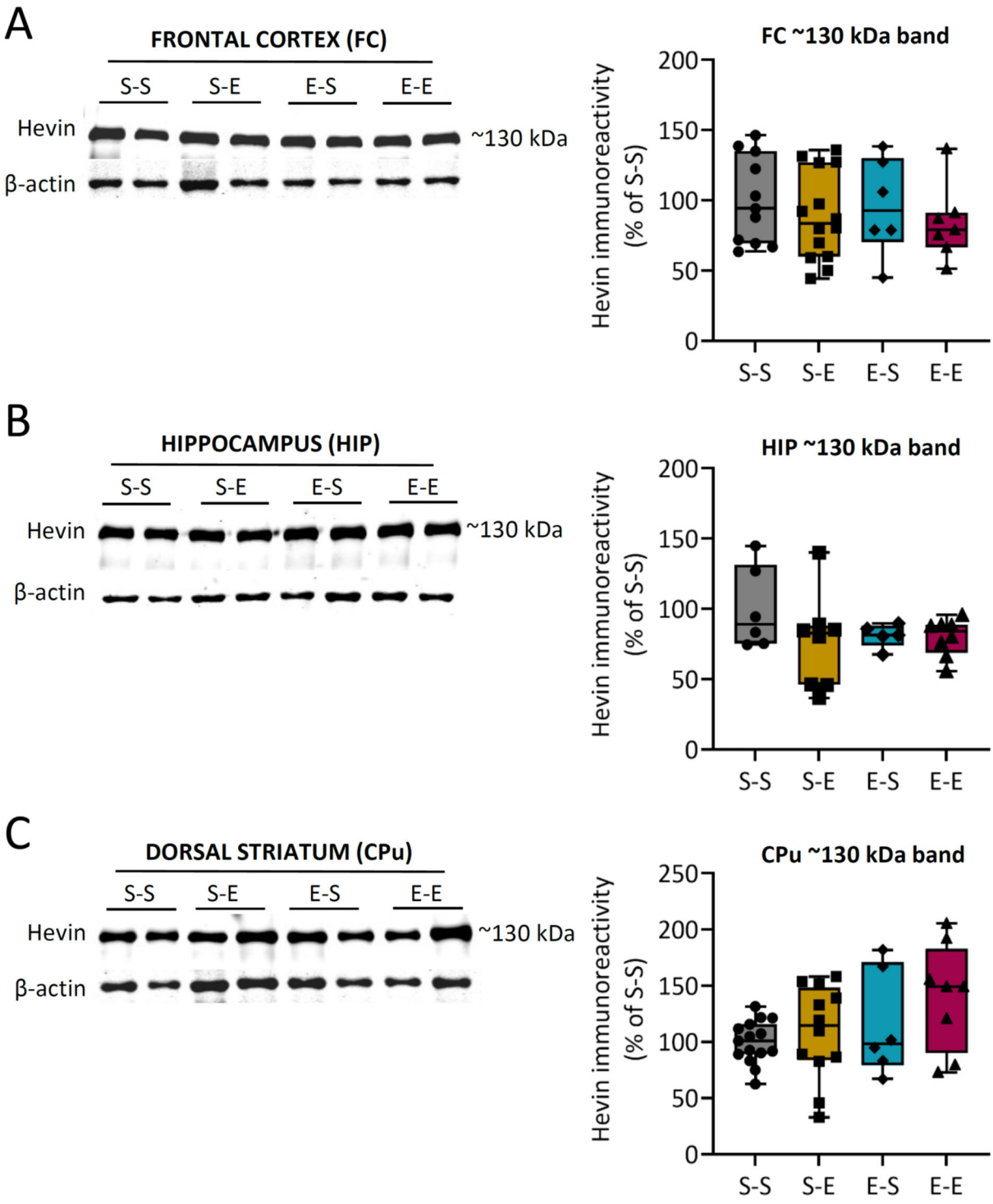

Figure 4.32. Effect of ethanol i.p. treatment on hevin protein in mouse frontal cortex (A), hippocampus (B) and dorsal striatum (C). A representative Western Blot image for the three brain regions *(FC: frontal cortex, HIP: hippocampus: CPu (caudate-putamen): dorsal striatum)* and the graphics representing the β-actin-normalized quantification of the hevin ˜130 kDa band in the four administered ethanol treatments (S-S: saline – saline (n, FC= 11, HIP= 6 and CPu =15), S-E: saline – ethanol (n, FC= 14, HIP= 8 and CPu =12), E-S: ethanol-saline (n, FC= 6, HIP= 5 and CPu =6) and E-E: ethanol-ethanol (n, FC= 7, HIP= 8 and CPu =8)). Kruskal-Wallis followed by Dunn's post hoc test was used for the comparison. Two different mouse samples were run for each treatment group and experiments were performed in triplicates. The quantification is represented in box-and-whiskers plots, where "box" shows the median and the 25th and 75th percentile and the "whiskers" depict the 5th and 95th percentile. Dots represent the average value of each individual in the performed experiments.

4.3.1.2. Effect of ethanol treatments on hevin expression in mouse plasma

The consequences of different ethanol i.p. administrations (see section 3.2.2.) in hevin expression levels in mice's plasma were also analyzed. In addition to the ~130 kDa band, an additional band with a molecular weight around 47 kDa was analyzed due to the high immunoreactivity signal of this band in most of the samples.

The ˜130 kDa plasmatic band showed similar profile to the one described in the mouse nucleus accumbens indwith the same ethanol treatment. Specifically, mouse plasma showed statistically significant greater levels of hevin ˜130 kDa band in the E-E group (ethanol chronic treatment followed by a single dose ethanol challenge after a withdrawal period) in comparison to the E-S group (ethanol chronic treatment followed by a withdrawal period) (˜130 kDa band: E-E 127% ± 23, E-S: 62% ± 26 increase, p=0.0396). It should be noted that two individuals from the E-S group barely expressed ˜130 kDa band **(Figure 4.33)**.

In addition, mouse plasma showed high variability in the expression levels of the ˜47 kDa band between individuals, with some of them expressing high levels of this form, as for two of the E-S group, and almost undetectable levels for others. Altogether, no significant differences in hevin expression levels were detected between the ethanol treatments for the ˜47 kDa band.

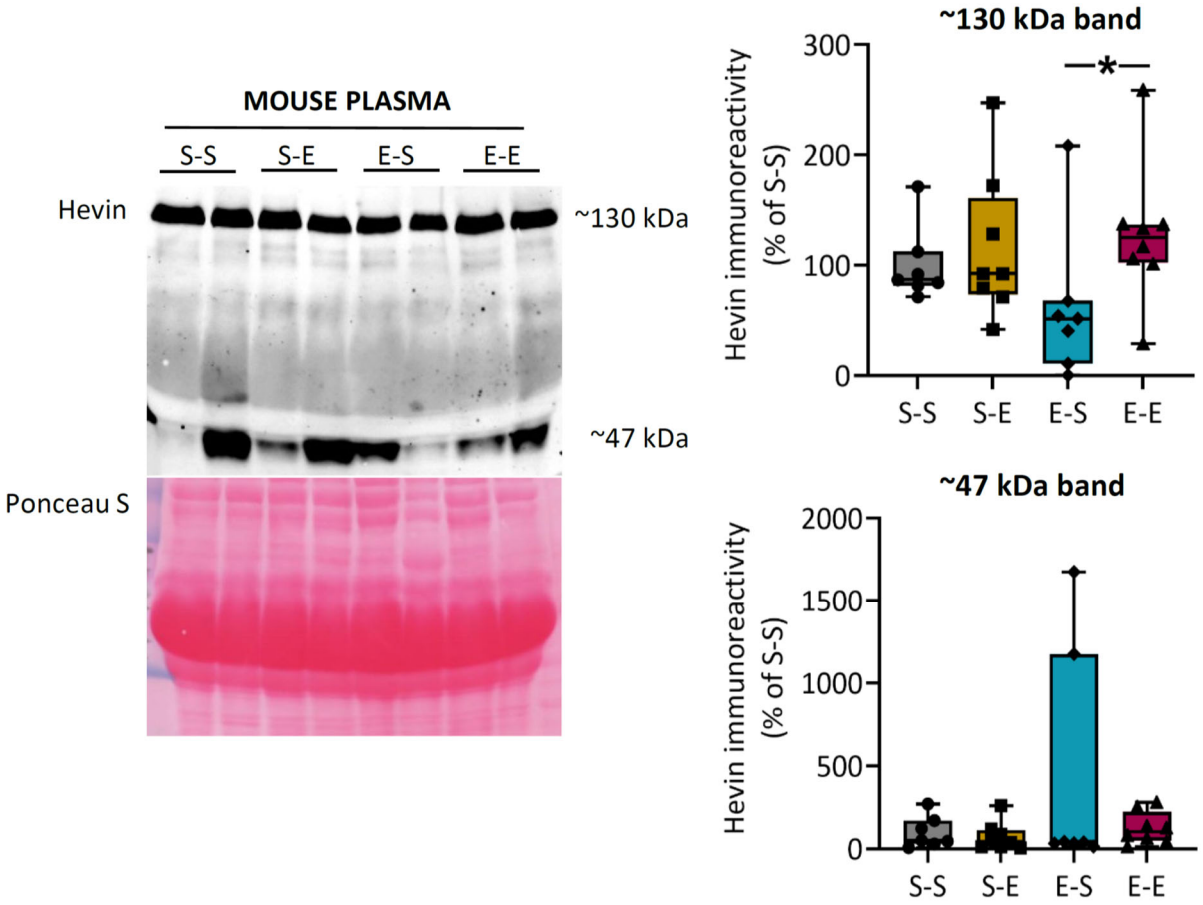

Fig. 4.33. Effect of ethanol i.p. treatment on hevin protein in mouse plasma. A representative Western Blot for hevin in mouse plasma and its Ponceau S stain images; the graphics representing the quantification of ~130 kDa and ~47 kDa hevin bands in the mouse plasma after the four administered ethanol treatments (S-S (n=7): saline – saline, S-E (n=8): saline – ethanol, E-S (n=7): ethanol-saline and E-E (n=8): ethanol-ethanol). Kruskal-Wallis followed by Dunn's post hoc test was used for the comparison (*$p < 0.05$). The quantification is represented in box-and-whiskers plots, where "box" shows the median and the 25th and 75th percentile and the "whiskers" depict the 5th and 95th percentile. Dots represent the average value of each individual in the performed experiments.

Finally, in order to assess if the expression of the lower band was the result of the cleavage of the ˜130 kDa band, the ratio of the immunoreactivity of both bands was also calculated (˜130 kDa/ ˜47 kDa), but no significant differences were detected between treatment groups (Fig. 4.34).

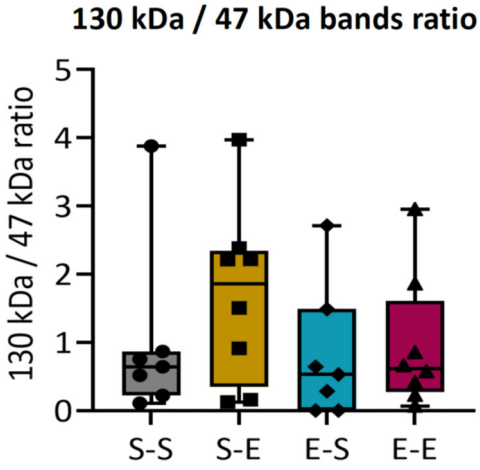

Fig. 4.34. Effect of ethanol i.p. treatment on hevin protein in mouse plasma. The graphic representing the 130 kDa band/47 kDa ratio in the mouse plasma after the four administered ethanol treatments (S-S (n=7): saline – saline, S-E (n=8): saline – ethanol, E-S (n=7): ethanol-saline and E-E (n=8): ethanol-ethanol). Kruskal-Wallis followed by Dunn's post hoc test was used for the comparison (*p< 0.05). The quantification is represented in box-and-whiskers plots, where "box" shows the median and the 25th and 75th percentile and the "whiskers" depict the 5th and 95th percentile. Dots represent the ration of each individual.

4.3.2. EVALUATION OF THE EFFECT OF HEVIN DOWNREGULATION IN ASTROCYTES OF THE NUCLEUS ACCUMBENS OF MICE ON THE REWARDING PROPERTIES OF ETHANOL

In order to test the role of hevin in the rewarding properties of ethanol, the expression levels of the protein were downregulated in the nucleus accumbens astrocytes by the RNA interference strategy (see section 3.2.3.) and the consumption of ethanol in a two-bottle choice paradigm was tested using IEA schedule (see section 3.5.5.).

4.3.2.1. Validation of the viral infection location and hevin downregulation in astrocytes of the nucleus accumbens

In order to confirm that the viral infection was correctly performed and the downregulation of hevin achieved in the nucleus accumbens astrocytes of the mice infected with the AAV2.5-GFAP-EmGFP-miR-hevin (hevin knockdown mice, KD), hevin protein was immunodetected in brain slices comprising the nucleus accumbens of perfused mice (see

section 3.2.3. for the viral infection specifications and 3.5.6. for immunohistochemistry assay details). In the same way, hevin immunoreactivity was also examined in brain slices containing the nucleus accumbens from the mice infected with the control viral vector AAV5.GFAP.eGFP.WPRE.hGH (control). In both cases, green fluorescent protein (GFP) was immunodetected as a control of the viral infection location and selectivity for astrocyte cell type. DAPI (4',6-diamidino-2-fenilindol) was also used for the identification of the cell bodies.

As expected, hevin knockdown mice showed almost a complete absence of the hevin protein in the nucleus accumbens astrocytes (the low expression made the quantification inviable). The localization of the injection and the expression of the transgene exclusively in the nucleus accumbens was demonstrated by GFP immunofluorescence signal in both hevin knockdown and control mice, with a very little spread to adjacent brain areas in the left hemisphere **(Figure 4.35)**.

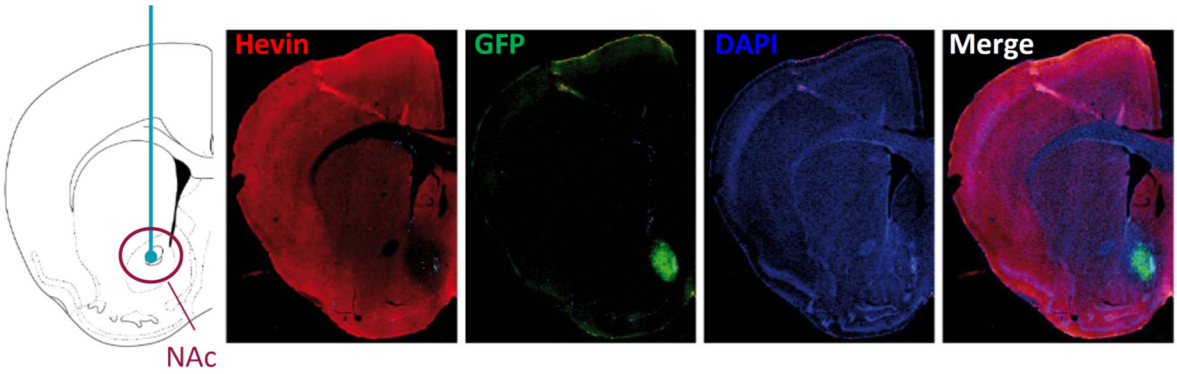

Figure 4.35. Validation of hevin downregulation in the mouse nucleus accumbens (NAc) astrocytes. Schematic representation of the viral injection performed in mouse NAc (modified from (Kaplan et al., 2011) followed by a representative immunohistochemical image of hevihn downregulation in mouse NAc after injection of miRNA containing viruses. Hevin immunofluorescence is shown in red, GFP in green and DAPI in blue.

4.3.2.2. Effect of hevin downregulation in the astrocytes of the nucleus accumbens on the rewarding properties of ethanol

In the IEA schedule (see section 3.5.5.), every day ethanol and water volumes drunk by each mouse were measured after 4h and 8h of the begging of the experiment. Both consumption (ingested ethanol expressed as g ethanol/kg) and preference (percentage of ethanol consumed from the total volume) were calculated for the first 4 h (from 0 h to 4 h) and for the last 4h (from 4 h to 8h). For the comparisons, only the third day of the setting of the

new ethanol concentration was used, as it was assumed that a period of two days was necessary for the mice to get used to the flavor.

The first 4 h (0-4 h) of the implemented IEA paradigm did not reveal alterations neither in the preference nor for the consumption of ethanol at low and medium concentrations (5%, 10% and 15%, w/v) administered the first 9 days **(Figures 4.36A and 4.37A)**. Nevertheless, the 12th day at 20% concentration of ethanol, the consumption was significantly higher in the hevin knockdown (KD) mice than in controls (hevin KD: 3.8 ± 0.4, control: 2.7 ± 0.2, p=0.0262) **(Figure 4.36A)**. Interestingly, the preference for ethanol between hevin knockdown and control mice was similar **(Figure 4.37A)**, suggesting that both ethanol and water intake were increasing at the same time. After a period of three days of withdrawal, when the mice were again submitted to the IEA paradigm with a 10% of ethanol concentration, the same ethanol intake profile as for the 20% of ethanol was found, i.e. an increased consumption in hevin knockdown mice (hevin KD: 3.3 ± 0.3, control: 2.3 ± 0.2, p=0.0379) **(Figure 4.36A)**. In addition, hevin knockdown group showed a greater ethanol consumption at the 12th day with a 20% ethanol concentration in comparison to the 3rd day at 5% ethanol concentration (5%: 2 ± 0.3, 20%: 3.8 ± 0.4, p=0.0072) **(Figure 4.36A)**. Altogether, these data show higher ethanol consumption in hevin knockdown animals, as an effect of the withdrawal period, while no differences were observed for ethanol preference.

In contrast, the last 4 h of the IEA experiment (from 4 h to 8 h) revealed that both, hevin knockdown and control mice, drunk as much water as ethanol **(Figures 4.36B and 4.37B)**.

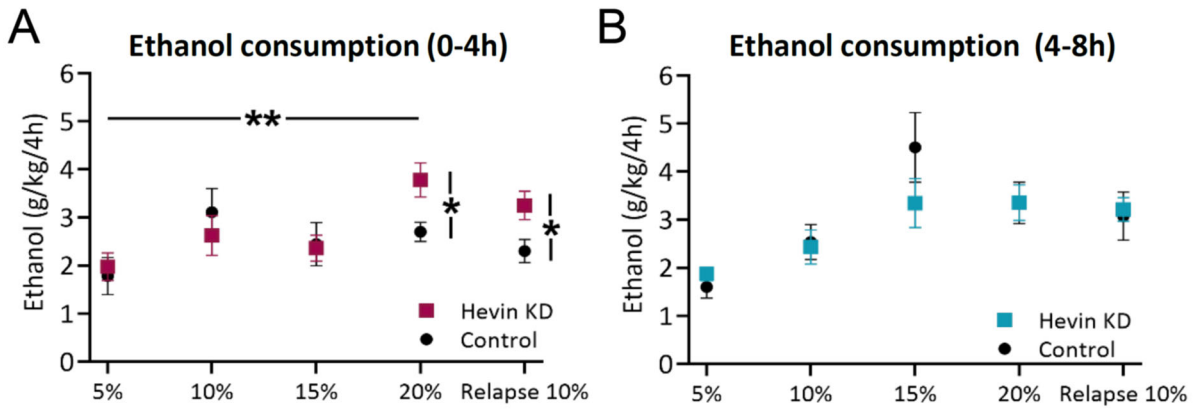

Figure 4.36. Effect of hevin downregulation in the nucleus accumbens astrocytes on the ethanol consumption (A-B). Ethanol consumption quantification every third day of each ethanol concentration. The ordinate represents the grams of ethanol per kg of mouse taken by hevin knockdown (KD) and control groups from 0 h to 4 h of the experiment **(A)** or from 4 h to 8 h **(B)**. The abscissa shows the ethanol concentration tested. Squares show the mean ± SEM from hevin KD mice values and circles show the mean ± SEM from control mice values. Mann-Whitney test was used for the comparison of the preference and consumption between the hevin KD and controls (*p< 0.05, **p< 0.01); and Friedman followed by Dunn's post hoc test was used for the comparison of the preference and consumption between ethanol concentrations.

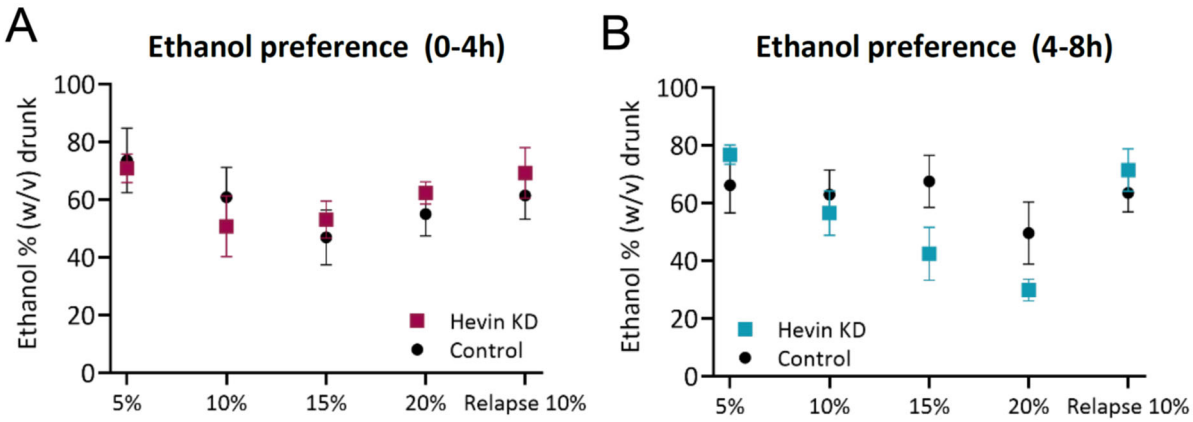

Figure 4.37. Effect of hevin downregulation in the nucleus accumbens astrocytes on the preference for ethanol (A-B). Ethanol preference quantification every third day of each ethanol concentration. The ordinate represents the average of the percentage of ethanol taken by hevin knockdown (KD) and control groups from 0 h to 4 h of the experiment **(A)** or from 4 h to 8 h **(B)**. The abscissa shows the ethanol concentration tested. Squares show the mean ± SEM from hevin KD mice values and circles show the mean ± SEM from control mice values.

5. DISCUSSION

The data collected in the present Doctoral Thesis provide new and original knowledge about the expression pattern of the matricellular protein hevin in human brain and its involvement in the pathophysiology of AUD.

Firstly, a deep characterization of the hevin protein expression was performed using different human tissues. Two glycosylated forms of the protein were detected in human brain. The expression of both hevin forms was measured and compared in four postmortem human brain areas (prefrontal cortex, hippocampus, caudate nucleus and cerebellum) and in their respective subcellular preparations (total homogenate, cytosol and P2 fraction). Hevin expression was also detected and compared between astrocytoma and meningioma brain tumors. Besides, hevin was found to be expressed in human CSF and plasma, but absent in any blood cell type.

Secondly, in order to asses if the protein hevin is implicated in AUD, hevin mRNA and protein expression levels were compared between subjects with AUD and controls, using postmortem human brain samples of prefrontal cortex, hippocampus, caudate nucleus and cerebellum; which showed hevin overexpression with brain area specificity.

Thirdly, in order to determine if the alterations detected in hevin expression levels in human brain were the consequence of the excessive and chronic consumption, adult male mice were administered with four different ethanol regimens and hevin protein expression was measured in these mice's brain and plasma. The data obtained in this study suggest that ethanol affects hevin brain expression, in a different manner depending on the brain area and the treatment.

Finally, to further elucidate the implication of hevin in the ethanol rewarding properties and assess whether the changes observed in humans could be related with the vulnerability to develop AUD, hevin expression was downregulated in mice's nucleus accumbens astrocytes and voluntary ethanol intake was measured. The obtained ethanol consumption measurements showed altered ethanol drinking, suggesting an involvement of hevin in the rewarding system.

The discussion of all these data has been divided into two major sections. The first section consists on the characterization study of hevin in human samples from control subjects. The second section refers the data from the study of hevin's role in AUD.

5.1. CHARACTERIZATION OF HEVIN EXPRESSION IN HUMAN SAMPLES

5.1.1. CHARACTERIZATION OF HEVIN EXPRESSION IN HUMAN BRAIN

Although the expression of hevin protein has been widely studied in rodents' tissues previously (Johnston et al., 1990; Kucukdereli et al., 2011; Lively & Brown, 2008b; Mendis, 1996a, 1996b; Weaver et al., 2011; Weaver et al., 2010), the data from the first section of the present Doctoral Thesis provide the first detailed description of hevin's physiological expression in human brain (Annex 1, Nuñez-delMoral et al., 2021). Two major hevin forms of different molecular weight were detected in total homogenates of human prefrontal cortex by Western blot, one intense band of ~130 kDa and a lower molecular weight band of ~100 kDa, which agrees to a great extent with previous results in the literature. Hevin immunoreactivity has mostly been described as a 120/116 kDa doublet in rat brain (Johnston et al., 1990; Lively & Brown, 2008a, 2008c; Mendis et al., 1996b), but ~130 kDa and 105 kDa hevin bands have also been described in human and mouse brain lysates (Brekken et al., 2004; Kucukdereli et al., 2011; Weaver et al., 2010).

It is necessary to mention that the reliability of the Western blot results rests on a thorough validation of the specificity of the selected antibody, which was indeed performed in this study. Immunoreactive signal of hevin in postmortem human brain disappeared when the antibody was previously incubated with the blocking peptide, and importantly, it was absent in mock-transfected cells and hevin knockout mouse brain lysate. Besides, the two hevin bands signal increased after the immunoprecipitation with the selected antibody and disappeared when immunoprecipitated with a non-specific antibody. In addition, the identity of the ~130 kDa and ~100 kDa immunoreactive bands were further confirmed by the LC-MS/MS analysis.

In order to investigate the nature of the main hevin bands, the hypothetical proteolytic relationship among them was studied first. Time- and temperature- dependent proteolysis assays ruled out the possibility that ~100 kDa hevin form as a degradation product of the ~130 kDa form. Furthermore, these assays confirm that any of the detected hevin bands were susceptible of the degradation by neither time nor temperature, under our experimental conditions.

Since several potential N-glycosylation sites have been proposed along hevin's protein sequence (Girard & Springer, 1995; Hambrock et al., 2003), glycosylation assays were also performed to further study these two hevin forms using common deglycosidases. Interestingly, both hevin bands appeared to be glycosylated as PNGaseF (a deglycosidase that cleaves almost all N-glycosylations) cleaved both forms (Freeze & Kranz, 2010). Part of those glycosylations corresponded to biantennary or tri-antennary fucosylation, as both bands were sensible to EnfoF3 cleavage. In addition, some of the glycosylations in the ~130 kDa band were N-linked high-mannose hybrid glycosylations, since they were sensible to the EndoH cleavage (Freeze & Kranz, 2010). In the ~100 kDa band PNGaseF deglycosylation led to a ~90 kDa band, which may correspond to native hevin with a calculated theoretical molecular weight of ~71 kDa (Johnston et al., 1990), or alternatively, to hevin with other post-translational modifications, such as phosphorylation or O-glycosilation, which do not confer a marked increase in the molecular weight. These results concord with those described in rat brain lysates and mouse recombinant hevin (Hambrock et al., 2003; Johnston et al., 1990). In particular, in a study performed on rat's brain homogenate in which two hevin protein bands were detected around 120 kDa and 116 kDa, both bands were cleaved by EndoF enzyme leading to ~110 kDa and ~105 kDa bands respectively; while, only the lower band was sensible to EndoH enzyme cleavage, leading to a band around ~105 kDa (Johnston et al., 1990). In addition, mouse recombinant full-length hevin, with a molecular weight around 94 kDa, was digested by both EndoF and EndoH enzymes leading to different hevin products (Hambrock et al., 2003)

Nevertheless, the differences between the ~130 kDa and ~100 kDa bands remain unknown. The LC-MS/MS analysis obtained in this work suggests that the difference between bands does not correspond to splicing or protein-truncating variants. Indeed, since the average molecular weight of an amino acid is 110 Da, the 30 kDa difference would correspond to a difference of approximately 272 aminoacids; however all but one of the peptides found were common for both bands and encompassed from amino acids 47-629 out the 664. Alternatively, the most probable explanation for this difference in the apparent molecular size may be the result of post-translational modifications. In the same way, previous reported Matrix-Assisted Laser Desorption/Ionization - Time-Of-Flight (MALDI-TOF) mass spectrometry indicates that hevin has more than 12kDa of post-translational modifications, which further suggests that the differences between both bands may be due to post-

translational modifications (Hambrock et al., 2003). One of the proposals includes O-glycosilations, with eight potential target sites in the hevin protein structure (Hambrock et al., 2003). Another possibility is that the two bands could correspond to different isoforms of the hevin protein, due to the alternative splicing of the hevin mRNA (Viloria et al., 2016).

In addition to the post-translational modifications, the discrepancy between the expected hevin molecular weight (~71 kDa) and the protein migration in the SDS-PAGE has been also related to the following possible factors: i) hevin could form homodimers and, thereby, the migration of the band appears the double of its molecular weight (~71 kDa vs ~140 kDa) or ii) because its high content of acidic residues confers a great negatively charged domain, producing the abnormal migration (Bendik et al., 1998; Brekken et al., 2004; Claeskens et al., 2000; Girard & Springer, 1996; Hambrock et al., 2003).

In this Doctoral Thesis, the characterization of hevin forms was further studied in regard to their enzymatic proteolysis by enzymes that endogenously cleave hevin in mice tissue and in the recombinant protein, but had never been studied in human hevin before. Proteolysis of hevin by ADAMTS4, MMP-3 and thrombin liberates the C-terminus portion of mouse and recombinant hevin (amino-acids 350–650), which possess 60% of identity to SPARC, and hence was named SPARC-Like fragment or SLF (Kucukdereli et al., 2011; Weaver et al., 2011; Weaver et al., 2010). SLF, like SPARC, antagonizes the synaptogenic activity of hevin (Kucukdereli et al., 2011). Furthermore, increased MMP-3 activity in the early phases after brain injury has been negatively correlated to hevin-calcyon interaction and impairing of hevin-mediated synaptogenesis, due to the MMP-3 Induced cleavage of hevin (Kim et al., 2021b). The data of the present Doctoral Thesis confirmed for the first time that human hevin is cleaved by these three enzymes. Incubation of human prefrontal cortex total homogenate samples with ADAMTS4 or MMP-3 produced a double band with similar molecular weight (~40 kDa) to that described in mouse brain (Weaver et al., 2011; Weaver et al., 2010). By contrast, the cleaved product of the recombinant human hevin was larger (~47 kDa). Differences in post-translational modifications in hevin prefrontal cortex or recombinant protein (in this case produced in a mouse myeloma cell line) could explain the observed molecular weight differences of the cleaved product. Hevin proteolysis by thrombin produced very different molecular weight fragments in both PFC and recombinant proteins, due to thrombin nonspecific cleavage sites (Rajalingam et al., 2008). Regardless of the protease identity, in vivo endogenous digestion of hevin in human brain

tissue also occurs, since the hypothetical SLF fragment was also detected in non-digested prefrontal cortex samples, despite very low levels compared to full-length hevin. Biochemical studies in ADAMTS4–null mice suggest that hevin is endogenously digested primarily by ADAMTS4, at least in the cerebellum (Weaver et al., 2010). Nevertheless, it has not been performed any similar in vivo study about the effect of the absence of MMP-3 and thrombin enzymes on hevin proteolysis, nor a direct comparison between these enzymes' activities with that of ADAMTS4 in brain tissue.

In the research on psychiatric diseases, studies using postmortem human tissue are of high value, since they represent the biological substrate of disease (the human) and include the environmental factors that can not be mimicked in animal models (Meana et al., 2014). However, the complexity of the samples makes it essential to consider some demographic and clinical measures as confounding factors, such as sex, age, PMD and storage time (McCullumsmith et al., 2014). In order to detect the influence of these variables in the expression of the hevin ~130 kDa and ~100 kDa bands, an immunoblot assay of a large cohort of control subjects composed of a total of 29 prefrontal cortex samples (11 of them females and 18 males) was performed. None of the confounding factors showed a significant correlation with the immunoreactivity signal of both hevin bands in our study. In terms of the differences between sexes, although no direct study on hevin protein has been performed, an analysis of the hevin's transcriptome on rat CNS tissue microglia did not show sex differences (Ewald et al., 2020). Furthermore, studies on tissue of patients with gastric adenocarcinoma or rectal cancer showed that the differences observed in hevin expression were independent of the sex factor (Jakharia et al., 2016; Kotti et al., 2014). However, a great correlation was detected between the ~130 kDa and ~100 kDa bands expression (i.e. subjects with intense ~130 kDa band also showed strong ~100 kDa band, and inversely), suggesting that the expression level of both hevin forms is commonly regulated.

5.1.2. HEVIN EXPRESSION IN HUMAN BRAIN, ASTROCYTOMA AND MENINGIOMA BRAIN TUMORS, CEREBROSPINAL FLUID AND BLOOD

In order to determine the subcellular expression profile of the two hevin forms in human brain, different subcellular fractions were prepared: total homogenate, cytosol and P2 fraction. The correct fractionation was confirmed by the enrichment of cytosolic proteins

(stathmin and IκBα) in the cytosolic (soluble) fraction and their impoverishment in the P2 fraction; and, conversely, the enrichment of synaptic proteins (syntaxin1A, VGLUT1, NR2A and PSD95) specifically in the P2 fraction, with relatively much lower expression in the cytosolic one. Thus, consistent with the wealth of experimental evidences showing hevin expression in synaptic junctions (Hambrock et al., 2003; Johnston et al., 1990; Mendis et al., 1996b; Singh et al., 2016), it was found that both human hevin forms, ~130 kDa and ~100 kDa, are strongly enriched in membranous, P2, fraction compared to cytosolic preparations in all brain regions tested. The enrichment in membrane preparation suggests that hevin is trapped in the complex mesh-like matrix of the synapses. However, hevin's presence (albeit lower) in the cytosolic fraction reflects its soluble nature and indicates that it can also attach to different targets before being secreted into the ECM (Ge et al., 2020; Hambrock et al., 2003; Sullivan et al., 2006).

Additionally, the two human hevin immunoreactive bands were detected in the four brain regions studied (prefrontal cortex, hippocampus, caudate nucleus and cerebellum), with the largest expression detected in the prefrontal cortex. This data is similar to the regional expression of hevin mRNA shown in mouse brain, with a strong expression in cortical regions (Mongrédien et al., 2019). Our group has previously observed also in adult human brain, that hevin mRNA is expressed in prefrontal cortex and caudate nucleus (Mongrédien et al., 2019). Thereby, the present results confirm that hevin mRNA is translated in adult human brain and add evidence for a region-specific expression of hevin. Importantly, the strong cortical expression of hevin detected in the present Doctoral Thesis, together with the previous evidences showing its role in the promotion of the glutamatergic synapses formation, maintenance and function (Espírito-Santo et al., 2021; Gan & Südhof, 2019, 2020; Kim et al., 2021b; Kucukdereli et al., 2011; Risher et al., 2014; Singh et al., 2016), suggests a major role of hevin in higher cognitive functions such as decision-making, social and emotional behavior, learning and memory. The expression of two post-translationally distinct forms of hevin with brain area specificity may suggest a particular role in adult physiological brain function.

Besides being expressed in the non-pathological brain, previous studies have demonstrated that hevin protein expression is induced in reactive astrocytes (Jones & Bouvier, 2014; Lively et al., 2011; McKinnon & Margolskee, 1996; Mendis et al., 2000), and abnormal

astrocyte activation has been related with tumor formation, such as astrocytoma (Gronseth et al., 2018; Yang et al., 2013). Upregulated hevin mRNA expression has also been reported in human meningioma or meningeal tumors (Dalan et al., 2017), which are typically slow-growing tumors of the meninges, where the arachnoid mater cells transform into meningioma cells (Buerki et al., 2018; Fathi & Roelcke, 2013). However, these studies did not distinguish between the different hevin forms. The data of the present Doctoral Thesis show that astrocytoma samples exhibited greater hevin immunoreactivity than meningioma samples, in both hevin bands, and the ~130 kDa isoform expression was increased in the astrocytoma samples in comparison to healthy brain tissue. However, no significant differences in the relative expression (ratio) of the ~130 kDa and ~100 kDa bands were detected between both types of tumors, suggesting that astrocytoma and meningioma tumors present similar alteration of both bands. These results are consistent with the well-known role of hevin and other ECM molecules in tumor invasion, and the proposal of hevin as a marker of glioblastoma and astrocytoma progression (He et al., 2016; Turtoi et al., 2012; Virga et al., 2018). Nevertheless, the fact that hevin expression is downregulated in other types of human cancers (e.g. prostate and colorectal cancers, gastric adenocarcinoma) (Han et al., 2018; Hurley et al., 2012; Jakharia et al., 2016; Nelson et al., 1998), has suggested that it may play different roles in tumor biology, as both oncogene and tumor suppressor, based on tumor type (Gagliardi et al., 2017). Overall, hevin's implication in cell adhesion, migration and proliferation highlight its role as a key protein in the regulation of tumor biology (Claeskens et al., 2000; Gagliardi et al., 2017; Sullivan & Sage, 2004).

Finally, the expression pattern of hevin in CSF and blood samples was also evaluated. The present data demonstrate that both hevin forms are secreted into the CSF in subjects without any psychiatric or neurological disorders. In contrast, a previous study showed that hevin protein was absent in normal/control CSF, albeit being upregulated in the CSF of multiple sclerosis patients (Hammack et al., 2004). As mentioned in the cited article, due to the sensitivity of the used proteomics it is possible that the hevin levels in the CSF of controls were undetectable, while the samples of patients with multiple sclerosis presented higher levels of hevin (Hammack et al., 2004). However, the origin of CSF hevin remains unknown; it may originate from brain's astrocytes and/or neurons, meninges or anywhere in the periphery, and arrive by bloodstream. In addition, although hevin was

clearly detected in blood plasma, none of the blood cell expressed it (platelets, erythrocytes and leucocytes). It suggests that the hevin present in blood derives from other organs where it is expressed, such as brain, liver, stomach, small intestine, esophagus, lung pancreas, heart, spleen or kidney (Bendik et al., 1998; Johnston et al., 1990; Klingler et al., 2020; Soderling et al., 1997; Weaver et al., 2011; Weaver et al., 2010). Interestingly, it was noted that, while ~130 kDa band was present in both CSF and serum, the ~100 kDa band was absent in these samples, and a novel ~90 kDa band was detected. This band may correspond to non-glycosylated form, as shown in deglycosylation assays. The different proportion of the two detected hevin forms in CSF and in blood suggests a different glycosylation/deglycosylation pattern and/or a different source of origin for hevin in each fluid (Barone et al., 2012; Karlsson et al., 2017).

Overall, the data from this section provide the first thorough characterization of hevin protein expression in postmortem human brain tissue. The data herein presented reveal that there are two forms of hevin, both glycosylated, whose expression is higher in the membrane-enriched fraction compared to the cytosolic (soluble) fraction. Furthermore, hevin expression is higher in the prefrontal cortex in comparison to other brain regions and in astrocytoma brain tumors in comparison to healthy tissue. It is also shown that hevin is expressed in human CSF and blood plasma, but not in blood cells, suggesting a potential role as a brain biomarker in these fluids. Taken together, these results constitute an essential resource for future studies of hevin in brain tissue under different pathological and non- pathological conditions.

5.2. THE ROLE OF HEVIN IN ALCOHOL USE DISORDER

5.2.1. HEVIN'S mRNA AND PROTEIN EXPRESSION LEVELS IN THE PREFRONTAL CORTEX, HIPPOCAMPUS, CAUDATE NUCLEUS AND CEREBELLUM OF SUBJECTS WITH ALCOHOL USE DISORDER

As it has been previously reviewed in the introduction, studies over the last decades are providing strong evidence about the implication of matricellular proteins in neuronal plasticity. In this way, the peculiarities of the protein hevin, such as its high expression in adult brain and its ability to promote synapse formation, have placed this protein in the focus of many studies in neuropsychiatric diseases.

In the present project, the main objective was to elucidate the possible implication of the protein hevin in AUD. For that purpose, hevin mRNA and protein expression levels were determined in postmortem human brain samples from subjects with no antemortem history of any neuropsychiatric disease (control group), subjects with antemortem diagnosis of AUD (AUD group) and subjects with antemortem diagnosis of major depression (depression group). Similarly to previous works performed using postmortem human samples, the depression group was included as a control of disease's specific changes (Erdozain et al., 2015; Ramos-Miguel et al., 2019; Rivero et al., 2015). It is important to note that each AUD and depression subject was matched by sex, age and PMD to a control, in order to avoid any confounding effect. Nevertheless, as it has been previously shown in the first part of this Doctoral Thesis, none of these demographic characteristics affected hevin expression (section 4.1.5).

Four brain areas were studied in the present study: prefrontal cortex, hippocampus, caudate nucleus and cerebellum. These regions were selected based on different aspects of AUD. Briefly, the prefrontal cortex was selected due to its crucial role on executive functions and cognitive control, such as decision-making, emotional control and impulse inhibition, among others (Abernathy et al., 2010; Friedman & Robbins, 2022; Jones & Graff-Radford, 2021). The hippocampus, was chosen because of its involvement on the memory consolidation, emotional processing, social cognition, motivation and, therefore, in the establishment of drug-context associations (Kennedy & Shapiro, 2009; Kutlu & Gould, 2016; Zhu et al., 2019). The caudate nucleus, together with the putamen, conform the main input nuclei of the basal ganglia and takes part in motivation, learning, feed-back processing and

goal-directed behaviors (Driscoll et al., 2022; Grahn et al., 2008). Last, the cerebellum was selected due to its role not only in the motor coordination, which is highly affected in long-term AUD, but also due to its involvement in the drug-related cue-memories (Miquel et al., 2016). Importantly, all these brain regions are functionally and structurally affected due to the excessive alcohol consumption, alterations that are shortly reviewed in the section 1.1.3.2.

Hevin gene expression was measured using the RT-qPCR technique, showing that, in the AUD group, every studied brain region presents higher relative hevin mRNA levels in comparison to the control group. No differences were detected between the depression and control group. In order to see if the same changes were observed in the protein levels, the immunoreactivity of the two previously detected hevin bands, at a molecular weight of ~130 kDa and ~100 kDa, was analyzed by Western blot and compared between the three groups of study.

The analysis of hevin protein expression was performed using the post nuclear total homogenate- preparations from each brain region. This fraction was used in order to increase the sample purity by the elimination of the nuclear fraction; and it was selected considering that it contains both fractions in which hevin is expressed (cytosolic and P2 fractions), as previously reported in the study of the subcellular distribution of hevin.

In this case, the results were not homogeneous for all brain areas. In accordance to the relative mRNA levels, the prefrontal cortex and cerebellum of the AUD group showed increased expression levels of the ~130 kDa and ~100 kDa hevin protein forms, in comparison to the control group; while, only the ~100 kDa band of the hippocampus presented higher signal than in the control group. In contrast, the hevin mRNA overexpression in the alcoholic group was not replicated in the protein expression in the caudate nucleus. As previously, the depression group did not show differences in the expression of the hevin protein in comparison to the control group.

Despite of this consistent data showing an overexpression of the hevin transcript in AUD, the mRNA levels of a cell does not have to necessarily correlate directly with the translated protein levels and/or function. There are many molecular mechanisms that take part in the gene expression pathway, which could explain the dissimilarities between the gene and protein expression (Buccitelli & Selbach, 2020; Greenbaum et al., 2003). For instance:

Firstly, mRNA alternative splicing can lead to different protein isoforms, as it has been proposed in order to explain the different hevin isoforms of around 110 kDa, 49 kDa and 39 kDa found in a pancreatic cell line (Viloria et al., 2016). Specifically, in this work an alternative splice variant of hevin lacking the signal peptide was detected by analyzing the splice variants and coding sequences databases. By RT-qPCR performed in this study, different hevin mRNA splice variants could be being detected and measured as a single transcript; while, by Western blot, both hevin isoforms (~130 kDa and ~100 kDa forms) are being measured independently. Thus, the differences between the AUD group and control group reported for the transcript would be diluted in the protein quantification.

Secondly, alternative polyadenylation phenomenon can cause the production of different protein isoforms. The polyadenylation of the pre- mRNA at the 3'-untranslated regions (3'UTRs) prevents its enzymatic degradation and mediates its export from the nucleus (Stewart, 2019; Zhang et al., 2021). Thus, improper functioning of polyadenylation polymerases in specific brain areas such as caudate nucleus could be causing hevin mRNA degradation or export blockade. In fact, in neurodegenerative diseases such as amyotrophic lateral sclerosis, Parkinson's and Alzheimer's diseases, different alternative polyadenylation profile has been identified among brain regions (Patel et al., 2019). Although there are still few evidences of the consequences of the polyadenylation alterations on disease, its implication in AUD is emerging with some preliminary studies trying to find alternative polyadenylation variants related to different alcohol consumption behaviors (Lusk et al., 2022). Furthermore, as one pre- mRNA might have more than one polyadenylation site, the mRNA can be cleavage or polyadenylated in different ways, creating many isoforms (Stewart, 2019; Zhang et al., 2021). Hevin mRNA presents more than one polyadenylation site, and, therefore, alternative polyadenylation could be mediating also the expression of different forms of the hevin protein (Jiang et al., 2022; Shen et al., 2022; Zhang et al., 2022).

Apart from the splicing or the polyadenylation of the 3'-terminus mentioned above, the mRNA suffers many other modifications to be transported from the nucleus to the cytoplasm or to be degraded. One is the capping of the 5'-terminus, a biological process that can alter the mRNA transport, and in which are involved many enzymes (Ramanathan et al., 2016).

Fourthly, a mRNA expressed in a given neuron can in some cases travel through the dendrites and axons to reach very distant sites, before being locally translated into protein (Das et al., 2019; Rodrigues et al., 2021) and this could in part explain the differences between mRNA and protein levels detected in the caudate nucleus. Thus, hevin mRNA may travel through the abundant inhibitory medium spiny neurons projections to be translated and secreted in other brain areas with higher glutamatergic synapse density or activity, such as prefrontal cortex, cerebellum or hippocampus, in agreement with the hevin protein overexpression detected in this brain areas (Consalez et al., 2021; Ferguson & Gao, 2018; Vigneault et al., 2015). In this way, hevin mRNA in the caudate nucleus may correspond to its expression in GABAergic parvalbumin local interneurons, while the mRNA and protein expression in glutamatergic projection neurons would be detected in other brain regions. (Gan & Südhof, 2020; Mongrédien et al., 2019).

Fifthly, even if the same unique transcript would be mediating the ~130 kDa and ~100 kDa protein translation, post-translational modifications (phosphorylation, ubiquitylation, glycosylation, addition of glycosaminoglycans) give rise to different hevin proteins and their subsequent independent detection and analysis, as it has been demonstrated in the present Doctoral Thesis (Buccitelli & Selbach, 2020). In fact, as mentioned before, the ~30 kDa difference in the molecular weight between the both bands might be caused by a wide range of post-translational modifications; some of them (e.g. ubiquitination) which could be mediating greater hevin protein degradation in the AUD group than in the control group, specifically in the caudate nucleus (Ravid & Hochstrasser, 2008). Indeed, altered transcriptome of elements implicated in the ubiquitination system have been reported in different brain areas of mice exposed to ethanol (Liu et al., 2006; Liu et al., 2022; Mignogna et al., 2019).

Finally, in the human brain both hevin forms are sensible to the cleavage by two proteases, ADAMTS4 and MMP-3. The activity of these enzymes might be regulating the levels of hevin ~130 kDa and ~100 kDa forms, as well as the ~47 kDa double band, identified as the possible SLF fragment. Therefore, it is possible that the activity or expression of these enzymes modulate the presence of hevin protein in response to ethanol with brain region specificity. Despite the current lack of information about the regional expression of ADAMTS4 and MMP-3 in the literature, there is an open access platform named The Human Protein Atlas (www.proteinatlas.org), that integrates and combines data from transcriptomics, single-

cell genomics, in situ hybridization and protein profiling (Sjöstedt et al., 2020). This website collects data from ADAMTS4 RNA-seq in human brain, showing that this protease is expressed with brain region specificity. In particular, ADAMTS4 is primarily expressed in basal ganglia, cerebellum and midbrain and, in a less extent, in the thalamus, hippocampus, hypothalamus and amygdala (data available from https://www.proteinatlas.org/ENSG00000158859-ADAMTS4/tissue). However, currently there is not reported data for the MMP-3 enzyme in the Human Brain Atlas. Importantly, the present Doctoral Thesis reveals that the hevin protein is altered in the brain of individuals suffering from AUD. Specifically, an overexpression of the ~130 kDa and ~100 kDa hevin forms in the prefrontal cortex and cerebellum, and of the ~100 kDa form in the hippocampus was detected in the AUD group in comparison to the control group. Even if the mechanisms underlying this feature or its consequences are difficult to determine in humans, several hypotheses can be postulated.

Hevin promotes the formation and maintenance of excitatory synapses specifically and modulates the refinement and stabilization of dendritic spines (Gan & Südhof, 2019; Kucukdereli et al., 2011; Risher et al., 2014; Singh et al., 2016). Therefore, the upregulation of hevin expression could be implicated in the profound structural rearrangement or adaptation that occurs in AUD (Avchalumov & Mandyam, 2020; Gass & Olive, 2012). Indeed, previous works have reported important loss in neurons, dendritic spines and neuronal structural proteins in AUD subjects (Bengochea & Gonzalo, 1990; Erdozain et al., 2014; Ferrer et al., 1986; Gass & Olive, 2012; Labisso et al., 2018). Furthermore, as previously mentioned (section 1.1.3.2), chronic alcohol consumption causes a loss of volume in the brain areas in which an increase of the hevin protein appears to be expressed (i.e. prefrontal cortex, cerebellum and hippocampus). Hevin increase could thus be an adaptive mechanism triggered in order to counteract ethanol's effects on neuronal structure.

Besides, at a molecular level, hevin increases NMDA receptor content and their function (Gan & Südhof, 2019, 2020; Singh et al., 2016). Hence, hevin could also mediate part of the synaptic plasticity occurring after chronic ethanol, such as long-term potentiation and NMDA receptor- dependent plasticity, as it has been widely described in preclinical studies as well as in postmortem human brain from subjects with AUD (Avchalumov & Mandyam, 2020; Burnett et al., 2016; Freund & Anderson, 1996; Loheswaran et al., 2017; Michaelis et al., 1993). Interestingly, despite its high expression in GABAergic parvalbumin interneurons,

hevin does not modulate inhibitory synapse formation or their transmission (Gan & Südhof, 2020; Mongrédien et al., 2019). Hence, the increase in hevin expression matches with the GABA/glutamate brain imbalance caused by alcohol (Wang et al., 2021).

Overall, the proposed hevin induced enhance in the excitatory transmission in the prefrontal cortex, cerebellum and hippocampus could be mediating the cognitive dysfunction and habituation of the behavior, which has previously been related to the glutamatergic signaling disruption in AUD (Burnett et al., 2016). In particular:

The prefrontal cortex is one of the main responsible areas for inhibitory control of the consumption and, thus, it moderates the drug craving and seeking behaviors. However, when the glutamatergic homeostasis is lost, the prefrontal cortex is overactivated and is not able to control properly these behaviors, thus promoting the preoccupation and anticipation of the drug consumption (Fish & Joffe, 2022; Yang et al., 2022). It is possible that hevin is taking part in this phase of the addiction cycle, due to its functions in the glutamatergic signaling. In regard to the cerebellum, during ethanol withdrawal the increase in the glutamatergic signaling has been related with neuron degeneration and the subsequent locomotor disturbances (i.e. ataxia) (Jung, 2015). Furthermore, the cerebellum controls the dopamine release in the prefrontal cortex through two glutamatergic pathways that reach the VTA, which suggest that it participates in the reward system (Miquel et al., 2016). The glutamatergic system also mediates the drug-induced sensitization in the cerebellum (Palomino et al., 2014). Although, further evidences are necessary to determine the implication of the cerebellar excitatory transmission in addiction disorders, hevin could be boosting all this processes in AUD by strengthening glutamatergic synapses.

In the same way, there is huge evidence in humans about the ethanol-induced hyperglutamatergic state in the hippocampus (e.g. elevated glutamate levels, increased expression of NMDA and AMPA receptors, downregulation of glutamate transporters) (Alasmari et al., 2018; Frischknecht et al., 2017). Since the hippocampus plays a critical role in the regulation of emotions, as well as in the contextual emotional memory, which are tightly regulated by the glutamatergic system, hevin might take part in the ethanol-related consolidation of memories and emotional dysregulation that occurs in AUD (Gonçalves-Ribeiro et al., 2019; Joyce et al., 2022).

On the other side, since hevin expression is increased in reactive astrocytes (McKinnon & Margolskee, 1996), another possible link between hevin overexpression and alcohol intake could be the astrocytic reactivity produced by alcohol (Tagliaferro et al., 2002). In fact, altered astrocytic gene expression has been reported in patients with AUD (Flatscher-Bader et al., 2005; Liu et al., 2007; Mayfield et al., 2002). Nevertheless, the large evidence on the ethanol-induced astrogliosis in preclinical models make more appropriate to discuss this hypothesis below, in the section referred to the results in animals (section 5.2.2).

Despite of the previously mentioned differences between the hevin mRNA and the protein, there is a linear correlation between the ~130 kDa and ~100 kDa bands immunoreactive signal in all brain regions for the three groups of study (Annex 3A-D). The linearity on the two bands expression shows that the both of them have similar expression pattern, when one is highly expressed, so is the other. This is especially relevant in the case of the hippocampus, in which, although the increase in the ~130 kDa band in the AUD group in comparison to controls did not reach statistical significance, the ~100 kDa band did. Therefore, the correlation in the expression between the both bands in both groups (AUD group: r= 0.8954, p<0.0001; Control: r=0.8491, p<0.0001) suggests that the ~130 kDa band may also be overexpressed in the hippocampus of AUD subjects, albeit not reaching statistical significance in our study.

Moreover, these data suggest that the extent of hevin's alterations in AUD are specific for each brain region: (i) percentage of increase, ii) whether the increase is observed in both protein and mRNA levels or only mRNA levels. Even if hevin's overexpression in subjects with AUD could be associated to the overall toxicity of the molecule, these region-dependent effects might suggest that hevin has a specific role in AUD's pathophysiology (Zink et al., 2020). In fact, distinct effects on synaptic plasticity has been reported depending on the phase of the dependence (acute and chronic intake, withdrawal or abstinence) and the brain region studied (Abrahao et al., 2017; Avchalumov & Mandyam, 2020).

Finally, consistent with a previous study and the results from the hevin transcript analysis, hevin protein expression was unaltered in the depression group, which was used as a control for disease specificity (Teyssier et al., 2011). This suggest that the alterations on the protein hevin might be characteristic for addictions disorders.

5.2.2. EFFECT OF ETHANOL TREATMENT ON THE EXPRESSION LEVELS OF THE PROTEIN HEVIN IN MOUSE BRAIN AND PLASMA

The data obtained in present Doctoral Thesis from the postmortem human brain raised the question of whether hevin overexpression is induced by ethanol or whether it is a pre-AUD state, suggesting vulnerability. In order to tackle this question, first a preclinical animal model of AUD was used to study the effects of ethanol administration on hevin protein expression and presence in both brain and plasma.

The C57BL/6J strain was selected since is the most widely used strain in neurobehavioral research and it has special sensitivity to addiction (Rhodes et al., 2007; Sloin et al., 2022). C57BL/6J male mice were injected i.p. with 1.75 g ethanol/kg, due to the ability of this dose to produce place preference in mice (Nocjar et al., 1999). Mice were submitted to four different ethanol treatments, which allowed the observation of the consequences of no alcohol consumption (S-S group), ethanol's acute effect (S-E group), the withdrawal effect (E-S group) and the effect of reinstatement after a withdrawal period (E-E group) (Bahi & Dreyer, 2012). The study of the withdrawal period outcome is of great interest since, as previously mentioned, the absence of the drug leads the brain in a hyperglutamatergic state and enhances stress and anxiety- like responses which produce neuroadaptative changes (Gerace et al., 2021; Hashimoto & Wiren, 2008; Patel et al., 2022; Yang et al., 2022).

The study of hevin expression in mouse brain was performed using total homogenate preparations, as the small amount of sample available from brain punches did not allow the use of post nuclear preparations (which was performed in the human brain study). Cortico-limbic brain regions involved in the neurocircuitry of drug addiction were selected, in particular nucleus accumbens, dorsal striatum (caudate nucleus and putamen), frontal cortex, hippocampus and amygdala (Koob & Volkow, 2016). In addition to the other brain areas mentioned before, the nucleus accumbens was selected as it is the main core of the mesocorticolimbic reward system and the amygdala due to its role in the reinforcement of negative emotional responses during alcohol withdrawal (Koob & Volkow, 2010; McCool, 2021; Roberto et al., 2021).

In respect to the mice´s brain Western blot analysis, only the main band of around ~130 kDa was detected in mice's cerebral tissue, which is consistent with previous reports in the literature (Brekken et al., 2004; Danjo et al., 2022; Kucukdereli et al., 2011; Wallingford et

al., 2017; Weaver et al., 2010). Regarding the study of the ethanol's acute effects on hevin expression, only the amygdala and the nucleus accumbens showed alterations after the ethanol treatment in comparison to the saline treatment.

In the amygdala, a decrease in hevin levels was observed after a single dose of ethanol, but not after chronic ethanol administration. In this context, acute and low doses of ethanol inhibit excitatory transmission and increase dendritic spines in rodents' amygdala, coinciding with anxiolytic effects (Harrison et al., 2017; Pandey et al., 2008; Roberto et al., 2021). Therefore, and according to the possible role of hevin in regulating the glutamatergic signaling and neuroplasticity in response to ethanol, hevin could be also taking part in the ethanol-mediated inhibition of the excitatory transmission in the amygdala. In contrast, chronic ethanol treatment increases glutamatergic transmission in rodents, causing tolerance to ethanol anxiolysis, while repeated withdrawal periods normalize dendritic arborization (Avegno et al., 2021; Pandey et al., 2008; Roberto et al., 2021; You et al., 2014). Although neither the ethanol withdrawal nor the reinstatement to which were submitted the mice produced alterations on hevin expression in the amygdala, it is possible that a prolonged ethanol treatment would be needed to activate the compensatory mechanisms in this key region.

On the contrary, in the nucleus accumbens, hevin was overexpressed only with a challenge dose after withdrawal, while no changes were observed after acute ethanol injection. It has already been described that chronic ethanol exposure and withdrawal in rodents' nucleus accumbens produces alterations in dendritic spine number, structure and organization, higher glutamate levels, as well as an increase in NMDA and AMPA receptors expression and function (Griffin et al., 2014; Ji et al., 2017; Kircher et al., 2019; Laguesse et al., 2017; Peterson et al., 2015; Uys et al., 2016; Zhou et al., 2007). This suggests that hevin increase observed in the nucleus accumbens could be the compensatory response to the ethanol-related glutamatergic inhibition. In this way, it is known that ethanol-mediated hyperglutamatergic state after prolonged intake is mediated, in part, by the increase in the NR2B containing NMDA receptors and their function (Burnett et al., 2016). Indeed, hevin increases the activity of these specific receptors (Chen et al., 2022; Singh et al., 2016). Furthermore, these results are also coherent with the alterations found in human brain, taking into account the high probability for alcoholic patients to experience withdrawal

periods followed by a relapse, even if this precise information was not available for the subjects included in the present Doctoral Thesis (Becker, 2008).

Overall, while changes in hevin's levels in the amygdala could be implicated in the acute alcohol experience, the increased hevin expression in the nucleus accumbens after chronic ethanol exposure suggests that hevin might also participate in the long-term adaptation to ethanol.

As noted, mouse and human brain showed different pattern of hevin expression levels in several regions (i.e. prefrontal cortex, hippocampus) after alcohol exposure. This difference could be explained by two essential factors largely discussed in the literature previously: i) the different regimen of alcohol exposure (time course, total drug intake and probable withdrawal period) which arises the question of what is the necessary cumulative effect of the drug to cause neuroplasticity, and ii) different psychosocial and environmental stressors (Koob & Volkow, 2010; Mackinnon et al., 2019).

How chronic alcohol exposure increases hevin brain expression remains unknown. Hevin has been found increased in reactive astrocytes in several pathological conditions, such as pilocarpine-induced epilepsy and ischemic models (Lively et al., 2011; Lively & Brown, 2007a, 2008b, 2008c; McKinnon & Margolskee, 1996). Both hevin expression and astrocytic activation and density are modulated by regulators of neuroinflammation (i.e. IL-10 induces hevin expression) (Blakely et al., 2015; Bull et al., 2014; Miguel-Hidalgo et al., 2006). Although in the present study the astrocytic reactivity has not been measured, since chronic ethanol intake induces reactive astrocytes (Tagliaferro et al., 2002; Teng et al., 2015; Vilpoux et al., 2022) and the upregulation of IL-10 (Patel et al., 2021), a possible explanation is that ethanol-induced astrogliosis led to the observed upregulation of hevin expression.

Regarding the study of hevin protein in the ethanol treated mice' plasma, two hevin bands were detected, the already described ~130 kDa band and additional band of around 47 kDa. Similar expression profile was obtained for the ~130 kDa band compared to that of the of nucleus accumbens, with increased hevin expression with a challenge dose after withdrawal. In this case, the increase was statistically significant only in comparison to the withdrawal period. However, the expression of ~47 kDa band appeared to be highly variable within the experimental groups, with some cases showing great immunoreactive signal and

other ones almost it absence. Although the identity of this band is not completely determined, it is possible that it corresponds to the hevin proteolytic cleavage product named SLF previously described at around 37-43 kDa for the murine hevin (Weaver et al., 2011; Weaver et al., 2010). Nevertheless, further experiments would be needed to verify the nature of this band and if its expression variability is due to altered activity of specific enzymes, such as ADMATS4 or MMP-3 which are present in plasma (Collazos et al., 2015; Kalebota et al., 2022; Zha et al., 2010).

The origin of hevin protein in blood plasma is still uncertain. As it has been demonstrated in the present Doctoral Thesis, hevin is not expressed by any blood cell type, but is expressed in other tissues than the brain, such as lung (Bendik et al., 1998), endothelial cells of high endothelial venules (Girard & Springer, 1995, 1996) or stomach (Klingler et al., 2020). The increase of the hevin ~130 kDa band in the plasma of ethanol-treated mice, suggests that hevin could be used as a biomarker in AUD relapse, as it has been proposed in the progression of the traumatic brain injury, severity of ischemic stroke, neurodegenerative diseases and several cancers (Ambrosius et al., 2018; Huang et al., 2019; Lau et al., 2006; Yin et al., 2009).

5.2.3. EFFECT OF HEVIN DOWNREGULATION IN THE ASTROCYTES OF THE NUCLEUS ACCUMBENS ON THE ETHANOL REWARDING PROPERTIES

In order to test the potential role of hevin on alcohol consumption, RNA interference strategy was used to downregulate hevin expression in the nucleus accumbens astrocytes, where it is essentially expressed (Mongrédien et al., 2019). Then, the consequence of hevin manipulation was evaluated in the intermittent ethanol access (IEA) model of voluntary ethanol intake. This animal model is one of the most used to study ethanol intake, since it induces ethanol intake escalation (Rosenwasser et al., 2013). Furthermore, the ethanol intake schedule has been selected based on the literature, since it allows to observe the effects of an abstinence period in the consumption reinstatement (Portero-Tresserra et al., 2018).

The downregulation of hevin was performed using hevin micro-RNA, a highly valuable tool that allows the selective repression of a given mRNA by promoting its degradation (Svoboda, 2020). The immunohistochemistry analysis of every mouse used in the study

verified the specific hevin knockdown and/ or the GFP expression in the astrocytes of the nucleus accumbens.

The obtained results indicate a disrupted reward system when hevin is downregulated. Specifically, in the first 4h, higher ethanol consumption was observed in hevin knockdown mice in comparison to control mice, in two cases: i) at high ethanol concentration (20%) administered after 12 days of intake, and ii) after three days of withdrawal with a medium ethanol concentration (10%). These findings suggest that ethanol addiction and withdrawal are associated with dysregulated hevin signaling. Since hevin increases excitatory synaptic plasticity, knocking-down hevin might disrupt the glutamatergic plasticity involved in the rewarding effects of ethanol (Alasmari et al., 2018; Griffin et al., 2014), making it necessary to increase alcohol consumption in order to reach the same hedonic response.

The effects of the hevin knockdown in the nucleus accumbens astrocytes on the ethanol intake, together with the observed increase in hevin expression in the nucleus accumbens after the reinstatement of the ethanol administration, suggest that hevin might be a key factor in the previously mentioned glutamatergic alterations subsequent to the chronic ethanol exposure and withdrawal (Griffin et al., 2014; Ji et al., 2017; Kircher et al., 2019; Laguesse et al., 2017; Peterson et al., 2015; Uys et al., 2016; Zhou et al., 2007).

To note, hevin knockdown mice drank significantly more of those preparations containing high ethanol concentration (20% at day 12) than those of low ethanol concentration (5% at day 3). This could either reflect the preference of hevin knockdown mice for higher ethanol containing beverages or, more probably, the need for a habituation period to make visible the behavioral consequences, as mentioned above.

Nevertheless, the consumption of ethanol in the last 4h of the experiment (4-8h) was similar between the hevin knockdown and control mice, and the ethanol preference analysis revealed that both groups drank as much water as ethanol, showing no differences in the preference at any dose and at any time. This suggests that mice undergo autoregulation in the water intake probably to avoid the dehydration produced by the higher ethanol intake.

In conclusion, the study of hevin implication in AUD data revealed increased hevin levels in various brain regions of subjects with AUD. In the same way, by the mouse model of chronic ethanol administration, it was found that relapse after chronic ethanol increases hevin in

the brain reward center, the nucleus accumbens. In addition, hevin manipulation in the astrocytes of the nucleus accumbens affected alcohol-related behavior, in particular, alcohol consumption. Therefore, these data suggest that hevin might be implicated both on ethanol's effects on the brain and/or on the processes leading to AUD. Thus, it is possible that chronic alcohol consumption in humans, coupled with repeated phases of abstinence and subsequent relapses could be altering hevin expression, which in turn would alter alcohol consumption, hence feeding the addiction cycle in AUD. Overall, the present Doctoral Thesis provides the first evidence for the role of hevin in alcohol consumption and addiction.

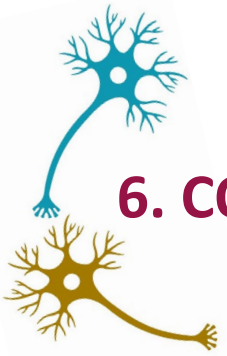

6. CONCLUSIONS

The main conclusions obtained from the present Doctoral Thesis are:

1. The matricellular protein hevin presents two immunodetectable isoforms in postmortem human brain, one migrating around 130 kDa and another one around 100 kDa.

2. The ~130 kDa and ~100 kDa hevin bands detected in human brain correspond to differently glycosilated hevin isoforms.

3. The ~130 kDa and ~100 kDa hevin bands in human brain are cleaved by ADAMTS4, MMP-3 and thrombin enzymes. The proteolytic cleavage of human hevin by ADAMTS4 and MMP-3 leads to a ~47 kDa fragment similar to that described as the SLF protein.

4. In control subjects, hevin expression is not affected by neither sex, age, PMD nor storage time; and there is a linear correlation between the expressions of both hevin isoforms.

5. The ~130 kDa and ~100 kDa hevin bands are strongly enriched in membranous fraction compared to cytosolic preparations, in all the studied regions (i.e. prefrontal cortex, hippocampus, caudate nucleus and cerebellum).

6. The ~130 kDa and ~100 kDa hevin bands are detected in the prefrontal cortex, hippocampus, caudate nucleus and cerebellum, with the largest expression detected in the prefrontal cortex.

7. Human astrocytoma samples exhibit greater expression of both hevin bands, with no significant differences in the relative expression of the ~130 kDa and ~100 kDa bands between both types of tumors. Additionally, the ~130 kDa isoform expression is increased in the astrocytoma samples in comparison to prefrontal cortex tissue.

8. Hevin is detected in CSF and plasma from control subjects, but it is absent from any blood cell type.

9. Hevin mRNA is significantly overexpressed in the prefrontal cortex, hippocampus, caudate nucleus and cerebellum of subjects with antemortem diagnosis of AUD in comparison to control subjects.

10. Subjects with AUD present increased expression of the ~130 kDa and ~100 kDa hevin isoforms in the prefrontal cortex and cerebellum, and increased expression of the ~100 kDa hevin isoform in the hippocampus, in comparison to controls.

11. In mice, a single dose of ethanol produces a decrease in hevin expression in the amygdala in comparison to the saline treatment, while in the nucleus accumbens, ethanol withdrawal and reinstatement leads to an increase in the hevin expression in comparison to the rest of the treatments. In addition, these mice' plasma show increased hevin expression after ethanol withdrawal and reinstatement in comparison to the withdrawal without reinstatement.

12. The downregulation of hevin mRNA in the nucleus accumbens astrocytes increases ethanol consumption in mice at high ethanol concentration administered after prolonged access to the drug, and after three days of withdrawal with a medium ethanol concentration. However, no differences are detected in the ethanol preference in these mice.

7. REFERENCES

Abernathy, K., Chandler, L. J., & Woodward, J. J. (2010). Alcohol and the prefrontal cortex. *International Review of Neurobiology*, *91*, 289–320.

Abrahao, K. P., Salinas, A. G., & Lovinger, D. M. (2017). Alcohol and the brain: neuronal molecular targets, synapses, and circuits. *Neuron*, *96*(6), 1223–1238.

Adams, J. C., Seed, B., & Lawler, J. (1998). Muskelin, a novel intracellular mediator of cell adhesive and cytoskeletal responses to thrombospondin-1. *The EMBO Journal*, *17*(17), 4964–4974.

Agabio, R., Trogu, E., & Pani, P. P. (2018). Antidepressants for the treatment of people with co-occurring depression and alcohol dependence. *The Cochrane Database of Systematic Reviews*, 4, CD008581.

Agrawal, A., & Lynskey, M. T. (2008). Are there genetic influences on addiction: Evidence from family, adoption and twin studies. *Addiction*, *103*(7), 1069–1081.

Alasmari, F., Goodwani, S., McCullumsmith, R. E., & Sari, Y. (2018). Role of glutamatergic system and mesocorticolimbic circuits in alcohol dependence. *Progress in Neurobiology*, *171*, 32–49.

Albrecht, C., von Der Kammer, H., Mayhaus, M., Klaudiny, J., Schweizer, M., & Nitsch, R. M. (2000). Muscarinic acetylcholine receptors induce the expression of the immediate early growth regulatory gene CYR61. *The Journal of Biological Chemistry*, *275*(37), 28929–28936.

Alexander, G. M., Graef, J. D., Hammarback, J. A., Nordskog, B. K., Burnett, E. J., Daunais, J. B., Bennett, A. J., Friedman, D. P., Suomi, S. J., & Godwin, D. W. (2012). Disruptions in serotonergic regulation of cortical glutamate release in primate insular cortex in response to chronic ethanol and nursery rearing. *Neuroscience*, *207*, 167–181.

Alhassoon, O. M., Sorg, S. F., Taylor, M. J., Stephan, R. A., Schweinsburg, B. C., Stricker, N. H., Gongvatana, A., & Grant, I. (2012). Callosal white matter microstructural recovery in abstinent alcoholics: A longitudinal diffusion tensor imaging study. *Alcoholism, Clinical and Experimental Research*, *36*(11), 1922–1931.

Allen, N. J., Bennett, M. L., Foo, L. C., Wang, G. X., Chakraborty, C., Smith, S. J., & Barres, B. A. (2012). Astrocyte glypicans 4 and 6 promote formation of excitatory synapses via GluA1 AMPA receptors. *Nature*, *486*(7403), 7403. https://doi.org/10.1038/nature11059

Allen, N. J., & Eroglu, C. (2017). Cell Biology of Astrocyte-Synapse Interactions. *Neuron*, *96*(3), 697–708.

Ambrosius, W., Michalak, S., Kazmierski, R., Lukasik, M., Andrzejewska, N., & Kozubski, W. (2018). The association between serum matricellular protein: secreted protein acidic and rich in cysteine-like 1 levels and ischemic stroke severity. *Journal of Stroke and Cerebrovascular Diseases*, *27*(3), 682–685.

American Psychiatric association (1994) *Diagnostic and statistical manual of mental disorders: DSM-IV.* In: Washington, DC.

American Psychiatric association (2000) *Diagnostic and statistical manual of mental disorders: DSM-IV-TR.* In: Washington, DC.

American Psychiatric association (2013) *Diagnostic and statistical manual of mental disorders: DSM-V.* In: Washington, DC.

Anton, R. F., Latham, P., Voronin, K., Book, S., Hoffman, M., Prisciandaro, J., & Bristol, E. (2020). Efficacy of gabapentin for the treatment of alcohol use disorder in patients with alcohol withdrawal symptoms: a randomized clinical trial. *JAMA Internal Medicine*, *180*(5), 728–736.

Anton, R. F., Schacht, J. P., Voronin, K. E., & Randall, P. K. (2017). Aripiprazole suppression of drinking in a clinical laboratory paradigm: influence of impulsivity and self-Control. *Alcoholism, Clinical and Experimental Research*, *41*(7), 1370–1380.

Ariwodola, O. J., & Weiner, J. L. (2004). Ethanol potentiation of GABAergic synaptic transmission may be self-limiting: role of presynaptic GABA(B) receptors. *The Journal of Neuroscience: The Official Journal of the Society for Neuroscience*, *24*(47), 10679–10686.

Arolfo, M. P., Yao, L., Gordon, A. S., Diamond, I., & Janak, P. H. (2004). Ethanol operant self-administration in rats is regulated by adenosine A2 receptors. *Alcoholism, Clinical and Experimental Research*, *28*(9), 1308–1316.

Asatryan, L., Nam, H. W., Lee, M. R., Thakkar, M. M., Dar, M. S., Davies, D. L., & Choi, D.-S. (2011). Implication of the purinergic system in alcohol use disorders. *Alcoholism, Clinical and Experimental Research*, *35*(4), 584–594.

Atwood, B. K., & Mackie, K. (2010). CB2: A cannabinoid receptor with an identity crisis. *British Journal of Pharmacology*, *160*(3), 467–479.

Avchalumov, Y., & Mandyam, C. D. (2020). Synaptic plasticity and its modulation by alcohol. *Brain Plasticity*, *6*(1), 103–111.

Avegno, E. M., Kasten, C. R., Snyder, W. B., Kelley, L. K., Lobell, T. D., Templeton, T. J., Constans, M., Wills, T. A., Middleton, J. W., & Gilpin, N. W. (2021). Alcohol dependence activates ventral tegmental area projections to central amygdala in male mice and rats. *Addiction Biology*, *26*(4), e12990.

Bahi, A., & Dreyer, J.-L. (2012). Involvement of nucleus accumbens dopamine D1 receptors in ethanol drinking, ethanol-induced conditioned place preference, and ethanol-induced psychomotor sensitization in mice. *Psychopharmacology*, *222*(1), 141–153.

Bailly, D., Vignau, J., Racadot, N., Beuscart, R., Servant, D., & Parquet, P. J. (1993). Platelet serotonin levels in alcoholic patients: Changes related to physiological and pathological factors. *Psychiatry Research*, *47*(1), 57–68.

Bajo, M., Cruz, M. T., Siggins, G. R., Messing, R., & Roberto, M. (2008). Protein kinase C epsilon mediation of CRF- and ethanol-induced GABA release in central amygdala. *Proceedings of the National Academy of Sciences*, *105*(24), 8410–8415.

Bare, D. J., McKinzie, J. H., & McBride, W. J. (1998). Development of rapid tolerance to ethanol-stimulated serotonin release in the ventral hippocampus. *Alcoholism, Clinical and Experimental Research*, *22*(6), 1272–1276.

Barone, R., Sturiale, L., Palmigiano, A., Zappia, M., & Garozzo, D. (2012). Glycomics of pediatric and adulthood diseases of the central nervous system. *Journal of Proteomics*, *75*(17), 5123–5139.

Barros, C. S., Franco, S. J., & Muller, U. (2011). Extracellular Matrix: Functions in the Nervous System. *Cold Spring Harbor Perspectives in Biology*, *3*(1), a005108–a005108.

Bartsch, S., Bartsch, U., Dörries, U., Faissner, A., Weller, A., Ekblom, P., & Schachner, M. (1992). Expression of tenascin in the developing and adult cerebellar cortex. *The Journal of Neuroscience: The Official Journal of the Society for Neuroscience*, *12*(3), 736–749.

Batel, P., Houchi, H., Daoust, M., Ramoz, N., Naassila, M., & Gorwood, P. (2008). A haplotype of the DRD1 gene is associated with alcohol dependence. *Alcoholism, Clinical and Experimental Research*, *32*(4), 567–572.

Becker, H. C. (2008). Alcohol dependence, withdrawal, and relapse. *Alcohol Research & Health*, *31*(4), 348–361.

Belmer, A., Patkar, O. L., Pitman, K. M., & Bartlett, S. E. (2016). Serotonergic neuroplasticity in alcohol addiction. *Brain Plasticity*, *1*(2), 177–206.

Bendik, I., Schraml, P., & Ludwig, C. U. (1998). Characterization of MAST9/hevin, a SPARC-like protein, that is down-regulated in non-small cell lung cancer. *Cancer Research*, *58*(4), 626–629.

Bengochea, O., & Gonzalo, L. M. (1990). Effect of chronic alcoholism on the human hippocampus. *Histology and Histopathology*, *5*(3), 349–357.

Bettinger, J. C., & Davies, A. G. (2014). The role of the BK channel in ethanol response behaviors: Evidence from model organism and human studies. *Frontiers in Physiology*, *5,* 346.

Bilbao, A., Neuhofer, D., Sepers, M., Wei, S.-P., Eisenhardt, M., Hertle, S., Lassalle, O., Ramos-Uriarte, A., Puente, N., Lerner, R., Thomazeau, A., Grandes, P., Lutz, B., Manzoni, O. J., & Spanagel, R. (2020). Endocannabinoid LTD in accumbal D1 neurons mediates reward-seeking behavior. *IScience*, *23*(3), 100951.

Blakely, P. K., Hussain, S., Carlin, L. E., & Irani, D. N. (2015). Astrocyte matricellular proteins that control excitatory synaptogenesis are regulated by inflammatory cytokines and

correlate with paralysis severity during experimental autoimmune encephalomyelitis. *Frontiers in Neuroscience*, *9, 344*.

Blednov, Y. A., Benavidez, J. M., Black, M., Leiter, C. R., Osterndorff-Kahanek, E., & Harris, R. A. (2015). Glycine receptors containing α2 or α3 subunits regulate specific ethanol-mediated behaviors. *Journal of Pharmacology and Experimental Therapeutics*, *353*(1), 181–191.

Bodhinathan, K., & Slesinger, P. A. (2013). Molecular mechanism underlying ethanol activation of G-protein–gated inwardly rectifying potassium channels. *Proceedings of the National Academy of Sciences*, *110*(45), 18309–18314.

Boikov, S. I., Sibarov, D. A., & Antonov, S. M. (2020). Ethanol inhibition of NMDA receptors in calcium-dependent and –independent modes. *Biochemical and Biophysical Research Communications*, *522*(4), 1046–1051.

Bolewska, P., Martin, B. I., Orlando, K. A., & Rhoads, D. E. (2019). Sequential changes in brain glutamate and adenosine a1 receptors may explain severity of adolescent alcohol withdrawal after consumption of High Levels of Alcohol. *Neuroscience Journal*, *2019*, e5950818.

Borea, P. A., Gessi, S., Merighi, S., Vincenzi, F., & Varani, K. (2018). Pharmacology of adenosine receptors: The State of the Art. *Physiological Reviews*, *98*(3), 1591–1625.

Bornstein, P. (1995). Diversity of function is inherent in matricellular proteins: an appraisal of thrombospondin 1. *Journal of Cell Biology*, *130*(3), 503–506.

Bornstein, P. (2009a). Matricellular proteins: an overview. *Journal of Cell Communication and Signaling*, *3*(3–4), 163–165.

Bornstein, P. (2009b). Thrombospondins function as regulators of angiogenesis. *Journal of Cell Communication and Signaling*, *3*(3–4), 189–200.

Bornstein, P., & Sage, E. H. (2002). Matricellular proteins: extracellular modulators of cell function. *Current Opinion in Cell Biology*, *14*(5), 608–616.

Bradford, M. M. (1976). A rapid and sensitive method for the quantitation of microgram quantities of protein utilizing the principle of protein-dye binding. *Analytical Biochemistry*, *72*(1), 248–254.

Brayman, V. L., Taetzsch, T., Miko, M., Dahal, S., Risher, W. C., & Valdez, G. (2021). Roles of the synaptic molecules Hevin and SPARC in mouse neuromuscular junction development and repair. *Neuroscience Letters*, *746*, 135663.

Brekken, R. A., & Sage, E. H. (2001). SPARC, a matricellular protein: at the crossroads of cell-matrix communication. *Matrix Biology: Journal of the International Society for Matrix Biology*, *19*(8), 816–827.

Brekken, R. A., Sullivan, M. M., Workman, G., Bradshaw, A. D., Carbon, J., Siadak, A., Murri, C., Framson, P. E., & Sage, E. H. (2004). Expression and characterization of murine hevin (SC1), a member of the SPARC family of matricellular proteins. *Journal of Histochemistry & Cytochemistry*, *52*(6), 735–748.

Buccitelli, C., & Selbach, M. (2020). mRNAs, proteins and the emerging principles of gene expression control. *Nature Reviews Genetics*, *21*(10), 10.

Buck, S. A., Torregrossa, M. M., Logan, R. W., & Freyberg, Z. (2021). Roles of dopamine and glutamate co-release in the nucleus accumbens in mediating the actions of drugs of abuse. *The FEBS Journal*, *288*(5), 1462–1474.

Buerki, R. A., Horbinski, C. M., Kruser, T., Horowitz, P. M., James, C. D., & Lukas, R. V. (2018). An overview of meningiomas. *Future Oncology*, *14*(21), 2161–2177.

Bull, C., Freitas, K. C. C., Zou, S., Poland, R. S., Syed, W. A., Urban, D. J., Minter, S. C., Shelton, K. L., Hauser, K. F., Negus, S. S., Knapp, P. E., & Bowers, M. S. (2014). Rat nucleus accumbens core astrocytes modulate reward and the motivation to self-administer ethanol after abstinence. *Neuropsychopharmacology, 39*(12), 2835–2845.

Burnett, E. J., Chandler, L. J., & Trantham-Davidson, H. (2016). Glutamatergic plasticity and alcohol dependence-induced alterations in reward, affect and cognition. *Progress in Neuro-Psychopharmacology & Biological Psychiatry*, *65*, 309–320.

Burnette, E. M., Nieto, S. J., Grodin, E. N., Meredith, L. R., Hurley, B., Miotto, K., Gillis, A. J., & Ray, L. A. (2022). Novel Agents for the pharmacological treatment of alcohol use disorder. *Drugs*, *82*(3), 251–274.

Butler, T. R., & Prendergast, M. A. (2012). Neuroadaptations in adenosine receptor signaling following long-term ethanol exposure and withdrawal. *Alcoholism, Clinical and Experimental Research*, *36*(1), 4–13.

Cannady, R., Rinker, J. A., Nimitvilai, S., Woodward, J. J., & Mulholland, P. J. (2018). Chronic alcohol, intrinsic excitability, and potassium channels: neuroadaptations and drinking behavior. *Handbook of Experimental Pharmacology*, *248*, 311–343.

Cao, J., Liu, X., Han, S., Zhang, C. K., Liu, Z., & Li, D. (2014). Association of the HTR2A Gene with alcohol and heroin abuse. *Human Genetics*, *133*(3), 357–365.

Cardenas, V. A., Studholme, C., Gazdzinski, S., Durazzo, T. C., & Meyerhoff, D. J. (2007). Deformation-based morphometry of brain changes in alcohol dependence and abstinence. *NeuroImage*, *34*(3), 879–887.

Ceccarini, J., Hompes, T., Verhaeghen, A., Casteels, C., Peuskens, H., Bormans, G., Claes, S., & Laere, K. V. (2014). Changes in cerebral CB1 Receptor availability after acute and chronic alcohol abuse and monitored abstinence. *Journal of Neuroscience*, *34*(8), 2822–2831.

Ceraso, A., Lin, J. J., Schneider-Thoma, J., Siafis, S., Tardy, M., Komossa, K., Heres, S., Kissling, W., Davis, J. M., & Leucht, S. (2020). Maintenance treatment with antipsychotic drugs for schizophrenia. *Cochrane Database of Systematic Reviews*, *8*.

Chanraud, S., Leroy, C., Martelli, C., Kostogianni, N., Delain, F., Aubin, H.-J., Reynaud, M., & Martinot, J.-L. (2009). Episodic memory in detoxified alcoholics: contribution of grey matter microstructure alteration. *PLOS ONE*, *4*(8), e6786.

Chen, G., Xu, J., Luo, H., Luo, X., Singh, S. K., Ramirez, J. J., James, M. L., Mathew, J. P., Berger, M., Eroglu, C., & Ji, R.-R. (2022). Sparcl1/Hevin drives pathological pain through spinal cord astrocyte and NMDA receptor signaling. *JCI Insight*.

Chin, J. H., & Goldstein, D. B. (1981). Membrane-disordering action of ethanol: Variation with membrane cholesterol content and depth of the spin label probe. *Molecular Pharmacology*, *19*(3), 425–431.

Christopherson, K. S., Ullian, E. M., Stokes, C. C. A., Mullowney, C. E., Hell, J. W., Agah, A., Lawler, J., Mosher, D. F., Bornstein, P., & Barres, B. A. (2005). Thrombospondins Are Astrocyte-Secreted Proteins that Promote CNS Synaptogenesis. *Cell*, *120*(3), 421–433.

Claeskens, A., Ongenae, N., Neefs, J. M., Cheyns, P., Kaijen, P., Cools, M., & Kutoh, E. (2000). Hevin is down-regulated in many cancers and is a negative regulator of cell growth and proliferation. *British Journal of Cancer*, *82*(6), 1123–1130.

Clarke, R. B. C., & Adermark, L. (2010). Acute ethanol treatment prevents endocannabinoid-mediated long-lasting disinhibition of striatal output. *Neuropharmacology*, *58*(4), 799–805.

Clarke, R. B. C., Adermark, L., Chau, P., Söderpalm, B., & Ericson, M. (2014). Increase in nucleus accumbens dopamine levels following local ethanol administration is not mediated by acetaldehyde. *Alcohol and Alcoholism*, *49*(5), 498–504.

Collazos, J., Asensi, V., Martin, G., Montes, A. H., Suárez-Zarracina, T., & Valle-Garay, E. (2015). The effect of gender and genetic polymorphisms on matrix metalloprotease (MMP) and tissue inhibitor (TIMP) plasma levels in different infectious and non-infectious conditions. *Clinical and Experimental Immunology*, *182*(2), 213–219.

Collins, M. A., An, J., Peller, D., & Bowser, R. (2015). Total protein is an effective loading control for cerebrospinal fluid western blots. *Journal of Neuroscience Methods*, *251*, 72–82.

Consalez, G. G., Goldowitz, D., Casoni, F., & Hawkes, R. (2021). Origins, development, and compartmentation of the granule cells of the cerebellum. *Frontiers in Neural Circuits*, *14,* 611841.

Costa, E. T., Soto, E. E., Cardoso, R. A., Olivera, D. S., & Valenzuela, C. F. (2000). Acute effects of ethanol on kainate receptors in cultured hippocampal neurons. *Alcoholism, Clinical and Experimental Research*, *24*(2), 220–225.

Costardi, J. V. V., Nampo, R. A. T., Silva, G. L., Ribeiro, M. A. F., Stella, H. J., Stella, M. B., & Malheiros, S. V. P. (2015). A review on alcohol: From the central action mechanism to chemical dependency. *Revista Da Associação Médica Brasileira*, *61*(4), 381–387.

Courville, C. B. (1955). *Effects of alcohol on the nervous system of man* (p. 102). San Lucas Press (316 N. Bailey St.).

Cowen, M. S., & Lawrence, A. J. (1999). The role of opioid-dopamine interactions in the induction and maintenance of ethanol consumption. *Progress in Neuro-Psychopharmacology & Biological Psychiatry*, *23*(7), 1171–1212.

Crabbe, J. C., Phillips, T. J., Feller, D. J., Hen, R., Wenger, C. D., Lessov, C. N., & Schafer, G. L. (1996). Elevated alcohol consumption in null mutant mice lacking 5-HT1B serotonin receptors. *Nature Genetics*, *14*(1), 98–101.

Cruz, M. T., Herman, M. A., Kallupi, M., & Roberto, M. (2012). nociceptin/orphanin fq blockade of corticotropin-releasing factor-induced gamma-aminobutyric acid release in central amygdala is enhanced after chronic ethanol exposure. *Biological Psychiatry*, *71*(8), 666–676.

Cuzon Carlson, V. C. (2018). GABA and Glutamate Synaptic Coadaptations to Chronic Ethanol in the Striatum. In K. A. Grant & D. M. Lovinger (Eds.), *The Neuropharmacology of Alcohol* (pp. 79–112). Springer International Publishing.

Dalan, A. B., Gulluoglu, S., Tuysuz, E. C., Kuskucu, A., Yaltirik, C. K., Ozturk, O., Ture, U., & Bayrak, O. F. (2017). Simultaneous analysis of miRNA-mRNA in human meningiomas by integrating transcriptome: A relationship between PTX3 and miR-29c. *BMC Cancer*, *17*(1).

Danjo, Y., Shigetomi, E., Hirayama, Y. J., Kobayashi, K., Ishikawa, T., Fukazawa, Y., Shibata, K., Takanashi, K., Parajuli, B., Shinozaki, Y., Kim, S. K., Nabekura, J., & Koizumi, S. (2022). Transient astrocytic mGluR5 expression drives synaptic plasticity and subsequent chronic pain in mice. *Journal of Experimental Medicine*, *219*(4), e20210989.

Dar, M. S., Mustafa, S. J., & Wooles, W. R. (1983). Possible role of adenosine in the CNS effects of ethanol. *Life Sciences*, *33*(14), 1363–1374.

Das, S., Singer, R. H., & Yoon, Y. J. (2019). The travels of mRNAs in neurons: Do they know where they are going? *Current Opinion in Neurobiology*, *57*, 110–116.

Daurio, A. M., Deschaine, S. L., Modabbernia, A., & Leggio, L. (2020). Parsing out the role of dopamine D4 receptor gene (DRD4) on alcohol-related phenotypes: A meta-analysis and systematic review. *Addiction Biology*, *25*(3), e12770.

Daviet, R., Aydogan, G., Jagannathan, K., Spilka, N., Koellinger, P. D., Kranzler, H. R., Nave, G., & Wetherill, R. R. (2022). Associations between alcohol consumption and gray and white matter volumes in the UK Biobank. *Nature Communications*, *13*(1175).

de la Vega Gallardo, N., Dittmer, M., Dombrowski, Y., & Fitzgerald, D. C. (2019). Regenerating CNS myelin: Emerging roles of regulatory T cells and CCN proteins. *Neurochemistry International*, *130*, 104349.

De Rubeis, S., He, X., Goldberg, A. P., Poultney, C. S., Samocha, K., Cicek, A. E., Kou, Y., Liu, L., Fromer, M., Walker, S., Singh, T., Klei, L., Kosmicki, J., Fu, S.C., Aleksic, B., Biscaldi, M., Bolton, P. F., Brownfeld, J. M., Cai, J., …& Buxbaum, J. D. (2014). Synaptic, transcriptional, and chromatin genes disrupted in autism. *Nature*, *515*(7526), 209–215.

Deak, J. D., Miller, A. P., & Gizer, I. R. (2019). Genetics of alcohol use disorder: A review. *Current Opinion in Psychology*, *27*, 56–61.

Deehan, G. A., Jr, Knight, C. P., Waeiss, R. A., Engleman, E. A., Toalston, J. E., McBride, W. J., Hauser, S. R., & Rodd, Z. A. (2016). Peripheral administration of ethanol results in a correlated increase in dopamine and serotonin within the posterior ventral tegmental area. *Alcohol and Alcoholism*, *51*(5), 535–540.

DePoy, L., Daut, R., Brigman, J. L., MacPherson, K., Crowley, N., Gunduz-Cinar, O., Pickens, C. L., Cinar, R., Saksida, L. M., Kunos, G., Lovinger, D. M., Bussey, T. J., Camp, M. C., & Holmes, A. (2013). Chronic alcohol produces neuroadaptations to prime dorsal striatal learning. *Proceedings of the National Academy of Sciences*, *110*(36), 14783–14788.

Di Chiara, G., & Imperato, A. (1988). Drugs abused by humans preferentially increase synaptic dopamine concentrations in the mesolimbic system of freely moving rats. *Proceedings of the National Academy of Sciences of the United States of America*, *85*(14), 5274–5278.

Dopico, A. M., Bukiya, A. N., & Martin, G. E. (2014). Ethanol modulation of mammalian BK channels in excitable tissues: Molecular targets and their possible contribution to alcohol-induced altered behavior. *Frontiers in Physiology*, *5*, 466.

Downs, A. M., & McElligott, Z. A. (2022). Noradrenergic circuits and signaling in substance use disorders. *Neuropharmacology*, *208*, 108997.

Driscoll, M. E., Bollu, P. C., & Tadi, P. (2022). *Neuroanatomy, Nucleus Caudate*. Treasure Island (FL): StatPearls Publishing.

Durazzo, T. C., Mon, A., Gazdzinski, S., Yeh, P.-H., & Meyerhoff, D. J. (2015). Serial longitudinal magnetic resonance imaging data indicate non-linear regional gray matter volume recovery in abstinent alcohol-dependent individuals. *Addiction Biology*, *20*(5), 956–967.

Easton, A. C., Lucchesi, W., Lourdusamy, A., Lenz, B., Solati, J., Golub, Y., Lewczuk, P., Fernandes, C., Desrivieres, S., Dawirs, R. R., Moll, G. H., Kornhuber, J., Frank, J., Hoffmann, P., Soyka, M., Kiefer, F., GESGA Consortium, Schumann, G., Peter Giese, K., … Rietschel, M. (2013). ACaMKII autophosphorylation controls the establishment of alcohol drinking behavior. *Neuropsychopharmacology*, *38*(9), 1636–1647.

Edenberg, H. J., & McClintick, J. N. (2018). Alcohol dehydrogenases, aldehyde dehydrogenases, and alcohol use disorders: a critical review. *Alcoholism: Clinical and Experimental Research*, *42*(12), 2281–2297.

Egervari, G., Siciliano, C. A., Whiteley, E. L., & Ron, D. (2021). Alcohol and the brain: From genes to circuits. *Trends in Neurosciences*, S0166-2236(21)00187-9.

Elu, N., Osinalde, N., Beaskoetxea, J., Ramirez, J., Lectez, B., Aloria, K., Rodriguez, J. A., Arizmendi, J. M., & Mayor, U. (2019). Detailed dissection of UBE3A-mediated DDI1 ubiquitination. *Frontiers in Physiology*, *10*, 534.

Emanuele, M. A., Wezeman, F., & Emanuele, N. V. (2002). Alcohol's effects on female reproductive function. *Alcohol Research & Health: The Journal of the National Institute on Alcohol Abuse and Alcoholism*, *26*(4), 274–281.

Engleman, E. A., McBride, W. J., Wilber, A. A., Shaikh, S. R., Eha, R. D., Lumeng, L., Li, T. K., & Murphy, J. M. (2000). Reverse microdialysis of a dopamine uptake inhibitor in the nucleus accumbens of alcohol-preferring rats: Effects on dialysate dopamine levels and ethanol intake. *Alcoholism, Clinical and Experimental Research*, *24*(6), 795–801.

Erdozain, A. M., & Callado, L. F. (2011). Involvement of the endocannabinoid system in alcohol dependence: The biochemical, behavioral and genetic evidence. *Drug and Alcohol Dependence*, *117*(2), 102–110.

Erdozain, A. M., Morentin, B., Bedford, L., King, E., Tooth, D., Brewer, C., Wayne, D., Johnson, L., Gerdes, H. K., Wigmore, P., Callado, L. F., & Carter, W. G. (2014). Alcohol-related brain damage in humans. *PLOS ONE*, *9*(4), e93586.

Erdozain, A. M., Rubio, M., Meana, J. J., Fernández-Ruiz, J., & Callado, L. F. (2015). Altered CB1 receptor coupling to G-proteins in the post-mortem caudate nucleus and cerebellum of alcoholic subjects. *Journal of Psychopharmacology (Oxford, England)*, *29*(11), 1137–1145.

Erdozain, A. M., Rubio, M., Valdizan, E. M., Pazos, A., Meana, J. J., Fernández-Ruiz, J., Alexander, S. P. H., & Callado, L. F. (2015). The endocannabinoid system is altered in the post-mortem prefrontal cortex of alcoholic subjects. *Addiction Biology*, *20*(4), 773–783.

Erickson, E. K., DaCosta, A. J., Mason, S. C., Blednov, Y. A., Mayfield, R. D., & Harris, R. A. (2021). Cortical astrocytes regulate ethanol consumption and intoxication in mice. *Neuropsychopharmacology*, *46*(3), 500–508. https://doi.org/10.1038/s41386-020-0721-0

Eroglu, C. (2009). The role of astrocyte-secreted matricellular proteins in central nervous system development and function. *Journal of Cell Communication and Signaling*, *3*(3–4), 167–176.

Eroglu, Ç., Allen, N. J., Susman, M. W., O'Rourke, N. A., Park, C. Y., Özkan, E., Chakraborty, C., Mulinyawe, S. B., Annis, D. S., Huberman, A. D., Green, E. M., Lawler, J., Dolmetsch, R., Garcia, K. C., Smith, S. J., Luo, Z. D., Rosenthal, A., Mosher, D. F., & Barres, B. A. (2009).

Gabapentin receptor α2δ-1 is a neuronal thrombospondin receptor responsible for excitatory CNS synaptogenesis. *Cell*, *139*(2), 380–392.

Espírito-Santo, S., Coutinho, V. G., Dezonne, R. S., Stipursky, J., Santos-Rodrigues, A. dos, Batista, C., Paes-de-Carvalho, R., Fuss, B., & Gomes, F. C. A. (2021). Astrocytes as a target for Nogo-A and implications for synapse formation in vitro and in a model of acute demyelination. *Glia*, *69*(6), 1429–1443.

Ewald, A. C., Kiernan, E. A., Roopra, A. S., Radcliff, A. B., Timko, R. R., Baker, T. L., & Watters, J. J. (2020). Sex- and Region-Specific Differences in the Transcriptomes of Rat Microglia from the Brainstem and Cervical Spinal Cord. *Journal of Pharmacology and Experimental Therapeutics*, *375*(1), 210–222.

Fan, S., Gangwar, S. P., Machius, M., & Rudenko, G. (2021). Interplay between hevin, SPARC, and MDGAs: Modulators of neurexin-neuroligin transsynaptic bridges. *Structure 29*(7)*: 664-678*.

Fang, T., Dong, H., Xu, X.-H., Yuan, X.-S., Chen, Z.-K., Chen, J.-F., Qu, W.-M., & Huang, Z.-L. (2017). Adenosine A2A receptor mediates hypnotic effects of ethanol in mice. *Scientific Reports*, *7*:12678.

Fathi, A.-R., & Roelcke, U. (2013). Meningioma. *Current Neurology and Neuroscience Reports*, *13*(4): 337.

Federici, M., Nisticò, R., Giustizieri, M., Bernardi, G., & Mercuri, N. B. (2009). Ethanol enhances GABAB-mediated inhibitory postsynaptic transmission on rat midbrain dopaminergic neurons by facilitating GIRK currents. *The European Journal of Neuroscience*, *29*(7), 1369–1377.

Ferguson, B. R., & Gao, W.-J. (2018). PV interneurons: critical regulators of E/I balance for prefrontal cortex-dependent behavior and psychiatric disorders. *Frontiers in Neural Circuits*, *12,* 37.

Ferhat, L., Chevassus au Louis, N., Jorquera, I., Niquet, J., Khrestchatisky, M., Ben-Ari, Y., & Represa, A. (1996). Transient increase of tenascin-C in immature hippocampus: Astroglial and neuronal expression. *Journal of Neurocytology*, *25*(1), 53–66.

Ferrer, I., Fábregues, I., Rairiz, J., & Galofré, E. (1986). Decreased numbers of dendritic spines on cortical pyramidal neurons in human chronic alcoholism. *Neuroscience Letters*, *69*(1), 115–119.

Fish, K., & Joffe, M. (2022). Targeting prefrontal cortex GABAergic microcircuits for the treatment of alcohol use disorder. *Frontiers in Synaptic Neuroscience*, *14,* 936911.

Flatscher-Bader, T., van der Brug, M., Hwang, J. W., Gochee, P. A., Matsumoto, I., Niwa, S.-I., & Wilce, P. A. (2005). Alcohol-responsive genes in the frontal cortex and nucleus accumbens of human alcoholics. *Journal of Neurochemistry*, *93*(2), 359–370.

Forero, D. A., López-León, S., Shin, H. D., Park, B. L., & Kim, D.-J. (2015). Meta-analysis of six genes (BDNF, DRD1, DRD3, DRD4, GRIN2B and MAOA) involved in neuroplasticity and the risk for alcohol dependence. *Drug and Alcohol Dependence*, *149*, 259–263.

Förstera, B., Castro, P. A., Moraga-Cid, G., & Aguayo, L. G. (2016). Potentiation of gamma aminobutyric acid receptors ($GABA_AR$) by ethanol: how are inhibitory receptors affected? *Frontiers in Cellular Neuroscience*, *10*, 114.

Förstera, B., Muñoz, B., Lobo, M. K., Chandra, R., Lovinger, D. M., & Aguayo, L. G. (2017). Presence of ethanol-sensitive glycine receptors in medium spiny neurons in the mouse nucleus accumbens. *Journal of Physiology*, *595*(15), 5285–5300.

Framson, P. E., & Sage, E. H. (2004). SPARC and tumor growth: where the seed meets the soil? *Journal of Cellular Biochemistry*, *92*(4), 679–690.

Freeze, H. H., & Kranz, C. (2010). Endoglycosidase and glycoamidase release of N-Linked glycans. *Current Protocols in Molecular Biology*, *8*.

Freund, G., & Anderson, K. J. (1996). Glutamate receptors in the frontal cortex of alcoholics. *Alcoholism, Clinical and Experimental Research*, *20*(7), 1165–1172.

Freund, G., & Anderson, K. J. (1999). Glutamate receptors in the cingulate cortex, hippocampus, and cerebellar vermis of alcoholics. *Alcoholism, Clinical and Experimental Research*, *23*(1), 1–6.

Friedman, N. P., & Robbins, T. W. (2022). The role of prefrontal cortex in cognitive control and executive function. *Neuropsychopharmacology*, *47*(1), 1.

Frischknecht, U., Hermann, D., Tunc-Skarka, N., Wang, G.-Y., Sack, M., van Eijk, J., Demirakca, T., Falfan-Melgoza, C., Krumm, B., Dieter, S., Spanagel, R., Kiefer, F., Mann, K. F., Sommer, W. H., Ende, G., & Weber-Fahr, W. (2017). Negative association between MR-spectroscopic glutamate markers and gray matter volume after alcohol withdrawal in the hippocampus: A Translational Study in Humans and Rats. *Alcoholism, Clinical and Experimental Research*, *41*(2), 323–333.

Gagliardi, F., Narayanan, A., & Mortini, P. (2017). SPARCL1 a novel player in cancer biology. *Critical Reviews in Oncology/Hematology*, *109*, 63–68.

Gan, K. J., & Südhof, T. C. (2019). Specific factors in blood from young but not old mice directly promote synapse formation and NMDA-receptor recruitment. *Proceedings of the National Academy of Sciences*, *116*(25), 12524–12533.

Gan, K. J., & Südhof, T. C. (2020). SPARCL1 promotes excitatory but not inhibitory synapse formation and function independent of neurexins and neuroligins. *The Journal of Neuroscience*, *40*(42), 8088–8102.

Gass, J. T., & Olive, M. F. (2012). Neurochemical and neurostructural plasticity in alcoholism. *ACS Chemical Neuroscience*, *3*(7), 494–504.

Gazdzinski, S., Durazzo, T. C., & Meyerhoff, D. J. (2005). Temporal dynamics and determinants of whole brain tissue volume changes during recovery from alcohol dependence. *Drug and Alcohol Dependence*, *78*(3), 263–273.

Ge, L., Zhuo, Y., Wu, P., Liu, Y., Qi, L., Teng, X., Duan, D., Chen, P., & Lu, M. (2020). Olfactory ensheathing cells facilitate neurite sprouting and outgrowth by secreting high levels of hevin. *Journal of Chemical Neuroanatomy*, *104*, 101728.

Gerace, E., Ilari, A., Caffino, L., Buonvicino, D., Lana, D., Ugolini, F., Resta, F., Nosi, D., Grazia Giovannini, M., Ciccocioppo, R., Fumagalli, F., Pellegrini-Giampietro, D. E., Masi, A., & Mannaioni, G. (2021). Ethanol neurotoxicity is mediated by changes in expression, surface localization and functional properties of glutamate AMPA receptors. *Journal of Neurochemistry*, *157*(6), 2106–2118.

Gessa, G. L., Muntoni, F., Collu, M., Vargiu, L., & Mereu, G. (1985). Low doses of ethanol activate dopaminergic neurons in the ventral tegmental area. *Brain Research*, *348*(1), 201–203.

Gilpin, N. W. (2008). Neurobiology of alcohol dependence. *Neurobiology of Alcohol Dependence*, *31*(3), 11.

Gimeno, C., Dorado, M. L., Roncero, C., Szerman, N., Vega, P., Balanzá-Martínez, V., & Alvarez, F. J. (2017). Treatment of comorbid alcohol dependence and anxiety disorder: review of the scientific evidence and recommendations for treatment. *Frontiers in Psychiatry*, *8*, 173.

Girard, J.-P., Baekkevold, E. S., Yamanaka, T., Haraldsen, G., Brandtzaeg, P., & Amalric, F. (1999). Heterogeneity of endothelial cells: the specialized phenotype of human high endothelial venules characterized by suppression subtractive hybridization. *The American Journal of Pathology*, *155*(6), 2043–2055.

Girard, J.-P., & Springer, T. A. (1995). Cloning from purified high endothelial venule cells of hevin, a close relative of the antiadhesive extracellular matrix protein SPARC. *Immunity*, *2*(1), 113–123.

Girard, J.-P., & Springer, T. A. (1996). Modulation of endothelial cell adhesion by hevin, an acidic protein associated with high endothelial venules. *Journal of Biological Chemistry*, *271*(8), 4511–4517.

Gleich, T., Spitta, G., Butler, O., Zacharias, K., Aydin, S., Sebold, M., Garbusow, M., Rapp, M., Schubert, F., Buchert, R., Heinz, A., & Gallinat, J. (2021). Dopamine D2/3 receptor availability in alcohol use disorder and individuals at high risk: towards a dimensional approach. *Addiction Biology*, *26*(2), e12915.

Goldstein, D. B. (1984). The effects of drugs on membrane fluidity. *Annual Review of Pharmacology and Toxicology*, *24*, 43–64.

Gonçalves-Ribeiro, J., Pina, C. C., Sebastião, A. M., & Vaz, S. H. (2019). Glutamate transporters in hippocampal LTD/LTP: not just prevention of excitotoxicity. *Frontiers in Cellular Neuroscience*, *13*, 357.

Gongidi, V., Ring, C., Moody, M., Brekken, R., Sage, E. H., Rakic, P., & Anton, E. S. (2004). SPARC-like 1 regulates the terminal phase of radial glia-guided migration in the cerebral cortex. *Neuron*, *41*(1), 57–69.

Goodwani, S., Saternos, H., Alasmari, F., & Sari, Y. (2017). Metabotropic and ionotropic glutamate receptors as potential targets for the treatment of alcohol use disorder. *Neuroscience and Biobehavioral Reviews*, *77*, 14–31.

Grahn, J. A., Parkinson, J. A., & Owen, A. M. (2008). The cognitive functions of the caudate nucleus. *Progress in Neurobiology*, *86*(3), 141–155.

Greenbaum, D., Colangelo, C., Williams, K., & Gerstein, M. (2003). Comparing protein abundance and mRNA expression levels on a genomic scale. *Genome Biology*, *4*(9), 117.

Griffin, W. C., Haun, H. L., Hazelbaker, C. L., Ramachandra, V. S., & Becker, H. C. (2014). Increased extracellular glutamate in the nucleus accumbens promotes excessive ethanol drinking in ethanol dependent mice. *Neuropsychopharmacology*, *39*(3), 707–717.

Gronseth, E., Wang, L., Harder, D. R., & Ramchandran, R. (2018). The Role of Astrocytes in Tumor Growth and Progression. *Astrocyte - Physiology and Pathology*.

Grover, T., Gupta, R., Arora, G., Bal, C. S., Ambekar, A., Basu Ray, S., Vaswani, M., & Sharma, A. (2020). Dopamine transporter availability in alcohol and opioid dependent subjects—a ^{99m}Tc-TRODAT-1SPECT imaging and genetic association study. *Psychiatry Research. Neuroimaging*, *305*, 111187.

Haass-Koffler, C. L., Swift, R. M., & Leggio, L. (2018). Noradrenergic targets for the treatment of alcohol use disorder. *Psychopharmacology*, *235*(6), 1625–1634.

Halim, A., Rüetschi, U., Larson, G., & Nilsson, J. (2013). LC–MS/MS characterization of o-glycosylation sites and glycan structures of human cerebrospinal fluid glycoproteins. *Journal of Proteome Research*, *12*(2), 573–584.

Hambrock, H. O., Nitsche, D. P., Hansen, U., Bruckner, P., Paulsson, M., Maurer, P., & Hartmann, U. (2003). SC1/Hevin: an extracellular calcium-modulated protein that binds collagen I. *Journal of Biological Chemistry*, *278*(13), 11351–11358.

Hammack, B. N., Fung, K. Y. C., Hunsucker, S. W., Duncan, M. W., Burgoon, M. P., Owens, G. P., & Gilden, D. H. (2004). Proteomic analysis of multiple sclerosis cerebrospinal fluid. *Multiple Sclerosis (Houndmills, Basingstoke, England)*, *10*(3), 245–260.

Hampton, W. H., Hanik, I. M., & Olson, I. R. (2019). Substance abuse and white matter: findings, limitations, and future of diffusion tensor imaging research. *Drug and Alcohol Dependence*, *197*, 288–298.

Han, W., Cao, F., Ding, W., Gao, X.-J., Chen, F., Hu, Y.-W., & Ding, H.-Z. (2018). Prognostic value of SPARCL1 in patients with colorectal cancer. *Oncology Letters*, *15*(2), 1429–1434.

Harris, R. A., Mihic, S. J., Dildy-Mayfield, J. E., & Machu, T. K. (1995). Actions of anesthetics on ligand-gated ion channels: Role of receptor subunit composition. *FASEB Journal: Official Publication of the Federation of American Societies for Experimental Biology*, *9*(14), 1454–1462.

Harrison, N. L., Skelly, M. J., Grosserode, E. K., Lowes, D. C., Zeric, T., Phister, S., & Salling, M. C. (2017). Effects of acute alcohol on excitability in the CNS. *Neuropharmacology*, *122*, 36–45.

Hashimoto, J. G., & Wiren, K. M. (2008). Neurotoxic Consequences of Chronic Alcohol Withdrawal: Expression Profiling Reveals Importance of Gender Over Withdrawal Severity. *Neuropsychopharmacology*, *33*(5), 1084-96.

Hashimoto, N., Sato, T., Yajima, T., Fujita, M., Sato, A., Shimizu, Y., Shimada, Y., Shoji, N., Sasano, T., & Ichikawa, H. (2016). SPARCL1-containing neurons in the human brainstem and sensory ganglion. *Somatosensory & Motor Research*, *33*(2), 112–117.

He, X., Lee, B., & Jiang, Y. (2016). Cell-ECM Interactions in Tumor Invasion. In Rejniak K. (Ed.), *Systems Biology of Tumor Microenvironment* (Vol. 936, pp. 73–91). Advances in Experimental Medicine and Biology, Springer.

Heilig, M., MacKillop, J., Martinez, D., Rehm, J., Leggio, L., & Vanderschuren, L. J. M. J. (2021). Addiction as a brain disease revised: why it still matters, and the need for consilience. *Neuropsychopharmacology*, *46,* 1715–1723.

Heinz, A., Daedelow, L. S., Wackerhagen, C., & Di Chiara, G. (2020). Addiction theory matters-Why there is no dependence on caffeine or antidepressant medication. *Addiction Biology*, *25*(2), e12735.

Heinz, A., Jones, D. W., Mazzanti, C., Goldman, D., Ragan, P., Hommer, D., Linnoila, M., & Weinberger, D. R. (2000). A relationship between serotonin transporter genotype and in vivo protein expression and alcohol neurotoxicity. *Biological Psychiatry*, *47*(7), 643–649.

Heinz, A., Ragan, P., Jones, D. W., Hommer, D., Williams, W., Knable, M. B., Gorey, J. G., Doty, L., Geyer, C., Lee, K. S., Coppola, R., Weinberger, D. R., & Linnoila, M. (1998). Reduced central serotonin transporters in alcoholism. *The American Journal of Psychiatry*, *155*(11), 1544–1549.

Heinz, A., Reimold, M., Wrase, J., Hermann, D., Croissant, B., Mundle, G., Dohmen, B. M., Braus, D. F., Braus, D. H., Schumann, G., Machulla, H.-J., Bares, R., & Mann, K. (2005). Correlation of stable elevations in striatal mu-opioid receptor availability in detoxified alcoholic patients with alcohol craving: A positron emission tomography study using carbon 11-labeled carfentanil. *Archives of General Psychiatry*, *62*(1), 57–64.

Heinz, A., Siessmeier, T., Wrase, J., Hermann, D., Klein, S., Grüsser-Sinopoli, S. M., Flor, H., Braus, D. F., Buchholz, H. G., Gründer, G., Schreckenberger, M., Smolka, M. N., Rösch, F., Mann, K., & Bartenstein, P. (2004). Correlation Between Dopamine D2 Receptors in the Ventral Striatum and Central Processing of Alcohol Cues and Craving. *American Journal of Psychiatry*, *161*(10), 1783–1789.

Henderson-Redmond, A. N., Guindon, J., & Morgan, D. J. (2016). Roles for the endocannabinoid system in ethanol-motivated behavior. *Progress in Neuro-Psychopharmacology and Biological Psychiatry*, *65*, 330–339.

Hennekinne, L., Colasse, S., Triller, A., & Renner, M. (2013). Differential control of thrombospondin over synaptic glycine and AMPA receptors in spinal cord neurons. *Journal of Neuroscience*, *33*(28), 11432–11439.

Henricks, A. M., Berger, A. L., Lugo, J. M., Baxter-Potter, L. N., Bieniasz, K. V., Petrie, G., Sticht, M. A., Hill, M. N., & McLaughlin, R. J. (2017). Sex- and hormone-dependent alterations in alcohol withdrawal-induced anxiety and corticolimbic endocannabinoid signaling. *Neuropharmacology*, *124*, 121–133.

Herkenham, M., Lynn, A. B., de Costa, B. R., & Richfield, E. K. (1991). Neuronal localization of cannabinoid receptors in the basal ganglia of the rat. *Brain Research*, *547*(2), 267–274.

Hermann, D., Hirth, N., Reimold, M., Batra, A., Smolka, M. N., Hoffmann, S., Kiefer, F., Noori, H. R., Sommer, W. H., Reischl, G., la Fougère, C., Mann, K., Spanagel, R., & Hansson, A. C. (2017). Low μ-opioid receptor status in alcohol dependence identified by combined positron emission tomography and post-mortem brain analysis. *Neuropsychopharmacology*, *42*(3), 606–614.

Hinckers, A. S., Laucht, M., Schmidt, M. H., Mann, K. F., Schumann, G., Schuckit, M. A., & Heinz, A. (2006). Low level of response to alcohol as associated with serotonin transporter genotype and high alcohol intake in adolescents. *Biological Psychiatry*, *60*(3), 282–287.

Hirvonen, J., Goodwin, R. S., Li, C.-T., Terry, G. E., Zoghbi, S. S., Morse, C., Pike, V. W., Volkow, N. D., Huestis, M. A., & Innis, R. B. (2012). Reversible and regionally selective downregulation of brain cannabinoid CB1 receptors in chronic daily cannabis smokers. *Molecular Psychiatry*, *17*(6), :642-49.

Hirvonen, J., Zanotti-Fregonara, P., Umhau, J. C., George, D. T., Rallis-Frutos, D., Lyoo, C. H., Li, C.-T., Hines, C. S., Sun, H., Terry, G. E., Morse, C., Zoghbi, S. S., Pike, V. W., Innis, R. B., & Heilig, M. (2013). Reduced cannabinoid CB1 receptor binding in alcohol dependence measured with positron emission tomography. *Molecular Psychiatry*, *18*(8), 916-921.

Ho, M.-F., Zhang, C., Wei, L., Zhang, L., Moon, I., Geske, J. R., Skime, M. K., Choi, D.-S., Biernacka, J. M., Oesterle, T. S., Frye, M. A., Seppala, M. D., Karpyak, V. M., Li, H., & Weinshilboum, R. M. (2022). Genetic variants associated with acamprosate treatment response in alcohol use disorder patients: A multiple omics study. *British Journal of Pharmacology*, *179*(13), 3330–3345.

Ho, P.-S., Shih, M.-C., Ma, K.-H., Huang, W.-S., Ho, K. K.-J., Yen, C.-H., Lu, R.-B., & Huang, S.-Y. (2011). Availability of the serotonin transporter in patients with alcohol dependence. *The World Journal of Biological Psychiatry: The Official Journal of the World Federation of Societies of Biological Psychiatry*, *12*(2), 134–142.

Hodge, C. W., Samson, H. H., Lewis, R. S., & Erickson, H. L. (1993). Specific decreases in ethanol- but not water-reinforced responding produced by the 5-HT3 antagonist ICS 205-930. *Alcohol (Fayetteville, N.Y.)*, *10*(3), 191–196.

Hu, J., Henry, S., Gallezot, J.-D., Ropchan, J., Neumaier, J. F., Potenza, M. N., Sinha, R., Krystal, J. H., Huang, Y., Ding, Y.-S., Carson, R. E., & Neumeister, A. (2010). Serotonin 1B receptor imaging in alcohol dependence. *Biological Psychiatry*, *67*(9), 800–803.

Huang, H.-B., Yang, S.-B., Shen, L.-J., Lv, Q.-W., Guo, M., Zhou, J., Li, Z., Yang, C.-S., Wang, L.-Y., & Zhang, H. (2019). A prospective study on serum secreted protein acidic and rich in cysteine-like 1 as a prognostic marker for severe traumatic brain injury. *Clinica Chimica Acta; International Journal of Clinical Chemistry*, *491*, 19–23.

Hurley, P. J., Marchionni, L., Simons, B. W., Ross, A. E., Peskoe, S. B., Miller, R. M., Erho, N., Vergara, I. A., Ghadessi, M., Huang, Z., Gurel, B., Park, B. H., Davicioni, E., Jenkins, R. B., Platz, E. A., Berman, D. M., & Schaeffer, E. M. (2012). Secreted protein, acidic and rich in cysteine-like 1 (SPARCL1) is down regulated in aggressive prostate cancers and is prognostic for poor clinical outcome. *Proceedings of the National Academy of Sciences*, *109*(37), 14977–14982.

Hurt, R. T., Ebbert, J. O., Croghan, I. T., Schroeder, D. R., Hurt, R. D., & Hays, J. T. (2018). Varenicline for tobacco-dependence treatment in alcohol-dependent smokers: A randomized controlled trial. *Drug and Alcohol Dependence*, *184*, 12–17.

Ikemoto, S., McBride, W. J., Murphy, J. M., Lumeng, L., & Li, T. K. (1997). 6-OHDA-lesions of the nucleus accumbens disrupt the acquisition but not the maintenance of ethanol consumption in the alcohol-preferring P line of rats. *Alcoholism, Clinical and Experimental Research*, *21*(6), 1042–1046.

Irintchev, A., Rollenhagen, A., Troncoso, E., Kiss, J. Z., & Schachner, M. (2005). Structural and Functional Aberrations in the Cerebral Cortex of Tenascin-C Deficient Mice. *Cerebral Cortex*, *15*(7), 950–962.

Jacquemont, M.-L., Sanlaville, D., Redon, R., Raoul, O., Cormier-Daire, V., Lyonnet, S., Amiel, J., Le Merrer, M., Heron, D., de Blois, M.-C., Prieur, M., Vekemans, M., Carter, N. P., Munnich, A., Colleaux, L., & Philippe, A. (2006). Array-based comparative genomic hybridisation identifies high frequency of cryptic chromosomal rearrangements in patients with syndromic autism spectrum disorders. *Journal of Medical Genetics*, *43*(11), 843–849.

Jakharia, A., Borkakoty, B., & Singh, S. (2016). Expression of SPARC like protein 1 (SPARCL1), extracellular matrix-associated protein is down regulated in gastric adenocarcinoma. *Journal of Gastrointestinal Oncology*, *7*(2), 278–283.

Jayakumar, A. R., Apeksha, A., & Norenberg, M. D. (2017). Role of matricellular proteins in disorders of the central nervous system. *neurochemical research*, *42*(3), 858–875.

Ji, X., Saha, S., Kolpakova, J., Guildford, M., Tapper, A. R., & Martin, G. E. (2017). Dopamine receptors differentially control binge alcohol drinking-mediated synaptic plasticity of the core nucleus accumbens direct and indirect pathways. *The Journal of Neuroscience: The Official Journal of the Society for Neuroscience*, *37*(22), 5463–5474.

Jiang, Q., Wang, H., Yuan, D., Qian, X., Ma, X., Yan, M., & Xing, W. (2022). Circular_0086414 induces SPARC like 1 (SPARCL1) production to inhibit esophageal cancer cell proliferation, invasion and glycolysis and induce cell apoptosis by sponging miR-1290. *Bioengineered*, *13*(5), 12099–12114.

Job, M. O., Tang, A., Hall, F. S., Sora, I., Uhl, G. R., Bergeson, S. E., & Gonzales, R. A. (2007). Mu (μ) Opioid Receptor Regulation of Ethanol-Induced Dopamine Response in the Ventral Striatum: Evidence of Genotype Specific Sexual Dimorphic Epistasis. *Biological Psychiatry*, *62*(6), 627–634.

Joffe, M. E., Centanni, S. W., Jaramillo, A. A., Winder, D. G., & Conn, P. J. (2018). Metabotropic Glutamate Receptors in Alcohol Use Disorder: Physiology, Plasticity, and Promising Pharmacotherapies. *ACS Chemical Neuroscience*, *9*(9), 2188–2204.

Johnson, B. A., Roache, J. D., Ait-Daoud, N., Zanca, N. A., & Velazquez, M. (2002). Ondansetron reduces the craving of biologically predisposed alcoholics. *Psychopharmacology*, *160*(4), 408–413.

Johnson, K. A., & Lovinger, D. M. (2020). Allosteric modulation of metabotropic glutamate receptors in alcohol use disorder: Insights from preclinical investigations. *Advances in Pharmacology*, *88*, 193–232.

Johnston, I. G., Paladino, T., Gurd, J. W., & Brown, I. R. (1990). Molecular cloning of SC1: A putative brain extracellular matrix glycoprotein showing partial similarity to osteonectin/BM40/SPARC. *Neuron*, *4*(1), 165–176.

Jonas, D. E., Amick, H. R., Feltner, C., Bobashev, G., Thomas, K., Wines, R., Kim, M. M., Shanahan, E., Gass, C. E., Rowe, C. J., & Garbutt, J. C. (2014). Pharmacotherapy for adults with alcohol use disorders in outpatient settings: A systematic review and meta-analysis. *JAMA*, *311*(18), 1889–1900.

Jones, D. T., & Graff-Radford, J. (2021). Executive Dysfunction and the Prefrontal Cortex. *Continuum (Minneapolis, Minn.)*, *27*(6), 1586–1601.

Jones, E. V., Bernardinelli, Y., Tse, Y. C., Chierzi, S., Wong, T. P., & Murai, K. K. (2011). Astrocytes Control Glutamate Receptor Levels at Developing Synapses through SPARC- -Integrin Interactions. *Journal of Neuroscience*, *31*(11), 4154–4165.

Jones, E. V., & Bouvier, D. S. (2014). Astrocyte-secreted matricellular proteins in cns remodelling during development and disease. *Neural Plasticity*, *2014*, 1–12.

Joyce, M. K. P., Marshall, L. G., Banik, S. L., Wang, J., Xiao, D., Bunce, J. G., & Barbas, H. (2022). Pathways for memory, cognition and emotional context: hippocampal, subgenual area 25, and amygdalar axons show unique interactions in the primate thalamic reuniens nucleus. *Journal of Neuroscience*, *42*(6), 1068–1089.

Jung, M. E. (2015). Alcohol withdrawal and cerebellar mitochondria. *The Cerebellum*, *14*(4), 421–437.

Jung, Y., Montel, R. A., Shen, P.-H., Mash, D. C., & Goldman, D. (2019). Assessment of the association of D2 dopamine receptor gene and reported allele frequencies with alcohol use disorders: a systematic review and meta-analysis. *JAMA Network Open*, *2*(11), e1914940.

Kähler, A. K., Djurovic, S., Kulle, B., Jönsson, E. G., Agartz, I., Hall, H., Opjordsmoen, S., Jakobsen, K. D., Hansen, T., Melle, I., Werge, T., Steen, V. M., & Andreassen, O. A. (2008). Association analysis of schizophrenia on 18 genes involved in neuronal migration: MDGA1 as a new susceptibility gene. *American Journal of Medical Genetics Part B: Neuropsychiatric Genetics*, *147B*(7), 1089–1100.

Kaij, L., & Rosenthal, D. (1961). Alcoholism in Twins. Studies on the Etiology and Sequels of Abuse of Alcohol. *The Journal of Nervous and Mental Disease*, *133*(3), 272.

Kalebota, N., Salai, G., Peric, P., Hrkac, S., Novak, R., Durmis, K. K., & Grgurevic, L. (2022). ADAMTS-4 as a possible distinguishing indicator between osteoarthritis and haemophilic arthropathy. *Haemophilia*, *28*(4), 656–662.

Kalinichenko, L. S., Hammad, L., Reichel, M., Kohl, Z., Gulbins, E., Kornhuber, J., & Müller, C. P. (2019). Acid sphingomyelinase controls dopamine activity and responses to appetitive stimuli in mice. *Brain Research Bulletin*, *146*, 310–319.

Kalk, N. J., & Lingford-Hughes, A. R. (2014). The clinical pharmacology of acamprosate. *British Journal of Clinical Pharmacology*, *77*(2), 315–323.

Kamimura, K., & Maeda, N. (2021). Glypicans and heparan sulfate in synaptic development, neural plasticity, and neurological disorders. *Frontiers in Neural Circuits*, *15*, 595596.

Kaplan, G. B., Leite-Morris, K. A., Fan, W., Young, A. J., & Guy, M. D. (2011). Opiate sensitization induces FosB/ΔFosB expression in prefrontal cortical, striatal and amygdala brain regions. *PLOS ONE*, *6*(8), e23574.

Kärkkäinen, O., Laukkanen, V., Haukijärvi, T., Kautiainen, H., Tiihonen, J., & Storvik, M. (2015). Lower [3H]citalopram binding in brain areas related to social cognition in alcoholics. *Alcohol and Alcoholism*, *50*(1), 46–50.

Karlsson, I., Ndreu, L., Quaranta, A., & Thorsén, G. (2017). Glycosylation patterns of selected proteins in individual serum and cerebrospinal fluid samples. *Journal of Pharmaceutical and Biomedical Analysis*, *145*, 431–439.

Karriker-Jaffe, K. J., Room, R., Giesbrecht, N., & Greenfield, T. K. (2018). Alcohol's harm to others: opportunities and challenges in a public health framework. *Journal of Studies on Alcohol and Drugs*, *79*(2), 239–243.

Kendler, K. S., Schmitt, E., Aggen, S. H., & Prescott, C. A. (2008). Genetic and environmental influences on alcohol, caffeine, cannabis, and nicotine use from early adolescence to middle adulthood. *Archives of General Psychiatry*, *65*(6), 674–682.

Kennedy, P. J., & Shapiro, M. L. (2009). Motivational states activate distinct hippocampal representations to guide goal-directed behaviors. *Proceedings of the National Academy of Sciences*, *106*(26), 10805–10810.

Khatri, S. N., Wu, W.-C., Yang, Y., & Pugh, J. R. (2019). Direction of action of presynaptic GABAA receptors is highly dependent on the level of receptor activation. *Journal of Neurophysiology*, *121*(5), 1896–1905.

Kim, H.-B., Morris, J., Miyashiro, K., Lehto, T., Langel, Ü., Eberwine, J., & Sul, J.-Y. (2021a). Astrocytes promote ethanol-induced enhancement of intracellular Ca2+ signals through intercellular communication with neurons. *IScience*, *24*(5), 102436.

Kim, J.-H., Jung, H.-G., Kim, A., Shim, H. S., Hyeon, S. J., Lee, Y.-S., Han, J., Jung, J. H., Lee, J., Ryu, H., Park, J.-Y., Hwang, E. M., & Suk, K. (2021b). Hevin–calcyon interaction promotes synaptic reorganization after brain injury. *Cell Death & Differentiation*, *28*, 2571-2588.

King, A., Vena, A., de Wit, H., Grant, J. E., & Cao, D. (2022). Effect of combination treatment with varenicline and nicotine patch on smoking cessation among smokers who drink heavily: a randomized clinical trial. *JAMA Network Open*, *5*(3), e220951.

Kircher, D. M., Aziz, H. C., Mangieri, R. A., & Morrisett, R. A. (2019). Ethanol experience enhances glutamatergic ventral hippocampal inputs to D1 receptor-expressing medium spiny neurons in the nucleus accumbens shell. *The Journal of Neuroscience: The Official Journal of the Society for Neuroscience*, *39*(13), 2459–2469.

Kishi, T., Sevy, S., Chekuri, R., & Correll, C. U. (2013). Antipsychotics for primary alcohol dependence: A systematic review and meta-analysis of placebo-controlled trials. *The Journal of Clinical Psychiatry*, *74*(7), e642-654.

Klein, M. O., Battagello, D. S., Cardoso, A. R., Hauser, D. N., Bittencourt, J. C., & Correa, R. G. (2019). Dopamine: functions, signaling, and association with neurological diseases. *Cellular and Molecular Neurobiology*, *39*(1), 31–59.

Klingler, A., Regensburger, D., Tenkerian, C., Britzen-Laurent, N., Hartmann, A., Stürzl, M., & Naschberger, E. (2020). Species-, organ- and cell-type-dependent expression of SPARCL1 in human and mouse tissues. *PLOS ONE*, *15*(5), e0233422.

Kobayashi, T., Ikeda, K., Kojima, H., Niki, H., Yano, R., Yoshioka, T., & Kumanishi, T. (1999). Ethanol opens G-protein-activated inwardly rectifying K+ channels. *Nature Neuroscience*, *2*(12), 1091-1097.

Koistinen, M., Tuomainen, P., Hyytiä, P., & Kiianmaa, K. (2001). Naltrexone suppresses ethanol intake in 6-hydroxydopamine-treated rats. *Alcoholism, Clinical and Experimental Research*, *25*(11), 1605–1612.

Koob, G. F. (2021). Drug Addiction: hyperkatifeia/negative reinforcement as a framework for medications development. *Pharmacological Reviews*, *73*(1), 163–201.

Koob, G. F., & Volkow, N. D. (2010). Neurocircuitry of Addiction. *Neuropsychopharmacology*, *35*(1), 217–238.

Koob, G. F., & Volkow, N. D. (2016). Neurobiology of addiction: A neurocircuitry analysis. *The Lancet Psychiatry*, *3*(8), 760–773.

Kotti, A., Holmqvist, A., Albertsson, M., & Sun, X.-F. (2014). SPARCL1 expression increases with preoperative radiation therapy and predicts better survival in rectal cancer patients. *International Journal of Radiation Oncology·Biology·Physics*, *88*(5), 1196–1202.

Koulentaki, M., & Kouroumalis, E. (2018). GABAA receptor polymorphisms in alcohol use disorder in the GWAS era. *Psychopharmacology*, *235*(6), 1845–1865.

Kranzler, H. R., Pierucci-Lagha, A., Feinn, R., & Hernandez-Avila, C. (2003). Effects of ondansetron in early- versus late-onset alcoholics: A prospective, open-label study. *Alcoholism, Clinical and Experimental Research*, *27*(7), 1150–1155.

Kranzler, H. R., & Soyka, M. (2018). Diagnosis and Pharmacotherapy of Alcohol Use Disorder: A Review. *JAMA*, *320*(8), 815–824.

Krystal, J. H. & Tobakoff B. (2002). Ethanol abuse, dependence, and withdrawal: neurobiology and clinical implications. In Kenneth L. D., Dennis C., Joseph T. C. & Charles N. (eds), *Neuropsychopharmacology: The Fifth Generation of Progress* (pp. 1425-1443). American College of Neuropsychopharmacology.

Kucukdereli, H., Allen, N. J., Lee, A. T., Feng, A., Ozlu, M. I., Conatser, L. M., Chakraborty, C., Workman, G., Weaver, M., Sage, E. H., Barres, B. A., & Eroglu, C. (2011). Control of excitatory CNS synaptogenesis by astrocyte-secreted proteins Hevin and SPARC. *Proceedings of the National Academy of Sciences of the United States of America*, *108*(32), E440-449.

Kumar, S., Porcu, P., Werner, D. F., Matthews, D. B., Diaz-Granados, J. L., Helfand, R. S., & Morrow, A. L. (2009). The role of $GABA_A$ receptors in the acute and chronic effects of ethanol: A decade of progress. *Psychopharmacology*, *205*(4), 529.

Kumar, S., Ren, Q., Beckley, J., O'Buckley, T., Gigante, E., Santerre, J., Werner, D., & Morrow, A. L. (2012). Ethanol Activation of protein kinase A Regulates $GABA_A$ receptor subunit expression in the cerebral cortex and contributes to ethanol-induced hypnosis. *Frontiers in Neuroscience*, *6*, 44.

Kutlu, M. G., & Gould, T. J. (2016). Effects of drugs of abuse on hippocampal plasticity and hippocampus-dependent learning and memory: Contributions to development and maintenance of addiction. *Learning & Memory*, *23*(10), 515–533.

Kyzar, E. J., & Pandey, S. C. (2015). Molecular mechanisms of synaptic remodeling in alcoholism. *Neuroscience Letters*, *601*, 11–19.

La Vignera, S., Condorelli, R. A., Balercia, G., Vicari, E., & Calogero, A. E. (2013). Does alcohol have any effect on male reproductive function? A review of literature. *Asian Journal of Andrology*, *15*(2), 221–225.

Labisso, W. L., Raulin, A.-C., Nwidu, L. L., Kocon, A., Wayne, D., Erdozain, A. M., Morentin, B., Schwendener, D., Allen, G., Enticott, J., Gerdes, H. K., Johnson, L., Grzeskowiak, J., Drizou, F., Tarbox, R., Osna, N. A., Kharbanda, K. K., Callado, L. F., & Carter, W. G. (2018). The Loss of α- and β-tubulin proteins are a pathological hallmark of chronic alcohol consumption and natural brain ageing. *Brain Sciences*, *8*(9), E175.

Lacagnina, M. J., Rivera, P. D., & Bilbo, S. D. (2017). Glial and neuroimmune mechanisms as critical modulators of drug use and abuse. *Neuropsychopharmacology*, *42*(1), 156–177.

Laguesse, S., Morisot, N., Shin, J. H., Liu, F., Adrover, M. F., Sakhai, S. A., Lopez, M. F., Phamluong, K., Griffin, W. C., Becker, H. C., Bender, K. J., Alvarez, V. A., & Ron, D. (2017). Prosapip1-Dependent synaptic adaptations in the nucleus accumbens drive alcohol intake, seeking, and reward. *Neuron*, *96*(1), 145-159.e8.

Laramée, P., Kusel, J., Leonard, S., Aubin, H.-J., François, C., & Daeppen, J.-B. (2013). The economic burden of alcohol dependence in Europe. *Alcohol and Alcoholism*, *48*(3), 259–269.

Lasek, A. W. (2016). Effects of Ethanol on Brain Extracellular Matrix: Implications for Alcohol Use Disorder. *Alcoholism: Clinical and Experimental Research*, *40*(10), 2030–2042.

Lau, C.-Y., Poon, R.-P., Cheung, S.-T., Yu, W.-C., & Fan, S.-T. (2006). SPARC and Hevin expression correlate with tumour angiogenesis in hepatocellular carcinoma. *The Journal of Pathology*, *210*(4), 459–468.

Lê, A. D., Funk, D., Harding, S., Juzytsch, W., Fletcher, P. J., & Shaham, Y. (2006). Effects of dexfenfluramine and 5-HT3 receptor antagonists on stress-induced reinstatement of alcohol seeking in rats. *Psychopharmacology*, *186*(1), 82–92.

Le Berre, A.-P., Fama, R., & Sullivan, E. V. (2017). Executive functions, memory, and social cognitive deficits and recovery in chronic alcoholism: a critical review to inform future research. *Alcoholism, Clinical and Experimental Research*, *41*(8), 1432–1443.

LeMarquand, D., Pihl, R. O., & Benkelfat, C. (1994). Serotonin and alcohol intake, abuse, and dependence: Clinical evidence. *Biological Psychiatry*, *36*(5), 326–337.

Li, D., Sulovari, A., Cheng, C., Zhao, H., Kranzler, H. R., & Gelernter, J. (2014). Association of gamma-aminobutyric acid A receptor α2 gene (GABRA2) with alcohol use disorder. *Neuropsychopharmacology*, *39*(4), 907–918.

Li, L., Yu, H., Liu, Y., Meng, Y.-J., Li, X.-J., Zhang, C., Liang, S., Li, M.-L., Guo, W., Qiang W., null, Deng, W., Ma, X., Coid, J., & Li, T. (2021). Lower regional grey matter in alcohol use disorders: Evidence from a voxel-based meta-analysis. *BMC Psychiatry*, *21*(1), 247.

Liu, J., Lewohl, J. M., Harris, R. A., Dodd, P. R., & Mayfield, R. D. (2007). Altered gene expression profiles in the frontal cortex of cirrhotic alcoholics. *Alcoholism: Clinical and Experimental Research*, *31*(9), 1460–1466.

Liu, J., Lewohl, J. M., Harris, R. A., Iyer, V. R., Dodd, P. R., Randall, P. K., & Mayfield, R. D. (2006). Patterns of gene expression in the frontal cortex discriminate alcoholic from nonalcoholic individuals. *Neuropsychopharmacology*, *31*(7), 1574–1582.

Liu, M., Guo, S., Huang, D., Hu, D., Wu, Y., Zhou, W., & Song, W. (2022). Chronic alcohol exposure alters gene expression and neurodegeneration pathways in the brain of adult mice. *Journal of Alzheimer's Disease*, *86*(1), 315–331.

Lively, S., & Brown, I. R. (2007a). Analysis of the extracellular matrix protein SC1 during reactive gliosis in the rat lithium–pilocarpine seizure model. *Brain Research*, *1163*, 1–9.

Lively, S., & Brown, I. R. (2008a). Extracellular matrix protein SC1/hevin in the hippocampus following pilocarpine-induced status epilepticus. *Journal of Neurochemistry*, *107*(5), 1335–1346.

Lively, S., & Brown, I. R. (2008b). The extracellular matrix protein SC1/hevin localizes to excitatory synapses following status epilepticus in the rat lithium-pilocarpine seizure model. *Journal of Neuroscience Research*, *86*(13), 2895–2905.

Lively, S., & Brown, I. R. (2008c). Localization of the Extracellular Matrix Protein SC1 Coincides with Synaptogenesis During Rat Postnatal Development. *Neurochemical Research*, *33*(9), 1692–1700.

Lively, S., Moxon-Emre, I., & Schlichter, L. C. (2011). SC1/hevin and reactive gliosis after transient ischemic stroke in young and aged rats. *Journal of Neuropathology and Experimental Neurology*, *70*(10), 913–929.

Lively, S., Ringuette, M. J., & Brown, I. R. (2007b). Localization of the Extracellular Matrix Protein SC1 to Synapses in the Adult Rat Brain. *Neurochemical Research*, *32*(1), 65–71.

Lloyd-Burton, S., & Roskams, A. J. (2012). SPARC-like 1 (SC1) is a diversely expressed and developmentally regulated matricellular protein that does not compensate for the absence of SPARC in the CNS. *The Journal of Comparative Neurology*, *520*(12), 2575–2590.

Loftén, A., Adermark, L., Ericson, M., & Söderpalm, B. (2021). An acetylcholine-dopamine interaction in the nucleus accumbens and its involvement in ethanol's dopamine-releasing effect. *Addiction Biology*, *26*(3), e12959.

Logge, W. B., Morley, K. C., & Haber, P. S. (2022). GABAB Receptors and Alcohol Use Disorders: Clinical Studies. In S. Vlachou & K. Wickman (Eds.), *Behavioral Neurobiology of GABAB Receptor Function* (pp. 195–212). Springer International Publishing.

Loheswaran, G., Barr, M. S., Zomorrodi, R., Rajji, T. K., Blumberger, D. M., Foll, B. L., & Daskalakis, Z. J. (2017). Impairment of neuroplasticity in the dorsolateral prefrontal cortex by alcohol. *Scientific Reports*, *7*(1), 5276.

Lopez-Leon, S., González-Giraldo, Y., Wegman-Ostrosky, T., & Forero, D. A. (2021). Molecular genetics of substance use disorders: An umbrella review. *Neuroscience & Biobehavioral Reviews*, *124*, 358–369.

López-Murcia, F. J., Terni, B., & Llobet, A. (2015). SPARC triggers a cell-autonomous program of synapse elimination. *Proceedings of the National Academy of Sciences of the United States of America*, *112*(43), 13366–13371.

Lovinger, D. M., & White, G. (1991). Ethanol potentiation of 5-hydroxytryptamine3 receptor-mediated ion current in neuroblastoma cells and isolated adult mammalian neurons. *Molecular Pharmacology*, *40*(2), 263–270.

Lovinger, D. M., White, G., & Weight, F. F. (1989). Ethanol inhibits NMDA-activated ion current in hippocampal neurons. *Science*, *243*(4899), 1721–1724.

Lovinger, D. M., White, G., & Weight, F. F. (1990). NMDA receptor-mediated synaptic excitation selectively inhibited by ethanol in hippocampal slice from adult rat. *The Journal of Neuroscience: The Official Journal of the Society for Neuroscience*, *10*(4), 1372–1379.

Lu, H.-C., & Mackie, K. (2021). Review of the endocannabinoid system. *Biological Psychiatry. Cognitive Neuroscience and Neuroimaging*, *6*(6), 607–615.

Lusk, R., Hoffman, P. L., Mahaffey, S., Rosean, S., Smith, H., Silhavy, J., Pravenec, M., Tabakoff, B., & Saba, L. M. (2022). Beyond genes: inclusion of alternative splicing and alternative polyadenylation to assess the genetic architecture of predisposition to voluntary alcohol consumption in brain of the HXB/BXH recombinant inbred rat panel. *Frontiers in Genetics*, *13*, 821026.

Lv, J., & Liu, F. (2017). The Role of Serotonin beyond the Central Nervous System during Embryogenesis. *Frontiers in Cellular Neuroscience*, *11*, 74.

Mackinnon, N., Bhatia, U., & Nadkarni, A. (2019). The onset and progression of alcohol use disorders: A qualitative study from Goa, India. *Journal of Ethnicity in Substance Abuse*, *18*(1), 89–102.

Mailliard, W. S., & Diamond, I. (2004). Recent advances in the neurobiology of alcoholism: The role of adenosine. *Pharmacology & Therapeutics*, *101*(1), 39–46.

Maley, F., Trimble, R. B., Tarentino, A. L., & Plummer, T. H. (1989). Characterization of glycoproteins and their associated oligosaccharides through the use of endoglycosidases. *Analytical Biochemistry*, *180*(2), 195–204.

Malik, A. R., Liszewska, E., & Jaworski, J. (2015). Matricellular proteins of the Cyr61/CTGF/NOV (CCN) family and the nervous system. *Frontiers in Cellular Neuroscience*, *9*, 237.

Mantere, T., Tupala, E., Hall, H., Särkioja, T., Räsänen, P., Bergström, K., Callaway, J., & Tiihonen, J. (2002). Serotonin transporter distribution and density in the cerebral cortex of alcoholic and nonalcoholic comparison subjects: a whole-hemisphere autoradiography study. *American Journal of Psychiatry*, *159*(4), 599–606.

Manzanares, J., Cabañero, D., Puente, N., García-Gutiérrez, M. S., Grandes, P., & Maldonado, R. (2018). Role of the endocannabinoid system in drug addiction. *Biochemical Pharmacology*, *157*, 108–121.

Marty, V. N., Mulpuri, Y., Munier, J. J., & Spigelman, I. (2020). Chronic alcohol disrupts hypothalamic responses to stress by modifying CRF and NMDA receptor function. *Neuropharmacology*, *167*, 107991.

Maurer, P., Hohenadl, C., Hohenester, E., Göhring, W., Timpl, R., & Engel, J. (1995). The C-terminal portion of BM-40 (SPARC/osteonectin) is an autonomously folding and crystallisable domain that binds calcium and collagen IV. *Journal of Molecular Biology*, *253*(2), 347–357.

Mayfield, R. D., Lewohl, J. M., Dodd, P. R., Herlihy, A., Liu, J., & Harris, R. A. (2002). Patterns of gene expression are altered in the frontal and motor cortices of human alcoholics. *Journal of Neurochemistry*, *81*(4), 802–813.

McCool, B. A. (2021). Ethanol modulation of cortico-basolateral amygdala circuits: Neurophysiology and behavior. *Neuropharmacology*, *197*, 108750.

McCullumsmith, R. E., Hammond, J. H., Shan, D., & Meador-Woodruff, J. H. (2014). Postmortem brain: an underutilized substrate for studying severe mental illness. *Neuropsychopharmacology*, *39*(1), 65–87.

McKinnon, P. J., & Margolskee, R. F. (1996). SC1: A marker for astrocytes in the adult rodent brain is upregulated during reactive astrocytosis. *Brain Research*, *709*(1), 27–36.

McKinnon, P. J., McLaughlin, S. K., Kapsetaki, M., & Margolskee, R. F. (2000). Extracellular Matrix-Associated Protein Sc1 Is Not Essential for Mouse Development. *Molecular and Cellular Biology*, *20*(2), 656–660.

Meana, J. J., Callado, L. F., & Morentin, B. (2014). ¿Qué aportan a la Psiquiatría los estudios en cerebro post mórtem? *Revista de Psiquiatría y Salud Mental - Journal of Psychiatry and Mental Health*, *7*(3), 101–103.

Mendis, D. (1996a). SC1, a brain extracellular matrix glycoprotein related to SPARC and follistatin, is expressed by rat cerebellar astrocytes following injury and during development. *Brain Research*, *730*(1–2), 95–106.

Mendis, D. B., Ivy, G. O., & Brown, I. R. (2000). Induction of SC1 mRNA encoding a brain extracellular matrix glycoprotein related to sparc following lesioning of the adult rat forebrain. *Neurochemical Research*, *25*(12), 1637–1644.

Mendis, D. B., Shahin, S., Gurd, J. W., & Brown, I. R. (1994). Developmental expression in the rat cerebellum of SC1, a putative brain extracellular matrix glycoprotein related to SPARC. *Brain Research*, *633*(1–2), 197–205.

Mendis, D. B., Shahin, S., Gurd, J. W., & Brown, I. R. (1996b). SC1, A SPARC-related glycoprotein, exhibits features of an ECM component in the developing and adult brain. *Brain Research*, *713*(1), 53–63.

Mews, P., Egervari, G., Nativio, R., Sidoli, S., Donahue, G., Lombroso, S., Alexander, D., Riesche, S., Heller, E., Nestler, E., Garcia, B., & Berger, S. (2019). Alcohol metabolism contributes to brain histone acetylation. *Nature*, *574*(7780), 717–721.

Michaelis, E. K., Michaelis, M. L., Freed, W. J., & Foye, J. (1993). Glutamate receptor changes in brain synaptic membranes during chronic alcohol intake. *Alcohol and Alcoholism. Supplement*, *2*, 377–381.

Mignogna, K. M., Bacanu, S. A., Riley, B. P., Wolen, A. R., & Miles, M. F. (2019). Cross-species alcohol dependence-associated gene networks: Co-analysis of mouse brain gene expression and human genome-wide association data. *PLOS ONE*, *14*(4), e0202063.

Miguel-Hidalgo, J. J. (2018). Molecular Neuropathology of Astrocytes and Oligodendrocytes in Alcohol Use Disorders. *Frontiers in Molecular Neuroscience*, *11*, 78.

Miguel-Hidalgo, J. J., Overholser, J. C., Meltzer, H. Y., Stockmeier, C. A., & Rajkowska, G. (2006). Reduced glial and neuronal packing density in the orbitofrontal cortex in alcohol dependence and its relationship with suicide and duration of alcohol dependence. *Alcoholism, Clinical and Experimental Research*, *30*(11), 1845–1855.

Miller, C. N., & Kamens, H. M. (2020). The role of nicotinic acetylcholine receptors in alcohol-related behaviors. *Brain Research Bulletin*, *163*, 135–142.

Minozzi S, Saulle R, & Rösner S. (2018). Baclofen for alcohol use disorder. *The Cochrane Database of Systematic Reviews*, *11*, *CD012557*.

Miquel, M., Vazquez-Sanroman, D., Carbo-Gas, M., Gil-Miravet, I., Sanchis-Segura, C., Carulli, D., Manzo, J., & Coria-Avila, G. A. (2016). Have we been ignoring the elephant in the

room? Seven arguments for considering the cerebellum as part of addiction circuitry. *Neuroscience & Biobehavioral Reviews*, *60*, 1–11.

Miranda, R., O'Malley, S. S., Treloar Padovano, H., Wu, R., Falk, D. E., Ryan, M. L., Fertig, J. B., Chun, T. H., Muvvala, S. B., & Litten, R. Z. (2020). Effects of alcohol cue reactivity on subsequent treatment outcomes among treatment-seeking individuals with alcohol use disorder: a multisite randomized, double-blind, placebo-controlled clinical trial of varenicline. *Alcoholism, Clinical and Experimental Research*, *44*(7), 1431–1443.

Mitchell, J. M., O'Neil, J. P., Janabi, M., Marks, S. M., Jagust, W. J., & Fields, H. L. (2012). Alcohol consumption induces endogenous opioid release in the human orbitofrontal cortex and nucleus accumbens. *Science Translational Medicine*, *4*(116), 116ra6.

Miyata, S., & Kitagawa, H. (2017). Formation and remodeling of the brain extracellular matrix in neural plasticity: Roles of chondroitin sulfate and hyaluronan. *Biochimica Et Biophysica Acta. General Subjects*, *1861*(10), 2420–2434.

Mongrédien, R., Erdozain, A. M., Dumas, S., Cutando, L., del Moral, A. N., Puighermanal, E., Rezai Amin, S., Giros, B., Valjent, E., Meana, J. J., Gautron, S., Callado, L. F., Fabre, V., & Vialou, V. (2019). Cartography of hevin-expressing cells in the adult brain reveals prominent expression in astrocytes and parvalbumin neurons. *Brain Structure and Function*. *224*(3), 1219–1244.

Most, D., Ferguson, L., & Harris, R. A. (2014). Molecular basis of alcoholism. *Handbook of Clinical Neurology*, *125*, 89–111.

Mothe, A. J., & Brown, I. R. (2000). Selective transport of SC1 mRNA, encoding a putative extracellular matrix glycoprotein, during postnatal development of the rat cerebellum and retina. *Molecular Brain Research*, *76*(1), 73–84.

Müller, C. P., Schumann, G., Kornhuber, J., & Kalinichenko, L. S. (2020). Chapter 41—The role of serotonin in alcohol use and abuse. In Müller C. P. & Cunningham K. A. (Eds.), *Handbook of Behavioral Neuroscience* (Vol. 31, pp. 803–827). Elsevier.

Munro, S., Thomas, K. L., & Abu-Shaar, M. (1993). Molecular characterization of a peripheral receptor for cannabinoids. *Nature*, *365*(6441), 61–65.

Murphy-Ullrich, J. E. (2001). The de-adhesive activity of matricellular proteins: Is intermediate cell adhesion an adaptive state? *Journal of Clinical Investigation*, *107*(7), 785–790.

Murphy-Ullrich, J. E., & Sage, E. H. (2014). Revisiting the matricellular concept. *Matrix Biology : Journal of the International Society for Matrix Biology*, *37*, 1–14.

Naassila, M., & Pierrefiche, O. (2019). GluN2B Subunit of the NMDA Receptor: The Keystone of the Effects of Alcohol During Neurodevelopment. *Neurochemical Research*, *44*(1), 78–88.

Nagai, J., Rajbhandari, A. K., Gangwani, M. R., Hachisuka, A., Coppola, G., Masmanidis, S. C., Fanselow, M. S., & Khakh, B. S. (2019). Hyperactivity with Disrupted Attention by Activation of an Astrocyte Synaptogenic Cue. *Cell*, *177*(5), 1280-1292.

Nair, A., Treiber, J. M., Shukla, D. K., Shih, P., & Müller, R.-A. (2013). Impaired thalamocortical connectivity in autism spectrum disorder: A study of functional and anatomical connectivity. *Brain*, *136*(6), 1942–1955.

Naudet, F., Fitzgerald, N., & Braillon, A. (2016). Nalmefene for alcohol dependence: a nice decision? *The Lancet Psychiatry*, *3*(12), 1104–1105.

Nedic Erjavec, G., Bektic Hodzic, J., Repovecki, S., Nikolac Perkovic, M., Uzun, S., Kozumplik, O., Tudor, L., Mimica, N., Svob Strac, D., & Pivac, N. (2021). Alcohol-related phenotypes and platelet serotonin concentration. *Alcohol*, *97*, 41–49.

Nelson, P. S., Plymate, S. R., Wang, K., True, L. D., Ware, J. L., Gan, L., Liu, A. Y., & Hood, L. (1998). Hevin, an antiadhesive extracellular matrix protein, is down-regulated in metastatic prostate adenocarcinoma. *Cancer Research*, *58*(2), 232–236.

Nestler, E. J., & Lüscher, C. (2019). The molecular basis of drug addiction: linking epigenetic to synaptic and circuit mechanisms. *Neuron*, *102*(1), 48–59.

Nicholson, C., & Hrabětová, S. (2017). Brain Extracellular Space: The Final Frontier of Neuroscience. *Biophysical Journal*, *113*(10), 2133–2142.

Nilsson, J., Rüetschi, U., Halim, A., Hesse, C., Carlsohn, E., Brinkmalm, G., & Larson, G. (2009). Enrichment of glycopeptides for glycan structure and attachment site identification. *Nature Methods*, *6*(11), 809–811.

Nishikawa, M., Diksic, M., Sakai, Y., Kumano, H., Charney, D., Palacios-Boix, J., Negrete, J., & Gill, K. (2009). Alterations in brain serotonin synthesis in male alcoholics measured using positron emission tomography. *Alcoholism: Clinical and Experimental Research*, *33*(2), 233–239.

Nocente, R., Vitali, M., Balducci, G., Enea, D., Kranzler, H. R., & Ceccanti, M. (2013). Varenicline and neuronal nicotinic acetylcholine receptors: A new approach to the treatment of co-occurring alcohol and nicotine addiction? *The American Journal on Addictions*, *22*(5), 453–459.

Nocjar, C., Middaugh, L. D., & Tavernetti, M. (1999). Ethanol consumption and place-preference conditioning in the alcohol-preferring C57BL/6 mouse: relationship with motor activity patterns. *Alcoholism: Clinical and Experimental Research*, *23*(4), 683–692.

Nummenmaa, L., Saanijoki, T., Tuominen, L., Hirvonen, J., Tuulari, J. J., Nuutila, P., & Kalliokoski, K. (2018). μ-opioid receptor system mediates reward processing in humans. *Nature Communications*, *9*(1), 1.

Nuñez-delMoral, A., Brocos-Mosquera, I., Vialou, V., Callado, L. F., & Erdozain, A. M. (2021). Characterization of hevin (SPARCL1) immunoreactivity in postmortem human brain homogenates. *Neuroscience*. *467*, 91-109

Nutt, D., Hayes, A., Fonville, L., Zafar, R., Palmer, E. O. C., Paterson, L., & Lingford-Hughes, A. (2021). Alcohol and the Brain. *Nutrients*, *13*(11), 3938.

Nutt, D. J., King, L. A., & Phillips, L. D. (2010). Drug harms in the UK: A multicriteria decision analysis. *The Lancet*, *376*(9752), 1558–1565.

Observatorio Español de las Drogas y las Adicciones. (2021a). *Informe 2021. Alcohol, tabaco y drogas ilegales en España*. Madrid: Ministerio de Sanidad. Delegación del Gobierno para el Plan Nacional sobre Drogas.

Observatorio Español de las Drogas y las Adicciones, C. (2021b). *Monografía. Alcohol 2021: Consumo y consecuencias*. Madrid: Ministerio de Sanidad. Delegación del Gobierno para el Plan Nacional sobre Drogas.

Oh, K. H., Haney, J. J., Wang, X., Chuang, C.-F., Richmond, J. E., & Kim, H. (2017). ERG-28 controls BK channel trafficking in the ER to regulate synaptic function and alcohol response in C. Elegans. *ELife*, *6*, e24733.

Olive, M. F., Koenig, H. N., Nannini, M. A., & Hodge, C. W. (2001). Stimulation of endorphin neurotransmission in the nucleus accumbens by ethanol, cocaine, and amphetamine. *The Journal of Neuroscience*, *21*(23), RC184.

Olsen, R. W. (2018). $GABA_A$ receptor: Positive and negative allosteric modulators. *Neuropharmacology*, *136*(Pt A), 10–22.

Olsen, R. W., & Liang, J. (2017). Role of $GABA_A$ receptors in alcohol use disorders suggested by chronic intermittent ethanol (CIE) rodent model. *Molecular Brain*, *10*(1), 45.

Oritani, K., Kanakura, Y., Aoyama, K., Yokota, T., Copeland, N. G., Gilbert, D. J., Jenkins, N. A., Tomiyama, Y., Matsuzawa, Y., & Kincade, P. W. (1997). Matrix glycoprotein SC1/ECM2 augments B lymphopoiesis. *Blood*, *90*(9), 3404–3413.

Palmisano, M., & Pandey, S. C. (2017). Epigenetic mechanisms of alcoholism and stress-related disorders. *Alcohol*, *60*, 7–18.

Palomino, A., Pavón, F.-J., Blanco-Calvo, E., Serrano, A., Arrabal, S., Rivera, P., Alén, F., Vargas, A., Bilbao, A., Rubio, L., Rodríguez de Fonseca, F., & Suárez, J. (2014). Effects of acute versus repeated cocaine exposure on the expression of endocannabinoid signaling-related proteins in the mouse cerebellum. *Frontiers in Integrative Neuroscience*, *8*, 22.

Palpacuer, C., Duprez, R., Huneau, A., Locher, C., Boussageon, R., Laviolle, B., & Naudet, F. (2018). Pharmacologically controlled drinking in the treatment of alcohol dependence or alcohol use disorders: A systematic review with direct and network meta-analyses on nalmefene, naltrexone, acamprosate, baclofen and topiramate. *Addiction*, *113*(2), 220–237.

Pandey, S. C., Zhang, H., Ugale, R., Prakash, A., Xu, T., & Misra, K. (2008). Effector immediate-early gene arc in the amygdala plays a critical role in alcoholism. *The Journal of Neuroscience: The Official Journal of the Society for Neuroscience*, *28*(10), 2589–2600.

Pang, K. Y., Braswell, L. M., Chang, L., Sommer, T. J., & Miller, K. W. (1980). The perturbation of lipid bilayers by general anesthetics: A quantitative test of the disordered lipid hypothesis. *Molecular Pharmacology*, *18*(1), 84–90.

Patel, R., Brophy, C., Hickling, M., Neve, J., & Furger, A. (2019). Alternative cleavage and polyadenylation of genes associated with protein turnover and mitochondrial function are deregulated in Parkinson's, Alzheimer's and ALS disease. *BMC Medical Genomics*, *12*(1), 60.

Patel, R. R., Wolfe, S. A., Bajo, M., Abeynaike, S., Pahng, A., Borgonetti, V., D'Ambrosio, S., Nikzad, R., Edwards, S., Paust, S., Roberts, A. J., & Roberto, M. (2021). IL-10 normalizes aberrant amygdala GABA transmission and reverses anxiety-like behavior and dependence-induced escalation of alcohol intake. *Progress in Neurobiology*, *199*, 101952.

Patel, R. R., Wolfe, S. A., Borgonetti, V., Gandhi, P. J., Rodriguez, L., Snyder, A. E., D'Ambrosio, S., Bajo, M., Domissy, A., Head, S., Contet, C., Dayne Mayfield, R., Roberts, A. J., & Roberto, M. (2022). Ethanol withdrawal-induced adaptations in prefrontal corticotropin releasing factor receptor 1-expressing neurons regulate anxiety and conditioned rewarding effects of ethanol. *Molecular Psychiatry*, 1–11.

Patkar, O. L., Belmer, A., Holgate, J. Y., Klenowski, P. M., & Bartlett, S. E. (2019). Modulation of serotonin and noradrenaline in the BLA by pindolol reduces long-term ethanol intake. *Addiction Biology*, *24*(4), 652–663.

Patkar, O. L., Belmer, A., Holgate, J. Y., Tarren, J. R., Shariff, M. R., Morgan, M., Fogarty, M. J., Bellingham, M. C., Bartlett, S. E., & Klenowski, P. M. (2017). The antihypertensive drug pindolol attenuates long-term but not short-term binge-like ethanol consumption in mice. *Addiction Biology*, *22*(3), 679–691.

Pavón, F. J., Serrano, A., Stouffer, D. G., Polis, I., Roberto, M., Cravatt, B. F., Martin-Fardon, R., Rodríguez de Fonseca, F., & Parsons, L. H. (2019). Ethanol-induced alterations in endocannabinoids and relevant neurotransmitters in the nucleus accumbens of fatty acid amide hydrolase knockout mice. *Addiction Biology*, *24*(6), 1204–1215.

Paxinos, G., & Franklin, K. B. J. (2001). *The mouse brain in stereotaxic coordinates* (2nd ed). Academic Press.

Peñasco, S., Rico-Barrio, I., Puente, N., Fontaine, C. J., Ramos, A., Reguero, L., Gerrikagoitia, I., de Fonseca, F. R., Suarez, J., Barrondo, S., Aretxabala, X., García del Caño, G., Sallés, J., Elezgarai, I., Nahirney, P. C., Christie, B. R., & Grandes, P. (2020). Intermittent ethanol exposure during adolescence impairs cannabinoid type 1 receptor-dependent long-term depression and recognition memory in adult mice. *Neuropsychopharmacology*, *45*(2), 2.

Peoples, R. W., Li, C., & Weight, F. F. (1996). Lipid vs protein theories of alcohol action in the nervous system. *Annual Review of Pharmacology and Toxicology*, *36*, 185–201.

Peterson, V. L., McCool, B. A., & Hamilton, D. A. (2015). Effects of ethanol exposure and withdrawal on dendritic morphology and spine density in the nucleus accumbens core and shell. *Brain Research*, *1594*, 125–135.

Pfefferbaum, A., Rosenbloom, M. J., Chu, W., Sassoon, S. A., Rohlfing, T., Pohl, K. M., Zahr, N. M., & Sullivan, E. V. (2014). White matter microstructural recovery with abstinence and decline with relapse in alcoholism: interaction with normal aging revealed with longitudinal DTI. *The Lancet. Psychiatry*, *1*(3), 202–212.

Pitchon, D. N., Zook, M., & Rhoads, D. E. (2013). A pattern of adolescent caffeine consumption that reduces alcohol withdrawal severity. *Journal of Caffeine Research*, *3*(3), 131–137.

Pitel, A.-L., Chételat, G., Le Berre, A. P., Desgranges, B., Eustache, F., & Beaunieux, H. (2012). Macrostructural abnormalities in Korsakoff syndrome compared with uncomplicated alcoholism. *Neurology*, *78*(17), 1330–1333.

Portero-Tresserra, M., Gracia-Rubio, I., Cantacorps, L., Pozo, O. J., Gómez-Gómez, A., Pastor, A., López-Arnau, R., de la Torre, R., & Valverde, O. (2018). Maternal separation increases alcohol-drinking behaviour and reduces endocannabinoid levels in the mouse striatum and prefrontal cortex. *European Neuropsychopharmacology*, *28*(4), 499–512.

Praharaj, S. K., Munoli, R. N., Shenoy, S., Udupa, S. T., & Thomas, L. S. (2021). High-dose thiamine strategy in Wernicke–Korsakoff syndrome and related thiamine deficiency conditions associated with alcohol use disorder. *Indian Journal of Psychiatry*, *63*(2), 121–126.

Pucci, M., Micioni Di Bonaventura, M. V., Wille-Bille, A., Fernández, M. S., Maccarrone, M., Pautassi, R. M., Cifani, C., & D'Addario, C. (2019). Environmental stressors and alcoholism development: Focus on molecular targets and their epigenetic regulation. *Neuroscience and Biobehavioral Reviews*, *106*, 165–181.

Purcell, A. E., Jeon, O. H., Zimmerman, A. W., Blue, M. E., & Pevsner, J. (2001). Postmortem brain abnormalities of the glutamate neurotransmitter system in autism. *Neurology*, *57*(9), 1618.

Rajalingam, D., Kathir, K. M., Ananthamurthy, K., Adams, P. D., & Kumar, T. K. S. (2008). A method for the prevention of thrombin-induced degradation of recombinant proteins. *Analytical Biochemistry*, *375*(2), 361–363

Ramanathan, A., Robb, G. B., & Chan, S.-H. (2016). mRNA capping: Biological functions and applications. *Nucleic Acids Research*, *44*(16), 7511–7526.

Ramirez, J. J., Bindu, D. S., & Eroglu, C. (2021). Building and destroying synaptic bridges: How do Hevin/Sparcl1, SPARC, and MDGAs modify trans-synaptic neurexin-neuroligin interactions? *Structure*, *29*(7), 635–637.

Ramos-Miguel, A., Gicas, K., Alamri, J., Beasley, C. L., Dwork, A. J., Mann, J. J., Rosoklija, G., Cai, F., Song, W., Barr, A. M., & Honer, W. G. (2019). Reduced SNAP25 protein fragmentation contributes to SNARE complex dysregulation in schizophrenia postmortem brain. *Neuroscience*, *420*, 112–128.

Ravid, T., & Hochstrasser, M. (2008). Diversity of degradation signals in the ubiquitin–proteasome system. *Nature Reviews Molecular Cell Biology*, *9*(9), 9.

Ray, L. A., Meredith, L. R., Kiluk, B. D., Walthers, J., Carroll, K. M., & Magill, M. (2020). Combined Pharmacotherapy and Cognitive Behavioral Therapy for Adults With Alcohol or Substance Use Disorders: A Systematic Review and Meta-analysis. *JAMA Network Open*, *3*(6), e208279.

Regensburger, D., Tenkerian, C., Pürzer, V., Schmid, B., Wohlfahrt, T., Stolzer, I., López-Posadas, R., Günther, C., Waldner, M. J., Becker, C., Sticht, H., Petter, K., Flierl, C., Gass, T., Thoenissen, T., Geppert, C. I., Britzen-Laurent, N., Méniel, V. S., Ramming, A., … Naschberger, E. (2021). Matricellular protein SPARCL1 regulates blood vessel integrity and antagonizes inflammatory bowel disease. *Inflammatory Bowel Diseases*, *27*(9), 1491–1502.

Rehm, J., Mathers, C., Popova, S., Thavorncharoensap, M., Teerawattananon, Y., & Patra, J. (2009). Global burden of disease and injury and economic cost attributable to alcohol use and alcohol-use disorders. *The Lancet*, *373*(9682), 2223–2233.

Reiner, A., & Levitz, J. (2018). Glutamatergic signaling in the central nervous system: ionotropic and metabotropic receptors in concert. *Neuron*, *98*(6), 1080–1098.

Rhodes, J. S., Ford, M. M., Yu, C.-H., Brown, L. L., Finn, D. A., Garland, T., & Crabbe, J. C. (2007). Mouse inbred strain differences in ethanol drinking to intoxication. *Genes, Brain, and Behavior*, *6*(1), 1–18.

Ringuette, M., Rogers, I., Varmuza, S., Rush, S., & Brown, I. R. (1998). Expression of SC1 is associated with the migration of myotomes along the dermomyotome during somitogenesis in early mouse embryos. *Development Genes and Evolution*, *208*(7), 403–406.

Risher, W. C., & Eroglu, C. (2012). Thrombospondins as key regulators of synaptogenesis in the central nervous system. *Matrix Biology*, *31*(3), 170–177.

Risher, W. C., Patel, S., Kim, I. H., Uezu, A., Bhagat, S., Wilton, D. K., Pilaz, L.-J., Singh Alvarado, J., Calhan, O. Y., Silver, D. L., Stevens, B., Calakos, N., Soderling, S. H., & Eroglu, C. (2014). Astrocytes refine cortical connectivity at dendritic spines. *ELife*, *3*, e04047.

Rivero, G., Gabilondo, A. M., García-Sevilla, J. A., La Harpe, R., Morentín, B., & Meana, J. J. (2015). Up-regulated 14-3-3β and 14-3-3ζ proteins in prefrontal cortex of subjects with schizophrenia: Effect of psychotropic treatment. *Schizophrenia Research*, *161*(2), 446–451.

Roberto, M., Kirson, D., & Khom, S. (2021). The Role of the Central Amygdala in Alcohol Dependence. *Cold Spring Harbor Perspectives in Medicine*, *11*(2), a039339.

Roberts, A. J., McArthur, R. A., Hull, E. E., Post, C., & Koob, G. F. (1998). Effects of amperozide, 8-OH-DPAT, and FG 5974 on operant responding for ethanol. *Psychopharmacology*, *137*(1), 25–32.

Rodd, Z. A., Bell, R. L., Melendez, R. I., Kuc, K. A., Lumeng, L., Li, T.-K., Murphy, J. M., & McBride, W. J. (2004a). Comparison of intracranial self-administration of ethanol within the posterior ventral tegmental area between alcohol-preferring and Wistar rats. *Alcoholism, Clinical and Experimental Research*, *28*(8), 1212–1219.

Rodd, Z. A., Melendez, R. I., Bell, R. L., Kuc, K. A., Zhang, Y., Murphy, J. M., & McBride, W. J. (2004b). Intracranial self-administration of ethanol within the ventral tegmental area of male Wistar rats: Evidence for involvement of dopamine neurons. *The Journal of Neuroscience: The Official Journal of the Society for Neuroscience*, *24*(5), 1050–1057.

Rodrigues, E. C., Grawenhoff, J., Baumann, S. J., Lorenzon, N., & Maurer, S. P. (2021). Mammalian neuronal mRNA transport complexes: the few knowns and the many unknowns. *Frontiers in Integrative Neuroscience*, *15,* 692948.

Rodriguez, L., Kirson, D., Wolfe, S. A., Patel, R. R., Varodayan, F. P., Snyder, A. E., Gandhi, P. J., Khom, S., Vlkolinsky, R., Bajo, M., & Roberto, M. (2022). Alcohol dependence induces CRF sensitivity in female central amygdala GABA synapses. *International Journal of Molecular Sciences*, *23*(14), 7842.

Rodriguez-Chavez, V., Moran, J., Molina-Salinas, G., Zepeda Ruiz, W. A., Rodriguez, M. C., Picazo, O., & Cerbon, M. (2021). Participation of glutamatergic ionotropic receptors in excitotoxicity: the neuroprotective role of prolactin. *Neuroscience*, *461*, 180–193.

Rojo-Mira, J., Pineda-Álvarez, M., & Zapata-Ospina, J. P. (2022). Efficacy and safety of anticonvulsants for the inpatient treatment of alcohol withdrawal syndrome: a systematic review and meta-analysis. *Alcohol and Alcoholism*, *57*(2), 155–164.

Rosenwasser, A. M., Fixaris, M. C., Crabbe, J. C., Brooks, P. C., & Ascheid, S. (2013). Escalation of Intake Under Intermittent Ethanol Access in Diverse Mouse Genotypes. *Addiction Biology*, *18*(3), 496–507. https://doi.org/10.1111/j.1369-1600.2012.00481.x

Rossetti, Z. L., Hmaidan, Y., & Gessa, G. L. (1992). Marked inhibition of mesolimbic dopamine release: A common feature of ethanol, morphine, cocaine and amphetamine abstinence in rats. *European Journal of Pharmacology*, *221*(2-3), 227–234.

Rubio, M., de Miguel, R., Fernández-Ruiz, J., Gutiérrez-López, D., Carai, M. A. M., & Ramos, J. A. (2009). Effects of a short-term exposure to alcohol in rats on FAAH enzyme and CB1 receptor in different brain areas. *Drug and Alcohol Dependence*, *99*(1–3), 354–358.

Rubio, M., Fernández-Ruiz, J., de Miguel, R., Maestro, B., Michael Walker, J., & Ramos, J. A. (2008). CB1 receptor blockade reduces the anxiogenic-like response and ameliorates the neurochemical imbalances associated with alcohol withdrawal in rats. *Neuropharmacology*, *54*(6), 976–988.

Sage, E. H., & Bornstein, P. (1991). Extracellular proteins that modulate cell-matrix interactions. SPARC, tenascin, and thrombospondin. *The Journal of Biological Chemistry*, *266*(23), 14831–14834.

SanMiguel, N., López-Cruz, L., Müller, C. E., Salamone, J. D., & Correa, M. (2019). Caffeine modulates voluntary alcohol intake in mice depending on the access conditions: Involvement of adenosine receptors and the role of individual differences. *Pharmacology, Biochemistry, and Behavior*, *186*, 172789.

Schurman, L. D., Lu, D., Kendall, D. A., Howlett, A. C., & Lichtman, A. H. (2020). Molecular mechanism and cannabinoid pharmacology. *Handbook of Experimental Pharmacology*, *258*, 323–353.

Seddighi, S., Varma, V. R., An, Y., Varma, S., Beason-Held, L. L., Tanaka, T., Kitner-Triolo, M. H., Kraut, M. A., Davatzikos, C., & Thambisetty, M. (2018). SPARCL1 accelerates symptom onset in alzheimer's disease and influences brain structure and function during aging. *Journal of Alzheimer's Disease: JAD*, *61*(1), 401–414.

Segobin, S. H., Chételat, G., Berre, A.-P. L., Lannuzel, C., Boudehent, C., Vabret, F., Eustache, F., Beaunieux, H., & Pitel, A.-L. (2014). Relationship between brain volumetric changes and interim drinking at six months in alcohol-dependent patients. *Alcoholism: Clinical and Experimental Research*, *38*(3), 739–748.

Šekeljić, V., & Andjus, P. R. (2012). Tenascin-C and its functions in neuronal plasticity. *The International Journal of Biochemistry & Cell Biology*, *44*(6), 825–829.

Sellers, E. M., Toneatto, T., Romach, M. K., Somer, G. R., Sobell, L. C., & Sobell, M. B. (1994). Clinical efficacy of the 5-HT3 antagonist ondansetron in alcohol abuse and dependence. *Alcoholism, Clinical and Experimental Research*, *18*(4), 879–885.

Seneviratne, C., Gorelick, D. A., Lynch, K. G., Brown, C., Romer, D., Pond, T., Kampman, K., & Kranzler, H. R. (2022). A randomized, double-blind, placebo-controlled, pharmacogenetic study of ondansetron for treating alcohol use disorder. *Alcoholism, Clinical and Experimental Research*.

Serrano, A., & Natividad, L. A. (2022). *Alcohol-Endocannabinoid Interactions: Implications for Addiction-Related Behavioral Processes*. *42*(1), 19.

Shanmugarajah, P. D., Hoggard, N., Currie, S., Aeschlimann, D. P., Aeschlimann, P. C., Gleeson, D. C., Karajeh, M., Woodroofe, N., Grünewald, R. A., & Hadjivassiliou, M. (2016). Alcohol-related cerebellar degeneration: Not all down to toxicity? *Cerebellum & Ataxias*, *3*(1), 17.

Shen, C., Han, L., Liu, B., Zhang, G., Cai, Z., Yin, X., Yin, Y., Chen, Z., & Zhang, B. (2022). The KDM6A-SPARCL1 axis blocks metastasis and regulates the tumour microenvironment of gastrointestinal stromal tumours by inhibiting the nuclear translocation of p65. *British Journal of Cancer*, *126*(10), 10.

Shen, W. W. (2018). Anticraving therapy for alcohol use disorder: A clinical review. *Neuropsychopharmacology Reports*, *38*(3), 105–116.

Shibasaki, M., Watanabe, K., Takeda, K., Itoh, T., Tsuyuki, T., Narita, M., Mori, T., & Suzuki, T. (2013). Effect of chronic ethanol treatment on μ-opioid receptor function, interacting proteins and morphine-induced place preference. *Psychopharmacology*, *228*(2), 207–215.

Shield, K. D., Parry, C., & Rehm, J. (2014). Chronic diseases and conditions related to alcohol use. *Alcohol Research: Current Reviews*, *35*(2), 155–171.

Sidhpura, N., & Parsons, L. H. (2011). Endocannabinoid-mediated synaptic plasticity and addiction-related behavior. *Neuropharmacology*, *61*(7), 1070–1087.
4
Sigel, E., & Steinmann, M. E. (2012). Structure, function, and modulation of $GABA_A$ receptors. *Journal of Biological Chemistry*, *287*(48), 40224–40231.

Singh, S. K., Stogsdill, J. A., Pulimood, N. S., Dingsdale, H., Kim, Y. H., Pilaz, L.-J., Kim, I. H., Manhaes, A. C., Rodrigues-Junior, W. S., Pamukcu, A., Enustun, E., Ertuz, Z., Scheiffele, P., Soderling, S., Silver, D. L., Ji, R.-R., Medina, A. E., & Eroglu, C. (2016). Astrocytes assemble thalamocortical synapses by bridging Nrx1α and NL1 via hevin. *Cell*, *164*(0), 183–196.

Sjöstedt, E., Zhong, W., Fagerberg, L., Karlsson, M., Mitsios, N., Adori, C., Oksvold, P., Edfors, F., Limiszewska, A., Hikmet, F., Huang, J., Du, Y., Lin, L., Dong, Z., Yang, L., Liu, X., Jiang, H., Xu, X., Wang, J., … Mulder, J. (2020). An atlas of the protein-coding genes in the human, pig, and mouse brain. *Science*, *367*(6482), eaay5947.

Sloin, H. E., Bikovski, L., Levi, A., Amber-Vitos, O., Katz, T., Spivak, L., Someck, S., Gattegno, R., Sivroni, S., Sjulson, L., & Stark, E. (2022). Hybrid offspring of C57BL/6J mice exhibit improved properties for neurobehavioral research. *ENeuro*, *9*(4).

Snyder, A. E., Salimando, G. J., Winder, D. G., & Silberman, Y. (2019). Chronic intermittent ethanol and acute stress similarly modulate BNST CRF neuron activity via noradrenergic signaling. *Alcoholism, Clinical and Experimental Research*, *43*(8), 1695–1701.

Soderling, J. A., Reed, M. J., Corsa, A., & Sage, E. H. (1997). Cloning and expression of murine SC1, a gene product homologous to SPARC. *Journal of Histochemistry & Cytochemistry*, *45*(6), 823–835.

Song, I., & Dityatev, A. (2018). Crosstalk between glia, extracellular matrix and neurons. *Brain Research Bulletin*, *136*, 101–108.

Soyka, M., Friede, M., & Schnitker, J. (2016). Comparing nalmefene and naltrexone in alcohol dependence: are there any differences? results from an indirect meta-analysis. *Pharmacopsychiatry*, *49*(02), 66–75.

Spanagel, R., Herz, A., & Shippenberg, T. S. (1992). Opposing tonically active endogenous opioid systems modulate the mesolimbic dopaminergic pathway. *Proceedings of the National Academy of Sciences of the United States of America*, *89*(6), 2046–2050.

Spanagel, R., & Kiefer, F. (2008). Drugs for relapse prevention of alcoholism: Ten years of progress. *Trends in Pharmacological Sciences*, *29*(3), 109–115.

Spanagel, R., Zink, M., & Sommer, W. H. (2016). Alcohol: neurobiology of alcohol addiction. In. Pfaff D. W & Volkow N. D. (Eds.), *Neuroscience in the 21st Century: From Basic to Clinical* (pp. 3593–3623). Springer.

Stewart, M. (2019). Polyadenylation and nuclear export of mRNAs. *The Journal of Biological Chemistry*, *294*(9), 2977–2987.

Storvik, M., Häkkinen, M., Tupala, E., & Tiihonen, J. (2009). 5-HT(1A) receptors in the frontal cortical brain areas in Cloninger type 1 and 2 alcoholics measured by whole-hemisphere autoradiography. *Alcohol and Alcoholism (Oxford, Oxfordshire)*, *44*(1), 2–7.

Storvik, M., Haukijärvi, T., Tupala, E., & Tiihonen, J. (2008). Correlation between the SERT binding densities in hypothalamus and amygdala in Cloninger type 1 and 2 alcoholics. *Alcohol and Alcoholism*, *43*(1), 25–30.

Storvik, M., Tiihonen, J., Haukijärvi, T., & Tupala, E. (2006). Lower serotonin transporter binding in caudate in alcoholics. *Synapse*, *59*(3), 144–151.

Strunz, M., Jarrell, J. T., Cohen, D. S., Rosin, E. R., Vanderburg, C. R., & Huang, X. (2019). Modulation of SPARC/Hevin Proteins in Alzheimer's Disease Brain Injury. *Alzheimer's Disease*, *68*(2), 695–710.

Sullivan, E. V., Marsh, L., Mathalon, D. H., Lim, K. O., & Pfefferbaum, A. (1995). Anterior hippocampal volume deficits in nonamnesic, aging chronic alcoholics. *Alcoholism, Clinical and Experimental Research*, *19*(1), 110–122.

Sullivan, E. V., & Pfefferbaum, A. (2009). Neuroimaging of the Wernicke–Korsakoff syndrome. *Alcohol and Alcoholism*, *44*(2), 155–165.

Sullivan, E. V., & Pfefferbaum, A. (2019). Brain-behavior relations and effects of aging and common comorbidities in alcohol use disorder: a review. *Neuropsychology*, *33*(6), 760–780.

Sullivan, M. M., Barker, T. H., Funk, S. E., Karchin, A., Seo, N. S., Höök, M., Sanders, J., Starcher, B., Wight, T. N., Puolakkainen, P., & Sage, E. H. (2006). Matricellular Hevin

regulates decorin production and collagen assembly. *Journal of Biological Chemistry*, *281*(37), 27621–27632.

Sullivan, M. M., & Sage, E. H. (2004). Hevin/SC1, a matricellular glycoprotein and potential tumor-suppressor of the SPARC/BM-40/Osteonectin family. *The International Journal of Biochemistry & Cell Biology*, *36*(6), 991–996.

Sung, K. W., Engel, S. R., Allan, A. M., & Lovinger, D. M. (2000). 5-HT(3) receptor function and potentiation by alcohols in frontal cortex neurons from transgenic mice overexpressing the receptor. *Neuropharmacology*, *39*(12), 2346–2351.

Svoboda, P. (2020). Key Mechanistic Principles and Considerations Concerning RNA Interference. *Frontiers in Plant Science*, *11*, 1237.

Swift, R. M. (2013). Naltrexone and nalmefene: any meaningful difference? *Biological Psychiatry*, *73*(8), 700–701.

Swift, R. M., & Aston, E. R. (2015). Pharmacotherapy for alcohol use disorder: current and emerging therapies. *Harvard Review of Psychiatry*, *23*(2), 122–133.

Szabo, Z., Owonikoko, T., Peyrot, M., Varga, J., Mathews, W. B., Ravert, H. T., Dannals, R. F., & Wand, G. (2004). Positron emission tomography imaging of the serotonin transporter in subjects with a history of alcoholism. *Biological Psychiatry*, *55*(7), 766–771.

Szumlinski, K. K., Diab, M. E., Friedman, R., Henze, L. M., Lominac, K. D., & Bowers, M. S. (2007). Accumbens neurochemical adaptations produced by binge-like alcohol consumption. *Psychopharmacology*, *190*(4), 415–431.

Tagliaferro, P., Vega, M. D., Evrard, S. G., Ramos, A. J., & Brusco, A. (2002). Alcohol exposure during adulthood induces neuronal and astroglial alterations in the hippocampal CA-1 area. *Annals of the New York Academy of Sciences*, *965*, 334–342.

Taketomi, T., Yasuda, T., Morita, R., Kim, J., Shigeta, Y., Eroglu, C., Harada, R., & Tsuruta, F. (2022). Autism-associated mutation in Hevin/Sparcl1 induces endoplasmic reticulum stress through structural instability. *Scientific Reports*, *12*(1), 11891.

Teng, S. X., Katz, P. S., Maxi, J. K., Mayeux, J. P., Gilpin, N. W., & Molina, P. E. (2015). Alcohol exposure after mild focal traumatic brain injury impairs neurological recovery and exacerbates localized neuroinflammation. *Brain, Behavior, and Immunity*, *45*, 145–156.

Terunuma, M. (2018). Diversity of structure and function of $GABA_B$ receptors: A complexity of $GABA_B$-mediated signaling. *Proceedings of the Japan Academy. Series B, Physical and Biological Sciences*, *94*(10), 390–411.

Teyssier, J.-R., Ragot, S., Chauvet-Gélinier, J.-C., Trojak, B., & Bonin, B. (2011). Activation of a ΔFOSB dependent gene expression pattern in the dorsolateral prefrontal cortex of patients with major depressive disorder. *Journal of Affective Disorders*, *133*(1–2), 174–178.

Thompson, P. M., Cruz, D. A., Olukotun, D. Y., & Delgado, P. L. (2012). Serotonin receptor, SERT mRNA and correlations with symptoms in males with alcohol dependence and suicide. *Acta Psychiatrica Scandinavica*, *126*(3), 165–174.

Timary, P. de, Cani, P. D., Duchemin, J., Neyrinck, A. M., Gihousse, D., Laterre, P.-F., Badaoui, A., Leclercq, S., Delzenne, N. M., & Stärkel, P. (2012). The loss of metabolic control on alcohol drinking in heavy drinking alcohol-dependent subjects. *PLOS ONE*, *7*(7), e38682.

Topiwala, A., Allan, C. L., Valkanova, V., Zsoldos, E., Filippini, N., Sexton, C., Mahmood, A., Fooks, P., Singh-Manoux, A., Mackay, C. E., Kivimäki, M., & Ebmeier, K. P. (2017). Moderate alcohol consumption as risk factor for adverse brain outcomes and cognitive decline: Longitudinal cohort study. *BMJ*, *357*, j2353.

Trindade, P., Hampton, B., Manhães, A. C., & Medina, A. E. (2016). Developmental alcohol exposure leads to a persistent change on astrocyte secretome. *Journal of Neurochemistry*, *137*(5), 730–743.

Tupala, E., Hall, H., Särkioja, T., Räsänen, P., & Tiihonen, J. (2000). Dopamine-transporter density in nucleus accumbens of type-1 alcoholics. *The Lancet*, *355*(9201), 380.

Turtoi, A., Musmeci, D., Naccarato, A. G., Scatena, C., Ortenzi, V., Kiss, R., Murtas, D., Patsos, G., Mazzucchelli, G., De Pauw, E., Bevilacqua, G., & Castronovo, V. (2012). Sparc-Like Protein 1 is a new marker of human glioma progression. *Journal of Proteome Research*, *11*(10), 5011–5021.

Underwood, M. D., Kassir, S. A., Bakalian, M. J., Galfalvy, H., Dwork, A. J., Mann, J. J., & Arango, V. (2018). Serotonin receptors and suicide, major depression, alcohol use disorder and reported early life adversity. *Translational Psychiatry*, *8*(1), 279.

Uys, J. D., McGuier, N. S., Gass, J. T., Griffin III, W. C., Ball, L. E., & Mulholland, P. J. (2016). Chronic intermittent ethanol exposure and withdrawal leads to adaptations in nucleus accumbens core postsynaptic density proteome and dendritic spines. *Addiction Biology*, *21*(3), 560–574.

Vafadar-Isfahani, B., Ball, G., Coveney, C., Lemetre, C., Boocock, D., Minthon, L., Hansson, O., Miles, A. K., Janciauskiene, S. M., Warden, D., Smith, A. D., Wilcock, G., Kalsheker, N., Rees, R., Matharoo-Ball, B., & Morgan, K. (2012). Identification of SPARC-like 1 protein as part of a biomarker panel for alzheimer's disease in cerebrospinal Fluid. *Journal of Alzheimer's Disease*, *28*(3), 625–636.

Van Sickle, M. D., Duncan, M., Kingsley, P. J., Mouihate, A., Urbani, P., Mackie, K., Stella, N., Makriyannis, A., Piomelli, D., Davison, J. S., Marnett, L. J., Di Marzo, V., Pittman, Q. J., Patel, K. D., & Sharkey, K. A. (2005). Identification and functional characterization of brainstem cannabinoid CB2 receptors. *Science*, *310*(5746), 329–332.

Varga, Z. V., Matyas, C., Paloczi, J., & Pacher, P. (2017). Alcohol misuse and kidney injury: epidemiological evidence and potential mechanisms. *Alcohol Research : Current Reviews*, *38*(2), 283–288.

Varodayan, F. P., Correia, D., Kirson, D., Khom, S., Oleata, C. S., Luu, G., Schweitzer, P., & Roberto, M. (2017). CRF modulates glutamate transmission in the central amygdala of naïve and ethanol-dependent rats. *Neuropharmacology*, *125*, 418–428.

Varodayan, F. P., Patel, R. R., Matzeu, A., Wolfe, S. A., Curley, D. E., Khom, S., Gandhi, P. J., Rodriguez, L., Bajo, M., D'Ambrosio, S., Sun, H., Kerr, T. M., Gonzales, R. A., Leggio, L., Natividad, L. A., Haass-Koffler, C. L., Martin-Fardon, R., & Roberto, M. (2022). The amygdala noradrenergic system is compromised with alcohol use disorder. *Biological Psychiatry*, *91*(12), 1008–1018.

Verhulst, B., Neale, M. C., & Kendler, K. S. (2015). The heritability of alcohol use disorders: A meta-analysis of twin and adoption studies. *Psychological Medicine*, *45*(5), 1061–1072.

Vialou, V., Robison, A. J., LaPlant, Q. C., Covington, H. E., Dietz, D. M., Ohnishi, Y. N., Mouzon, E., Rush, A. J., Watts, E. L., Wallace, D. L., Iniguez, S. D., Ohnishi, Y. H., Steiner, M. A., Warren, B., Krishnan, V., Neve, R. L., Ghose, S., Berton, O., Tamminga, C. A., & Nestler, E. J. (2010). ΔFosB in brain reward circuits mediates resilience to stress and antidepressant responses. *Nature Neuroscience*, *13*(6), 745–752.

Vigneault, É., Poirel, O., Riad, M., Prud'homme, J., Dumas, S., Turecki, G., Fasano, C., Mechawar, N., & El Mestikawy, S. (2015). Distribution of vesicular glutamate transporters in the human brain. *Frontiers in Neuroanatomy*, *9,* 23.

Viloria, K., Munasinghe, A., Asher, S., Bogyere, R., Jones, L., & Hill, N. J. (2016). A holistic approach to dissecting SPARC family protein complexity reveals FSTL-1 as an inhibitor of pancreatic cancer cell growth. *Scientific Reports*, *6*(1), 1.

Vilpoux, C., Fouquet, G., Deschamps, C., Lefebvre, E., Gosset, P., Antol, J., Zabijak, L., Marcq, I., Naassila, M., & Pierrefiche, O. (2022). Astrogliosis and compensatory neurogenesis after the first ethanol binge drinking-like exposure in the adolescent rat. *Alcoholism: Clinical and Experimental Research*, *46*(2), 207–220.

Virga, J., Bognár, L., Hortobágyi, T., Zahuczky, G., Csősz, É., Kalló, G., Tóth, J., Hutóczki, G., Reményi-Puskár, J., Steiner, L., & Klekner, A. (2018). Tumor Grade versus Expression of Invasion-Related Molecules in Astrocytoma. *Pathology & Oncology Research*, *24*(1), 35–43.

Virkkunen, M., Goldman, D., Nielsen, D. A., & Linnoila, M. (1995). Low brain serotonin turnover rate (low CSF 5-HIAA) and impulsive violence. *Journal of Psychiatry & Neuroscience: JPN*, *20*(4), 271–275.

Volkow, N. D., Wang, G. J., Fowler, J. S., Logan, J., Hitzemann, R., Ding, Y. S., Pappas, N., Shea, C., & Piscani, K. (1996). Decreases in dopamine receptors but not in dopamine transporters in alcoholics. *Alcoholism, Clinical and Experimental Research*, *20*(9), 1594–1598.

Volkow, N. D., Wiers, C. E., Shokri-Kojori, E., Tomasi, D., Wang, G.-J., & Baler, R. (2017). Neurochemical and metabolic effects of acute and chronic alcohol in the human brain: Studies with positron emission tomography. *Neuropharmacology*, *122*, 175–188.

Vonghia, L., Leggio, L., Ferrulli, A., Bertini, M., Gasbarrini, G., & Addolorato, G. (2008). Acute alcohol intoxication. *European Journal of Internal Medicine*, *19*(8), 561–567.

Walker, C. D., Risher, W. C., & Risher, M.-L. (2020). Regulation of synaptic development by astrocyte signaling factors and their emerging roles in substance Abuse. *Cells*, *9*(2), 297.

Wall, T. L., Luczak, S. E., & Hiller-Sturmhöfel, S. (2016). Biology, Genetics, and Environment. *Alcohol Research: Current Reviews*, *38*(1), 59–68.

Wallingford, J., Scott, A. L., Rodrigues, K., & Doering, L. C. (2017). Altered Developmental Expression of the Astrocyte-Secreted Factors Hevin and SPARC in the Fragile X Mouse Model. *Frontiers in Molecular Neuroscience*, *10*, 268.

Wang, G., Weber-Fahr, W., Frischknecht, U., Hermann, D., Kiefer, F., Ende, G., & Sack, M. (2021). Cortical glutamate and GABA changes during early abstinence in alcohol dependence and their associations with benzodiazepine medication. *Frontiers in Psychiatry*, *12*, 656468.

Wang, J., Holt, L. M., Huang, H. H., Sesack, S. R., Nestler, E. J., & Dong, Y. (2021). Astrocytes in cocaine addiction and beyond. *Molecular Psychiatry*, *27*, 652–668.

Wang, S. (2019). Historical review: opiate addiction and opioid receptors. *Cell Transplantation*, *28*(3), 233–238.

Weaver, M. S., Workman, G., Cardo-Vila, M., Arap, W., Pasqualini, R., & Sage, E. H. (2010). Processing of the matricellular protein hevin in mouse brain is dependent on ADAMTS4. *Journal of Biological Chemistry*, *285*(8), 5868–5877.

Weaver, M., Workman, G., Schultz, C. R., Lemke, N., Rempel, S. A., & Sage, E. H. (2011). Proteolysis of the matricellular protein hevin by matrix metalloproteinase-3 produces a SPARC-like fragment (SLF) associated with neovasculature in a murine glioma model. *Journal of Cellular Biochemistry*, *112*(11), 3093–3102.

Weiss, F., & Porrino, L. J. (2002). Behavioral neurobiology of alcohol addiction: Recent advances and challenges. *The Journal of Neuroscience: The Official Journal of the Society for Neuroscience*, *22*(9), 3332–3337.

Werner, D. F., Porcu, P., Boyd, K. N., O'Buckley, T. K., Carter, J. M., Kumar, S., & Morrow, A. L. (2016). Ethanol-induced $GABA_A$ receptor α4 subunit plasticity involves phosphorylation and neuroactive steroids. *Molecular and Cellular Neurosciences*, *72*, 1–8.

Whiting, P. J., McKernan, R. M., & Wafford, K. A. (1995). Structure and pharmacology of vertebrate $GABA_A$ receptor subtypes. *International Review of Neurobiology*, *38*, 95–138.

WHO (2018). *Global status report on alcohol and health 2018*. In: Poznyak V. & Rekv D. (eds.). World Health Organization.

Wilson, D. F., & Matschinsky, F. M. (2020). Ethanol metabolism: the good, the bad, and the ugly. *Medical Hypotheses*, *140*, 109638.

Wilson, S., Bair, J. L., Thomas, K. M., & Iacono, W. G. (2017). Problematic alcohol use and reduced hippocampal volume: A meta-analytic review. *Psychological Medicine*, *47*(13), 2288–2301.

Wirkner, K., Eberts, C., Poelchen, W., Allgaier, C., & Illes, P. (2000). Mechanism of inhibition by ethanol of NMDA and AMPA receptor channel functions in cultured rat cortical neurons. *Naunyn-Schmiedeberg's Archives of Pharmacology*, *362*(6), 568–576.

Witkiewitz, K., Litten, R. Z., & Leggio, L. (2019). Advances in the science and treatment of alcohol use disorder. *Science Advances*, *5*(9), eaax4043.

Witkiewitz, K., Saville, K., & Hamreus, K. (2012). Acamprosate for treatment of alcohol dependence: Mechanisms, efficacy, and clinical utility. *Therapeutics and Clinical Risk Management*, *8*, 45–53.

Wrase, J., Makris, N., Braus, D. F., Mann, K., Smolka, M. N., Kennedy, D. N., Caviness, V. S., Hodge, S. M., Tang, L., Albaugh, M., Ziegler, D. A., Davis, O. C., Kissling, C., Schumann, G., Breiter, H. C., & Heinz, A. (2008). Amygdala Volume Associated With Alcohol Abuse Relapse and Craving. *American Journal of Psychiatry*, *165*(9), 1179–1184.

Xu, J., Xiao, N., & Xia, J. (2010). Thrombospondin 1 accelerates synaptogenesis in hippocampal neurons through neuroligin 1. *Nature Neuroscience*, *13*(1), 22–24.

Yan, Q. S. (1999). Extracellular dopamine and serotonin after ethanol monitored with 5-minute microdialysis. *Alcohol*, *19*(1), 1–7.

Yan, Q., & Sage, E. H. (1999). SPARC, a Matricellular Glycoprotein with Important Biological Functions. *Journal of Histochemistry & Cytochemistry*, *47*(12), 1495–1505.

Yang, B.-Z., Arias, A. J., Feinn, R., Krystal, J. H., Gelernter, J., & Petrakis, I. L. (2017). GRIK1 and GABRA2 variants have distinct effects on the dose-related subjective response to intravenous alcohol in healthy social drinkers. *Alcoholism, Clinical and Experimental Research*, *41*(12), 2025–2032.

Yang, C., Rahimpour, S., Yu, A. C. H., Lonser, R. R., & Zhuang, Z. (2013). Regulation and dysregulation of astrocyte activation and implications in tumor formation. *Cellular and Molecular Life Sciences: CMLS*, *70*(22), 4201–4211.

Yang, W., Singla, R., Maheshwari, O., Fontaine, C. J., & Gil-Mohapel, J. (2022). Alcohol use disorder: neurobiology and therapeutics. *Biomedicines*, *10*(5), 5.

Yang, X., Tian, F., Zhang, H., Zeng, J., Chen, T., Wang, S., Jia, Z., & Gong, Q. (2016). Cortical and subcortical gray matter shrinkage in alcohol-use disorders: a voxel-based meta-analysis. *Neuroscience and Biobehavioral Reviews*, *66*, 92–103.

Yen, C.-H., Yeh, Y.-W., Liang, C.-S., Ho, P.-S., Kuo, S.-C., Huang, C.-C., Chen, C.-Y., Shih, M.-C., Ma, K.-H., Peng, G.-S., Lu, R.-B., & Huang, S.-Y. (2015). Reduced dopamine transporter availability and neurocognitive deficits in male patients with alcohol dependence. *PLoS ONE*, *10*(6), e0131017.

Yim, H. J., & Gonzales, R. A. (2000). Ethanol-induced increases in dopamine extracellular concentration in rat nucleus accumbens are accounted for by increased release and not uptake inhibition. *Alcohol*, *22*(2), 107–115

Yin, G. N., Lee, H. W., Cho, J.-Y., & Suk, K. (2009). Neuronal pentraxin receptor in cerebrospinal fluid as a potential biomarker for neurodegenerative diseases. *Brain Research*, *1265*, 158–170.

You, C., Zhang, H., Sakharkar, A. J., Teppen, T., & Pandey, S. C. (2014). Reversal of deficits in dendritic spines, BDNF and Arc expression in the amygdala during alcohol dependence by HDAC inhibitor treatment. *International Journal of Neuropsychopharmacology*, *17*(2), 313–322.

Zaso, M. J., Goodhines, P. A., Wall, T. L., & Park, A. (2019). Meta-Analysis on Associations of Alcohol Metabolism Genes With Alcohol Use Disorder in East Asians. *Alcohol and Alcoholism*, *54*(3), 216–224.

Zha, Y., Chen, Y., Xu, F., Zhang, J., Li, T., Zhao, C., & Cui, L. (2010). Elevated level of ADAMTS4 in plasma and peripheral monocytes from patients with acute coronary syndrome. *Clinical Research in Cardiology: Official Journal of the German Cardiac Society*, *99*(12), 781–786.

Zhang, H.-P., Wu, J., Liu, Z.-F., Gao, J.-W., & Li, S.-Y. (2022). SPARCL1 is a novel prognostic biomarker and correlates with tumor microenvironment in colorectal cancer. *BioMed Research International*, *2022*, e1398268.

Zhang, Y., Liu, L., Qiu, Q., Zhou, Q., Ding, J., Lu, Y., & Liu, P. (2021). Alternative polyadenylation: methods, mechanism, function, and role in cancer. *Journal of Experimental & Clinical Cancer Research*, *40*(1), 51.

Zhou, F. C., Anthony, B., Dunn, K. W., Lindquist, W. B., Xu, Z. C., & Deng, P. (2007). Chronic alcohol drinking alters neuronal dendritic spines in the brain reward center nucleus accumbens. *Brain Research*, *1134*, 148–161.

Zhou, H., Sealock, J. M., Sanchez-Roige, S., Clarke, T.-K., Levey, D. F., Cheng, Z., Li, B., Polimanti, R., Kember, R. L., Smith, R. V., Thygesen, J. H., Morgan, M. Y., Atkinson, S. R., Thursz, M. R., Nyegaard, M., Mattheisen, M., Børglum, A. D., Johnson, E. C., Justice, A. C., … Gelernter, J. (2020). Genome-wide meta-analysis of problematic alcohol use in 435,563 individuals yields insights into biology and relationships with other traits. *Nature Neuroscience*, *23*(7), 809–818.

Zhou, Q., Verdoorn, T. A., & Lovinger, D. M. (1998). Alcohols potentiate the function of 5-HT3 receptor-channels on NCB-20 neuroblastoma cells by favouring and stabilizing the open channel state. *The Journal of Physiology*, *507 (Pt 2)*, 335–352.

Zhu, Y., Gao, H., Tong, L., Li, Z., Wang, L., Zhang, C., Yang, Q., & Yan, B. (2019). Emotion regulation of hippocampus using real-time fMRI neurofeedback in healthy human. *Frontiers in Human Neuroscience*, *13*, 242.

Zink, A., Conrad, J., Telugu, N. S., Diecke, S., Heinz, A., Wanker, E., Priller, J., & Prigione, A. (2020). Assessment of ethanol-induced toxicity on IPSC-derived human neurons using a novel high-throughput mitochondrial neuronal health (MNH) assay. *Frontiers in Cell and Developmental Biology*, *8*, 590540.

Zlebnik, N. E., & Cheer, J. F. (2016). Drug-Induced Alterations of Endocannabinoid-Mediated Plasticity in Brain Reward Regions. *Journal of Neuroscience*, *36*(40), 10230–10238.

Zorick, T., Okita, K., Mandelkern, M. A., London, E. D., & Brody, A. L. (2019). Effects of Citalopram on Cue-Induced Alcohol Craving and Thalamic D2/3 Dopamine Receptor Availability. *International Journal of Neuropsychopharmacology*, *22*(4), 286–291.

Zou, X., Durazzo, T. C., & Meyerhoff, D. J. (2018). Regional Brain Volume Changes in Alcohol-Dependent Individuals During Short-Term and Long-Term Abstinence. *Alcoholism, Clinical and Experimental Research*, *42*(6), 1062–1072.

ANNEXES

ANNEX 1

Characterization of Hevin (SPARCL1) Immunoreactivity in Postmortem Human Brain Homogenates

Amaia Nuñez-delMoral, Iria Brocos-Mosquera, Vincent Vialou, Luis F. Callado and Amaia M. Erdozain

Neuroscience (2021), *467*, 91-109

DOI: 10.1016/j.neuroscience.2021.05.017

NEUROSCIENCE
RESEARCH ARTICLE
A. Nuñez-delMoral et al. / Neuroscience 467 (2021) 91–109

Characterization of Hevin (SPARCL1) Immunoreactivity in *Postmortem* Human Brain Homogenates

Amaia Nuñez-delMoral, [a,b] **Iria Brocos-Mosquera,** [a,b] **Vincent Vialou,** [c,d,e*†] **Luis F. Callado** [a,b,f] **and Amaia M. Erdozain** [a,b*‡]

[a] *Department of Pharmacology, University of the Basque Country, UPV/EHU, Leioa, Bizkaia, Spain*

[b] *Centro de Investigación Biomédica en Red de Salud Mental (CIBERSAM), Spain*

[c] *Sorbonne Université, Neuroscience Paris Seine – IBPS, Team Neurobiology of Psychiatric Disorders, Paris, France*

[d] *CNRS UMR8246, Neuroscience Paris Seine - IBPS, Team Neurobiology of Psychiatric Disorders, Paris, France*

[e] *Inserm U1130, Neuroscience Paris Seine – IBPS, Team Neurobiology of Psychiatric Disorders, Paris, France*

[f] *BioCruces Bizkaia Health Research Institute, Barakaldo, Bizkaia, Spain*

Abstract—Hevin is a matricellular glycoprotein that plays important roles in neural developmental processes such as neuronal migration, synaptogenesis and synaptic plasticity. In contrast to other matricellular proteins whose expression decreases when development is complete, hevin remains highly expressed, suggesting its involvement in adult brain function. *In vitro* studies have shown that hevin can have different post-translational modifications. However, the glycosylation pattern of hevin in the human brain remains unknown, as well as its relative distribution and localization. The present study provides the first thorough characterization of hevin protein expression by Western blot in *postmortem* adult human brain. Our results demonstrated two major specific immunoreactive bands for hevin: an intense band migrating around 130 kDa, and a band migrating around 100 kDa. Biochemical assays revealed that both hevin bands have a different glycosylation pattern. Subcellular fractionation showed greater expression in membrane-enriched fraction than in cytosolic preparation, and a higher expression in prefrontal cortex (PFC) compared to hippocampus (HIP), caudate nucleus (CAU) and cerebellum (CB). We confirmed that a disintegrin and metalloproteinase with thrombospondin motifs 4 (ADAMTS4) and matrixmetalloproteinase 3 (MMP-3) proteases digestion led to an intense double band with similar molecular weight to that described as SPARC-like fragment (SLF). Finally, hevin immunoreactivity was also detected in human astrocytoma, meningioma, cerebrospinal fluid and serum samples, but was absent from any blood cell type.

Key words: hevin, SPARCL1, human brain, *postmortem*, Western blot.

INTRODUCTION

Hevin, also called SPARC-like1 (SPARCL1 or SC1), ECM2 or Mast9, is a matricellular glycoprotein of the secreted protein acidic and rich in cysteine (SPARC) family (Girard and Springer, 1996; Johnston et al., 1990; Soderling et al., 1997). Non-structural matricellular proteins (including hevin, SPARC, thrombospondin and tenascin families) are extracellular matrix (ECM) molecules that do not act directly as scaffold molecules, but interact with other ECM proteins as well as cytokines, proteases, neurotrophic factors and cell surface receptors (Bornstein, 1995). As a consequence of their cell–cell and cell–ECM interactions during brain development, these proteins take part in cell proliferation, differentiation, neuronal migration and synaptogenesis (Bornstein, 2009; Bornstein and Sage, 2002; Eroglu, 2009; Murphy-Ullrich and Sage, 2014). Hevin distribution along radial glial fibers in the developing cortex signals the end of neuronal

*Corresponding authors. Addresses: Sorbonne Université, INSERM, CNRS, Neuroscience Paris Seine, 75005 Paris, France. Fax: +33-144276069. (V. Vialou). Department of Pharmacology, University of the Basque Country (UPV/EHU), Barrio Sarriena s/n, 48940 Leioa, Bizkaia, Spain. Fax: +34-946013220 (A. M. Erdozain).
E-mail addresses: vincent.vialou@inserm.fr (V. Vialou), amaia_erdozain@ehu.eus (A. M. Erdozain).
† ORCID ID: 0000-0002-8212-751X.
‡ ORCID ID: 0000-0003-0207-9122.

Abbreviations: PFC, prefrontal cortex; HIP, hippocampus; CAU, caudate nucleus; CB, cerebellum; ECM, extracellular matrix; CSF, cerebrospinal fluid; ADAMTS4, a disintegrin and metalloproteinase with thrombospondin motifs 4; MMP-3, matrixmetalloproteinase 3; EndoF3, endoglycosidase F3; EndoH, endoglycosidase H; PNGaseF, N-glycosidase F; CNS, central nervous system; WT, wild-type; P2, membrane-enriched fraction; PMD, *postmortem* delay; SLF, SPARC-like fragment, IKβα, NFKB inhibitor alpha; VGLUT1, vesicular glutamate transporter 1; NR2A, N-methyl D-aspartate receptor subtype 2A; PSD95, postsynaptic density protein 95.

https://doi.org/10.1016/j.neuroscience.2021.05.017
0306-4522/

migration in the appropriate cortical layer due to its antiadhesive properties (Gongidi et al., 2004). During synaptogenesis, hevin expression in astrocytes promotes the formation of excitatory synapses during brain development (Kucukdereli et al., 2011; Risher et al., 2014), probably by bridging non-interacting presynaptic neurexin-1α and postsynaptic neuroligin-1B proteins (Singh et al., 2016).

Whereas most of the matricellular proteins are expressed mostly during brain development, hevin remains highly expressed in adult brain (Eroglu, 2009; Lively et al., 2007; Lloyd-Burton and Roskams, 2012; Weaver et al., 2011). Recently, we identified hevin cellular expression profile in adult human brain, specifically in astrocytes and in various types of neurons, in particular in GABAergic parvalbumin-positive neurons, as well as other GABAergic neuronal subtypes and some glutamatergic neurons (Mongrédien et al., 2019). The systematic comparison between mouse and human adult brain revealed a conserved cellular expression pattern for hevin (Mongrédien et al., 2019; Weaver et al., 2011). Hevin is found in all mouse brain regions by virtue of its astrocytic expression and has been observed in every human brain region studied so far including prefrontal cortex (PFC), caudate nucleus (CAU), brainstem and sensory ganglion neurons (Hashimoto et al., 2016; Mongrédien et al., 2019). Its physiological role in adult brain has been investigated mainly in animal models of brain diseases such as brain injury, ischemic infarction and epilepsy. Thus, hevin expression is enhanced in reactive astrocytes after ischemic infarction or localized brain injury in adult rodents (Lively et al., 2011; McKinnon and Margolskee, 1996; Mendis et al., 2000). In a study of behavioral adaptation to stress, hevin was induced in resilient individuals and its overexpression by viral-mediated transgenesis reversed the effects of social defeat in mice acting like an antidepressant (Vialou et al., 2010). Accordingly, hevin is one of the most downregulated transcripts in the frontopolar cortex of depressed/suicide victims (Zhurov et al., 2012). Hevin has also been looked at as a potential biomarker of neurodegenerative disorders and has been found in the cerebrospinal fluid (CSF) of individuals with Parkinson's and Alzheimer's diseases (Yin et al., 2009).

Post-translational modifications are essential to the physiological function of extracellular proteins (Correia et al., 2019). Hevin is a 80 kDa protein that is post-translationally modified, mainly by glycosylation. The glycosylation pattern of hevin was first described in rat brain in 1990 (Johnston et al., 1990); it was thereafter studied in recombinant hevin in an eukaryotic expression system (Hambrock et al., 2003), and described in human CSF (Halim et al., 2013; Nilsson et al., 2009). However, so far no study has assessed hevin's glycosylation pattern in human brain tissue. In addition, despite being characterized as a synaptic junction protein in rodents (Kucukdereli et al., 2011; Risher et al., 2014; Singh et al., 2016), the subcellular distribution of the protein hevin in human brain remains unknown. In the present study, we provide the first detailed characterization of hevin immunoreactivity by Western blot in several *postmortem* human brain regions. First, we performed the biochemical characterization of hevin proteolysis, deglycosylation and protease cleavage pattern. Second, we performed regional and subcellular expression analyses of hevin in human PFC, hippocampus (HIP), cerebellum (CB) and CAU. Sex and age-differences in hevin immunoreactivities in human PFC were also analyzed. In addition, we explored the expression levels of hevin protein in human astrocytomas, meningiomas, CSF and blood samples.

EXPERIMENTAL PROCEDURES

Materials

The different primary antibodies used in this study (catalogue number, type, dilutions) are detailed in Table 1. Goat-IgG anti-mouse biotin (B 2763) was obtained from ThermoFisher Scientific. Recombinant human hevin (2728-SL) and recombinant human ADAMTS4 (A Disintegrin and Metalloproteinase with Thrombospondin motifs 4, 4307-AD) proteins were obtained from R&D Systems. Thrombin, was purchased from Sigma-Aldrich (605195) and human MMP-3 protein (Matrixmetalloproteinase 3, 10467-HNAE) from Sino Biological. EndoF3 (Endoglycosidase F3, P0771S), EndoH (Endoglycosidase H, P0702S) and PNGaseF (N-Glycosidse F, P0708S) recombinant enzymes were obtained from New England BioLabs.

Human samples

Human samples from subjects who died by sudden and violent causes were obtained at autopsy in the Basque Institute of Legal Medicine, Bilbao, Spain. All the subjects died by sudden and violent causes; *postmortem* tissue examinations and medical histories determined they were free of psychiatric or neurological disorders. At the time of autopsy, samples from the brain PFC, CAU, HIP, CB and CSF were extracted, at the time of autopsy and immediately stored at −70 °C until assayed. Small pieces of brain tissue containing tumor were collected at the time of craniotomy for tumor resection at the Neurosurgery Service, Cruces Hospital (Bizkaia, Spain) and stored at −70 °C until assays were performed. Samples were also taken from each patient for diagnosis by neuropathologists according to the International Classification of CNS (central nervous system) tumors drafted under the auspices of the World Health Organization. The tumors were diagnosed as anaplastic astrocytoma (grade III) or meningioma. Samples of blood were immediately processed after extraction from living subjects. The demographic characteristics and the number of the subjects included in the different types of experiments are shown in Table 2. The study was performed in compliance with legal policy and ethical review boards for *postmortem* brain studies.

Hevin knock out mouse brain samples

Hevin-null mice were obtained from C. Eroglu (Duke University, North Carolina, USA). Hevin-null mice were generated using homologous recombination of the

Table 1. References and dilutions of the primary antibodies used in this study

Primary antibody	Trading house	Catalog number	Antibody type	Immunized specie	Dilution
Anti-human SPARCL1	R&D Systems	AF2728	Polyclonal	Goat	1:3000
Anti-human SPARCL1	Santa Cruz Biotechnology	sc-514275	Monoclonal	Mouse	1:500
Anti-mouse SPARCL1	R&D Systems	AF2836	Polyclonal	Goat	1:2000
Anti-human β-actin	Sigma-aldrich	A1978	Monoclonal	Mouse	1: 100.000
Anti-human Syntaxin1A	Merck Millipore	MAB336	Polyclonal	Mouse	1:2000
Anti-human Vglut1	Donated by Salah El Mestikawy	——	Polyclonal	Rabbit	1:1000
Anti-human NR2A	Santa Cruz Biotechnology	sc-1468	Polyclonal	Goat	1:1000
Anti-human PSD95	Merck Millipore	MAB1596	Monoclonal	Mouse	1:1000
Anti-human Stathmin	Cell Signaling Technology	#3352	Polyclonal	Rabbit	1:200
Anti-human Ikb-α	Santa Cruz Biotechnology	Sc-371	Polyclonal	Rabbit	1:500

Table 2. Demographic characteristics and number of the subjects included in each assay of this study

Type of assay	Sample number (*N*)	Age (Mean ± SEM)	Sex (female/male)
Antibody specificity, degradation and enzymatic assays	Pool preparation containing samples from 4 different subjects	45 ± 2	4 M
Regional and subcellular expression assays	6 PFC 6 HIP 6 CAU 6 CB	44 ± 1	6 M
Correlations with different variables	29 PFC	50 ± 2	11F/18 M
Astrocytoma	3	49 ± 8	3 M
Meningioma	3	61 ± 7	2F/1M
Cerebrospinal fluid	4	65 ± 7	4 M
Blood	4	28 ± 3	4F

second exon at the transcription start codon resulting in the absence of hevin protein expression (McKinnon et al., 2000). Hevin-null mice were backcrossed to C57BL/6J for 10 generations. Experiments were performed on brains of 2–4 months old hevin-null, wild-type (WT) littermates and C57BL/6J mice, after sacrifice. Briefly, mice were decapitated and their brain quickly removed. CB was dissected and stored at −80 °C. Samples were homogenized by sonication in 200 μl of RIPA buffer 1× containing protease inhibitor at 1/1000 on ice (Sigma, Protease Inhibitor Cocktail #11836153001). Protein concentrations were determined by Bradford assay (Bradford, 1976). Proteins samples (50 μg) were suspended in NuPage LDS sample buffer 25% (Invitrogen, Carlsbad, CA, USA, #NP0008) and DTT 1 M, heated at 90 °C for 10 min, and then analyzed by western blot. All experiments were performed in conformity with the European Union laws and policies for use of animals in neuroscience research (European Committee Council Directive 2010/63/EU), and were approved by the local animal research committee. C57BL6J mice were housed in groups under conditions at 22 ± 1 °C and a 12 h light/-dark cycle, with food and water provided *ad libitum*.

Hevin expressing cells

Human carcinoid BON cells maintained in 1:1 DMEM/F12 supplemented with 10% fetal bovine serum and 100 U–100 μg/ml of penicillin–streptomycin, at 37 °C in a humidified 5% CO_2 incubator, were transiently transfected with mHevin or mock-transfected, using Lipofectamine 2000 standard protocol. Cells were lysed in 5 mM Tris-HCl pH 7.4 with a sonicator and then analysed by Western blot.

Preparation of brain subcellular fractions

Human brain samples were prepared in order to obtain total homogenates, cytosolic/soluble fractions and membrane-enriched (P2) fraction, as previously described (Brocos-Mosquera et al., 2018), with minor modifications.

Preparation of CSF samples and blood fractionation

Human *postmortem* CSF samples were centrifuged for 10 min (4 °C) at 1100×*g* to remove cell and debris, as previously published (Collins et al., 2015). For blood fractionation (n = 4), 5 mL of blood were added slowly to a 5 mL density bar (0.9 mL Optiprep™, 0.85% (w/v) NaCl, 20 nM HEPES–NaOH pH 7.4, 1 mM EDTA) to avoid mixing the two phases, and centrifuged 15 min (20 °C) at 350×*g* on a swinging rotor (Eppendorf centrifuge 5810 R, A-4-62 rotor). Whole blood was separated into four phases that were recovered separately, corresponding to serum (top phase), platelets (intermediate thin layer), leucocytes (intermediate layer, under platelets) and ery-

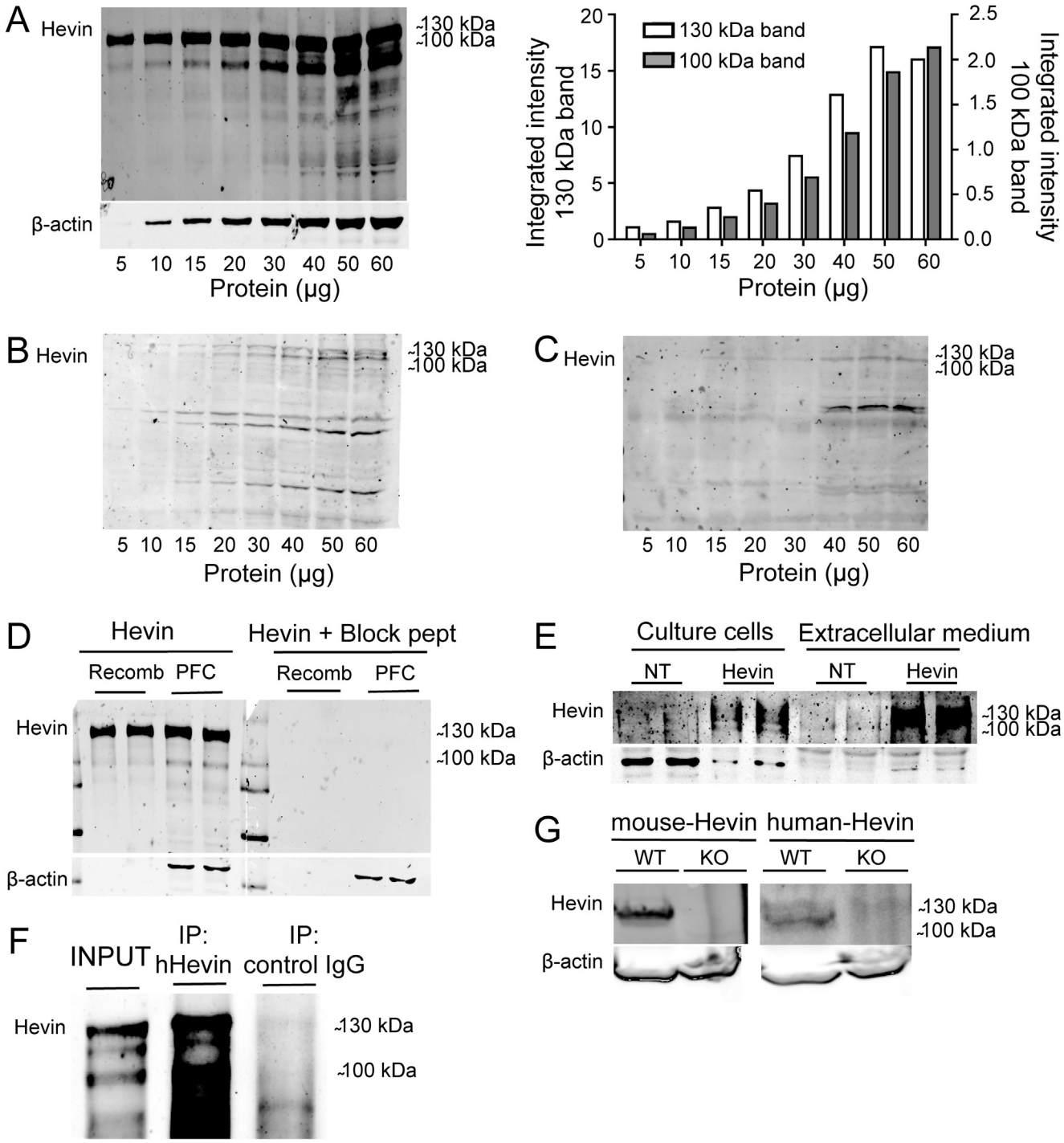

Fig. 1. Validation of human hevin antibody specificity. **(A)** Protein dependent-curve of hevin immunoreactivity in PFC total homogenate pool (5–60 μg) with goat anti-human hevin antibody (and the corresponding quantification of ~130 kDa and ~100 kDa hevin bands), **(B)** with goat anti-mouse hevin antibody and **(C)** with mouse anti-human hevin antibody. Blots A, B and C were run in parallel with the same sample and blot A was incubated with β-actin. **(D)** Hevin immunoreactivity with goat anti-human hevin antibody in PFC total homogenate and in human recombinant hevin (Recomb), in the presence or absence of its blocking peptide. **(E)** Hevin immunoreactivity with goat anti-human hevin antibody in cell culture lysate and in the extracellular medium of mock-transfected (NT) and hevin-tranfected BON cells. **(F)** Immunoblotting with goat anti-human hevin after immunoprecipitating hevin protein with goat anti-human hevin or control IgG in PFC total homogenate. The input loaded in the gel corresponds to 1:20 fraction of the tissue used in the assays. **(G)** Hevin immunoreactivity in wild-type (WT) and hevin knockout (KO) mouse brain homogenates (50 μg), with goat anti-mouse antibody or goat anti-human hevin antibody. Molecular weights are shown on the figure. Samples in **(D, E)** were run in duplicate.

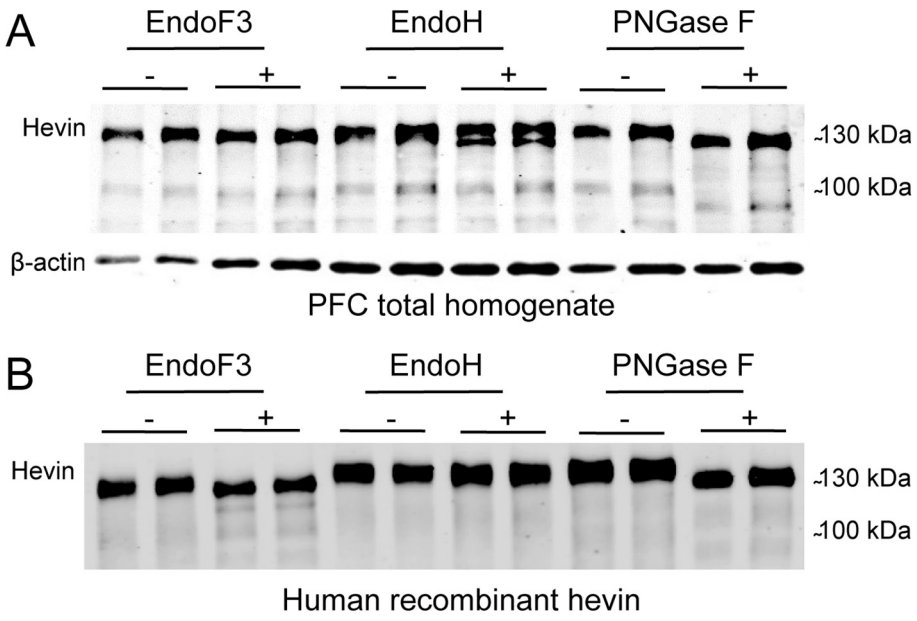

Fig. 2. Distinct glycosylation patterns of hevin in human brain. **(A, B)** Hevin immunoreactivity in a PFC total homogenate **(A)** and in human recombinant **(B)** hevin after treatment with EndoF3, EndoH or PNGaseF enzymes for 5 h at 37 °C. Experiments were performed in triplicates. Representative Western blot image for each experiment is shown.

throcytes (bottom phase) enriched fractions. To remove any serum content of fractions enriched in platelets and leucocytes, they were centrifuged again (5 min, 20 °C 600×*g*) and the supernatants were discharged. The pellet was resuspended in 500 μL of resuspending solution (0.85% (w/v) NaCl, 20 nM HEPES–NaOH pH 7.4, 1 mM EDTA) and centrifuged again. Homogenization buffer supplemented with protease and phosphatase inhibitors was added to each blood fraction and sonicated for 15 s (QSONICA Q55). Protein content was measured by the Bradford method (Collins et al., 2015) and stored at −70 °C until analyzed by Western blot.

Western blot

Western blot assays were performed as previously described (Brocos-Mosquera et al., 2018) with the exception of degradation assays and specificity assays, in which the primary antibody was incubated (1 h at room temperature) with the blocking peptide (R&D Systems 2728-SL, 1:150) in the same incubation solution prior to incubation with the nitrocellulose membrane. The hevin immunoreactivity values were normalized to β-actin signal. A standard pool of total homogenate was processed on the same gels and used as external reference sample.

Immunoprecipitation assay

Immunoprecipitation assays were performed as previously described (Brocos-Mosquera et al., 2018). Polyclonal goat anti-hSPARCL1 antibody (R&D Systems AF2728) was used for immunoprecipitations and goat IgG were used as isotype control of unspecific binding. Lysates were precleared 1 h at 4 °C with protein A/G agarose (Santa Cruz, sc-2003) and incubated with 10 μg antibody for 100 μg of tissue and protein A/G agarose beads at 4 °C overnight. After three washes with lysis buffer, samples were heated at 95 °C for 7 min in loading buffer for elution and centrifuged to pellet the agarose beads. Western blot was used to analyze the supernatants.

Protein identification by LC–MS/MS

Selected bands were excised manually from the gel and subjected to in-gel endopeptidase digestion as previously published (Shevchenko et al., 1996), with minor modifications. Gel pieces were incubated with DTT (10 mM in 50 mM NH_4HCO_3, 56 °C, 45 min) and Iodoacetamide (25 mM in 50 mM NH_4HCO_3, room temperature, 30 min, dark) and digested with proteomics grade trypsin (12.5 ng/μl in 50 mM NH_4HCO_3, 37 °C, overnight). The recovered peptides were dried in a SpeedVac (Thermo Fisher Scientific) and desalted with homemade C18 tips (3 M Empore C18). Mass spectrometric analyses were performed on an EASY-nLC 1200 liquid chromatography system interfaced with a Q Exactive HF-X mass spectrometer (Thermo Scientific) via a nanospray flex ion source. Desalted peptides were loaded onto an Acclaim PepMap100 precolumn (75 μm × 2 cm, Thermo Scientific) connected to an Acclaim PepMap RSLC (75 μm × 25 cm, Thermo Scientific) analytical column. Peptides were eluted using a linear gradient of 2.4–24% acetonitrile in 0.1% formic acid at a flow rate of 300 nL min^{-1} over 18 min. Full MS scans were acquired from *m*/*z* 375 to 1800 with a resolution of 120,000 at *m*/*z* 200. The 10 most intense ions were fragmented by higher energy C-trap dissociation with normalized collision energy of 28 and MS/MS spectra were recorded with a resolution of 15,000 at *m*/*z* 200. The maximum ion injection time was 100 ms for survey and 120 ms for MS/MS scans, whereas AGC target values of 3×10^6 and 5×10^5 were used for survey and MS/MS scans, respectively (Elu et al., 2019). Raw files were processed with Proteome Discoverer 2.2 (Thermo Scientific) and searches were performed against a UniProtKB-SwissProt Human (2020_02) database. Precursor and fragment mass tolerances were set to 10 ppm and 0.02 Da respectively and up to 1 missed cleavage was allowed. Carbamidomethylation of Cys was set as fixed modification and oxidation of Met as variable modification. Peptide and protein FDR were set to 1%.

Deglycosylation assays

Following the manufacturers recommendations, 8 μg of total homogenates obtained from a pool of human PFC

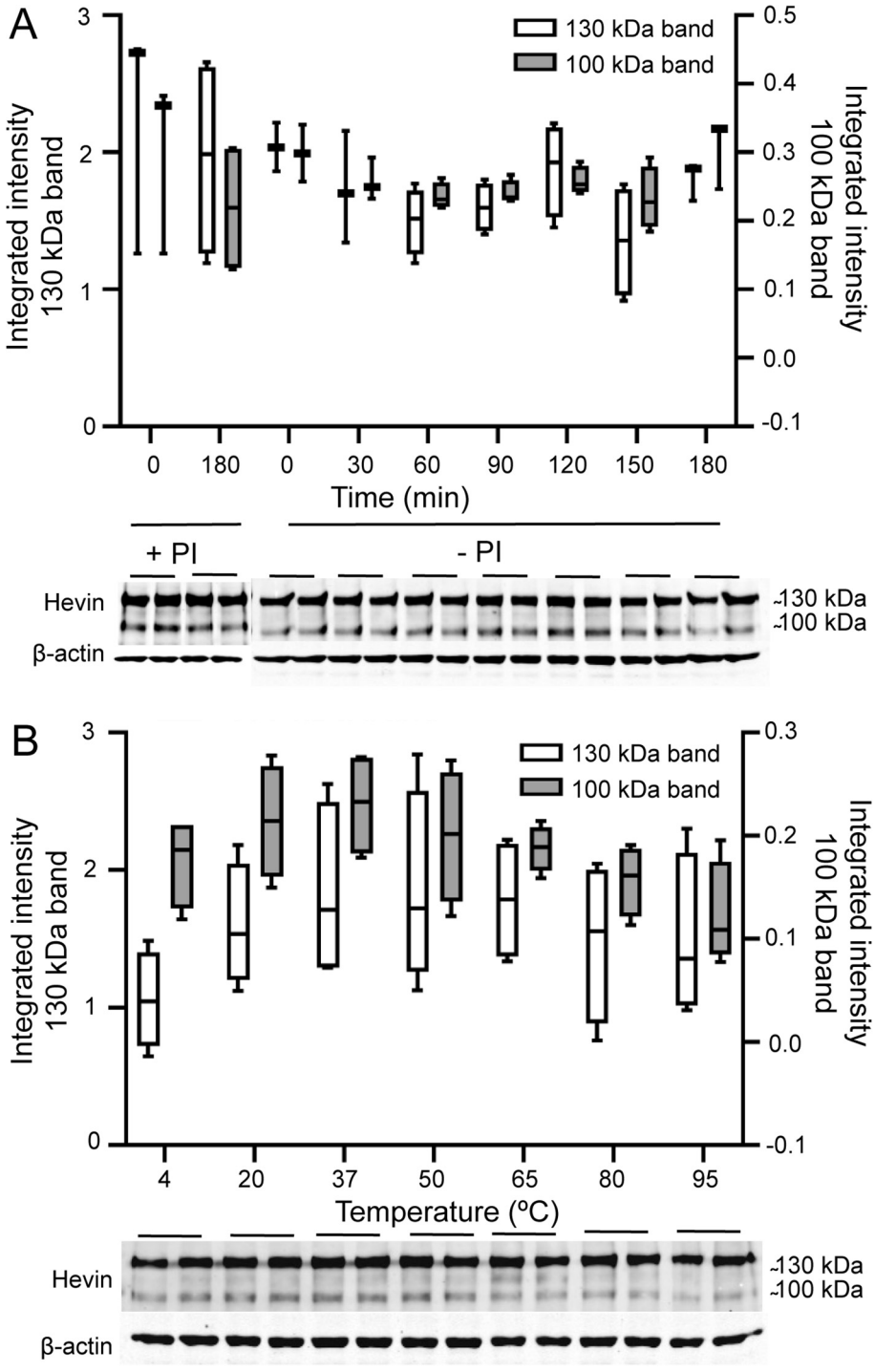

Fig. 3. Proteolytic degradation of hevin in human brain. **(A)** Hevin immunoreactivity and corresponding β-actin-normalized quantification in a PFC total homogenate pool (20 μg) after incubation with (+PI) or without (−PI) protease inhibitors for a duration of 0–180 min at 37 °C. **(B)** Hevin immunoreactivity and corresponding β-actin-normalized quantification in a PFC total homogenate pool (20 μg) after incubation at different temperatures (4–95 °C) for 15 min. Experiments were performed in triplicates. Representative Western blot image for each experiment is shown.

or 50 ng of human recombinant hevin (R&D Systems, 2728-SL) as positive control were treated with three deglycosylases separately: EndoF3 (50 U), EndoH (5000 U) and PNGase F (1000 U). Briefly, samples were incubated in the appropriate reaction buffer (final volume of 20 μl), in the presence or absence of the enzyme, for 5 h at 37 °C. The reaction was stopped by addition of a final concentration of PMSF 2 mM, DTT 100 mM, Laemmli buffer (2% SDS, 8% glycerol, 0.01% Bromophenol Blue), and by heating for 5 min at 98 °C, before being analyzed by Western blot.

Proteolysis study

A pool of total homogenates obtained from human PFC was prepared in the presence or absence of protease inhibitors, as previously published (Brocos-Mosquera et al., 2018), and incubated at 37 °C for a range of time (0–180 min). Then samples were prepared in the loading buffer, heated at 95 °C for 5 min and analyzed by western blot. In temperature-dependent proteolysis assays, a range of different temperatures (4 °C–95 °C, for 15 min) was used to heat the samples in the loading buffer.

ADAMTS4, MMP-3 and thrombin proteases digestion

One-hundred and forty micrograms of total protein of PFC pool were combined with 2 μg of ADAMTS4 or 0.4 μg of MMP-3 in 100 μl incubation buffer B1 (50 mM Tris-HCl, 125 mM NaCl, 5 mM H_2OCaCl_2, pH 7.5) and incubated 1 h or 5 h at 37 °C. In the case of thrombin, 70 μg of total protein of PFC pool were combined with 1 U of enzyme in 50 μl buffer B2 (20 mM Tris-HCl, 0.15 M NaCl, 2.5 mM H_2OCaCl_2, pH 8.4) and incubated 15 h at 37 °C. Four-hundred nanograms and 20 ng of human recombinant hevin (R&D Systems, 2728-SL) were used as positive controls for ADAMTS4/MMP-3 and thrombin digestions, respectively. For negative controls, samples were treated in the same way but without the enzyme. In all cases, the reaction was stopped by addition of PMSF 2 mM, DTT 100 mM, Laemmli buffer (2% SDS, 8% glycerol, 0.01% Bromophenol Blue) and heated 10 min at 75 °C, before being analyzed by Western blot.

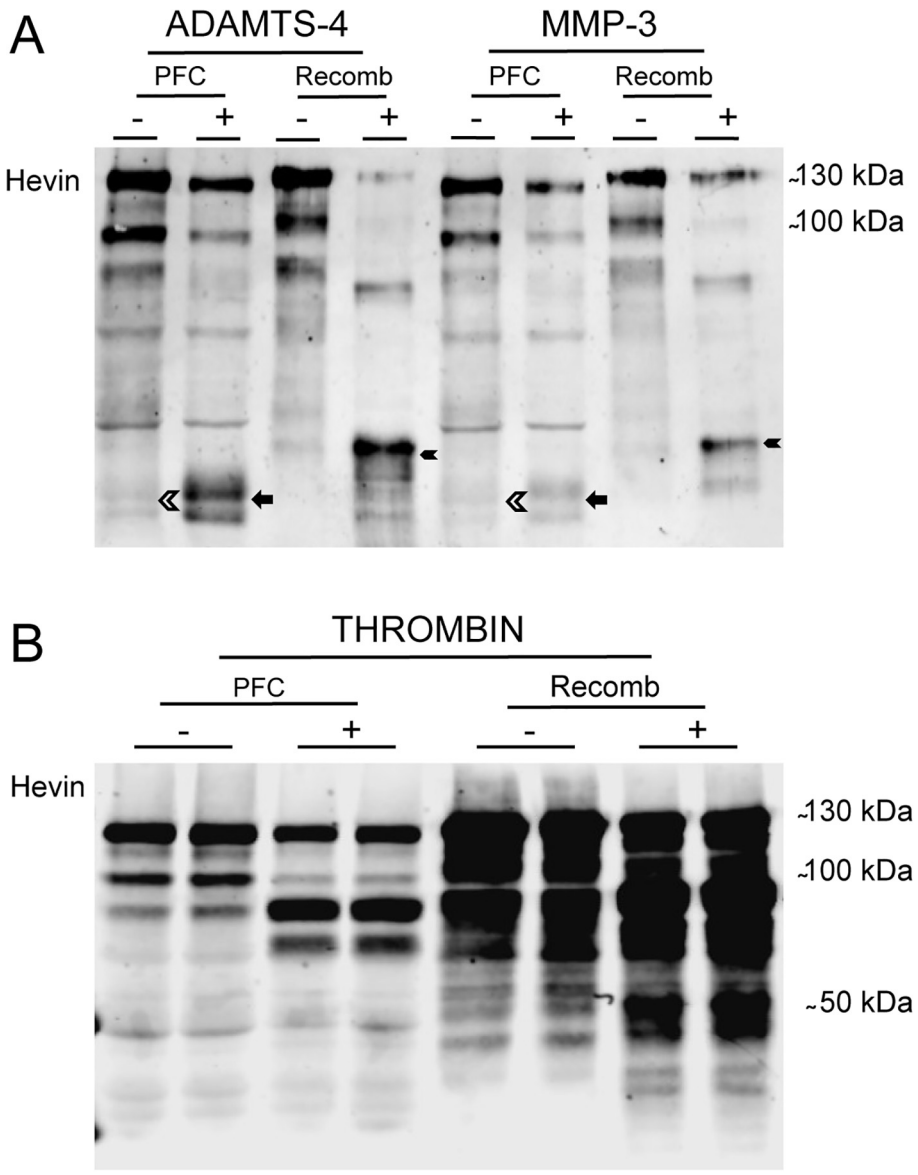

Fig. 4. Sensitivity of human hevin to matrix metalloproteases and the serine protease thrombin. **(A)** Hevin immunoreactivity in a PFC total homogenate and in human recombinant hevin after treatment with after treatment with ADAMTS4 or MMP-3 enzymes for 5 h at 37 °C (*arrow*: ~40 kDa double band detected in digested-PFC; *filled arrowhead*: ~47 kDa double band detected in digested-recombinant protein; *empty arrowhead*: hypothetical ~40 kDa SLF fragment in non-digested PFC). **(B)** Hevin immunoreactivity of PFC total homogenate pool (70 μg) or human recombinant hevin (20 ng) after 15 h (37 °C) of incubation in the presence or absence of thrombin (1 U). Experiments were performed in duplicate and a representative Western blot image is shown.

Data analysis

Results are shown in box-and-whiskers plots with the ''box" depicting the median and the 25th and 75th quartiles and the ''whisker" showing the 5th and 95th percentile. All statistical calculations were performed using GraphPad Prism 7®. Prior to analysis, all data sets were tested for two criteria: (i) normal distribution and (ii) equality of variances. The normal distribution was tested by applying a D'Agostino and Pearson normality test. The equality of variances was tested with an *F*-test. In the case of normal distribution and of equal variances, statistical comparisons were made with Student's unpaired t test. Otherwise, non-parametric tests were used as detailed below. All used statistical models were fixed-effect models. Results were considered statistically significant when p value < 0.05. Significance levels are symbolized with asterisks if $p < 0.05$ (*), $p < 0.01$ (**) or $p < 0.001$ (***).

Subcellular and regional expression pattern for both full-length forms of hevin at ~130 and ~100 kDa. Comparison of hevin levels in total homogenates, cytosolic and membrane-enriched (P2) fraction, and in PFC, HIP, CAU and CB were performed from brain samples of 8 individuals ($n = 6$). Because these data displayed a non-parametric distribution, they were analyzed with a Kruskal–Wallis test followed by a Dunn's multiple comparisons test.

Sex differences on the expression of hevin bands. The data set composed of 29 PFC samples from 11 females and 18 males passed the normality test, and had equal variance. Student's unpaired t test was used and showed no significant differences.

Correlation with age, postmortem delay (PMD), storage time and hevin isoform levels. A simple linear regression analysis was performed to determine the correlation between hevin isoform levels and age, PMD, storage time and in between isoforms. No significant correlation was observed except between hevin isoform ($r = 0.8313$, $p \leq 0.0001$).

Astrocytoma and meningioma. Full-length forms of hevin at ~130 and ~100 kDa in astrocytoma ($n = 3$), meningioma ($n = 3$) and PFC ($n = 6$) did not passed normality test. These data were analyzed with Mann–Whitney tests.

RESULTS

Specificity of hevin immunoreactivity

Three antibodies against hevin were tested for specificity by western blotting on human PFC total homogenate pool. Anti-human hevin antibody (R&D systems, AF2728) showed two marked bands at the expected molecular weight (Fig. 1A, left), while neither anti-mouse hevin (R&D Systems, AF2836) nor anti-human hevin (Santa Cruz, sc-514275) antibodies showed specific

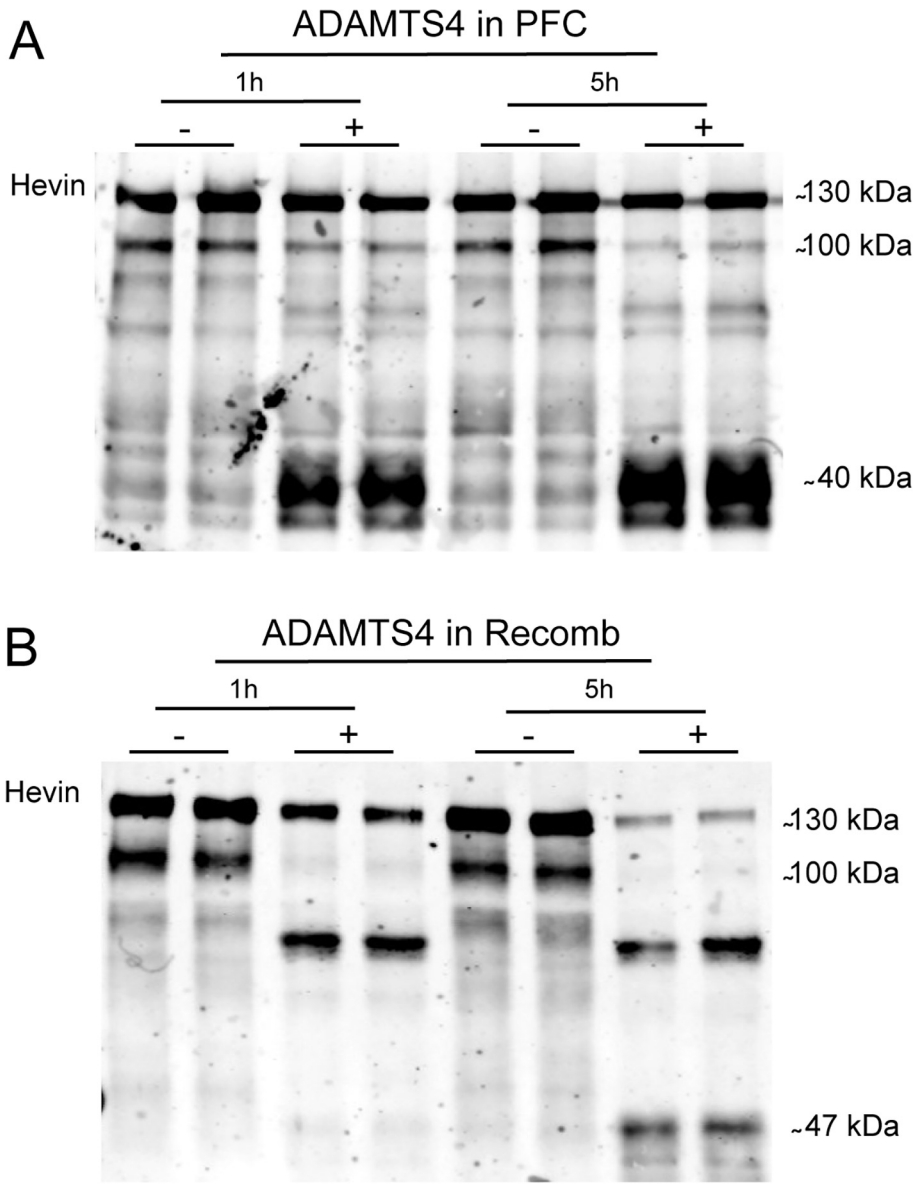

Fig. 5. ADAMTS4-dependent proteolysis of human hevin. **(A)** Hevin immunoreactivity of PFC total homogenate pool (50 μg), **(B)** and human recombinant hevin (140 ng) after 1 h or 5 h (37 °C) of incubation in the presence or absence of ADAMTS4 (2 μg) protease. Experiments were performed in duplicate and a representative Western blot image is shown.

immunoreactivity at the expected size (Fig. 1B, C). Hevin immunoreactive upper band migrated at 130 kDa and the lower band at around 100 kDa, similar to what has been described by other authors (Brekken et al., 2004; Johnston et al., 1990; Kucukdereli et al., 2011; Lively and Brown, 2008a, 2008b; Mendis, 1996b; Weaver et al., 2010, 2011). Intensity of the immunoblot signal increased in a dose-dependent manner (Fig. 1A, right), suggesting specificity. These two bands also appeared when the recombinant hevin protein was loaded (Fig. 1D) and their immunoreactivity was blocked by preincubating the antibody with the blocking peptide (recombinant human hevin, R&D systems, Fig. 1D), supporting the specificity of both bands corresponding to hevin. In addition, we performed Western blot experiments on cell extracts and its extracellular medium of BON cells transfected with mouse hevin. Hevin immunoreactivity was detected in hevin-transfected cells and its extracellular medium, but not in mock-transfected cells (Fig. 1E). To further assess the specificity of the selected antibody (R&D AF2728), immunoprecipitation of hevin from PFC total homogenate samples revealed the same bands (~130 and ~100 kDa), which were absent with control IgGs (Fig. 1F). To further assess the specificity of the selected antibody (R&D AF2728), immunoprecipitation of hevin from PFC total homogenate samples revealed the same bands (~130 and ~100 kDa), which were absent with control IgGs (Fig. 1F). Importantly, protein bands at these molecular weights were removed and analyzed by LC–MS/MS, which unambiguously identified hevin protein (UniProtKB Q14515) in both ~130 and ~100 kDa bands (sequence coverage 36% and 18% respectively). Although more unique peptides were found in ~130 kDa band (19 vs 8, probably due to a higher amount of the ~130 kDa isoform), all but one peptide found in the 100 kDa isoforms are common to the ~130 kDa and encompassed almost the entire protein sequence from amino acids A47 to R629 (Supplementary Figure). This proteomic analysis suggests that the 30 kDa difference observed between the two bands are not splicing variants but the result of differential post-translational modifications. Finally, in total homogenates of mouse brain samples, we observed hevin immunoreactivity at ~120 kDa with both anti-mouse hevin (R&D Systems, AF2836) and anti-human hevin (R&D Systems, AF2728) antibodies (Fig. 1G), which was absent in hevin knockout mice. Altogether, these results demonstrate the specificity of the R&D anti-human hevin antibody. We selected this antibody to further characterize hevin protein in human brain tissue.

Deglycosylation, endogenous proteolysis and proteases digestion assays

We determined to study the glycosylation pattern of hevin, its endogenous proteolytic degradation, and its proteolysis by matrix metalloproteases. Firstly, several deglycosylation assays were carried out in order to gain

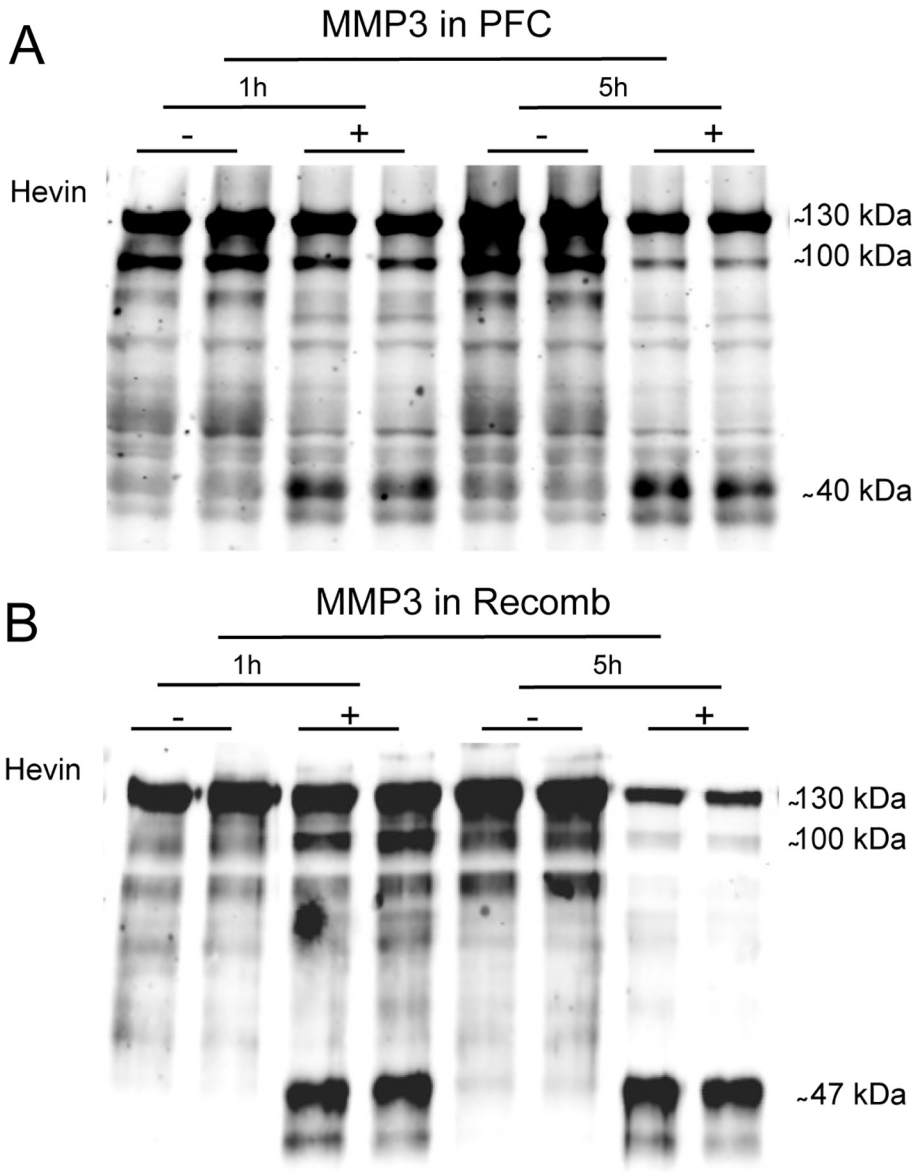

Fig. 6. MMP3-dependent proteolysis of human hevin. **(A)** Hevin immunoreactivity of PFC total homogenate pool (50 μg), **(B)** and human recombinant hevin (140 ng) after 1 h or 5 h (37 °C) of incubation in the presence or absence of MMP-3 protease (0.4 μg). Experiments were performed in duplicate and a representative Western blot image is shown.

more insight into the structure of the carbohydrate moieties of each of the hevin bands observed in human brain. Human PFC total homogenate pool and human recombinant hevin (R&D Systems, AF2728) were incubated in the presence of PNGase F, EndoF3 or EndoH deglycosylases, enzymes that remove different types of N-glycosylations. PNGase F (almost all N-glycan, asparagine-linked chains hydrolyzing enzyme (Maley et al., 1989): high mannose, hybrid, bi-, tri- and tetra-antennary) produced a marked shift in both hevin bands of PFC and recombinant protein, leading to lower molecular weight bands of ~125 and ~90 kDa (Fig. 2A, B). These results indicate that both hevin bands are glycosylated proteins. EndoF3 (asparagine-linked fucosylated-bi-antennary and tri-antennary complex oligosaccharides cleaving enzyme) (Maley et al., 1989) seemed to produce a slight shift of both bands in PFC and recombinant protein to lower molecular weight bands, although not as pronounced as PNGaseF. And finally, in the presence of EndoH enzyme (high mannose cleaving enzyme (Maley et al., 1989), only a fraction of the ~130 kDa band suffered a migration shift in both PFC and recombinant protein, which might suggest that this apparent unique band corresponds to a mix of slightly different isoforms or is even a doublet (Fig. 2A, B). Altogether these results confirm that both hevin bands in human brain are glycosylated but in different manner, as in rodent brain (Johnston et al., 1990).

Second, we wanted to determine if the ~100 kDa band derived from the ~130 kDa band via proteolytic degradation. We incubated PFC total homogenate samples at 37 °C in the absence of protease inhibitors for a range of times, then denatured the samples at 95 °C for 5 min and immediately processed them by western blot. Immunoreactive intensity of the bands was remained unchanged throughout the entire 3 h experiment (Fig. 3A), suggesting the absence of endogenous proteolysis. We next tested the effect of increasing temperatures on hevin proteolysis. PFC total homogenate samples were incubated for 15 min in temperature ranging from 4 to 95 °C, then immediately processed for western blot. Temperature-dependent proteolysis did not alter the intensity of the two bands (Fig. 3B). These results suggest that the lower ~100 kDa band is not a degradation product of the ~130 kDa band.

The matrix metalloproteases ADAMTS4, MMP-3 and thrombin have been described to cleave hevin in rodent brains resulting in a C-terminal SPARC-like fragment (SLF), which shares a high homology with SPARC, a close homologue of hevin, and which antagonizes hevin's synaptogenic function (Weaver et al., 2010, 2011). To confirm the sensitivity of human hevin towards ADAMTS4, MMP-3 and thrombin, we preformed proteolysis assays incubating PFC pool preparations and human recombinant hevin with the three proteases. As expected,

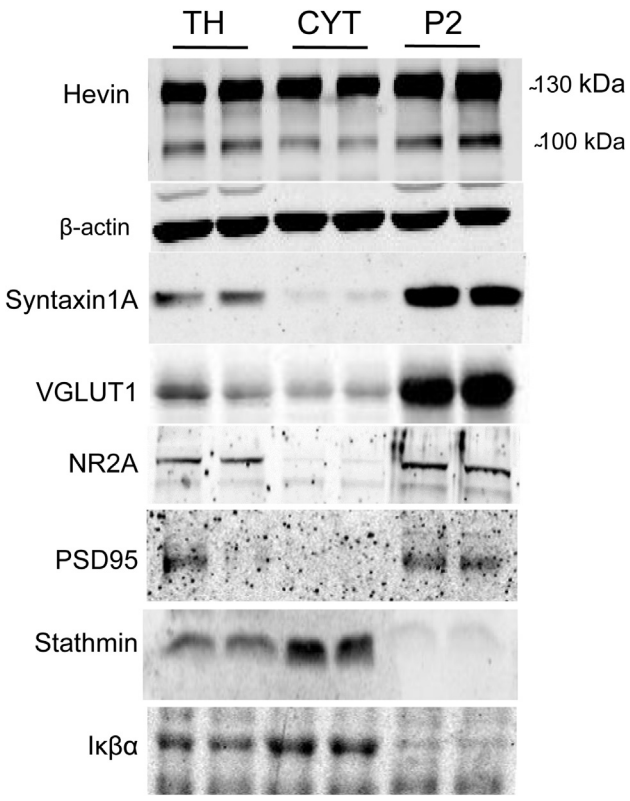

Fig. 7. Human hevin expression in membrane-enriched and cytosolic fraction. Validation of the subcellular isolation of cytosol and P2 fractions from human PFC samples. Immunoreactivities of synaptic proteins (Syntaxin1A, VGLUT1, NR2A, PSD95) are enriched in P2 membrane fraction. Immunoreactivities of cytosolic proteins (Stathmin, IKβα) are enriched in cytosolic fraction. Western blot experiments were performed using a goat anti-human hevin antibody (R&D Systems, AF2728) and those specified in Table 1. Experiments were performed in duplicate and a representative Western blot image is shown. TH: total homogenate, CYT: cytosol, P2: membrane-enriched fraction.

incubation with ADAMTS4 or MMP-3 enzymes in human PFC led to a marked decreased in the intensity of the ~130 kDa and ~100 kDa bands with a concomitant appearance of an intense ~40 kDa double band (Fig. 4A, arrow), that seems to correspond to the SLF fragment (Weaver et al., 2010, 2011). Likewise, proteolysis of human recombinant hevin decreased the intensity of full-length hevin protein bands. Surprisingly, the band corresponding to the hypothesized SLF had slightly greater molecular weight (Fig. 4A, filled arrowhead). In contrast, hevin proteolytic cleavage by thrombin in both PFC and recombinant proteins, which decreased levels of the ~130 kDa and ~100 kDa bands, produced many fragments higher than 50 kDa (Fig. 4B). In both ADAMTS4 (Fig. 5) and MMP-3 (Fig. 6) dependent-proteolysis assays, pronounced effects were observed when increasing the incubation time (1 h or 5 h of incubation). Importantly, the SLF fragment was identified in non-digested PFC samples, although it showed lower intensity level compared to the ~130 kDa and ~100 kDa bands (Fig. 4A, open arrowhead).

Subcellular and regional distribution of hevin in the human brain

We studied the subcellular distribution of both full-length forms of hevin at ~130 and ~100 kDa in human brain by Western blot using cellular fractionation of brain samples into both a cytosolic and a membrane-enriched (P2) fraction. The expression of stathmin and IKβα (NFKB inhibitor alpha) in the cytosolic fraction, together with the enrichment of syntaxin1A, VGLUT1 (Vesicular glutamate transporter 1), NR2A (N-methyl D-aspartate receptor subtype 2A) and PSD95 (postsynaptic density protein 95) and in P2 neuronal membranes confirmed the correct fractionation of brain preparations (Fig. 7). Both hevin ~130 and ~100 kDa bands were strongly enhanced in the membrane-enriched P2 fraction compared to the cytosolic fraction. This subcellular expression pattern was observed in all brain areas (Fig. 8A–D).

For each subcellular fraction (total homogenate, cytosols and P2), similar regional distribution was observed for the ~130 and ~100 kDa hevin forms, i.e. PFC showed the highest expression of hevin bands in all cases (Fig. 9A–C). In addition, greater levels were detected in ~130 kDa and ~100 kDa bands of total homogenate and ~100 kDa band of cytosol fractions in CAU compared to CB ($p < 0.05$, $p < 0.01$ and $p < 0.01$, respectively); and in ~100 kDa band of cytosol in HIP compared to CB ($p < 0.05$).

Effect of sex, age, PMD and storage time on hevin immunoreactivity

To test for sex and age differences on the expression of hevin bands, a larger control cohort of 29 PFC samples, composed of 11 females and 18 males ranging from 18 to 71 years old, was analyzed. Neither sex (11 females vs 18 males), nor age (18–71 years) showed significant differences or correlation with the immunoreactivity of any of the two detected bands (sex ~130 kDa band $p = 0.3544$; ~100 kDa band $p = 0.9787$; age ~130 kDa $p = 0.9248$ and ~100 kDa $p = 0.0514$; Fig. 10A–D). Importantly, no correlation was observed between hevin expression levels and *postmortem* delay (3–39 h) and storage time (18–244 months; PMD ~130 kDa $p = 0.5809$ and ~100 kDa $p = 0.3022$; storage time ~130 kDa $p = 0.5252$ and ~100 kDa $p = 0.9477$; Fig. 10E–H). Interestingly, analyzing this larger control cohort there was found to be a positive correlation between the ~130 kDa and ~100 kDa bands in human PFC ($p < 0.0001$), indicating that subjects that showed high levels for one form also showed high levels for the other and conversely (Fig. 10I).

Hevin expression in astrocytomas, meningiomas, CSF and blood

Next the relative contribution of the two forms of hevin in astrocytoma tumors ($n = 3$) in comparison with meningioma brain tumors ($n = 3$) were evaluated. Hevin protein expression, clearly detectable in both tumors, was significantly increased in astrocytoma

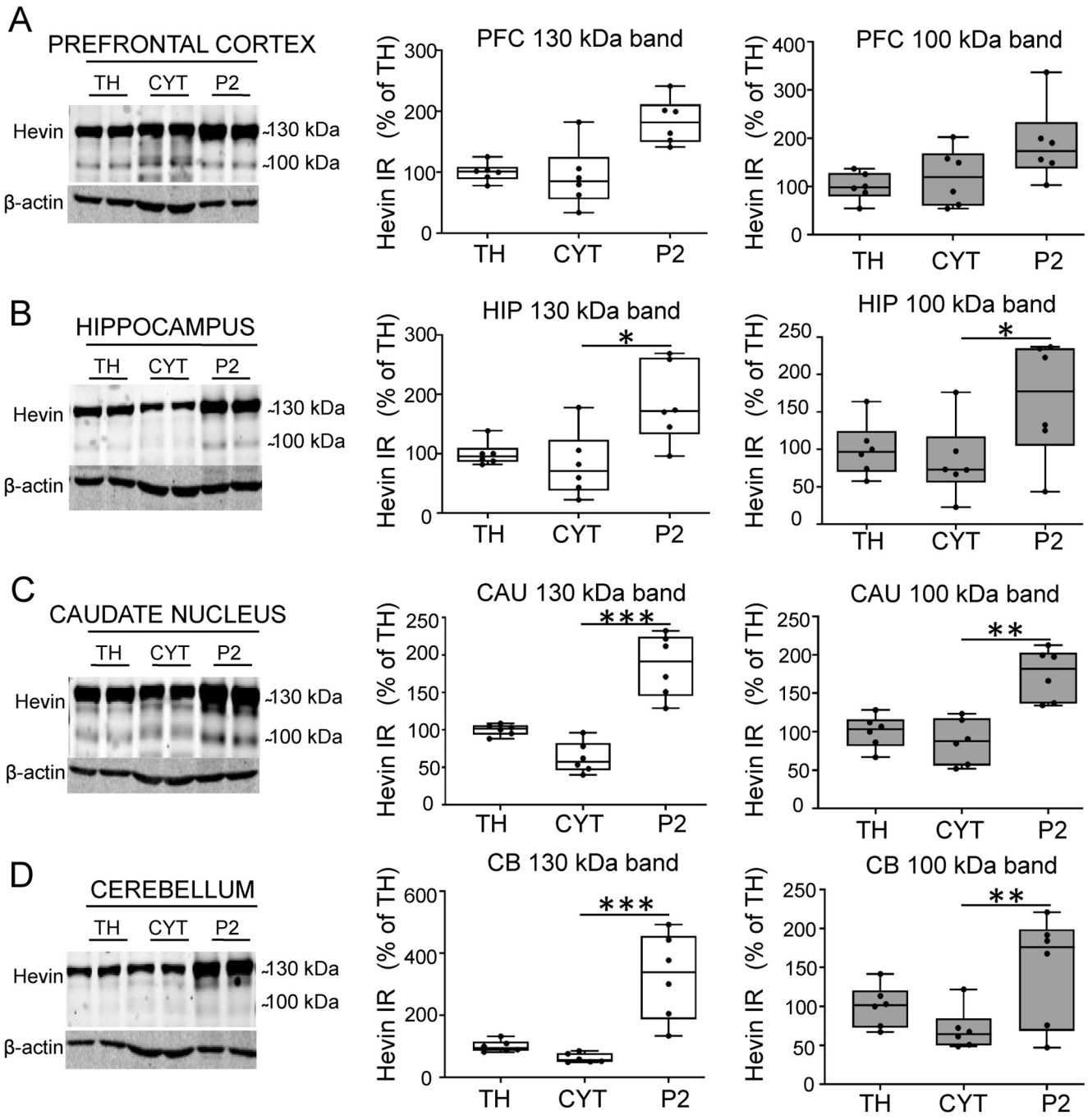

Fig. 8. Prominent expression of hevin in membrane-enriched fraction along different brain regions. **(A–D)** Hevin immunoreactivity and its ~130 kDa and ~100 kDa bands quantification (β-actin-normalized) in different cellular preparations (TH: total homogenate, CYT: cytosol, P2: membrane-enriched fraction) obtained from prefrontal cortex **(A)**, hippocampus **(B)**, caudate nucleus **(C)** and cerebellum **(D)**. Representative Western blot images are shown in the figure. Kruskal-Wallis followed by Dunn's multiple comparisons test was used for each comparison. IR: immunoreactivity. PFC 130 kDa: $H_2 = 9.696$; CYT vs P2: $p = 0.004$; PFC 100 kDa: $H_2 = 5.626$; CYT vs P2: $p = 0.117$; HIP 130 kDa: $H_2 = 7.17$; CYT vs P2: $p = 0.011$; HIP 100 kDa: $H_2 = 4.363$; CYT vs P2: $p = 0.04$; CAU 130 kDa: $H_2 = 14.36$; CYT vs P2: $p = 0.0002$; CAU 100 kDa: $H_2 = 11.66$; CYT vs P2: $p = 0.0014$; CB 130 kDa: $H_2 = 14.75$; CYT vs P2: $p = 0.0001$; CB 100 kDa: $H_2 = 4.994$; CYT vs P2: $p = 0.0266$. Significance levels: $^*p < 0.05$, $^{**}p < 0.01$, $^{***}p < 0.001$, $^{****}p < 0.0001$. Brain regions were collected from six individuals. Experiments were performed in duplicate. Data points are added to the box-and-whiskers plot.

tumors compared with meningioma tumors (~130 kDa band: astrocytoma 200% ± 37 and meningioma 15% ± 7; ~100 kDa band: astrocytoma 121% ± 44 and meningioma 4% ± 1; Fig. 11A). However, the relative expression of the ~130 kDa and ~100 kDa bands (calculated as the 130/100 ratio) was similar in both brain tumors (astrocytoma 34 ± 9 and meningioma 47 ± 13). In contrast, the relative 130/100 hevin bands ratio seems to be increased in both tumor types compared to control PFC brain regions (ratio of 6 ± 1, and $p = 0.002$ in both cases).

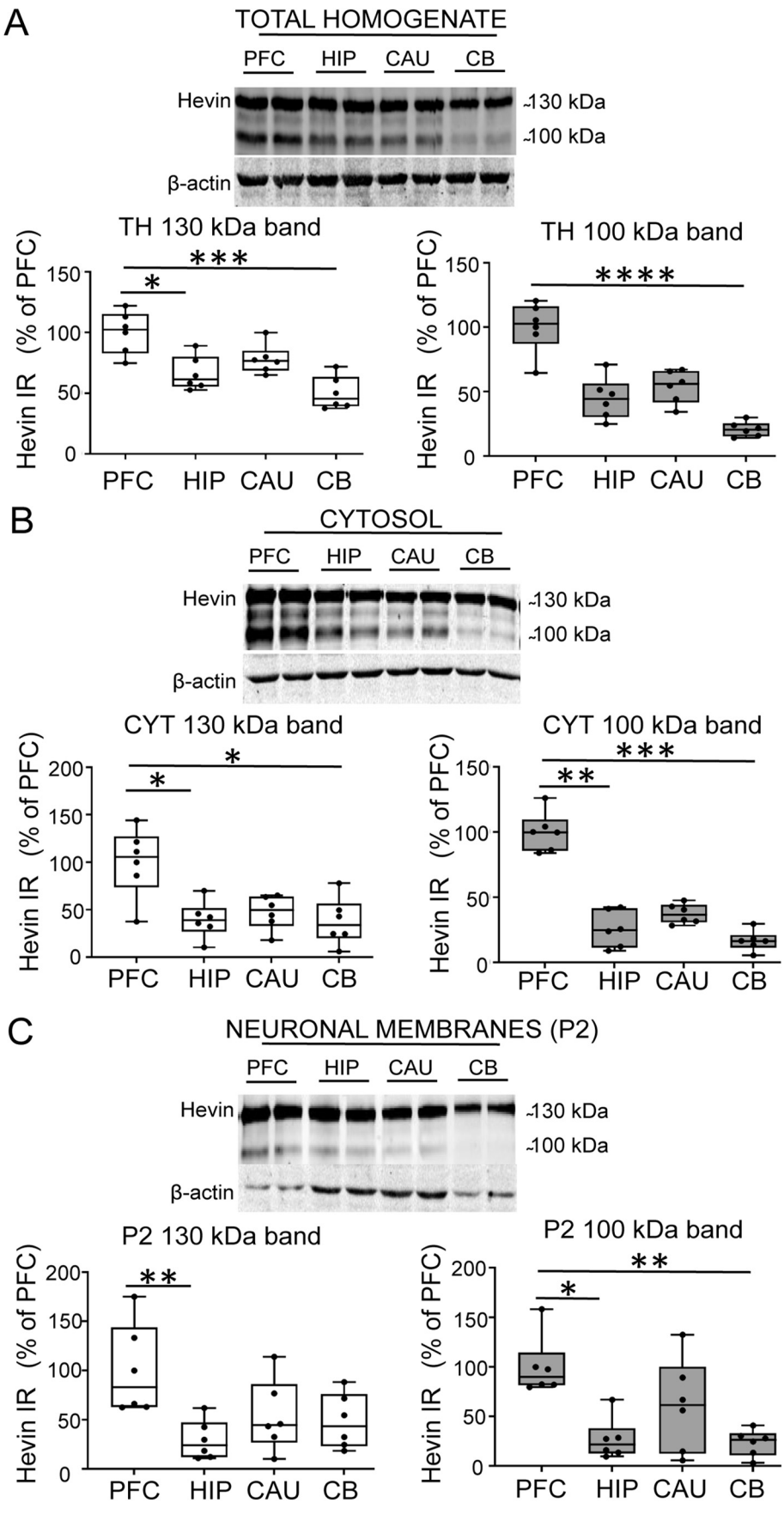

Hevin protein expression was also detected in CSF (n = 4) and serum (n = 4), with apparent higher levels in the CSF (Fig. 11B). Significantly, a new pattern of hevin immunoreactivity was observed in both fluids. A shorter novel band of ~90 kDa band and the ~130 kDa band were detected, without the ~100 kDa band (Fig. 11B).

The presence of hevin in the serum raises the question of its source of expression. We tested the expression of hevin in different blood fractions (serum, platelets, erythrocytes and leucocytes) in order to assess if hevin is produced by blood cells or derives from other organs that would secrete it. Western blot analysis revealed that hevin, which was highly expressed in serum, was absent in any blood cell fraction (~130 kDa and ~90 kDa bands; Fig. 11C), suggesting that hevin is transported into the bloodstream and not synthesized by any blood cell type.

DISCUSSION

In recent years, a number of glycoproteins that constitute the ECM have been shown to participate in synaptic function (Trinidad et al., 2012). These matricellular proteins are often secreted by astrocytes and play essential roles during development in synapse formation and plasticity. Among these matricellular proteins, hevin function has been well characterized during development (Eroglu, 2009; Kucukdereli et al., 2011; Lively and Brown, 2008b; Lloyd-Burton and Roskams, 2012; Mendis, 1996a; Mendis et al., 1996b, 2000; Risher et al., 2014), but its level remains high during adulthood, suggesting a physiological role in adult synaptic plasticity (Johnston et al., 1990; Lively et al., 2007; Lively and Brown, 2008b, 2010; Mendis et al., 1996a; Mongrédien et al., 2019). In rodents, astrocytic secretion of hevin is increased after brain injury (Lively et al., 2011; McKinnon and Margolskee, 1996; Mendis et al.,

2000) and hevin expression is altered in models of neuropsychiatric disorders (Purcell et al., 2001; Yin et al., 2009). In humans, hevin has also been associated with several mental disorders (Yin et al., 2009; Zhurov et al., 2012). In this context, it is crucial to better characterize hevin protein expression in the human brain. Here, we provide a detailed characterization of hevin protein expression by Western blot in *postmortem* adult human brain.

The reliability of our Western blot results rests on a thorough validation of the specificity of the selected antibody. Immunodetection of hevin in *postmortem* human brain disappeared when the antibody was previously incubated with the blocking peptide, and was absent in mock-transfected cells and hevin knockout mouse brain lysate. Conversely, hevin signal increased in a protein-dependent manner and after antibody immunoprecipitation. In our study, two main hevin immunoreactive bands were detected in human brain, an intense band of ~130 kDa and a lower molecular weight band of ~100 kDa, which agrees to a great extent with previous results in the literature. Hevin immunoreactivity has mostly been described as a 116/120 kDa doublet in rat brain (Johnston et al., 1990; Lively and Brown, 2008a, 2008b; Mendis et al., 1996a), but ~130 kDa and 105 kDa hevin bands have also been described in human and mouse brain lysates (Brekken et al., 2004; Kucukdereli et al., 2011; Weaver et al., 2010).

In order to further investigate the nature of the main hevin bands, we performed several biochemical assays. Time- and temperature- dependent proteolysis assays discharged ~100 kDa hevin form as the degradation product of the ~130 kDa form. Hevin is a 664 amino-acids glycoprotein composed of a signal peptide, an acidic N-terminal domain, followed by a follistatin-like domain and an extracellular Ca^{2+} binding-domain at the C-terminus. Several potential N-glycosylation sites have been proposed along hevin's protein sequence, mainly in the acidic N-terminal and in the follistatin-like domain (Asn-444) (Bendik et al., 1998; Girard and Springer, 1995; Hambrock et al., 2003). Additionally, several O-glycosylation sites have also been experimentally observed in human CSF (Halim et al., 2013). Our deglycosylation assays demonstrated that both hevin forms in human brain are N-glycosylated (PNGaseF cleavage). In both bands, some glycosylations corresponded to bi-antennary or tri-antennary fucosylation (EnfoF3 cleavage, but less migration shift than PNGaseF), while some N-glycosylation were due to N-linked high-mannose hybrid glycosylation (EndoH cleavage) only in the ~130 kDa form (Freeze and Kranz, 2010). PNGaseF deglycosylation leads to a ~90 kDa band, which may correspond to native hevin -with a calculated theoretical Mw of ~71 kDa (Johnston et al., 1990), or to some form of hevin with other post-translational modifications such as phosphorylation. These results concord with those described in rat brain lysates and mouse recombinant hevin (Hambrock et al., 2003; Johnston et al., 1990). The expression of two post-translationally distinct forms of hevin in different species suggests a conserved role in adult physiological brain function.

Proteolysis of hevin by ADAMTS4, MMP-3 and thrombin liberates the C terminus portion of mouse and recombinant hevin (amino-acids 350–650), which possess 60% of identity to SPARC, and hence was named SLF (Kucukdereli et al., 2011; Weaver et al., 2010, 2011). SLF, like SPARC, antagonizes the synaptogenic activity of hevin (Kucukdereli et al., 2011). Here we confirmed that human hevin is cleaved by these three enzymes. Incubation of human PFC total homogenate samples with ADAMTS4 or MMP-3 produced a double band with similar molecular weight (~40 kDa) to that described in mouse brain (Weaver et al., 2010, 2011). By contrast, the cleaved product of the recombinant human hevin was larger (~47 kDa). Differences in post-translational modifications in hevin PFC or recombinant protein (in this case produced in a mouse myeloma cell line) could explain the observed molecular weight differences of the cleaved product. Hevin proteolysis by thrombin produced very different molecular weight fragments in both PFC and recombinant proteins, due to thrombin non-specific cleavage sites (Rajalingam et al., 2008). Regardless of the protease identity, *in vivo* digestion of hevin occurs as we could detect the hypothetical SLF fragment in non-digested PFC samples, despite very low levels compared to full-length hevin. Biochemical studies in ADAMTS4–null mice suggest that hevin is endogenously digested primarily by ADAMTS4 at least in the CB (Weaver et al., 2010). Future studies are needed to identify the proteases responsible for the cleavage of hevin in human brain. Based on the antagonistic role of SLF on hevin synaptogenic function, it would be relevant to include the quantification of SLF levels along with hevin in future studies on human neuropsychiatric disorders.

Consistent with the wealth of experimental evidences showing hevin expression in synaptic junctions (Hambrock et al., 2003; Johnston et al., 1990; Singh et al., 2016), we found that the two human hevin forms, ~130 kDa and ~100 kDa, are strongly enriched in membranous fraction compared to cytosolic preparations in

Fig. 9. Comparison of human hevin expression among different brain regions. **(A–D)** Hevin immunoreactivity and its ~130 kDa and ~100 kDa bands quantification (β-actin-normalized) in different brain areas (PFC: prefrontal cortex, HIP: hippocampus, CAU: caudate nucleus, CB: cerebellum). Representative Western blot images are shown in the figure. Kruskal–Wallis followed by Dunn's multiple comparisons test was used for each comparison. IR: immunoreactivity. TH 130 kDa: $H_3 = 15.02$; PFC vs HIP: $p = 0.043$; PFC vs CB: $p = 0.0006$; TH 100 kDa: $H_3 = 18.47$; PFC vs CB: $p = 0.0001$; CYT 130 kDa: $H_3 = 8.867$; PFC vs HIP: $p = 0.034$; PFC vs CB: $p = 0.027$; CYT 100 kDa: $H_3 = 17.21$; PFC vs HIP: $p = 0.006$; PFC vs CB: $p = 0.0003$; P2 130 kDa: $H_3 = 9.58$; PFC vs HIP: $p = 0.007$; P2 100 kDa: $H_3 = 11.49$; PFC vs HIP: $p = 0.013$; PFC vs CB: $p = 0.009$. Significance levels: $*p < 0.05$, $**p < 0.01$, $***p < 0.001$, $****p < 0.0001$. Brain regions were collected from six individuals. Experiments were performed in duplicate. Data points are added to the box-and-whiskers plot.

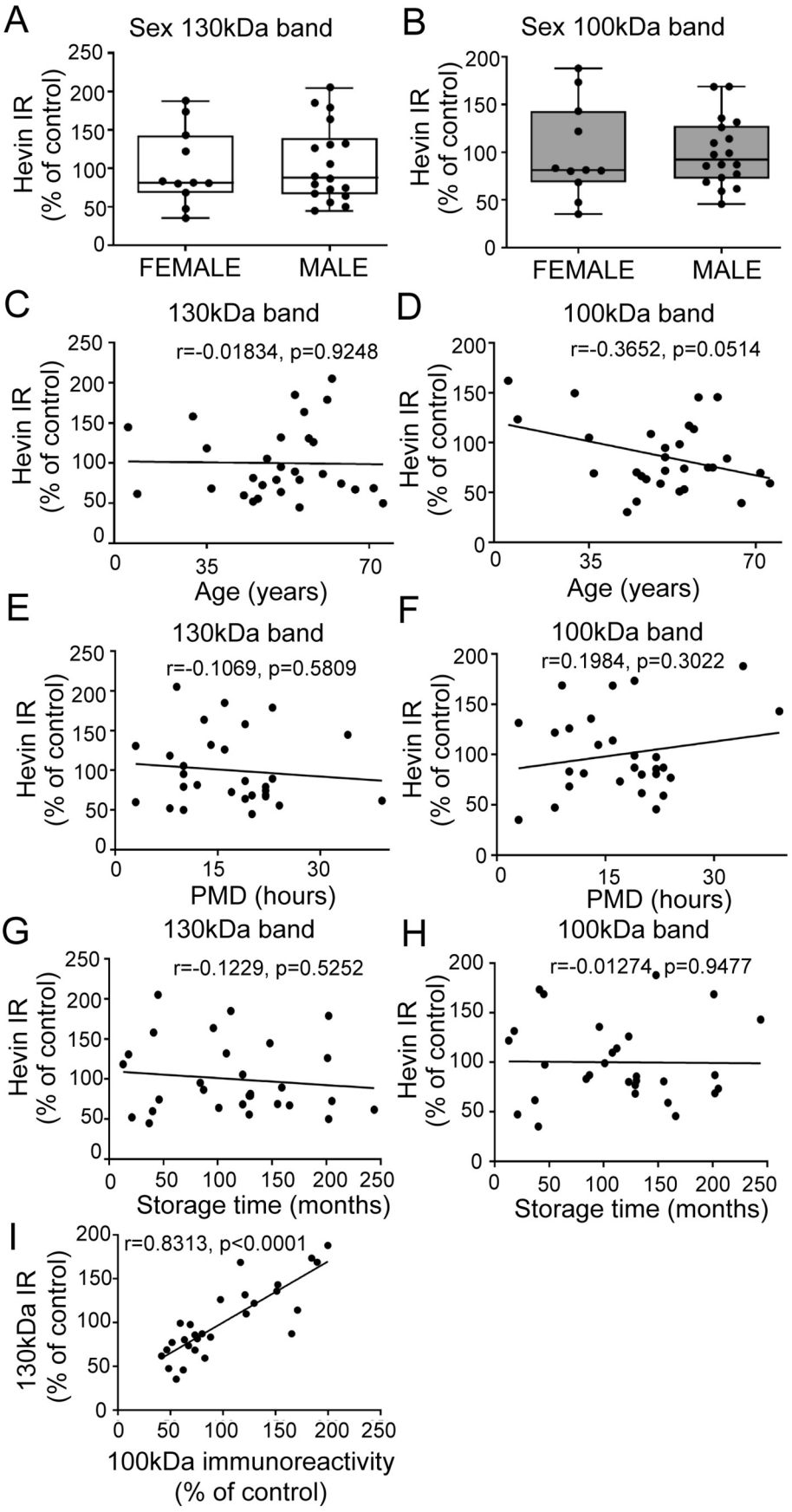

all brain region tested. The enrichment in membrane preparation suggests that hevin is trapped in the complex mesh-like matrix of the synapses. However, hevin's presence in the cytosolic (soluble) fraction reflects its soluble nature and also suggests that it can also attach to different targets before being secreted to the ECM (Ge et al., 2020; Hambrock et al., 2003; Sullivan et al., 2006). Additionally, the two human hevin immunoreactive bands were detected in the four brain regions studied with the largest expression detected in the PFC. This data is similar to the regional expression of hevin mRNA shown in mouse brain, with a strong expression in cortical regions (Mongrédien et al., 2019). In addition, we have previously observed in adult human brain, hevin mRNA expression in astrocytes and parvalbumin interneurons in PFC and CAU, and in glutamatergic neurons in PFC (Mongrédien et al., 2019). Our present results confirm that hevin mRNA is translated in adult human brain and add evidence for a region-specific expression of hevin. Hevin strong cortical expression suggests a major role in higher cognitive functions such as decision-making, social and emotional behavior, learning and memory. Thus, future analysis of hevin in several limbic brain regions of patients with psychiatric disorders such as depression, drug addiction and schizophrenia would be particularly relevant. In addition, based on recent evidence showing that post-translational modifications are crucial in synaptic functions (Zhang et al., 2018), analysis of hevin expression levels should differentiate between the two isoforms.

Besides being expressed in the non-pathological brain, previous studies have demonstrated that hevin protein expression is induced in reactive astrocytes (Jones and Bouvier, 2014; Lively et al., 2011; McKinnon and Margolskee, 1996; Mendis et al., 2000), and abnormal astrocyte activation has been related with tumor formation, such as astrocy-

toma (Gronseth et al., 2018; Yang et al., 2013). Upregulated hevin mRNA expression has also been reported in human meningiomas or meningeal tumors (Dalan et al., 2017), which are typically slow-growing tumors of the meninges, where the arachnoid mater cells transform into meningioma cells (Buerki et al., 2018; Fathi and Roelcke, 2013). However, these studies did not distinguish between the different hevin forms. Here we show that astrocytoma samples exhibited greater hevin immunoreactivity than meningioma samples, in both hevin bands. However no significant differences in the relative expression of the ~130 kDa and ~100 kDa bands (ratio) were detected between both types of tumors. These results are consistent with the well-known role of hevin and other ECM molecules in tumor invasion, and the proposal of hevin as a marker of glioblastoma and astrocytoma progression (He et al., 2016; Turtoi et al., 2012; Virga et al., 2018). Nevertheless, the fact that hevin expression is downregulated in other types of human cancers, has suggested it may play different roles in tumor biology, as both oncogene and tumor suppressor, based on tumor type (Gagliardi et al., 2017). Hevin's implication in cell adhesion, migration and proliferation highlight its role as a key protein in the regulation of tumor biology (Claeskens et al., 2000; Gagliardi et al., 2017; Sullivan and Sage, 2004).

Finally, we evaluated hevin expression pattern in CSF and blood samples. It has been shown that hevin protein is upregulated in the CSF of multiple sclerosis patients, while it is absent in normal CSF in the same study (Hammack et al., 2004). In contrast to that study, herein we demonstrate that two hevin forms are secreted into the CSF in subjects without psychiatric or neurological disorders. However, the origin of CSF hevin remains unknown; it may originate from brain's astrocytes and/or neurons, meninges or anywhere in the periphery and arrive by bloodstream. In addition, although we clearly detected hevin in blood plasma, none of the blood cell expressed it (platelets, erythrocytes and leucocytes), suggesting that hevin present in blood derives from other organs where hevin is expressed such as brain, endothelial cells of high endothelial venules (Girard and Springer, 1995, 1996), liver (Klingler et al., 2020), stomach (Klingler et al., 2020), small intestine (Klingler et al., 2020), oesophagus (Klingler et al., 2020), lung (Bendik et al., 1998; Klingler et al., 2020; Weaver et al., 2010), pancreas (Bendik et al., 1998; Weaver et al., 2010), heart (Bendik et al., 1998; Johnston et al., 1990; Weaver et al., 2011), spleen or kidney (Bendik et al., 1998; Soderling et al., 1997). Interestingly, it was noted that, while ~130 kDa band was present in both CSF and serum, the ~100 kDa band was absent and a ~90 kDa band was detected. This band may correspond to non-glycosylated form, as shown in deglycosylation assays. The different proportion of the two detected hevin forms in CSF and in blood suggests a different glycosylation/deglycosylation pattern and/or a different source of origin for hevin in each fluid (Barone et al., 2012; Karlsson et al., 2017).

The present study provides a thorough characterization of hevin protein expression by Western blot in *postmortem* human brain. The data herein presented reveal that there are two forms of hevin, both glycosylated, whose expression is higher in the membrane-enriched fraction compared to the cytosolic/soluble fraction. Furthermore, hevin expression is higher in the PFC in comparison to other brain regions. Hevin protein in PFC did not vary with age, nor sex. It is also shown that hevin is expressed in human CSF and blood plasma, but not in blood cells. Taken together, these results constitute an essential resource for future studies of hevin in brain tissue under pathological and non-pathological conditions.

ACKNOWLEDGEMENTS

Mass spectrometry analysis was performed by Kerman Aloria in the Proteomics Core Facility-SGIKER at the University of the Basque Country (member of ProteoRed-ISCIII).

AUTHOR CONTRIBUTIONS

A.E., L.C. and V.V. conceived the study. L.C. managed and provided the human post-mortem samples. A.N. and I.B. performed brain and blood fractionation. A.N. performed Western blot analysis. V.V. performed mouse brain dissection and mouse Western blot. A.N. and I.B. performed deglycosylation, proteolysis, immunoprecipitation assay. A.N. and A.E. participated in HPLC/MS analysis. L.C. provided key facilities, equipment and advice. A.E. coordinated the study. A.E.

Fig. 10. Influence of sex, age, PMD and storage time on hevin expression, and correlation between the two hevin isoforms. **(A, B)** Sex comparison between 11 females and 18 males of ~130 kDa **(A)** and ~100 kDa **(B)** hevin bands immunoreactivity (β-actin-normalized) in PFC total homogenates. Age **(C, D)**, *postmortem* delay **(E, F)** and storage time **(G, H)** correlation with the immunoreactivity of the ~130 kDa and ~100 kDa bands in total homogenate preparations obtained from human PFC of 29 control subjects. **(I)** Statistical linear correlation of hevin ~130 kDa and ~100 kDa bands immunoreactivities in PFC total homogenate pool of 29 subjects. IR: immunoreactivity. Statistical comparison between sexes was performed by two-tailed Student's *t*-test and correlation analyses by two-tailed Pearson's correlation test. No statistically significant linear correlations were observed (Pearson' *r* value and *p* value are shown in each correlation graph). Simple linear regression analysis showed correlation between the levels of the 130 kDa band with the 100 kDa band ($r = 0.8313$, $p \leq 0.0001$). Prefrontal cortex samples of 29 subjects were used and run in triplicate.

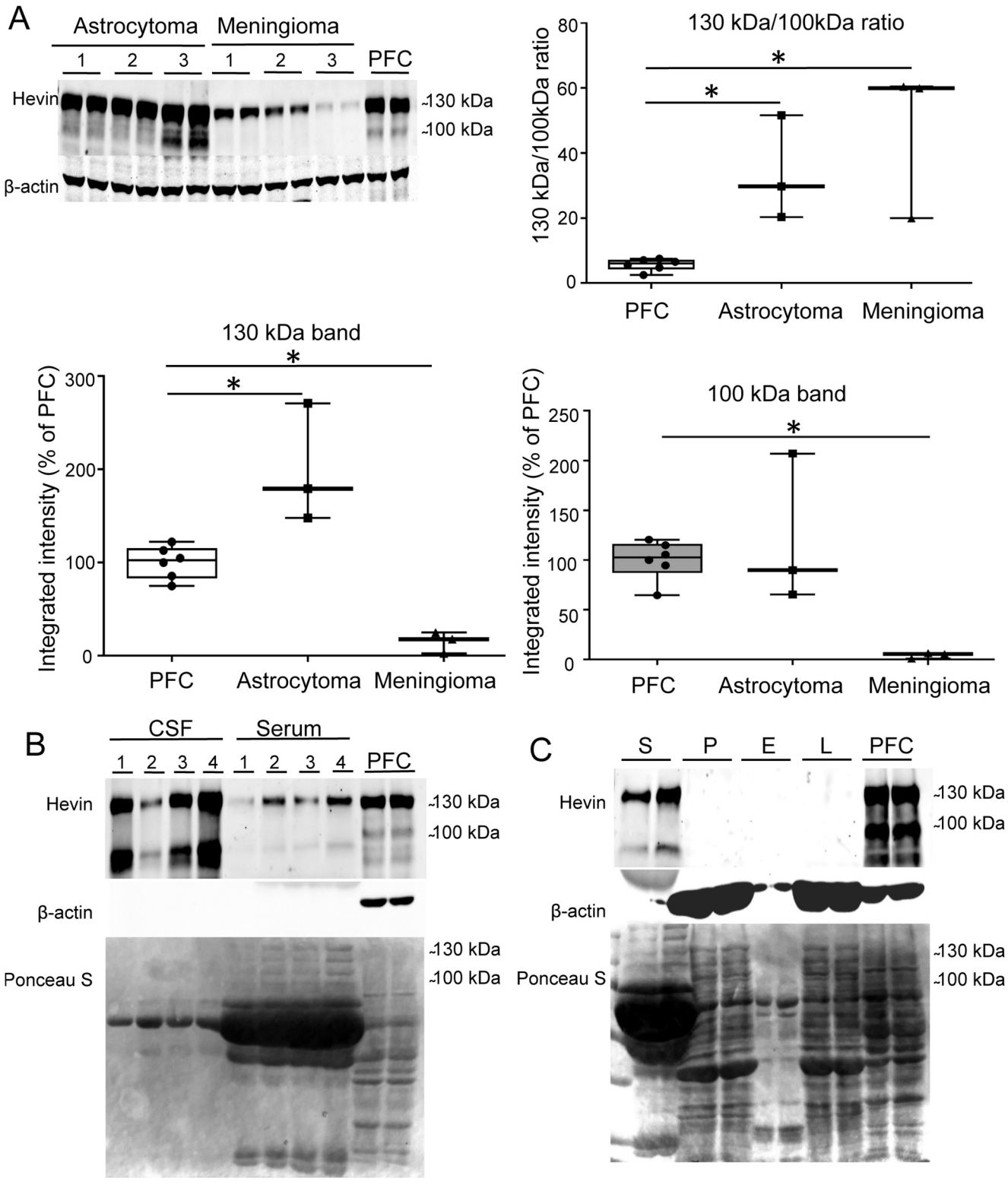

Fig. 11. Strong expression of hevin in astrocytoma, meningioma and CSF but not in any blood cell type. **(A)** Hevin immunoreactivity and corresponding β-actin-normalized quantifications in total homogenate preparations of 3 astrocytoma (18 μg), 3 meningioma (18 μg) and 6 PFC samples (15 μg). **(B)** Hevin immunoreactivity in 4 CSF (3.6 μg) and 4 serum samples (3.6 μg). **(C)** Hevin immunoreactivity in different blood fractions (S: serum, P: platelets, E: erythrocytes, L: leucocytes). The same amount of protein was loaded for each sample (37 μg) with the exception of leucocytes (8 μg, due to the sample concentration). β-Actin (only present in PFC and serum samples) and Ponceau S staining are also shown. Experiments were performed in duplicate. Representative Western blot image is shown. The statistical comparison between astrocytoma, meningioma and PFC was done by Mann–Whitney test. 130 kDa, PFC vs Astrocytoma: $U_{6,\,3} = 0.024$; 130 kDa, PFC vs Meningioma: $U_{6,\,3} = 0.024$; 100 kDa, Astrocytoma vs Meningioma: $U_{3,\,3} = 0.024$; 130 kDa / 100 kDa ratio, PFC vs Astrocytoma: $U_{6,\,3} = 0.024$; Astrocytoma vs Meningioma: $U_{3,\,3} = 0.024$. Samples were run in duplicate. Significance levels: $^{*}p < 0.05$. Data points are added to the box-and-whiskers plot.

and A.N. wrote the manuscript. All authors reviewed and approved the manuscript.

FUNDING SOURCES

This work was supported by The European Foundation for Alcohol Research (ERAB, EA 1819); Basque Government (IT1211-19); Fundación Vital (2018); Brain & Behavior Research Foundation (NARSAD, #17566), FP7 Marie Curie Actions Career Integration Grant (FP7-PEOPLE-2013-CIG #618807), Agence Nationale de la Recherche (ANR JCJC 2015). A. Nuñez-del Moral is recipient of a Predoctoral Fellowship from the Basque Government.

DECLARATIONS OF INTEREST

None.

REFERENCES

Barone R, Sturiale L, Palmigiano A, Zappia M, Garozzo D (2012) Glycomics of pediatric and adulthood diseases of the central nervous system. J Proteomics 75(17):5123–5139. https://doi.org/10.1016/j.jprot.2012.07.007.

Bendik I, Schraml P, Ludwig CU (1998) Characterization of MAST9/hevin, a SPARC-like protein, that is down-regulated in non-small cell lung cancer. Cancer Res 58(4):626–629.

Bornstein P (1995) Diversity of function is inherent in matricellular proteins: An appraisal of thrombospondin 1. J Cell Biol 130 (3):503–506.

Bornstein P (2009) Matricellular proteins: an overview. J Cell Commun Signaling 3(3–4):163–165. https://doi.org/10.1007/s12079-009-0069-z.

Bornstein P, Sage EH (2002) Matricellular proteins: Extracellular modulators of cell function. Curr Opin Cell Biol 14(5):608–616. https://doi.org/10.1016/S0955-0674(02)00361-7.

Bradford MM (1976) A rapid and sensitive method for the quantitation of microgram quantities of protein utilizing the principle of protein-dye binding. Anal Biochem 72(1):248–254. https://doi.org/10.1016/0003-2697(76)90527-3.

Brekken RA, Sullivan MM, Workman G, Bradshaw AD, Carbon J, Siadak A, Murri C, Framson PE, Sage EH (2004) Expression and characterization of murine hevin (SC1), a member of the SPARC family of matricellular proteins. J Histochem Cytochem 52 (6):735–748. https://doi.org/10.1369/jhc.3A6245.2004.

Brocos-Mosquera I, Nuñez Del Moral A, Morentin B, Meana JJ, Callado LF, Erdozain AM (2018) Characterisation of spinophilin immunoreactivity in postmortem human brain homogenates. Prog Neuro-Psychopharmacol Biol Psychiatry 81:236–242. https://doi.org/10.1016/j.pnpbp.2017.09.019.

Buerki RA, Horbinski CM, Kruser T, Horowitz PM, James CD, Lukas RV (2018) An overview of meningiomas. Future Oncol 14 (21):2161–2177. https://doi.org/10.2217/fon-2018-0006.

Claeskens A, Ongenae N, Neefs JM, Cheyns P, Kaijen P, Cools M, Kutoh E (2000) Hevin is down-regulated in many cancers and is a negative regulator of cell growth and proliferation. Br J Cancer 82 (6):1123–1130. https://doi.org/10.1054/bjoc.1999.1051.

Collins MA, An J, Peller D, Bowser R (2015) Total protein is an effective loading control for cerebrospinal fluid western blots. J Neurosci Methods 251:72–82. https://doi.org/10.1016/j.jneumeth.2015.05.011.

Correia SC, Carvalho C, Cardoso S, Moreira PI (2019) Post-translational modifications in brain health and disease. Biochim Biophys Acta (BBA) - Mol Basis Dis 1865(8):1947–1948. https://doi.org/10.1016/j.bbadis.2019.05.006.

Dalan AB, Gulluoglu S, Tuysuz EC, Kuskucu A, Yaltirik CK, Ozturk O, Ture U, Bayrak OF (2017) Simultaneous analysis of miRNA-mRNA in human meningiomas by integrating transcriptome: a relationship between PTX3 and miR-29c. BMC Cancer 17(1):207. https://doi.org/10.1186/s12885-017-3198-4.

Elu N, Osinalde N, Beaskoetxea J, Ramirez J, Lectez B, Aloria K, Rodriguez JA, Arizmendi JM, Mayor U (2019) Detailed dissection of UBE3A-mediated DDI1 ubiquitination. Front Physiol 10. https://doi.org/10.3389/fphys.2019.00534.

Eroglu C (2009) The role of astrocyte-secreted matricellular proteins in central nervous system development and function. J Cell Commun Signaling 3(3–4):167–176. https://doi.org/10.1007/s12079-009-0078-y.

Fathi A-R, Roelcke U (2013) Meningioma. Curr Neurol Neurosci Rep 13(4). https://doi.org/10.1007/s11910-013-0337-4.

Freeze HH, Kranz C (2010) Endoglycosidase and glycoamidase release of N-linked glycans. Curr Protoc Mol Biol 89(1):17. https://doi.org/10.1002/0471142727.mb1713as89.

Gagliardi F, Narayanan A, Mortini P (2017) SPARCL1 a novel player in cancer biology. Crit Rev Oncol/Hematol 109:63–68. https://doi.org/10.1016/j.critrevonc.2016.11.013.

Ge L, Zhuo Yi, Wu P, Liu Y, Qi L, Teng X, Duan Da, Chen P, Lu M (2020) Olfactory ensheathing cells facilitate neurite sprouting and outgrowth by secreting high levels of hevin. J Chem Neuroanat 104:101728. https://doi.org/10.1016/j.jchemneu.2019.101728.

Girard J-P, Springer TA (1995) Cloning from purified high endothelial venule cells of hevin, a close relative of the antiadhesive extracellular matrix protein SPARC. Immunity 2(1):113–123. https://doi.org/10.1016/1074-7613(95)90083-7.

Girard J-P, Springer TA (1996) Modulation of endothelial cell adhesion by hevin, an acidic protein associated with high endothelial venules. J Biol Chem 271(8):4511–4517. https://doi.org/10.1074/jbc.271.8.4511.

Gongidi V, Ring C, Moody M, Brekken R, Sage EH, Rakic P, Anton ES (2004) SPARC-like 1 regulates the terminal phase of radial glia-guided migration in the cerebral cortex. Neuron 41(1):57–69.

Gronseth E, Wang L, Harder DR, Ramchandran R (2018) The role of astrocytes in tumor growth and progression. Astrocyte Physiol Pathol. https://doi.org/10.5772/intechopen.72720.

Halim A, Rüetschi U, Larson G, Nilsson J (2013) LC–MS/MS characterization of O-glycosylation sites and glycan structures of human cerebrospinal fluid glycoproteins. J Proteome Res 12 (2):573–584. https://doi.org/10.1021/pr300963h.

Hambrock HO, Nitsche DP, Hansen U, Bruckner P, Paulsson M, Maurer P, Hartmann U (2003) SC1/Hevin: an extracellular calcium-modulated protein that binds collagen I. J Biol Chem 278(13):11351–11358. https://doi.org/10.1074/jbc.M212291200.

Hammack BN, Fung KYC, Hunsucker SW, Duncan MW, Burgoon MP, Owens GP, Gilden DH (2004) Proteomic analysis of multiple sclerosis cerebrospinal fluid. Mult Sclerosis (Houndmills, Basingstoke, England) 10(3):245–260. https://doi.org/10.1191/1352458504ms1023oa.

Hashimoto N, Sato T, Yajima T, Fujita M, Sato A, Shimizu Y, Shimada Y, Shoji N, Sasano T, Ichikawa H (2016) SPARCL1-containing neurons in the human brainstem and sensory ganglion. Somatosens Mot Res 33(2):112–117. https://doi.org/10.1080/08990220.2016.1197115.

He X, Lee B, Jiang Y (2016) Cell-ECM interactions in tumor invasion. In: Rejniak KA, editor. Systems biology of tumor microenvironment. Springer International Publishing. p. 73–91. https://doi.org/10.1007/978-3-319-42023-3_4.

Jones EV, Bouvier DS (2014) Astrocyte-secreted matricellular proteins in CNS remodelling during development and disease. Neural Plasticity. https://doi.org/10.1155/2014/321209 321209.

Johnston IG, Paladino T, Gurd JW, Brown IR (1990) Molecular cloning of SC1: A putative brain extracellular matrix glycoprotein showing partial similarity to osteonectin/BM40/SPARC. Neuron 4 (1):165–176. https://doi.org/10.1016/0896-6273(90)90452-L.

Karlsson I, Ndreu L, Quaranta A, Thorsén G (2017) Glycosylation patterns of selected proteins in individual serum and cerebrospinal fluid samples. J Pharm Biomed Anal 145:431–439. https://doi.org/10.1016/j.jpba.2017.04.040.

Klingler A, Regensburger D, Tenkerian C, Britzen-Laurent N, Hartmann A, Stürzl M, Naschberger E, Yao Y (2020) Species-, organ- and cell-type-dependent expression of SPARCL1 in human and mouse tissues. PLoS ONE 15(5):e0233422. https://doi.org/10.1371/journal.pone.0233422.

Kucukdereli H, Allen NJ, Lee AT, Feng A, Ozlu MI, Conatser LM, Chakraborty C, Workman G, Weaver M, Sage EH, Barres BA, Eroglu C (2011) Control of excitatory CNS synaptogenesis by astrocyte-secreted proteins Hevin and SPARC. Proc Natl Acad Sci 108(32):E440–E449. https://doi.org/10.1073/pnas.1104977108.

Lively S, Brown IR (2008a) Extracellular matrix protein SC1/hevin in the hippocampus following pilocarpine-induced status epilepticus. J Neurochem 107(5):1335–1346. https://doi.org/10.1111/j.1471-4159.2008.05696.x.

Lively S, Brown IR (2008b) Localization of the extracellular matrix protein SC1 coincides with synaptogenesis during rat postnatal development. Neurochem Res 33(9):1692–1700. https://doi.org/10.1007/s11064-008-9606-z.

Lively S, Brown IR (2010) The extracellular matrix protein SC1/Hevin localizes to multivesicular bodies in bergmann glial fibers in the adult rat cerebellum. Neurochem Res 35(2):315–322. https://doi.org/10.1007/s11064-009-0057-y.

Lively S, Moxon-Emre I, Schlichter LC (2011) SC1/hevin and reactive gliosis after transient ischemic stroke in young and aged rats. J Neuropathol Exp Neurol 70(10):913–929. https://doi.org/10.1097/NEN.0b013e318231151e.

Lively S, Ringuette MJ, Brown IR (2007) Localization of the extracellular matrix protein SC1 to synapses in the adult rat brain. Neurochem Res 32(1):65–71. https://doi.org/10.1007/s11064-006-9226-4.

Lloyd-Burton S, Roskams AJ (2012) SPARC-like 1 (SC1) is a diversely expressed and developmentally regulated matricellular protein that does not compensate for the absence of SPARC in the CNS. J Comp Neurol 520(12):2575–2590. https://doi.org/10.1002/cne.23029.

Maley F, Trimble RB, Tarentino AL, Plummer TH (1989) Characterization of glycoproteins and their associated oligosaccharides through the use of endoglycosidases. Anal Biochem 180(2):195–204. https://doi.org/10.1016/0003-2697(89)90115-2.

McKinnon PJ, Margolskee RF (1996) SC1: A marker for astrocytes in the adult rodent brain is upregulated during reactive astrocytosis. Brain Res 709(1):27–36. https://doi.org/10.1016/0006-8993(95)01224-9.

McKinnon PJ, McLaughlin SK, Kapsetaki M, Margolskee RF (2000) Extracellular matrix-associated protein Sc1 is not essential for mouse development. Mol Cell Biol 20(2):656–660. https://doi.org/10.1128/MCB.20.2.656-660.2000.

Mendis DB, Shahin S, Gurd JW, Brown IR (1996a) SC1, A SPARC-related glycoprotein, exhibits features of an ECM component in the developing and adult brain. Brain Res 713(1–2):53–63. https://doi.org/10.1016/0006-8993(95)01472-1.

Mendis DB, Ivy GO, Brown IR (1996b) SC1, a brain extracellular matrix glycoprotein related to SPARC and follistatin, is expressed by rat cerebellar astrocytes following injury and during development. Brain Res 730(1–2):95–106. https://doi.org/10.1016/S0006-8993(96)00440-4.

Mendis DB, Ivy GO, Brown IR (2000). Induction of SC1 mRNA encoding a brain extracellular matrix glycoprotein related to SPARC following lesioning of the adult rat forebrain. Neurochem Res, 25(12), 1637–1644. PubMed. https://doi.org/10.1023/a:1026626805612.

Mongrédien R, Erdozain AM, Dumas S, Cutando L, del Moral AN, Puighermanal E, Rezai Amin S, Giros B, Valjent E, Meana JJ, Gautron S, Callado LF, Fabre V, Vialou V (2019) Cartography of hevin-expressing cells in the adult brain reveals prominent expression in astrocytes and parvalbumin neurons. Brain Struct Funct 224(3):1219–1244. https://doi.org/10.1007/s00429-019-01831-x.

Murphy-Ullrich JE, Sage EH (2014) Revisiting the matricellular concept. Matrix Biol 37:1–14. https://doi.org/10.1016/j.matbio.2014.07.005.

Nilsson J, Rüetschi U, Halim A, Hesse C, Carlsohn E, Brinkmalm G, Larson G (2009) Enrichment of glycopeptides for glycan structure and attachment site identification. Nat Methods 6(11):809–811. https://doi.org/10.1038/nmeth.1392.

Purcell AE, Jeon OH, Zimmerman AW, Blue ME, Pevsner J (2001) Postmortem brain abnormalities of the glutamate neurotransmitter system in autism. Neurology 57(9):1618–1628. https://doi.org/10.1212/WNL.57.9.1618.

Rajalingam D, Kathir KM, Ananthamurthy K, Adams PD, Kumar TKS (2008) A method for the prevention of thrombin-induced degradation of recombinant proteins. Anal Biochem 375(2):361–363. https://doi.org/10.1016/j.ab.2008.01.014.

Risher WC, Patel S, Kim IH, Uezu A, Bhagat S, Wilton DK, Pilaz L-J, Singh Alvarado J, Calhan OY, Silver DL, Stevens B, Calakos N, Soderling SH, Eroglu C (2014) Astrocytes refine cortical connectivity at dendritic spines. ELife, 3, e04047. https://doi.org/10.7554/eLife.04047.

Shevchenko A, Wilm M, Vorm O, Mann M (1996) Mass spectrometric sequencing of proteins from silver-stained polyacrylamide gels. Anal Chem 68(5):850–858. https://doi.org/10.1021/ac950914h.

Singh S, Stogsdill J, Pulimood N, Dingsdale H, Kim Y, Pilaz L-J, Kim I, Manhaes A, Rodrigues W, Pamukcu A, Enustun E, Ertuz Z, Scheiffele P, Soderling SH, Silver D, Ji R-R, Medina A, Eroglu C (2016) Astrocytes assemble thalamocortical synapses by bridging Nrx1α and NL1 via Hevin. Cell 164(1-2):183–196. https://doi.org/10.1016/j.cell.2015.11.034.

Soderling JA, Reed MJ, Corsa A, Sage EH (1997) Cloning and expression of murine SC1, a gene product homologous to SPARC. J Histochem Cytochem 45(6):823–835. https://doi.org/10.1177/002215549704500607.

Sullivan MM, Barker TH, Funk SE, Karchin A, Seo NS, Höök M, Sanders J, Starcher B, Wight TN, Puolakkainen P, Sage EH (2006) Matricellular Hevin regulates decorin production and collagen assembly. J Biol Chem 281(37):27621–27632. https://doi.org/10.1074/jbc.M510507200.

Sullivan MM, Sage EH (2004) Hevin/SC1, a matricellular glycoprotein and potential tumor-suppressor of the SPARC/BM-40/Osteonectin family. Int J Biochem Cell Bio 36(6):991–996. https://doi.org/10.1016/j.biocel.2004.01.017.

Trinidad JC, Barkan DT, Gulledge BF, Thalhammer A, Sali A, Schoepfer R, Burlingame AL (2012) Global identification and characterization of both O-GlcNAcylation and phosphorylation at the murine synapse. Mol Cell Proteomics: MCP 11(8):215–229. https://doi.org/10.1074/mcp.O112.018366.

Turtoi A, Musmeci D, Naccarato AG, Scatena C, Ortenzi V, Kiss R, Murtas D, Patsos G, Mazzucchelli G, De Pauw E, Bevilacqua G, Castronovo V (2012) Sparc-like protein 1 is a new marker of human glioma progression. J Proteome Res 11(10):5011–5021. https://doi.org/10.1021/pr3005698.

Vialou V, Robison AJ, Laplant QC, Covington 3rd HE, Dietz DM, Ohnishi YN, Mouzon E, Rush AJ, Watts EL, Wallace DL, Iñiguez SD, Ohnishi YH, Steiner MA, Warren BL, Krishnan V, Bolaños CA, Neve RL, Ghose S, Berton O, Tamminga CA, Nestler EJ (2010) DeltaFosB in brain reward circuits mediates resilience to stress and antidepressant responses. Nat Neurosci 13(6):745–752. https://doi.org/10.1038/nn.2551.

Virga J, Bognár L, Hortobágyi T, Zahuczky G, Csősz É, Kalló G, Tóth J, Hutóczki G, Reményi-Puskár J, Steiner L, Klekner A (2018) Tumor grade versus expression of invasion-related molecules in astrocytoma. Pathol Oncol Res 24(1):35–43. https://doi.org/10.1007/s12253-017-0194-6.

Weaver MS, Workman G, Cardo-Vila M, Arap W, Pasqualini R, Sage EH (2010) Processing of the matricellular protein hevin in mouse brain is dependent on ADAMTS4. J Biol Chem 285(8):5868–5877. https://doi.org/10.1074/jbc.M109.070318.

Weaver M, Workman G, Schultz CR, Lemke N, Rempel SA, Sage EH (2011) Proteolysis of the matricellular protein hevin by matrix

metalloproteinase-3 produces a SPARC-like fragment (SLF) associated with neovasculature in a murine glioma model. J Cell Biochem 112(11):3093–3102. https://doi.org/10.1002/jcb.v112.1110.1002/jcb.23235.

Yang C, Rahimpour S, Yu ACH, Lonser RR, Zhuang Z (2013) Regulation and dysregulation of astrocyte activation and implications in tumor formation. Cell Mol Life Sci: CMLS 70 (22):4201–4211. https://doi.org/10.1007/s00018-013-1274-8.

Yin GN, Lee HW, Cho J-Y, Suk K (2009) Neuronal pentraxin receptor in cerebrospinal fluid as a potential biomarker for neurodegenerative diseases. Brain Res 1265:158–170. https://doi.org/10.1016/j.brainres.2009.01.058.

Zhang P, Lu H, Peixoto RT, Pines MK, Ge Y, Oku S, Siddiqui TJ, Xie Y, Wu W, Archer-Hartmann S, Yoshida K, Tanaka KF, Aricescu AR, Azadi P, Gordon MG, Sabatini BL, Wong ROL, Craig AM (2018) Heparan sulfate organizes neuronal synapses through neurexin partnerships. Cell 174(6):1450–1464.e23. https://doi.org/10.1016/j.cell.2018.07.002.

Zhurov V, Stead JDH, Merali Z, Palkovits M, Faludi G, Schild-Poulter C, Anisman H, Poulter MO, Yaragudri VK (2012) Molecular pathway reconstruction and analysis of disturbed gene expression in depressed individuals who died by suicide. PLoS ONE 7(10):e47581. https://doi.org/10.1371/journal.pone.0047581.

APPENDIX A. SUPPLEMENTARY DATA

Supplementary data to this article can be found online at https://doi.org/10.1016/j.neuroscience.2021.05.017.

(Received 12 March 2021, Accepted 13 May 2021)
(Available online 24 May 2021)

ANNEX 2

A novel role for the matricellular protein hevin in alcohol use disorder

Amaia Nuñez-delMoral, Paula C. Bianchi, Iria Brocos-Mosquera, Augusto Anesio, Paula Palombo, Rosana Camarini, Fabio C .Cruz, Luis F. Callado, Vincent Vialou, Amaia M. Erdozain

ABSTRACT

Astrocytic-secreted matricellular proteins have been shown to influence various aspects of synaptic function. More recently, they have been found altered in animal models of psychiatric disorders such as drug addiction. Hevin, a matricellular protein highly expressed in the adult brain, has been implicated in resilience to stress and antidepressant treatment suggesting a role in motivated behaviors. To address the possible role of hevin in drug addiction, we quantified its expression in human postmortem brains and in animal models of alcohol abuse. Hevin mRNA and protein expression were analyzed in postmortem human brain of subjects with an antemortem diagnosis of alcohol use disorder (AUD, n = 25) and respective controls (n=25). Overall, all the studied human brain regions (prefrontal cortex, hippocampus, caudate nucleus and cerebellum) showed an increase in hevin levels either at mRNA or/and protein levels. To test if this alteration was the result of alcohol exposure or indicative of a susceptible factor to alcohol consumption, mice were exposed to different regimens of intraperitoneal alcohol administration. Hevin protein expression was increased in nucleus accumbens (NAc) after alcohol withdrawal and reinstatement. The possible role of hevin on AUD was determined using an RNA interference strategy to downregulate hevin expression in NAc astrocytes, which led to increased ethanol consumption. Additionally, ethanol reinstatement after withdrawal increased hevin levels in blood plasma, suggesting that hevin could be used as a biomarker of alcohol abuse. Altogether, these results support a novel role for hevin in the neurobiology of AUD.

INTRODUCTION

Alcohol use disorder (AUD) is one of the psychiatric diseases that most negatively affect global health, society, and the economy [1,2]. Ethanol is considered the most dangerous and harmful drug of abuse with an estimated 5.1% of the total disease burden (*in terms of disability-adjusted life years*) and 5.3% of deaths worldwide [3,4]. AUD is characterized by compulsion to take or seek alcoholic beverages, craving, withdrawal symptoms, tolerance and relapse [5,6]. Chronic ethanol consumption alters the activity and the long-term function of brain regions such as the prefrontal cortex (PFC), hippocampus (HIP), striatum, amygdala (AMY) or cerebellum (CB), which result in cognitive impairments, learning and memory deficits, and a shift from positive to negative reinforcement [7,8]. An essential aspect of AUD is the high rate of relapse, depicted as recurrent abstinence periods followed by reinstatement of the consumption. This pathological pattern of alcohol consumption might take part in the progression and deepening of the disorder [9–11]. Ethanol's effects on the brain involve alterations in synaptic plasticity and morphological reorganization of circuits implicated in reward, stress and executive functions. Although the contribution of various molecular mediators has been recognized, including monoamines, neuropeptides, and stress hormones [8], no key genetic switch mediating significant traits of the AUD phenotype has been characterized.

Astrocytes play critical roles in central nervous system homeostasis and are implicated in the pathogenesis of neurological and psychiatric conditions, including drug dependence [12,13]. In regard to AUD, activation of mouse cortical astrocytes by chemogenetic approaches increases alcohol consumption and alters its locomotor and sedative effects [14]. Likewise, activation of the astrocytes of the nucleus accumbens (NAc) potentiates the rewarding properties of alcohol and decreases alcohol self-administration after prolonged abstinence [15]. Chronic alcohol exposure profoundly modifies the transcriptomic profile of astrocytes *in vitro*, *in utero* and *in vivo*, with changes in the expression of genes involved in cellular differentiation, metabolism, gene transcription, extracellular matrix composition and synaptogenesis [16–19]. Astrocytic synaptogenic factors promote excitatory synapse formation, maturation, and refinement during development [12,20–24]. In particular, it has been shown that in prenatal and postnatal animal models of AUD, hevin, a secreted synaptogenic astrocytic factor, is induced [18,25].

The matricellular protein hevin (SPARCL1 , SC1, ECM2 or Mast9) specifically promotes the formation and maintenance of thalamocortical excitatory synapses, by linking presynaptic neurexin-1α and the postsynaptic neuroligin-1B [21,22,24,26]. It is highly expressed in human and mouse adult brain [27–32], in astrocytes and parvalbumin interneurons, and in a restricted number of other neuronal subpopulations, including glutamatergic neurons in cortical and subcortical regions [30]. Importantly, hevin has been implicated in resilience to stress, showing an antidepressant-like effect in a model of social defeat [33].

Considering the effects of alcohol on the brain limbic system, and the role of hevin in structural and synaptic plasticity, the pattern of hevin expression was assessed in human cortico-limbic structures associated with AUD. Additionally, we assessed the status of hevin in brain and blood of mice exposed to different regimens of intraperitoneal alcohol administration.

MATERIALS AND METHODS

Human samples

Human samples were obtained at autopsy in the Basque Institute of Legal Medicine (Bilbao, Spain). Brain dissections were performed at the moment of the autopsy for the collection of PFC, HIP, caudate nucleus (CAU) and CB samples, which were immediately stored at -70°C until assay. A blood toxicological study by the National Institute of Toxicology (Madrid), using different standard methods (including radioimmunoassay, enzymatic immunoassay, high-performance liquid chromatography and gas chromatography-mass spectrometry) determined the presence or not of ethanol, antidepressants, antipsychotics and psychotropic drugs at the time of death. The study included 75 subjects divided into three experimental groups: 25 subjects with an antemortem diagnosis of AUD, 25 subjects with an antemortem diagnosis of major depression and 25 control subjects (with no antemortem history of any neuropsychiatric disease). The antemortem diagnosis were performed by psychiatrists based on DMS-IV and ICD-10 criteria. The depression group was included as a control of disease-specific changes. Each subject with AUD was matched by age, sex and PMD (postmortem delay) with a control and depression subject (summarized in Table 1); none of these parameters was statistically different between groups ($p > 0.05$, one-way ANOVA). A full description of the demographic characteristics of all the subjects is shown in Supplementary Table 1. Samples from matched AUD, depression and control subjects were processed and tested in parallel. The study was performed in compliance with legal policy and ethical review boards for postmortem brain studies.

Animals and treatments

All experiments were performed in strict conformity with the European Union laws and policies for use of animals in neuroscience research (European Committee Council Directive 2010/63/EU). C57BL6J mice were housed in groups of five animals per cage under the standard condition: 23°C and a 12 h light/dark cycle with food and water provided *ad libitum*. Experiments were performed on 2 to 4 months C57BL/6J mice.

Four ethanol regimens were performed in C57BL/6J mice (Fig. 3A) [34]. Mice were chronically treated either with saline or ethanol for 13 days, not injected for the following 3 days (withdrawal), and ultimately, given a challenge dose of saline or ethanol (reinstatement). The four resulting experimental groups were as follows: 1) saline – saline (S-S), 2) saline – ethanol (S-E), 3) ethanol-saline (E-S) and 4) ethanol-ethanol (E-E). The dose of 1.75 g ethanol/kg injected i.p. or a 0.9% NaCl saline solution i.p. were used [35]. Mice were killed 24h after the last injection, and brain dissections were performed immediately after. Five brain areas were collected with bilateral punches: frontal cortex (FC), amygdala (AMY), hippocampus (HIP), dorsal striatum (CPu) and nucleus accumbens (NAc). Blood was collected in EDTA-coated tubes and centrifuged. All the samples were stored at –70°C until their preparation for western blot assays.

For hevin downregulation in the astrocytes of the NAc, mice were anesthetized with an i.p. mixture containing 100 mg/kg of ketamine and 10 mg/kg of xylazine i.p.), placed in a stereotaxic frame, and injected with AAV2.5-GFAP-EmGFP-miR-hevin (9,4.1012vg/ml) or the control viral vector AAV5.GFAP.eGFP.WPRE.hGH (9.1x10e12 vg/ml, University of North Carolina, USA). Coordinates used to target NAc were: anteroposterior: +1,6, mediolateral: +1.45, dorsoventral: -4.3,

with an angle of 10° from the midline. 0.5 µl of the virus were injected at a rate of 0.1 µl/min. Behavioral tests were performed 3 weeks after surgery and monitored regularly. The correct injection site and the expression of the transgene were confirmed by immunohistochemistry.

Sample preparation

For Western blot experiments both human and animal brain samples were processed as previously described previously [31], with the following modifications: 1) in human brain samples the nuclear fraction was removed for all of the total homogenates, and 2) in mice brain punches the homogenization was performed by sonication (QSONICA Q55), due to the small sample volume. Protein content was measured by the Bradford method [36] and stored at -70°C until analyzed by Western blot. Regarding mouse plasma samples, they were homogenized in buffer supplemented with protease and phosphatase inhibitors (5mM Tris-HCl pH 7.4, 50 µL/g of Sigma protease inhibitor Cocktail, 5mM Na_3VO_4 and 10 mM NaF) before sonication (QSONICA Q55) and stored at -70°C until analyzed by Western blot.

Real-time reverse transcription polymerase chain reaction (RT-qPCR)

mRNA extraction, cDNA synthesis and qPCR of the four human brain regions were performed as previously described [37] with minor modifications. The qPCR reactions were performed on a StepOne™ system using TaqMan™ Fast Universal Master Mix (Thermo Fisher) reactive and the specific gene probes for hevin, glyceraldehyde 3-phosphate dehydrogenase (GAPDH) and ribosomal protein S13 (RPS13) (TaqMan® gene expression assay Hs00949886_m1, Hs99999905_m1 and Hs01945436_u1, respectively). The hevin's mRNA expression amounts were normalized to the expression of the GAPDH and RPS13 housekeeping genes and with a reference sample (pool of all samples for each brain region); and determined by the comparative Ct method (ΔΔCt), where ΔΔCt = $(Ct\ (hevin)_{sample} - Ct\ (housekeeping)_{sample})$-$(Ct\ (hevin)_{reference\ sample} - Ct\ (housekeeping)_{reference\ sample})$ using StepOne™ Software v2.1. A negative internal control (mQH_2O) was also included. The qPCRs were run in triplicates for each cDNA.

Western blot

Western blot experiments were performed as previously described [31]. In human and mouse brain samples hevin immunoreactivity was normalized by β-actin signal. For mouse plasma samples, the Ponceau S staining confirmed the equal amount of protein load. In all cases, a standard pool of total homogenate (from human or mouse origin, respectively) was used as an external reference sample. The primary and secondary antibodies used for the detection of hevin and β-actin proteins are detailed in the Supplementary Table 2.

Intermittent ethanol access schedule (IEA) in hevin knockdown mice

In order to measure the alcohol intake in the active period of the mice, one week before starting the experiment, their light cycle was changed to a light and dark cycle of 12 h, with water and food *ad libitum*. Lights were off at 9 a.m. and on at 9 p.m., starting the experiment at 9 a.m., when both hevin knockdown (KD, n=7) and control (n=7) mice were individually housed. Mice were first habituated to two bottles of water for 3 days. IEA was performed for a total of 18 days [38]; water and ethanol bottles were placed every day at 9 a.m. and removed at 5 p.m. in each cage. The consumed volume was measured after 4 h and 8 h of the beginning of the experiment, and the bottles' position was switched every day to avoid possible bottle side preference bias. Ethanol concentration

(w/v) was increased every 3 days in order to induce an alcohol intake behavior. The beginning ethanol concentration was 5%, followed by 10%, 15%, 20%, 3 days of ethanol withdrawal and a 10% of ethanol, as the reinstatement concentration. Ethanol solutions were prepared by mixing 96% (v/v) ethanol with tap water. Mice's weight was measured every 3 days. Ethanol preference (percentage of ethanol consumed from the total volume for each measurement; > 50% was considered as the preference for ethanol) and consumption (g ethanol/kg mouse ingested for each measurement) were calculated for each mouse.

Immunohistochemistry

Mice were anesthetized with a lethal dose of pentobarbital at 150 mg/kg i.p. and perfused intracardially with 4% paraformaldehyde in a phosphate-buffered solution. Brains were removed and stored at 4°C in 4% paraformaldehyde until use. Brains were cut on a vibratome in coronal sections of 40 µm. Slices were incubated in a blocking buffer containing 0.2% gelatin and 0.25% triton in PBS for 1 hour at room temperature, then treated with antibodies against hevin (R&D mSPARCL1 AF2836, 1:2000) or anti-GFP (A010-pGFP-5, Badrilla, 1:2000) overnight at 4°C. After washing, slices were incubated with a Cyanine Cy™3 conjugated secondary antibody for 2 hours at room temperature (Jackson Immunoresearch, USA). Slices were incubated with DAPI (4',6-diamidino-2-fenilindol, 1:15000, Sigma-Aldrich, D9542) before mounting with Fluoromount-G (20 min at RT). All the slices were scanned on a NanoZoomer 2.0-HT (Hamamatsu Photonics, Hamamatsu City, Japan) as previously described [30].

Statistical analysis

Statistical analysis was performed using GraphPad Prism 9®. Briefly, a comparison of mRNA and hevin protein levels in the human brain between the AUD, depression and control groups was performed using one-way ANOVA followed by Dunnett's multiple comparisons test. Taking into account the large sample size (n=25) and the high inter-subject variability in human brain morphology and configuration, data was considered normally distributed [39,40]. Data obtained in animal studies did not pass the D'Agostino and Pearson normality test and F-test for the equality of variances. As a result, non-parametric statistical tests were used in all these cases. More specifically, biochemical analyses in mouse brains and plasma were performed using the Kruskal-Wallis test followed by Dunn's multiple comparisons test. Differences between hevin KD mice and controls in ethanol preference and consumption were calculated by the Mann-Whitney test and the Friedman test was used for ethanol concentration data. Results were considered statistically significant when the p-value was <0.05. Significant differences are symbolized by asterisk, where if $p < 0.05$ (*), $p < 0.01$ (**), $p < 0.001$ (***) or $p < 0.0001$ (****).

RESULTS

Hevin expression in postmortem human brain of subjects with AUD

Hevin mRNA and protein expression levels were measured in four human brain areas (PFC, HIP, CAU and CB) from 75 subjects. Individuals were divided according to their antemortem psychiatric history: AUD (n = 25), depression (n = 25) and control (n = 25) groups. Interestingly, in all the studied brain areas an increase in hevin's mRNA was detected in the AUD group compared to the controls (PFC: 59% increase, $p = 0.0028$; HIP: 72% increase, $p = 0.0058$; CAU: 92% increase, $p = 0.0028$ and CB: 70% increase, $p = 0.0344$). However, no significant differences were detected between the depression and the control groups (Fig. 1A-D).

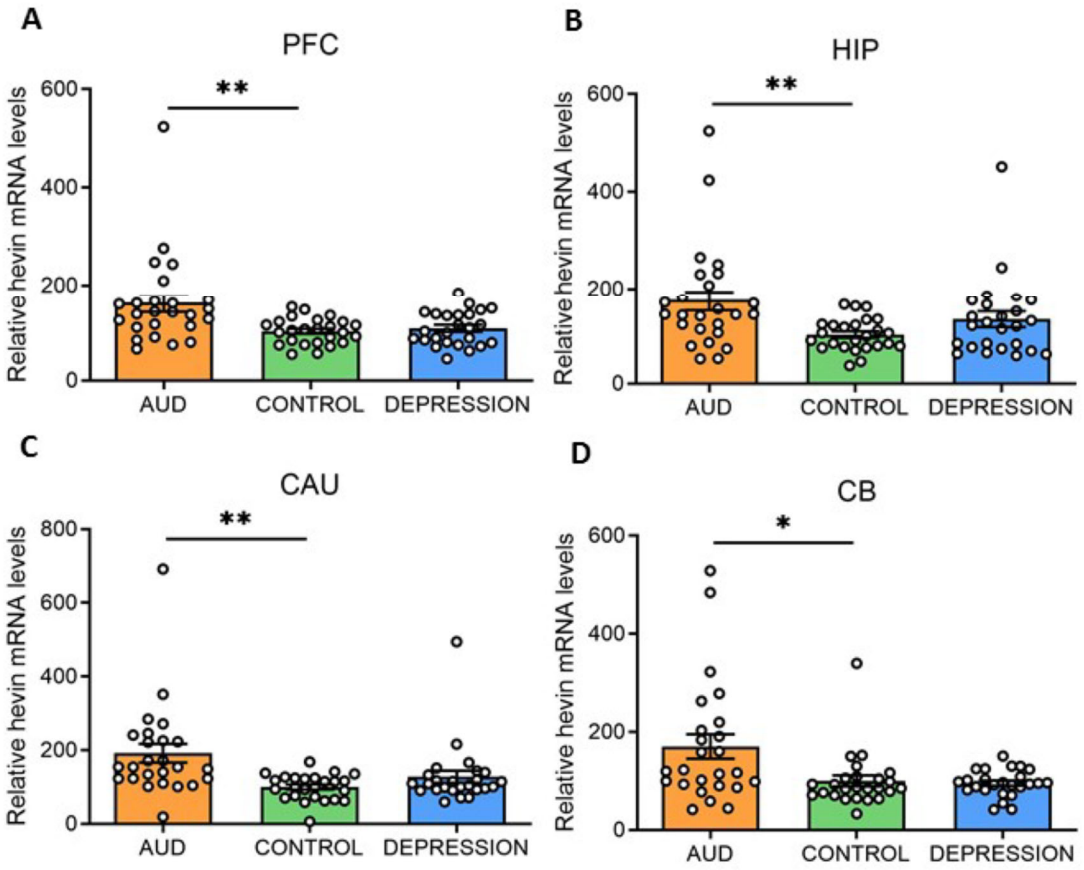

Fig. 1. mRNA expression of hevin in postmortem human brain of AUD subjects. Relative hevin mRNA levels quantified by RT-qPCR in human postmortem samples from subjects with AUD, depression and controls in PFC (A), HIP (B), CAU (C) and CB (D). n=25 per group. One- way ANOVA followed by Dunnett's post hoc test was used for the comparison (*p< 0.05, **p< 0.01). Samples were run in triplicate. The quantification is represented in box-and-whiskers plots, where "box" shows the median and the 25th and 75th percentile and the "whiskers" depict the 5th and 95th percentile. Dots represent the average value of each individual in the performed experiments.

To further elucidate whether hevin mRNA increase paralleled an enhancement in the translation process, the protein expression levels were also determined. Both previously described ~130 kDa and ~100 kDa hevin bands [22,31,41,42] were measured in total homogenates of PFC, HIP, CAU and CB. In accordance to the alterations observed in hevin's mRNA, an increase in the ˜130 kDa and ˜100 kDa forms was detected in PFC and CB of the AUD subjects in comparison to controls (PFC: 25% increase in ~130 kDa band, p = 0.0015 and 46% increase in ~100 kDa band, p <0.0001; CB: 32% increase in ~130 kDa band, p = 0.0344 and 38% increase in ~100 kDa band, p = 0,013) (Fig. 2A,D). In the HIP, only the ˜100 kDa band was significantly increased in AUD (56% increase in ~100 kDa band, p = 0.00384), although the ˜130 kDa band showed a similar trend (Fig. 2B). In contrast, in the CAU no significant differences were observed between both groups in the expression of any of the bands (Fig. 2C). Finally, the depression group did not show significant differences in the levels of protein expression in comparison to the control group in any brain area, as observed for the mRNA levels (Fig. 2A-D).

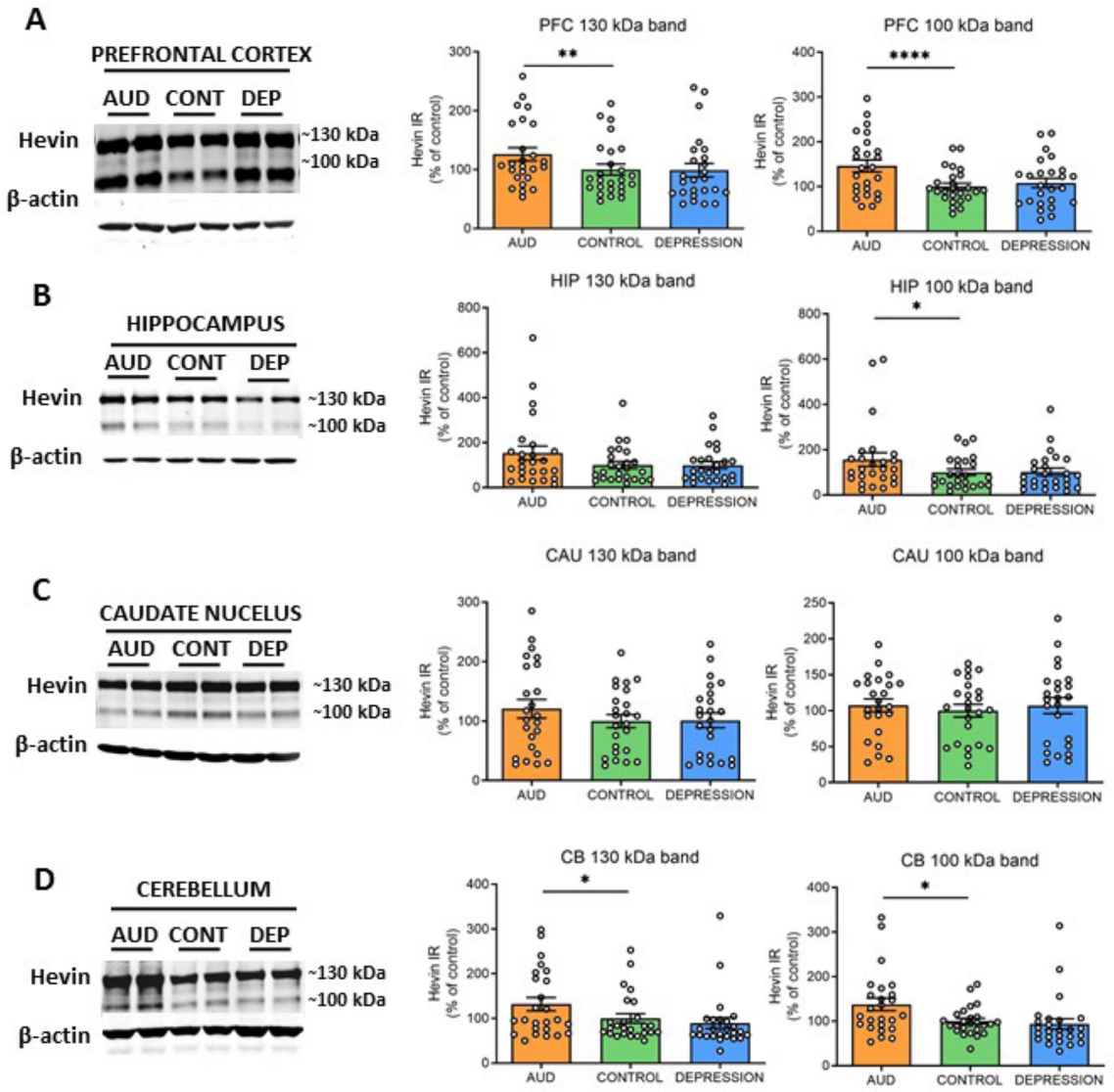

Fig. 2. Protein expression of hevin in postmortem human brain of AUD subjects. Hevin protein expression in human postmortem samples from subjects with AUD, depression and controls in PFC (A), HIP (B), CAU (C) and CB (D). Representative western blot images for each brain region are shown, along with the graphics representing the actin-normalized immunoreactivity (IR) of both ˜130 kDa and ˜100 kDa hevin bands. n=25 per group. One- way ANOVA followed by Dunnett's post hoc test was used for the comparison (*p< 0.05, **p< 0.01, ****p< 0.0001). Experiments were performed in triplicate. The quantification is represented in box-and-whiskers plots, where "box" shows the median and the 25th and 75th percentile and the "whiskers" depict the 5th and 95th percentile. Dots represent the average value of each individual in the performed experiments.

Hevin protein expression in mouse brain after ethanol administration

Hevin expression was evaluated in several mice brain regions (FC, AMY, HIP, CPu and NAc) after different ethanol regimens. Mice were intraperitoneally injected with ethanol (13 days) followed by a withdrawal period (3 days) and a challenge dose of ethanol or saline. In contrast to the human brain, mice did not express the ˜100 kDa

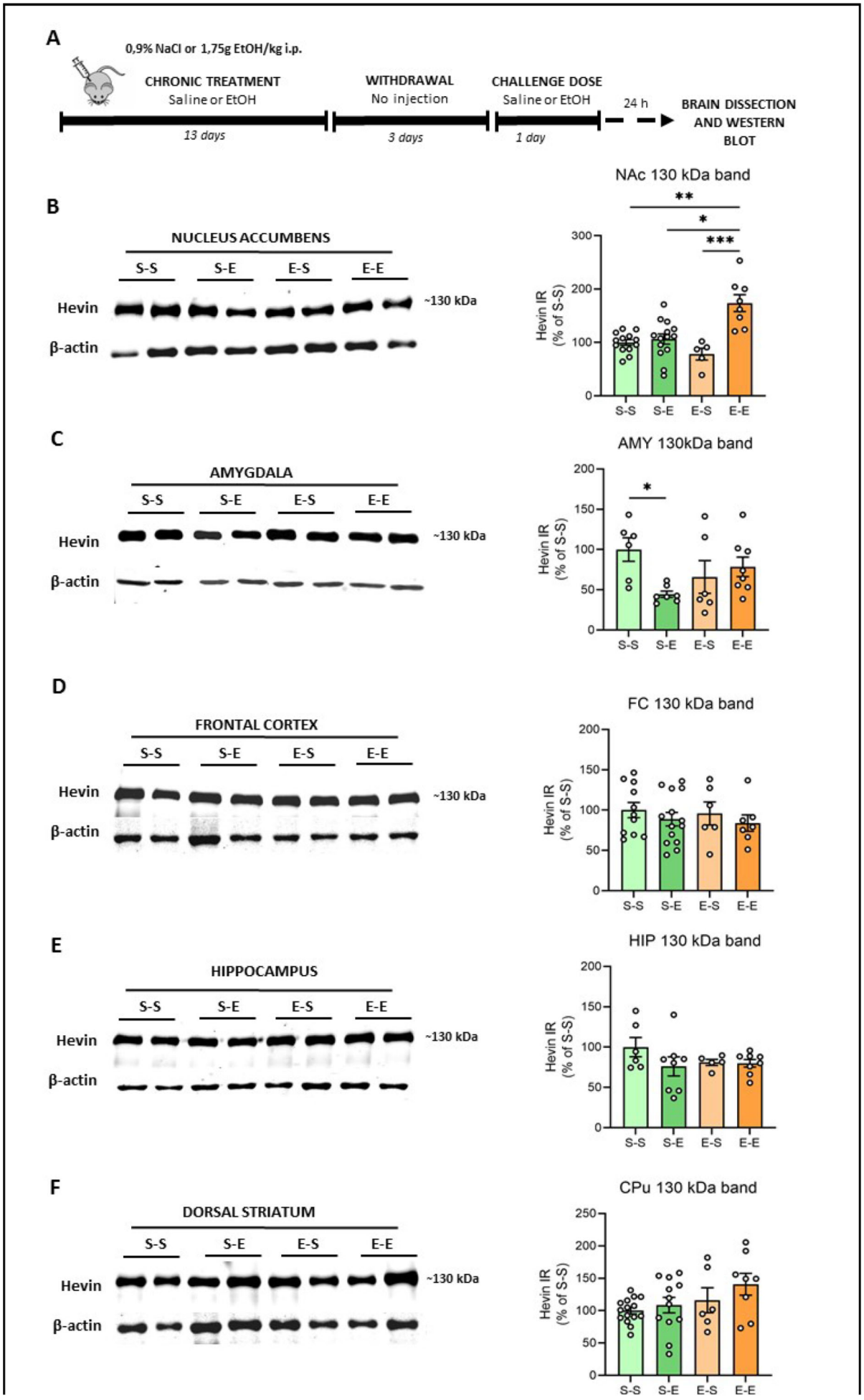
A
0,9% NaCl or 1,75g EtOH/kg i.p.
CHRONIC TREATMENT
Saline or EtOH
13 days
WITHDRAWAL
No injection
3 days
CHALLENGE DOSE
Saline or EtOH
1 day
24 h
BRAIN DISSECTION AND WESTERN BLOT
B
NUCLEUS ACCUMBENS
S-S S-E E-S E-E
Hevin
β-actin
~130 kDa
NAc 130 kDa band
Hevin IR (% of S-S)
C
AMYGDALA
AMY 130kDa band
D
FRONTAL CORTEX
FC 130 kDa band
E
HIPPOCAMPUS
HIP 130 kDa band
F
DORSAL STRIATUM
CPu 130 kDa band

Fig. 3. Hevin protein expression in the brain of mice exposed to different regimen of ethanol. A) Schematic figure showing the four ethanol treatments performed. (B-F) Representative western blot images for each brain region are shown, along with the graphics representing the actin-normalized immunoreactivity (IR) of ˜130 kDa band in the four administered ethanol treatments (S-S: saline – saline, S-E: saline – ethanol, E-S: ethanol-saline and E-E: ethanol-ethanol) in the following brain regions: B) *nucleus accumbens,* NAc, C) amygdala, AMY, D) frontal cortex, FC, E) hippocampus, HIP, and F) dorsal striatum, CPu. n=5-15 per group. Kruskal-Wallis followed by Dunn's post hoc test was used for the comparison (*p< 0.05, **p< 0.01, ***p< 0.001). Experiments were performed in triplicate. The quantification is represented in box-and-whiskers plots, where "box" shows the median and the 25th and 75th percentile and the "whiskers" depict the 5th and 95th percentile. Dots represent the average value of each individual in the performed experiments.

band, or its immunoreactive signal was too low to be analyzed, as it has been described before [42,43]. Therefore, the present data correspond only to the ˜130 kDa band. Twenty-four h after an ethanol challenge in animals treated repeatedly with ethanol injections, an increase in hevin protein expression was observed in the NAc in comparison to the other 3 treatments (saline, one single dose of ethanol and withdrawal period after repeated injections) (74% increase vs S-S, p = 0.0041; 68% increase vs S-E, p = 0.0232 and 98% increase vs E-S, p = 0.0007) (Fig. 3A). Acute ethanol injection reduced hevin protein levels in AMY (54% decrease vs S-S, p = 0.0471 (Fig. 3B). No significant changes were observed in the other brain regions.

Hevin protein expression in mouse plasma after ethanol treatment.

Hevin expression levels were also analyzed in mouse plasma after chronic ethanol treatment. The 100 kDa band was not identifiable in these samples. Concerning the 130 kDa band, ethanol challenge after withdrawal produced higher levels of hevin in comparison to the saline challenge after withdrawal (65% increase vs E-S, p=0.0396) (Fig. 4.). An additional band with a molecular weight around ˜47 kDa was also analyzed due to the high immunoreactivity signal of this band in most of the samples. Plasma showed high variability in the expression levels of the 47 kDa band among mice, with some of them expressing high levels of this form (i.e. two of the E-S group), and almost undetectable levels for others. As a result, no differences were detected in hevin expression levels between the ethanol treatments for the 47 kDa band (Fig. 4.). In order to assess if the expression of the lower band was the result of the cleavage of the 130 kDa band, the ratio of the immunoreactivity of both bands was also calculated (130 kDa/ 47 kDa). No significant differences were detected between treatment groups in the 130 kDa/ 47 kDa ratio (Fig. 4.).

Behavioral consequences of hevin downregulation in NAc astrocytes on ethanol consumption

To test the role of hevin in the long-term adaptation to ethanol, we downregulated hevin expression in NAc using an RNA interference strategy, and tested the consequences of this cell-specific and regional downregulation of hevin on the consumption of ethanol in an intermittent ethanol access schedule (IEA). The downregulation of hevin in the astrocytes of the NAc was verified by the immunohistochemistry of hevin protein and GFP in the mice's brain slices after the IEA schedule was completed. Indeed, immunohistochemistry assays revealed a complete deletion of hevin expression in

NAc astrocytes from mice infected with the miRNA-containing viruses (Fig. 5A).

Mice showed a high preference for the initial low dose of the ethanol solution (Fig. 5B). Preference for the ethanol bottle (calculated as the percentage of ethanol consumed from the total volume) was similar between hevin KD mice and control mice for every dose during the entire procedure (Fig. 5B). When measuring total alcohol consumption (ingested ethanol expressed as g ethanol/kg), hevin KD in NAc astrocytes did not affect consumption of ethanol at low and medium concentrations (5%, 10% and 15%, w/v) (Fig. 5C). However, when exposed to a higher concentration of ethanol (20%), hevin KD showed an increased consumption compared to the lowest dose (5%), while control animals maintained a similar intake over time (Fig. 5C). After three days of withdrawal, hevin KD mice showed a higher relapse to consuming 10% ethanol dose than controls (Fig. 5C). Interestingly, these effects were only observed in the first 4 h of ethanol access. The last 4 h of the IEA experiment (from 4 h to 8 h) revealed that both groups, hevin KD and control mice, drank as much water as ethanol. Altogether, these data demonstrate that hevin KD animals consume more ethanol at the highest concentration and after ethanol withdrawal, while having a similar preference for ethanol.

DISCUSSION

AUD is characterized by two main features, the loss of control over the consumption of alcoholic beverages, and the relentless necessity to consume alcohol during abstinence, known as craving [5,6].

However, their neurobiological bases remain mainly unknown. Postmortem brain samples from subjects with a reliable antemortem diagnosis of AUD, and appropriately matched control subjects, provide a unique opportunity to search for any clinical relevance of altered molecular expression of different proteins in patients with AUD [44]. In this line, the principal finding of the present study is that the matricellular protein hevin is overexpressed in the brain of subjects with AUD.

Human brain regions analyzed in this study were selected based on their implication in different aspects of AUD and on tissue availability. The PFC was chosen for its role in executive functions, such as control, planning and inhibitions of behaviors; the HIP for its important role in the association of particular environments and emotional states with the effect of the drug; the CAU, for its involvement in cognition, learning, memory, and feedback processing; and the CB, for its role in movement and balance incoordination after long-term alcohol consumption, in addition to its role in cognition, emotion and drug addiction [8]. Overall, all the studied regions showed an increase in hevin levels either at mRNA or/and protein levels in AUD subjects. This is the first evidence in humans for the role of hevin in the pathophysiology of AUD. Even if the mechanisms underlying this feature or its consequences are difficult to determine in humans, several hypotheses can be postulated. Hevin promotes the formation and maintenance of excitatory synapses specifically and modulates the refinement and stabilization of dendritic spines [22,24,26,45]; therefore, the upregulation of hevin expression could be implicated in the profound structural rearrangement/adaptation that occurs in AUD [46,47]. Indeed, we previously found an important loss in neuronal structural proteins in AUD subjects, and other authors have reported that AUD subjects also suffer neuronal and dendritic spines loss [47–51]. Hevin increase could thus be an adaptative mechanism triggered to counteract ethanol's effects on neuronal structure. Besides, at a molecular level, hevin increases NMDA-receptor (NMDA-R) expression and their function [21,24,45].

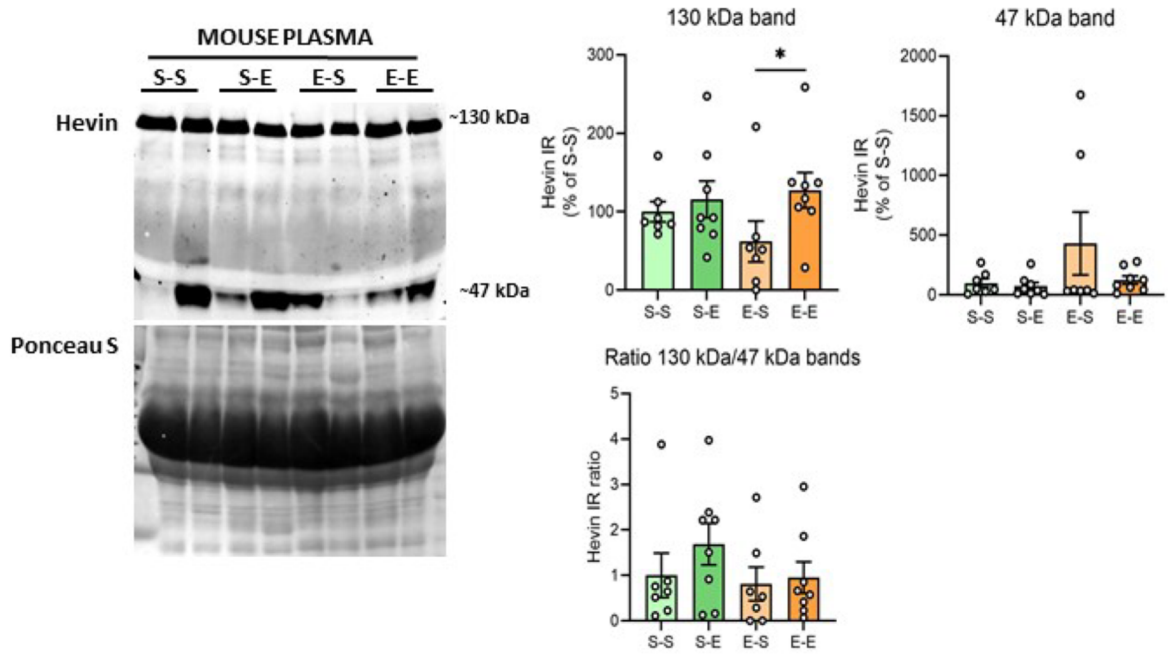

Fig. 4. Hevin protein expression in mouse plasma after different regimen of ethanol. A representative western blot for hevin in mouse plasma and its Ponceau S stain images, along with the graphics representing the actin-normalized immunoreactivity of ˜130 kDa and ˜47 kDa hevin bands and the ratio 130 kDa band/47 kDa in mouse plasma after the four administered ethanol treatments (S-S: saline – saline, S-E: saline – ethanol, E-S: ethanol-saline and E-E: ethanol-ethanol). n=7-8 per group. Kruskal-Wallis followed by Dunn's post hoc test was used for the comparison (*p< 0.05). Experiments were performed in triplicate. The quantification is represented in box-and-whiskers plots, where "box" shows the median and the 25th and 75th percentile and the "whiskers" depict the 5th and 95th percentile. Dots represent the average value of each individual in the performed experiments.

Hence, hevin could also mediate part of the synaptic plasticity occurring after chronic ethanol, such as long-term potentiation and NMDA-R dependent plasticity, as it has been widely described in preclinical studies as well as in postmortem human brain from subjects with AUD [46,52–54]. In our study we did not find any difference in hevin expression levels between sexes. As a control for disease specificity, a group of subjects with antemortem diagnoses of depression was added. Hevin expression was unaltered in the depression group in our study, consistent with a previous study [55]. These results in the human brain raise the question of whether hevin overexpression is induced by ethanol or if it is a *pre*-AUD *state*, suggesting vulnerability. We used preclinical models of AUD and compared the effects of chronic alcohol withdrawal, chronic alcohol relapse and acute alcohol administration on hevin protein levels in mouse brain. We selected cortico-limbic brain regions involved in the neurocircuitry of drug addiction, in particular ventral and dorsal striatum, PFC, HIP and AMY [8]. In contrast to human data, we observed hevin protein expression changes only in the AMY and NAc. In the AMY, a decrease in hevin levels was observed after a single dose of ethanol, but not after chronic ethanol administration. In this context, and according to the possible

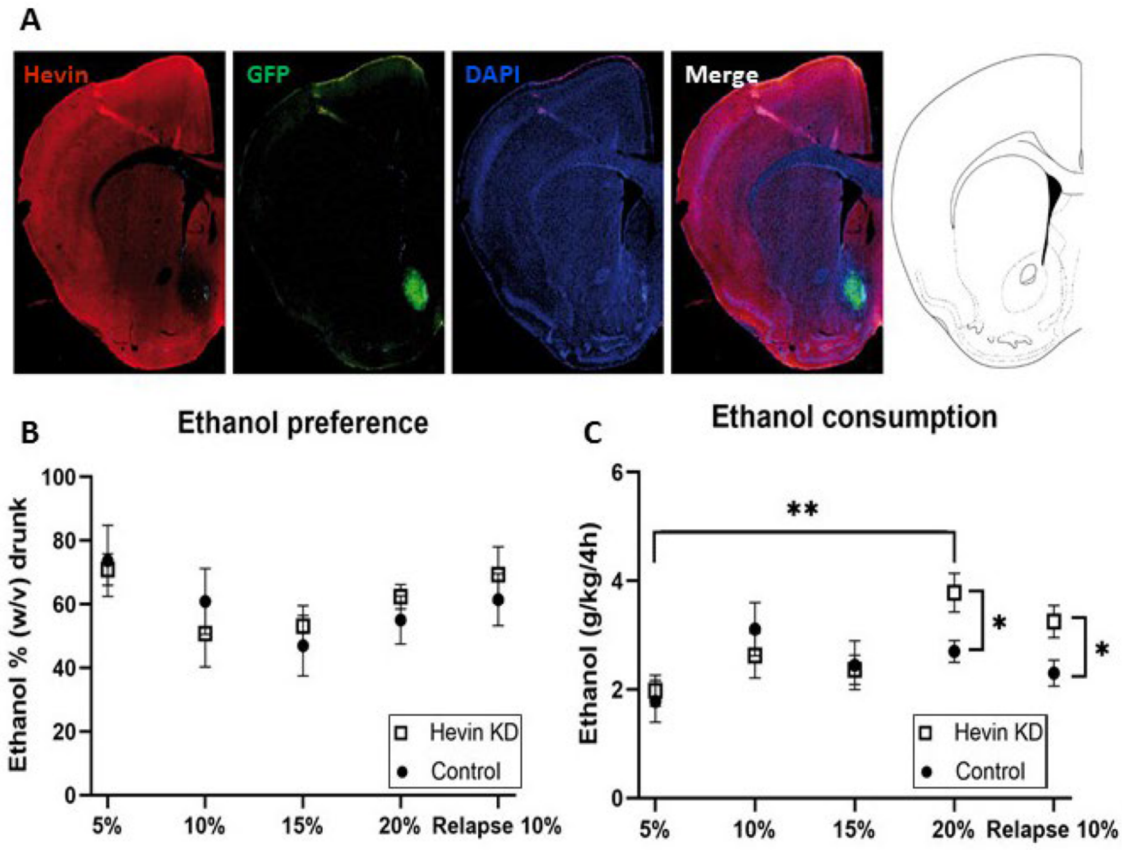

Fig.5. Effect of hevin protein downregulation in mouse NAc astrocytes on ethanol consumption. A) Immunohistochemical validation of hevin downregulation in mouse NAc after injection of miRNA-containing viruses (hevin immunofluorescence, in red, is absent in astrocytes infected with hevin miRNA and co-expressing EmGFP). B) Ethanol preference quantification every third day of each ethanol concentration. C) Ethanol consumption quantification every third day of each ethanol concentration. The ordinate represents the average of the percentage of ethanol taken by hevin KD and control groups (B) or the grams of ethanol per kg of mouse taken in 4h (C). The abscissa shows the ethanol concentration tested. N = 8/group. Empty squares show the mean ± SEM from hevin KD mice values and filled circles show the mean ± SEM from control mice values. Mann-Whitney test was used for the comparison of the preference and consumption between the hevin KD and controls (*p< 0.05, **p< 0.01); and Friedman followed by Dunn's post hoc test was used for the comparison of the preference and consumption between ethanol concentrations. Values represent the mean ± SEM.

role of hevin in regulating the glutamatergic signaling and neuroplasticity in response to ethanol, acute and low doses of ethanol decrease excitability and increase dendritic spines in rodents' AMY, coinciding with anxiolytic effects, while repeated withdrawal normalizes dendritic arborization, causing tolerance to ethanol anxiolysis [56–58]. On the contrary, in the NAc, hevin was overexpressed only with a challenging dose after withdrawal, while no change was observed after acute ethanol injection. It has already been described that chronic ethanol intake and withdrawal in rodents' NAc produce alterations in dendritic spine number, structure and

organization, as well as an increase in NMDA-R and AMPA-R expression and function, which suggests that hevin increase observed in NAc could be a compensatory response to the ethanol-related glutamatergic inhibition [59–64]. Overall, while changes in hevin levels in AMY could be implicated in the acute alcohol experience, the increased hevin expression in NAc after chronic ethanol exposure suggests that hevin might also participate in the long-term adaptation to ethanol. As noted, mouse and human brains showed a different pattern of hevin expression levels in several regions (i.e. PFC, HIP) after alcohol exposure. This difference could be explained by two essential factors largely discussed in the literature previously: 1) the different regimens of alcohol exposure (time course, total drug intake and probable withdrawal period) which arises the question of what is the necessary cumulative effect of the drug to cause neuroplasticity, and 2) different psychosocial and environmental stressors [65].

To test the potential role of hevin on alcohol consumption, we used RNA interference strategy to downregulate hevin expression in NAc astrocytes, where it is essentially expressed [30], and evaluated the consequence of hevin manipulation in the IEA model of voluntary ethanol intake. Our results indicate a disrupted reward system when hevin is downregulated (KD). Specifically, we detected a higher ethanol consumption in hevin KD mice in two cases: i) at high ethanol concentrations (20%), which were administered after 15 days of intake and ii) after three days of withdrawal with a medium ethanol concentration (10%). These findings suggest that ethanol addiction and withdrawal are associated with dysregulated hevin signaling. Since hevin increases excitatory synaptic plasticity, knocking-down hevin might disrupt the glutamatergic plasticity involved in the rewarding effects of ethanol [66], making it necessary to increase alcohol consumption in order to reach the same hedonic response [67]. Nevertheless, the ethanol preference analysis revealed that both hevin KD and control mice drank as much water as ethanol, showing no differences in the preference at any dose and at any time. We suggest that mice undergo autoregulation in the water intake probably to avoid the dehydration produced by the higher ethanol intake.

Finally, we tested whether hevin levels would be altered in the blood plasma of mice after chronic alcohol withdrawal, chronic alcohol relapse or acute alcohol administration. Interestingly, a very similar expression profile was obtained after the different ethanol treatments in plasma samples compared to NAc, with increased hevin expression only with a challenge dose after withdrawal. The origin of hevin protein in blood plasma is still uncertain. Hevin is not expressed by any blood cell type [31], but is expressed in other tissues than the brain, such as lung [68], endothelial cells of high endothelial venules [27,69] or stomach [70]. The increase of hevin in the plasma of ethanol-treated mice, suggests that hevin could be used as a biomarker in AUD relapse, as it has been proposed in neurodegenerative diseases and several cancers [71,72].

As a whole, this study sheds light on the role of hevin in the pathophysiology of AUD. In humans, we previously found that hevin is expressed in astrocytes and some glutamatergic and GABAergic neurons [30]. Although, the source of hevin overexpression in AUD subjects is unknown, our cell-specific RNA interference strategy in mice shows that hevin expression in NAc astrocytes is crucial for increased voluntary ethanol consumption. As described above, we hypothesized that hevin could take part in the acquisition of the addiction behavior by strengthening and promoting specific

synaptic signaling and/or modulating neuronal plasticity/adaptation in brain areas involved in AUD.

In conclusion, our postmortem brain analysis revealed an increase in hevin levels in various brain regions of subjects with AUD. In order to explore whether this increase was a consequence of alcohol intake, we used a mouse model of chronic ethanol administration and found that only chronic ethanol relapse increases hevin in the brain reward center, the NAc. In addition, we also evaluated whether alterations in hevin expression would affect alcohol-related behavior, and revealed that hevin manipulation in NAc astrocytes, where the vast majority of hevin is expressed in this region, modulates alcohol consumption. Overall, this study provides the first evidence for the role of hevin in alcohol consumption and addiction.

FUNDING

This work was supported by ERAB (The European Foundation for Alcohol Research, EA 18 19); Centro de Investigación Biomédica en Red de Salud Mental (CIBERSAM), Spain, the Basque Government (IT1512-22); Fundación Vital and FP7 Marie Curie Actions Career Integration Grant (FP7-PEOPLE- 2013-CIG #618807 to VV). A.N.-dM. is recipient of a predoctoral fellowship from the Basque Government and received an EMBO short-term fellowship.

REFERENCES

1. Heilig M, MacKillop J, Martinez D, Rehm J, Leggio L, Vanderschuren LJMJ. Addiction as a brain disease revised: why it still matters, and the need for consilience. Neuropsychopharmacology. 2021:1–9.

2. Rehm J, Mathers C, Popova S, Thavorncharoensap M, Teerawattananon Y, Patra J. Global burden of disease and injury and economic cost attributable to alcohol use and alcohol-use disorders. The Lancet. 2009;373:2223–2233.

3. Nutt DJ, King LA, Phillips LD. Drug harms in the UK: a multicriteria decision analysis. The Lancet. 2010;376:1558–1565.

4. WHO. World Health Organization. Global status report on alcohol and health 2018. https://www.who.int/publications/i/item/9789241565639.Report 27 September 2018.

5. Spanagel R, Zink M, Sommer WH. Alcohol: neurobiology of alcohol addiction. In: Pfaff DW, Volkow ND, editors. Neurosci. 21st Century Basic Clin., New York, NY: Springer; 2016. p. 3593–3623.

6. Weiss F, Porrino LJ. Behavioral neurobiology of alcohol addiction: recent advances and challenges. J Neurosci Off J Soc Neurosci. 2002;22:3332–3337.

7. Abrahao KP, Salinas AG, Lovinger DM. Alcohol and the brain: neuronal molecular targets, synapses, and circuits. Neuron. 2017;96:1223–1238.

8. Koob GF, Volkow ND. Neurobiology of addiction: a neurocircuitry analysis. Lancet Psychiatry. 2016;3:760–773.

9. Becker HC. Alcohol dependence, withdrawal, and relapse. Alcohol Res Health. 2008;31:348–361.

10. Koob GF, Le Moal M. Plasticity of reward neurocircuitry and the 'dark side' of drug addiction. Nat Neurosci. 2005;8:1442–1444.

11. Sliedrecht W, de Waart R, Witkiewitz K, Roozen HG. Alcohol use disorder relapse factors: A systematic review. Psychiatry Res. 2019;278:97–115.

12. Nagai J, Rajbhandari AK, Gangwani MR, Hachisuka A, Coppola G, Masmanidis SC, et al. Hyperactivity with disrupted attention by activation of an astrocyte synaptogenic cue. Cell. 2019;177:1280-1292.e20.

13. Wang J, Holt LM, Huang HH, Sesack SR, Nestler EJ, Dong Y. Astrocytes in cocaine addiction and beyond. Mol Psychiatry. 2021. 9 April 2021. https://doi.org/10.1038/s41380-021-01080-7.

14. Erickson EK, DaCosta AJ, Mason SC, Blednov YA, Mayfield RD, Harris RA. Cortical astrocytes regulate ethanol consumption and intoxication in mice. Neuropsychopharmacology. 2021;46:500–508.
15. Bull C, Freitas KCC, Zou S, Poland RS, Syed WA, Urban DJ, et al. Rat nucleus accumbens core astrocytes modulate reward and the motivation to self-administer ethanol after abstinence. Neuropsychopharmacol Off Publ Am Coll Neuropsychopharmacol. 2014;39:2835–2845.
16. Erickson EK, Farris SP, Blednov YA, Mayfield RD, Harris RA. Astrocyte-specific transcriptome responses to chronic ethanol consumption. Pharmacogenomics J. 2018;18:578–589.
17. Erickson EK, Blednov YA, Harris RA, Mayfield RD. Glial gene networks associated with alcohol dependence. Sci Rep. 2019;9:10949.
18. Trindade P, Hampton B, Manhães AC, Medina AE. Developmental alcohol exposure leads to a persistent change on astrocyte secretome. J Neurochem. 2016;137:730–743.
19. Pignataro L, Varodayan FP, Tannenholz LE, Protiva P, Harrison NL. Brief alcohol exposure alters transcription in astrocytes via the heat shock pathway. Brain Behav. 2013;3:114–133.
20. Christopherson KS, Ullian EM, Stokes CCA, Mullowney CE, Hell JW, Agah A, et al. Thrombospondins are astrocyte-secreted proteins that promote CNS synaptogenesis. Cell. 2005;120:421–433.
21. Gan KJ, Südhof TC. SPARCL1 promotes excitatory but not inhibitory synapse formation and function independent of neurexins and neuroligins. J Neurosci. 2020;40:8088–8102.
22. Kucukdereli H, Allen NJ, Lee AT, Feng A, Ozlu MI, Conatser LM, et al. Control of excitatory CNS synaptogenesis by astrocyte-secreted proteins Hevin and SPARC. Proc Natl Acad Sci U S A. 2011;108:E440-449.
23. Murphy-Ullrich JE, Sage EH. Revisiting the matricellular concept. Matrix Biol J Int Soc Matrix Biol. 2014;37:1–14.
24. Singh SK, Stogsdill JA, Pulimood NS, Dingsdale H, Kim YH, Pilaz L-J, et al. Astrocytes assemble thalamocortical synapses by bridging Nrx1α and NL1 via hevin. Cell. 2016;164:183–196.
25. Miguel-Hidalgo JJ. Molecular neuropathology of astrocytes and oligodendrocytes in alcohol use disorders. Front Mol Neurosci. 2018;11:78.
26. Risher WC, Patel S, Kim IH, Uezu A, Bhagat S, Wilton DK, et al. Astrocytes refine cortical connectivity at dendritic spines. ELife. 2014;3.
27. Girard J-P, Springer TA. Modulation of endothelial cell adhesion by hevin, an acidic protein associated with high endothelial venules. J Biol Chem. 1996;271:4511–4517.
28. Johnston IG, Paladino T, Gurd JW, Brown IR. Molecular cloning of SC1: a putative brain extracellular matrix glycoprotein showing partial similarity to osteonectin/BM40/SPARC. Neuron. 1990;4:165–176.
29. Lively S, Brown IR. The extracellular matrix protein SC1/hevin localizes to multivesicular bodies in bergmann glial fibers in the adult rat cerebellum. Neurochem Res. 2010;35:315–322.
30. Mongrédien R, Erdozain AM, Dumas S, Cutando L, del Moral AN, Puighermanal E, et al. Cartography of hevin-expressing cells in the adult brain reveals prominent expression in astrocytes and parvalbumin neurons. Brain Struct Funct. 2019; 224:, 1219–1244.
31. Nuñez-delMoral A, Brocos-Mosquera I, Vialou V, Callado LF, Erdozain AM. Characterization of hevin (SPARCL1) immunoreactivity in postmortem human brain homogenates. Neuroscience. 2021; 15;467:91-109.

32. Soderling JA, Reed MJ, Corsa A, Sage EH. Cloning and expression of murine SC1, a gene product homologous to SPARC. J Histochem Cytochem. 1997;45:823–835.
33. Vialou V, Robison AJ, LaPlant QC, Covington HE, Dietz DM, Ohnishi YN, et al. ΔFosB in brain reward circuits mediates resilience to stress and antidepressant responses. Nat Neurosci. 2010;13:745–752.
34. Bahi A, Dreyer J-L. Involvement of nucleus accumbens dopamine D1 receptors in ethanol drinking, ethanol-induced conditioned place preference, and ethanol-induced psychomotor sensitization in mice. Psychopharmacology (Berl). 2012;222:141–153.
35. Nocjar C, Middaugh LD, Tavernetti M. Ethanol consumption and place-preference conditioning in the alcohol-preferring C57BL/6 mouse: relationship with motor activity patterns. Alcohol Clin Exp Res. 1999;23:683–692.
36. Bradford MM. A rapid and sensitive method for the quantitation of microgram quantities of protein utilizing the principle of protein-dye binding. Anal Biochem. 1976;72:248–254.
37. Muguruza C, Miranda-Azpiazu P, Díez-Alarcia R, Morentin B, González-Maeso J, Callado LF, et al. Evaluation of 5-HT2A and mGlu2/3 receptors in postmortem prefrontal cortex of subjects with major depressive disorder: Effect of antidepressant treatment. Neuropharmacology. 2014;86:311–318.
38. Portero-Tresserra M, Gracia-Rubio I, Cantacorps L, Pozo OJ, Gómez-Gómez A, Pastor A, et al. Maternal separation increases alcohol-drinking behaviour and reduces endocannabinoid levels in the mouse striatum and prefrontal cortex. Eur Neuropsychopharmacol. 2018;28:499–512.
39. Dean B, Hyde TM, Kleinman JE. Using CNS autopsy tissue in psychiatric research: a practical guide. CRC Press; 2019.
40. Seghier ML, Price CJ. Interpreting and utilising intersubject variability in brain function. Trends Cogn Sci. 2018;22:517–530.
41. Brekken RA, Sullivan MM, Workman G, Bradshaw AD, Carbon J, Siadak A, et al. expression and characterization of murine Hevin (SC1), a member of the SPARC family of matricellular proteins. J Histochem Cytochem. 2004;52:735–748.
42. Weaver MS, Workman G, Cardo-Vila M, Arap W, Pasqualini R, Sage EH. Processing of the matricellular protein hevin in mouse brain is dependent on ADAMTS4. J Biol Chem. 2010;285:5868–5877.
43. Weaver M, Workman G, Schultz CR, Lemke N, Rempel SA, Sage EH. Proteolysis of the matricellular protein hevin by matrix metalloproteinase-3 produces a SPARC-like fragment (SLF) associated with neovasculature in a murine glioma model. J Cell Biochem. 2011;112:3093–3102.
44. McCullumsmith RE, Hammond JH, Shan D, Meador-Woodruff JH. Postmortem brain: an underutilized substrate for studying severe mental illness. Neuropsychopharmacology. 2014;39:65–87.
45. Gan KJ, Südhof TC. Specific factors in blood from young but not old mice directly promote synapse formation and NMDA-receptor recruitment. Proc Natl Acad Sci. 2019;116:12524–12533.
46. Avchalumov Y, Mandyam CD. Synaptic plasticity and its modulation by alcohol. Brain Plast. 2020;6:103–111.
47. Gass JT, Olive MF. Neurochemical and neurostructural plasticity in alcoholism. ACS Chem Neurosci. 2012;3:494–504.
48. Ferrer I, Fábregues I, Rairiz J, Galofré E. Decreased numbers of dendritic spines on cortical pyramidal neurons in human chronic alcoholism. Neurosci Lett. 1986;69:115–119.
49. Erdozain AM, Morentin B, Bedford L, King E, Tooth D, Brewer C, et al. Alcohol-related brain damage in humans. PLOS ONE. 2014;9:e93586.

50. Labisso WL, Raulin A-C, Nwidu LL, Kocon A, Wayne D, Erdozain AM, et al. The Loss of α- and β-tubulin proteins are a pathological hallmark of chronic alcohol consumption and natural brain ageing. Brain Sci. 2018;8:E175.
51. Bengochea O, Gonzalo LM. Effect of chronic alcoholism on the human hippocampus. Histol Histopathol. 1990;5:349–357.
52. Freund G, Anderson KJ. Glutamate receptors in the frontal cortex of alcoholics. Alcohol Clin Exp Res. 1996;20:1165–1172.
53. Michaelis EK, Michaelis ML, Freed WJ, Foye J. Glutamate receptor changes in brain synaptic membranes during chronic alcohol intake. Alcohol Alcohol Oxf Oxfs Suppl. 1993;2:377–381.
54. Loheswaran G, Barr MS, Zomorrodi R, Rajji TK, Blumberger DM, Foll BL, et al. Impairment of Neuroplasticity in the Dorsolateral Prefrontal Cortex by Alcohol. Sci Rep. 2017;7:5276.
55. Teyssier J-R, Ragot S, Chauvet-Gélinier J-C, Trojak B, Bonin B. Activation of a ΔFOSB dependent gene expression pattern in the dorsolateral prefrontal cortex of patients with major depressive disorder. J Affect Disord. 2011;133:174–178.
56. Harrison NL, Skelly MJ, Grosserode EK, Lowes DC, Zeric T, Phister S, et al. Effects of acute alcohol on excitability in the CNS. Neuropharmacology. 2017;122:36–45.
57. Pandey SC, Zhang H, Ugale R, Prakash A, Xu T, Misra K. Effector immediate-early gene arc in the amygdala plays a critical role in alcoholism. J Neurosci Off J Soc Neurosci. 2008;28:2589–2600.
58. You C, Zhang H, Sakharkar AJ, Teppen T, Pandey SC. Reversal of deficits in dendritic spines, BDNF and Arc expression in the amygdala during alcohol dependence by HDAC inhibitor treatment. Int J Neuropsychopharmacol. 2014;17:313–322.
59. Zhou FC, Anthony B, Dunn KW, Lindquist WB, Xu ZC, Deng P. Chronic alcohol drinking alters neuronal dendritic spines in the brain reward center nucleus accumbens. Brain Res. 2007;1134:148–161.
60. Peterson VL, McCool BA, Hamilton DA. Effects of ethanol exposure and withdrawal on dendritic morphology and spine density in the nucleus accumbens core and shell. Brain Res. 2015;1594:125–135.
61. Uys JD, McGuier NS, Gass JT, Griffin III WC, Ball LE, Mulholland PJ. Chronic intermittent ethanol exposure and withdrawal leads to adaptations in nucleus accumbens core postsynaptic density proteome and dendritic spines. Addict Biol. 2016;21:560–574.
62. Ji X, Saha S, Kolpakova J, Guildford M, Tapper AR, Martin GE. Dopamine receptors differentially control binge alcohol drinking-mediated synaptic plasticity of the core nucleus accumbens direct and indirect pathways. J Neurosci Off J Soc Neurosci. 2017;37:5463–5474.
63. Laguesse S, Morisot N, Shin JH, Liu F, Adrover MF, Sakhai SA, et al. Prosapip1-dependent synaptic adaptations in the nucleus accumbens drive alcohol intake, seeking and reward. Neuron. 2017;96:145-159.e8.
64. Kircher DM, Aziz HC, Mangieri RA, Morrisett RA. Ethanol experience enhances glutamatergic ventral hippocampal inputs to d1 receptor-expressing medium spiny neurons in the nucleus accumbens shell. J Neurosci Off J Soc Neurosci. 2019;39:2459–2469.
65. Koob GF, Volkow ND. Neurocircuitry of addiction. Neuropsychopharmacology. 2010;35:217–238.
66. Griffin WC, Haun HL, Hazelbaker CL, Ramachandra VS, Becker HC. Increased extracellular glutamate in the nucleus accumbens promotes excessive ethanol drinking in ethanol dependent mice. Neuropsychopharmacol Off Publ Am Coll Neuropsychopharmacol. 2014;39:707–717.
67. Cofresí RU, Bartholow BD, Piasecki TM. Evidence for incentive salience sensitization as a pathway to alcohol use

disorder. Neurosci Biobehav Rev. 2019;107:897–926.
68. Bendik I, Schraml P, Ludwig CU. Characterization of MAST9/Hevin, a SPARC-like Protein, That is Down-Regulated in Non-Small Cell Lung Cancer. Cancer Res. 1998;58:626–629.
69. Girard J-P, Springer TA. Cloning from purified high endothelial venule cells of hevin, a close relative of the antiadhesive extracellular matrix protein SPARC. Immunity. 1995;2:113–123.
70. Klingler A, Regensburger D, Tenkerian C, Britzen-Laurent N, Hartmann A, Stürzl M, et al. Species-, organ- and cell-type-dependent expression of SPARCL1 in human and mouse tissues. PLOS ONE. 2020;15:e0233422.
71. Lau C-Y, Poon R-P, Cheung S-T, Yu W-C, Fan S-T. SPARC and hevin expression correlate with tumour angiogenesis in hepatocellular carcinoma. J Pathol. 2006;210:459–468.
72. Yin GN, Lee HW, Cho J-Y, Suk K. Neuronal pentraxin receptor in cerebrospinal fluid as a potential biomarker for neurodegenerative diseases. Brain Res. 2009;1265:158–170.

ANNEX2. SUPPLEMENTARY MATERIAL

A novel role for the matricellular protein hevin in alcohol use disorder

Amaia Nuñez-delMoral, Paula C. Bianchi, Iria Brocos-Mosquera, Augusto Anesio, Paula Palombo, Rosana Camarini, Fabio C. Cruz, Luis F. Callado, Vincent Vialou, Amaia M. Erdozain

Case	Sex	Age (years)	PMD (hours)	Storage time (months)	Cause of dead	Psychiatric diagnosis	Drugs in blood
A1	M	59	22	11	Natural/ Cirrhosis	AUD	(-)
C1	M	57	3	18	Accident/ Crushing	Control	(-)
D1	M	55	20	95	Suicide/ Train	Depression	Antidepressants
A2	M	59	19	159	Natural/ CRF	AUD	(-)
C2	M	58	16	201	Accident/ Traffic	Control	(-)
D2	M	60	18	170	Suicide/ Hanging	Depression	Antidepressants
A3	M	61	34	20	Natural/ CRF	AUD	Ethanol
C3	M	62	9	45	Natural/ CRF	Control	(-)
D3	M	62	15	96	Suicide/ Knife	Depression	Antidepressants
A4	M	51	23	23	Natural/ CRF	AUD	(-)
C4	M	51	14	108	Accident/ Traffic	Control	Ethanol
D4	M	51	24	200	Suicide/ Hanging	Depression	Antidepressants
A5	M	55	11	36	Natural/ CRF	AUD	(-)
C5	M	56	13	96	Natural/ CRF	Control	(-)
D5	M	56	3	128	Natural/ Thromboembolism	Depression	Antidepressants
A6	M	61	27	162	Natural/ CRF	AUD	(-)
C6	M	61	23	202	Accident/ Traffic	Control	(-)
D6	M	60	24	111	Suicide/ Jumping	Depression	Antidepressants
A7	M	52	17	85	Natural/ CRF	AUD	(-)
C7	M	54	16	112	Accident/ Work	Control	(-)
D7	M	50	23	143	Suicide/ Gun	Depression	Antidepressants
A8	M	47	28	88	Natural/ Hemorrhage	AUD	Ethanol
C8	M	46	24	129	Natural/CRF	Control	(-)
D8	M	49	27	18	Natural/CRF	Depression	Antidepressants
A9	F	50	14	95	Natural/ Hemorrhage	AUD	Ethanol
C9	F	50	10	129	Natural/CRF	Control	(-)
D9	F	49	19	164	Suicide/ Jumping	Depression	Antidepressants
A10	F	38	22	165	Natural/ CRF	AUD	(-)
C10	F	36	20	123	Accident/ Train	Control	(-)
D10	F	36	32	152	Suicide/ Drug intoxication	Depression	Anxiolytics/ Antidepressants
A11	F	71	16	125	Natural/ CRF	AUD	(-)
C11	F	71	22	155	Accident/ Traffic	Control	(-)
D11	F	70	7	92	Suicide/ Jumping	Depression	Antidepressants
A12	M	64	9	104	Natural/ CRF	AUD	Ethanol
C12	M	64	22	46	Natural/ CRF	Control	(-)
D12	M	65	12	145	Suicide/ Hanging	Depression	Antidepressants
A13	M	73	2	168	Natural/ CRF	AUD	Ethanol
C13	M	73	10	202	Accident/ Jumping	Control	(-)
D13	M	73	11	39	Suicide/ Hanging	Depression	Antidepressants
A14	M	52	27	114	Natural/ CRF	AUD	(-)
C14	M	51	19	101	Accident/ Traffic	Control	(-)
D14	M	53	22	87	Suicide/ Hanging	Depression	Antidepressants
A15	M	49	10	115	Natural/ CRF	AUD	Ethanol
C15	M	48	10	123	Natural/CRF	Control	(-)
D15	M	50	24	118	Suicide/ Gun	Depression	Antidepressants
A16	M	56	24	129	Natural/ CRF	AUD	Ethanol
C16	M	55	22	130	Natural/CRF	Control	(-)
D16	M	56	22	119	Suicide/ Gun	Depression	Antidepressants
A17	F	54	7	142	Natural/ CRF	AUD	Ethanol
C17	F	51	10	84	Natural/CRF	Control	(-)
D17	F	54	18	169	Suicide/ Hanging	Depression	Antidepressants

A18	M	60	6	143	Natural/ CRF	AUD	(-)
C18	M	60	19	87	Natural/ CRF	Control	(-)
D18	M	61	5	198	Natural/ Aneurism	Depression	Antidepressants
A19	M	46	11	149	Natural/ Hemorrhage	AUD	(-)
C19	M	47	17	205	Natural/ CRF	Control	(-)
D19	M	47	18	167	Suicide/ Hanging	Depression	Antidepressants
A20	F	44	11	163	Natural/ CRF	AUD	(-)
C20	F	45	12	130	Natural/ CRF	control	(-)
D20	F	43	24	143	Natural/CRF	Depression	Antidepressants
A21	M	53	25	158	Natural/ CRF	AUD	(-)
C21	M	54	23	159	Accident/ Jumping	control	(-)
D21	M	53	39	191	Suicide/ Gun	Depression	Antidepressants
A22	M	65	5	159	Natural/ CRF	AUD	Ethanol
C22	M	67	22	166	Natural/ CRF	control	(-)
D22	M	65	11	94	Suicide/ Drug intoxication	Depression	Anxiolytics/ Antidepressants
A23	F	50	23	159	Natural/ CRF	AUD	Ethanol
C23	F	45	8	21	Natural/ Hemorrhage	Control	(-)
D23	F	49	18	142	Suicide/ Submersion	Depression	Antidepressants
A24	M	57	17	147	Natural/ CRF	AUD	(-)
C24	M	55	20	37	Accident/ Mountain	Control	(-)
D24	M	57	21	92	Suicide/ Jumping	Depression	Antidepressants
A25	F	46	19	156	Natural/ CRF	AUD	Ethanol
C25	F	43	3	40	Accident/ Traffic	Control	(-)
D25	F	45	21	89	Suicide/ Hanging	Depression	Antidepressants
A	7F/18M	55±2	17±2	119±10			
C	7F/18M	54±2	15±1	114±12			
D	7F/18M	55±2	19±2	127±9			

Supplementary table 1. Demographic characteristics, postmortem delay (PMD), storage time of the sample, cause of death, psychiatric diagnosis and toxicological findings of the subjects included in the study. A, AUD (alcohol use disorder); C, control; D, depression; M, male; F, female; CRF, cardiorespiratory failure.

Sample	Primary Ab	Primary Ab dilution	Secondary Ab	Secondary Ab dilution
Human brain (PFC, HIP, CAU, CB)	Goat anti-human hevin (R&D systems, AF2728)	1:3000	Alexa Fluor® 680 conjugated donkey anti-goat (Life Technologies, A21084)	1:5000
	Mouse anti- β-actin (Sigma-Aldrich, A1978)	1:100.000	DyLight™ 800 conjugated donkey anti-mouse (Rockland, 610-745-002)	1:5000
Mouse brain (FC, NAc, CPu, HIP, AMY) and plasma	Goat anti-mouse hevin (R&D systems, AF2836)	1:2000	Alexa Fluor® 680 conjugated donkey anti-goat (Life Technologies, A21084)	1:5000
	Rabbit anti- β-actin (Abcam, Ab8227)	1:5000	DyLight™ 800 conjugated donkey anti-rabbit (Rockland, 611-745-127)	1:5000

Supplementary table 2. Details of the primary and secondary antibodies used in western blot assays.

ANNEX 3

Correlation between both hevin protein isoforms

Statistical linear correlation between β-actin normalized ~130 kDa and ~100 kDa hevin bands immunoreactivity in post nuclear preparations from human prefrontal cortex **(A)**, cerebellum **(B)**, hippocampus **(C)** and caudate nucleus **(D)** of alcohol use disorder (AUD), control and depression groups of subjects. Correlation analysis was performed by two-tailed Pearson´s correlation test (Pearson' r value, *p* value and the regression line are shown). Dots represent the average value of each individual in the performed experiments.

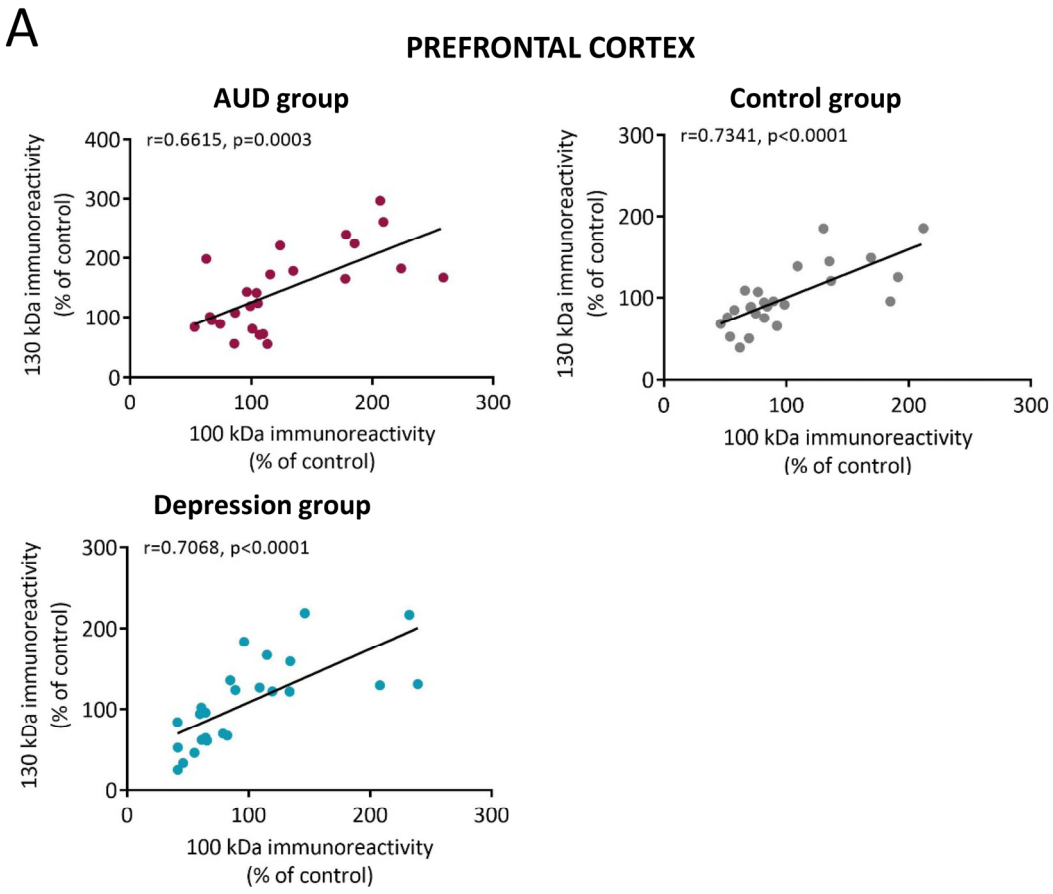

B

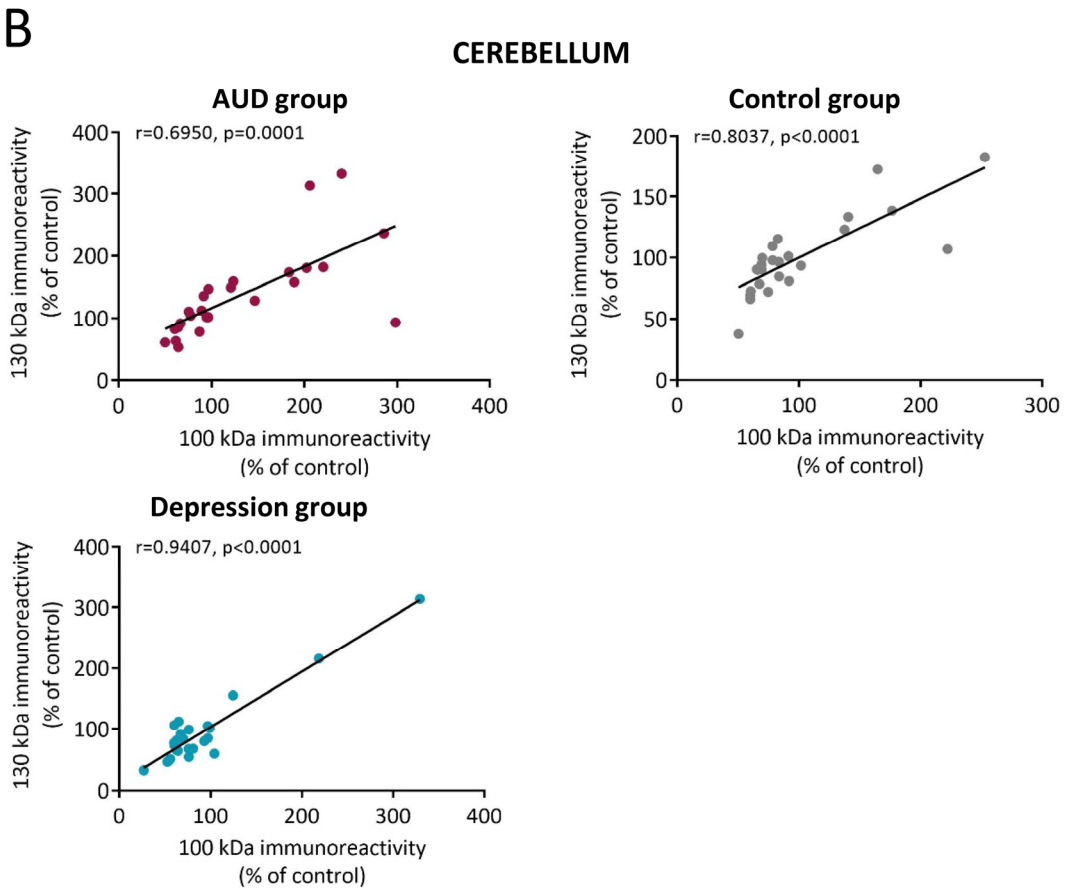
CEREBELLUM
AUD group
r=0.6950, p=0.0001
Control group
r=0.8037, p<0.0001
Depression group
r=0.9407, p<0.0001
130 kDa immunoreactivity (% of control)
100 kDa immunoreactivity (% of control)

C

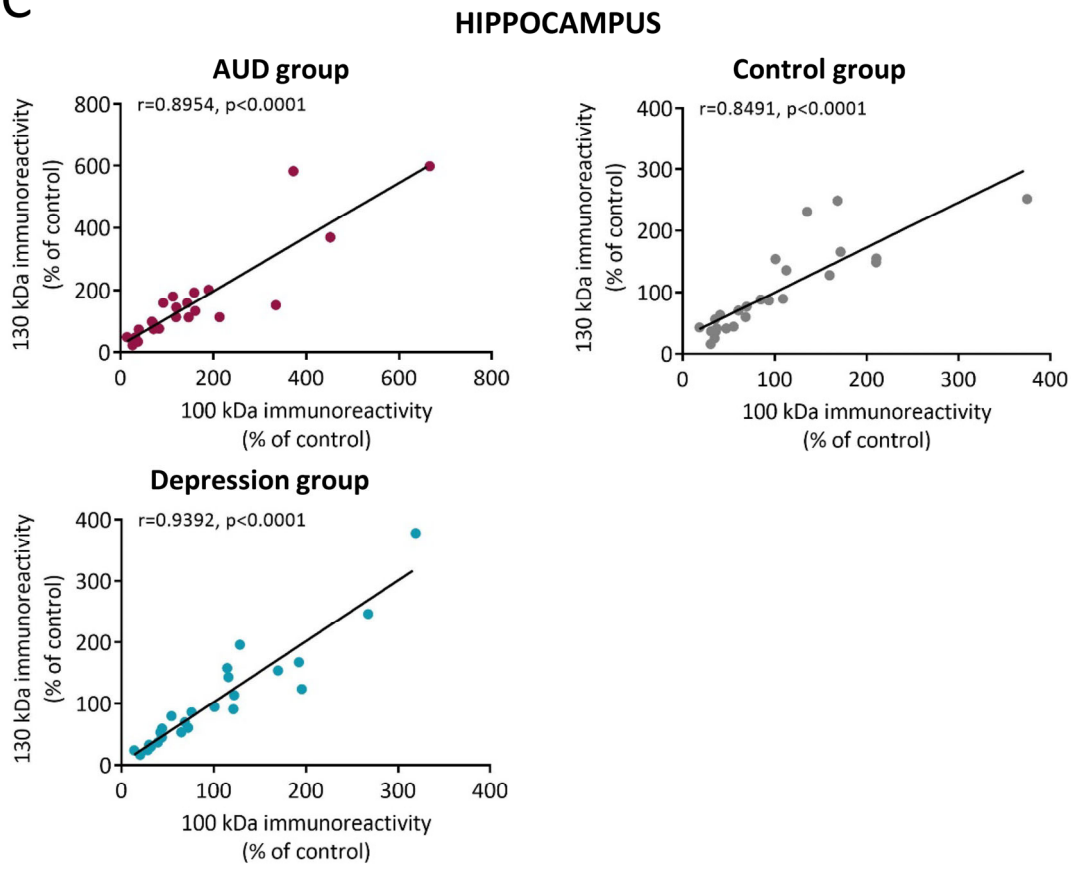
HIPPOCAMPUS
AUD group
r=0.8954, p<0.0001
Control group
r=0.8491, p<0.0001
Depression group
r=0.9392, p<0.0001
130 kDa immunoreactivity (% of control)
100 kDa immunoreactivity (% of control)

D

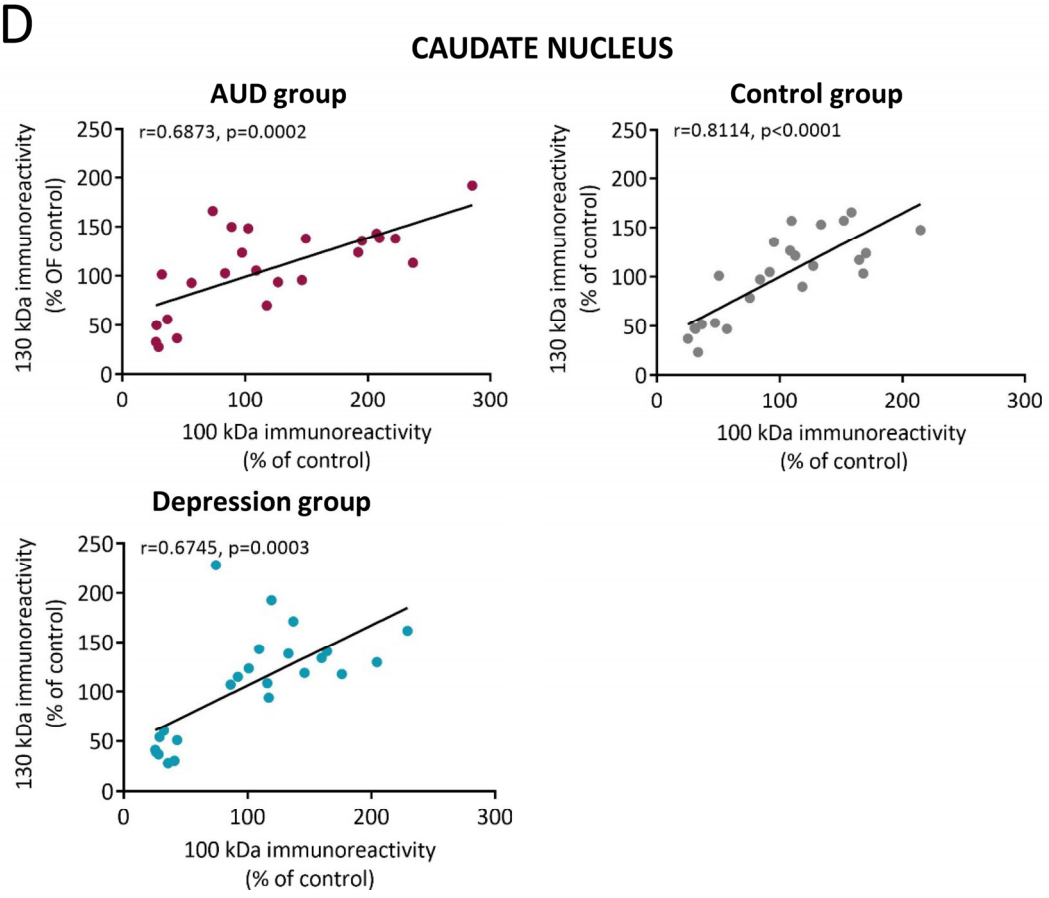
CAUDATE NUCLEUS
AUD group
r=0.6873, p=0.0002
130 kDa immunoreactivity
(% OF control)
100 kDa immunoreactivity
(% of control)
Control group
r=0.8114, p<0.0001
130 kDa immunoreactivity
(% of control)
100 kDa immunoreactivity
(% of control)
Depression group
r=0.6745, p=0.0003
130 kDa immunoreactivity
(% of control)
100 kDa immunoreactivity
(% of control)